Lunar and Planetary Laboratory
Department of Planetary Sciences

Washington State:

A Planetary Analogue in Flood Basalts and Flood Channels

Planetary Geology Field Practicum
PTYS 594a
September 20-26, 2002

The University of Arizona

Tucson, Arizona

Editor's Introduction

Fieldtrippers,

Welcome to the Washington State field trip! This is the second major trip that the Lab has undertaken, the first having been the Yellowstone trip in the fall of 1997. On both of these trips it has been a graduate student that has taken the initiative to get the ball rolling and line up support, but now, as then, the work of many dedicated volunteers has been what made the trip possible. In particular, I wish to thank Jani Radebaugh for helping me organize this whole thing; Lazslo Kezstheyi and Windy Jaeger for their efforts above and beyond the call of duty in helping to plan and scout the trip; Alfred McEwen and Vik Baker for serving as trip leaders; Noreen Conarro and Linda Hickox for patiently leading us through the bureaucratic minefield; Mike Drake and the Department of Planetary Sciences for their unswerving moral and financial support; and H. Jay Melosh for the creation of the field trip as one of LPL's most distinctive graduate institutions.

For the possible benefit of future generations of LPL graduate students, I have included the information from our proposal to Mike on page *v*. Also included in this chapter is the final budget for the trip, which I've included so that you know where it is that $500 you (may have) spent is going.

This year marks the LPL field trip's first foray into the world of electronic publishing, with the LaTeXtemplate (`http://c3po.lpl.arizona.edu/CRB`) that some participants utilized, and total booklet postscript (`http://c3po.lpl.arizona.edu/CRB/booklet`) that allowed the publication of this material online.

In converting Ralph's handout to LaTeX, I noted that he now holds the world record for most '~' characters in a handout — 18! I propose that in the spring Ralph be forced to give a talk on a subject that we actually know something about.

Finally, thank you to all of you who made my life easy — those that used the LaTeX template, those that scanned in their own stuff, and those that kept their handouts brief.

Now for the trip – I wish us all pleasant weather, engaging science, and fewer CFs than one might expect statistically based on a Monte-Carlo simulation.

Jason Barnes, ed.

Contents

Proposal

Field trip to Washington State: a Mars Analogue in Flood Basalts and Flood Channels

Prepared by Jason Barnes, Laszlo Keszthelyi, Windy Jaeger, and Jani Radebaugh

Introduction

In 1997, following a semester without a field trip, the Planetary Science Department undertook a field trip to Yellowstone National Park to study volcanic and hydrothermal processes. In a similar vein, we propose for Fall 2002 a field trip to Washington State to study flood basalts, planetary volcanism, and massive flood outflow channels as analogues to what might be found on Mars. This matter is particularly important when considering possible future Mars sample return missions — in order to properly understand samples they must be placed into context. The proposed trip is 7 days long, has an estimated total budget of $14,820, and will be led by Alfred McEwen, Vik Baker, and Lazlo Keszthelyi. A scientific summary along with a proposed itinerary, science discussion topics, and a budget for the trip are included below.

Science Summary

The focus of future NASA funding for Planetary Geology is (for better or worse) the search for water and life on Mars. The Mars Exploration Program already recieves about half of all the NASA funds for Solar System Exploration. The stated principle for the MEP is "Follow the Water" (http://mars.jpl.nasa.gov). For this reason, it is essential that the upcoming generation of planetary science students be familiar with the physics and geology associated with aqueous processes.

Perhaps the strongest evidence for water on Mars comes from the morphology of the massive outflow channels. The United States is exceedingly fortunate to be the home of some of the most recent catastrophic floods which approach the scale of the purported Martian floods. The Channeled Scablands of Washington State are the best terrestrial analogs for the massive channels on Mars (e.g., Baker, 1978). The University of Arizona is also extremely fortunate to have the world's acknowledged expert on the Channeled Scablands and catastrophic flooding. The students in this department deserve to be able to take advantage of both of these invaluable resources.

Of course, there are many conflicting hypotheses for the formation of every geomophologic feature suggested to indicate aqueous flow on Mars. Leading contenders for the eroding fluid include CO2-rich debris flows (suggested to behave like pyroclastic flows), mudflows, lava, and glaciers. The Cascades and Columbia River Basalts provide excellent examples of erosion by all of these processes.

We propose to tap the expertise of both people at LPL and their local contacts in the Washington area to lead a trip through the Cascades and Channeled Scablands. In addition to Vic Baker, Laszlo

Keszthelyi would come from LPL to describe the flood basalt lava flows. Baker and Keszthelyi will also invite experts from the local universities and the USGS Cascades Volcano Observatory to provide additional information.

While the emphasis will be on aqueous processes and other processes that have been suggested to mimic aqueous processes, this trip will provide the opportunity to examine other topics of interest to planetary scientists. Examples include: andesite formation on Earth and Mars, palagonite formation on Earth and Mars, plate tectonics on Earth and the other planets, life in extreme environments, and the role of impacts vs. volcanism in mass extinctions.

This trip would provide graduates from LPL with a critical scientific advantage over students from other departments. In particular, examining these types of features from the ground will prepare the new LPL graduates to interpret morphologic features on the scale that will be provided by the new rover and high resolution imaging experiments.

Science Topics

The way that LPL field trips are run, each student studies a particular scientific topic and becomes the expert for that topic over the course of the field trip, also giving a 10-15 minute talk on the subject. The following are suggested field trip topics, along with 4 special half-hour pre-trip talks on the overarching geological themes to be studied in the area. These talks will be given by local (U of A) experts.

EDITOR'S NOTE: THIS PRELIMINARY TOPIC LIST CHANGED SOMEWHAT BETWEEN THE PROPOSAL AND THE ACTUAL TRIP.

Science Topics	
Missoula Floods	**Mt. St. Helens**
Pleistocene Climate / Glacial History	Eruptive history of Mt. St. Helens
Lake Missoula and the Ice Dam	Lahars
J. Brentz and the Flood Saga	Physics of pyroclastic flows
Geology and History of Dry Falls	Magma chemistry
Giant flood ripples	Lava Tube formation
Loess deposits	Seismology of 1980 Eruption
Ephrata Gravel Fan / MPF Landing Site	Ash deposition from 1980
Palouse Falls and Canyon Formation	Gas emissions, 1980
Scabland Formation & Hydrology	Physics of 1980 Directed Blast
Wake-vortex scouring and the Flood	Lava dome
Wallula Gap / flood discharge rates	Landslide Tsunami
	Ecological succession after 1980
Other	Eyewitness accounts of 1980 eruption
Grand Coulee Dam / Salmon	
History of Hanford Nuclear reservation	**Columbia River Basalts**
Rootless Cones near Odessa, WA	Pillow Lava
Comparison of Remote Sensing to Ground	Columbia River Basalts source vents
	Other Massive Basalt Eruption Sequences
	Extent and Volume of CRB
	Timing and evolution of CRB eruptions
	Rate of CRB flow emplacement
Big pretrip talks	Yellowstone Mantle Plume
Geology and plate tectonics of WA.	
The Mt. Saint Helens eruption of 1980	
Columbia River Basalt	
Channeled Scabland Overview (Vic Baker?)	

Schedule

Although the specific timing and stops of the field trip are subject to airline scheduling and other presently unknown constraints, a preliminary schedule is proposed below.

EDITOR'S NOTE: I'VE OMITTED THE PRELINARY SCHEDULE FOR BREVITY, BUT IT WAS SIMILAR IN SCOPE AND DETAIL TO THE ONE PRINTED EARLIER, EXCEPT THAT SPECIFIC TALKS AT SPECIFIC STOPS WERE NOT ENUMERATED.

Budget

The budget included below assumes 30 field trip participants (similar to the number of participants in the Yellowstone field trip), and also provides money for a scouting trip by Laszlo Keszthelyi prior to the main trip. The trip as designed starts in Portland, Oregon and ends in Spokane, Washington, and provides for airfare between the two endpoints.

EDITOR'S NOTE: I REPLACED THE ORIGINAL, PRELIMINARY BUDGET WITH THE ACTUAL BUDGET FOR THE TRIP FOR ACCURACY AND TRANSPARENCY (I.E., TO SHOW WE'RE NOT ENRONNING THE MONEY FROM THE DEPARTMENT AND THOSE PEOPLE WHO ARE PAYING OUT OF POCKET). NOTE THAT THE ORIGINAL PROPOSAL WAS FOR 30 PEOPLE AND $15,000, OR $500 A PERSON, AND THAT WE ARE RIGHT ON THAT VALUE FOR THE ACTUAL BUDGET.

Budget Item	Cost (per)	Quantity	Cost (total)	Funding Source
Airline Flights	$244.48	28	$5867.52	LPL
Change Fees	$100	4	$400	LPL
15-Passenger Vans	$562.48	3	$1687.44	LPL/IND
Vans — Mileage	$0.25	3 × 800miles	$600.00	LPL/IND
Gas for Vans	$1.50/gallon	$3 \times \frac{1800\text{mi}}{12mpg}$	$675.00	LPL/IND
Pickup Truck (∞ miles)	$405.00	1	$405.00	LPL/IND
Gas for Truck	$1.50/gallon	$\frac{1800\text{mi}}{15mpg}$	$180.00	LPL/IND
Hotels	$75.79	34	$2580.26	LPL/IND
MSH Fees	$3	26	$78	LPL/IND
Recon	$43.33	1	$1300.00	LPL/IND
Total (LPL)	$491.90	28	$13772.20	LPL
Total (IND)	$220.76	6	$1324.54	IND

Itinerary

Friday, 20 September

5:00 am	Meet in front of the Delta ticket counter at Tucson International Airport.
6:44 am	Depart Tucson on Delta flight DL3989Q.
9:30 am	Arrive at Salt Lake City International Airport.
11:10 am	Depart Salt Lake City on Delta Flight DL1063Q.
11:55 am	Arrive at Portland International Airport & have lunch.
1:30 pm	Rent vehicles, then drive north to Kelso.
2:30 pm	Arrive in Kelso and check in to Motel 6.
	Spend the rest of the afternoon buying groceries and visiting the Mount St. Helens visitor's center (across the street from Motel 6).

Saturday, 21 September

8:00 am	Meet local experts from the Cascades Volcano Observatory and depart for Mount St. Helens.
9:00 am	Arrive at the Forest Learning Center.
	Presentations:
	Rachel Mastrapa — Cascades volcanism
	Jason Barnes — local ecology since the 1980 Mount St. Helens eruption
	Mike Bland — lahars
10:15 am	Depart the Forest Learning Center.
10:45 am	Arrive at the Johnston Ridge Observatory.
	Presentations:
	Rachel Mastrapa — seismology of the 1980 eruption
	Jim Richardson — debris flows
	John Weirich — the directed blast
	Dave O'Brien — physics of pyroclastic eruptions
	Mandy Proctor — physics of Plinian plumes and 1980 ash deposition
12:30 pm	Have lunch, purchase passes, and look around the visitor center, then watch the next showing of the visitor center's movie about the 1980 eruption.
	Presentations:
	Pete Lanagan — 1980 gas emissions and climate impact
2:30 pm	Drive to the Hummocks Trail where we will hike 2.4 miles.
	Presentation:
	Matt Pasek — Mount St. Helens magma chemistry and andesitic volcanism
4:00 pm	Drive back to Kelso.
	Optional stop: the sediment dam

Sunday, 22 September

7:00 am	Leave Kelso.
9:00 am	Arrive at the Bonneville Dam and meet Jim O'Connor's group.
	Presentations:
	Sally House — Bonneville landslide
	Ralph Lorenz — hydroelectric power, dams and salmon
10:45 am	Leave the Bonneville Dam.
	CB Presentation:
	Ross Beyer — jointing in basalts
11:45 am	Lunch at rest stop (mile post 72 or 73).
12:30 am	Leave rest stop.
12:45 pm	Arrive at The Dalles.
	Presentations:
	Moses Milazzo (a.k.a. Laszlo Keszthelyi) — pillow basalts
	Jani Radebaugh — palagonites on Earth and Mars
1:30 pm	Leave The Dalles.
2:00 pm	Stop at Maryhill
	Presentation:
	Jim O'Connor — overview of the Missoula Flood
2:30 pm	Leave Maryhill
2:45 pm	Arrive at Rock Creek Rd. (mile post 120).
	Presentations:
	Fred Cielsa (a.k.a. Laszlo Keszthelyi) — CRB eruption duration and solar system analogs
	Matt Chamberlain — Other terrestrial flood basalts
	Adam Showman — atmospheric impact of flood basalt eruptions
4:30 pm	Leave Rock Creek Road stop.
	CB Presentation:
	Gwen Bart — the Yellowstone plume
7:00 pm	Arrive at Sand Station Recreation Center for a view of the Walulla Gap (mile post 194).
	Presentation:
	Hirdy Miyamoto — modeling of floods
7:30 pm	Leave Sand Station.
8:10 pm	Arrive in Kennewick and check in to Super 8.

Monday, 23 September

8:00 am	Meet up with Steve Reidel and leave Kennewick.
9:00 am	Arrive at Rattlesnake Mountain Observatory.
	Presentations:
	Windy Jaeger — structure and origin of the Yakima fold belt
	Zibi Turtle — the Yakima folds as an analog for wrinkle ridges
	Joe Plassmann — history of the Hanford Nuclear Reservation
11:00 am	Leave Rattlesnake Mountain.
12:00 am	Lunch at Umtanum Ridge.
1:00 pm	Leave Umtanum Ridge.
1:40 pm	Arrive at the Sentinel Bluffs.
	Discussion:
	led by **Steve Reidel**.
2:10 pm	Leave Sentinel Bluffs
2:30 pm	Arrive at Ginkgo State Park.
	Presentation:
	Abby Wasserman — petrified wood
3:30 pm	Leave Ginkgo State Park
	Optional stop: lava and lake sediments roadcut
	Optional stop: peperite roadcut
3:40 pm	Arrive at Frenchman Spring Coulee.
	Presentation:
	Matt Tiscareno — scabland formation and wake-vortex scouring
4:40 pm	Leave Frenchman Spring Coulee.
	Optional stop: flood deposits around George
5:15 pm	Arrive at Moses Lake and check in to Motel 6.

Tuesday, 24 September

8:00 am	Leave Moses Lake.
9:00 am	Arrive at West Bar overlook (between mile posts 21 and 22).
	Presentations:
	Adina Alpert — giant ripples
10:00 am	Leave West Bar.
10:30 am	Stop in Moses Coulee.
	Presentation:
	Brandon Preblich — Hanging valleys.
11:00 am	Resume driving along Moses Coulee.
12:00	Lunch at Armour Draw and examine rubbly pahoehoe flow.
1:00 pm	Leave Armour Draw.
1:15 pm	Arrive at Jameson Lake.
	Presentation:
	Curtis Cooper — Pleistocene climate and glacial history

2:00 pm	Leave Jameson Lake.
2:45 pm	Arrive at Dry Falls.
	Presentations:
	Jonathan Fortney — geology and history of Dry Falls
	Abby Wasserman — rhinoceros mold
4:00 pm	Leave Dry Falls.
4:30 pm	Arrive at Soap Lake.
	Presentation:
	Oleg Amramov — extremophiles in Soap Lake and implications for life on Mars
5:00 pm	Leave Soap Lake.
5:15 pm	Arrive at the Ephrata boulder.
	Presentations:
	Adina Alpert — the Ephrata gravel fan/MPF landing site
6:00 pm	Leave boulder stop.
6:30 pm	Arrive in Moses Lake.

Wednesday, 25 September

7:00 am	Depart Moses Lake.
7:45 am	Examine scabland features in Crab Creek.
	Presentation:
	Jason Barnes — loess deposits
8:30 am	Continue along Crab Creek.
9:00 am	Arrive at Amphitheater Crater.
	Presentations:
	Devon Burr and **Windy Jaeger** — ring dikes
10:00 am	Depart Amphitheater Crater.
11:30 am	Arrive at Marengo Siding. Take lunch on 2 mile hike.
	Presentation:
	Jay Melosh — debate over numerous, smaller floods or fewer, larger floods from glacial Lake Missoula.
1:30 pm	Depart Marengo Siding.
	CB Presentation:
	Jay Melosh — Mima silt mounds
2:00 pm	Stop to see Loess Hills.
	Presentation:
	Devon Burr — formation of streamlined landforms
3:00 pm	Continue along McCall Road.
4:30 pm	Williams Lake Gravel Pit.
5:00 pm	Continue along Martin Road.
5:15 pm	Arrive at "Hole in the Ground"
5:45 pm	Depart "Hole in the Ground"
6:15 pm	Arrive Malden
	Optional stop: Malden gravel pit

7:30 pm	Arrive in Spokane, check-in at Budget Inn.

Thursday, 26 September

	Optional stop: Golf course in Hangman Creek.
12:00	Lunch
1:30 pm	Arrive at Spokane International Airport.
4:25 pm	Depart Spokane on Delta flight DL3944K
6:53 pm	Arrive at Salt Lake City International Airport
8:10 pm	Depart Salt Lake City on Delta flight DL3959K
8:52 pm	Arrive in Tucson

Driving Directions

Day 1: Friday, September 20

- *Portland (airport) — Kelso (Motel 6)* [1 hour]
  - ▶ left exit onto **I-205 N**
  - ▶ exit in ∼ 12 miles onto **I-5 N**
  - ▶ **exit 39**, then turn right (E) onto Allen St.
    - for **Motel 6**, take 1st left onto Minor Rd.
      — OR —
    - for **Safeway**, take 1st right onto Kelso Dr.

Day 2: Saturday, September 21

- *Kelso — Forest Center* [1 hour]
  - ▶ N onto **I-5**
  - ▶ **exit 49** at Castle Rock onto **S.R. 504 E**
  - ▶ **Elk Rock Forest Learning Center**o on right at **milepost 33**
- *Forest Center — Johnston Ridge Visitor Center* [30 minutes]
  - ▶ continue east on **S.R. 504**
  - ▶ do **not** go to Coldwater Ridge Visitor Center
  - ▶ parking lot at **milepost 52**
- *JRVC — Hummocks Trail* [15 minutes]
  - ▶ drive back **7 miles** on S.R. 504, parking lot on the left
- *Hummocks Trail — Sediment Dam* [1 hour]
  - ▶ continue west on S.R. 504 to **milepost 21**, take road to the left, park
- *Sediment Dam — Kelso* [30 minutes]
  - ▶ return to **S.R. 504**
  - ▶ turn left (west) and return to **I-5**
  - ▶ **exit 39** at Kelso, go under I-5 to return to Motel 6

Day 3: Sunday, September 22

- *Kelso — Bonneville Dam* [1hour, 30 minutes]
  - ▶ S on **I-5**
  - ▶ **exit 7** onto **I-205 S**
  - ▶ **exit 22** onto **I-84 E**
  - ▶ exit **milepost 40**, pass under interstate
  - ▶ stop at security checkpoint, proceed to dam (**not** fish hatchery)
  - ▶ **park** in main lot
- *Bonneville Dam — Lunch Stop* [45 minutes]

- ▶ continuing east on I-84, exit at **milepost 72.9**

- *Lunch — The Dalles* [20 minutes]
  - ▶ continue east on I-84 to **exit 87** (east side of The Dalles)
  - ▶ turn right, **park in pullout** on right
- *The Dalles — Maryhill overlook* [30 minutes]
  - ▶ return to **I-84 E**
  - ▶ take **Highway 97 N** at Biggs, **exit 104**
  - ▶ cross the Columbia River
  - ▶ turn right onto **S.R. 14 E** (to **Kennewick**)
  - ▶ turn right in ∼ 1 **mile** on road to "Maryhill Stonehenge"
  - ▶ drive ∼ 1 mile to **parking lot** and overlook
- *Maryhill — Rock Creek Road* [20 minutes]
  - ▶ return to **S.R. 14**, turn right
  - ▶ drive ∼ 15 miles to **milepost 120**, park on **left**
- *Rock Creek Road — Sand Point Recreational Area* [2 hours and 30 minutes]
  - ▶ continue ∼ 60 **miles** east on S.R. 14 to **I-82 S**
  - ▶ cross Columbia River to **Umatilla**
  - ▶ take **S.R. 730 E** in Umatilla
  - ▶ continue east ∼ 15 miles to **milepost 194**, east on the left into Sand Station Recreation Center
- *Sand Point — Kennewick* [40 minutes]
  - ▶ continue ∼ 12 miles east on 730 to **Wallula Junction**
  - ▶ turn left onto **U.S. Route 12 (to Pasco)**
  - ▶ continue west ∼ 17 miles to **Route 240 (Kennewick)** (exit 12A?)
  - ▶ exit **Columbia Center Boulevard**

Day 4: Monday, September 23

- *Kennewick — Rattlesnake Mountain Observatory* [1 hour]
  - ▶ W on **Highway 240** ∼ 10 **miles** to Highway 225
  - ▶ **Follow** Steve Reidel through gates to Observatory
- *Rattlesnake Mountain — Umtanum Ridge view* [1 hour]
  - ▶ return to **Highway 240**, turn left (northwest)
  - ▶ Highway 240 W becomes Highway **24 N** in about 20 miles
  - ▶ cross Columbia River and turn left onto **Highway 243**
  - ▶ pull off in about **3 miles**
- *Umtanum Ridge — Sentinel Bluffs* [15 minutes]
  - ▶ continue west on Highway 243 for about **15 miles** (note: expect to stop in **Desert Aire** gas station for rest stop)
- *Sentinel Bluffs — Gingko State Park* [20 minutes]
  - ▶ continue ∼ 10 miles north on 243, join **Highway 26**
  - ▶ exit onto I-90, **cross Columbia River, exit 136**
  - ▶ wind past Rock Shop to **State Park** visitor center and park
- *Gingko State Park — Optional road cut* [10 minutes]

- ▶ head toward **boat launch**
- ▶ turn left **(uphill)** instead of going down to the river
- ▶ park in **about 0.5 miles**

- *Gingko State Park — Frenchman Spring Coulee stops* [15 minutes]
  - ▶ wind back to **I-90 E**
  - ▶ **cross** Columbia River
  - ▶ **exit** on Silica Road in **7 miles**
  - ▶ *Optional stop* **ON EXIT RAMP**
  - ▶ turn left in $\sim$ 1 mile onto **Silica Road**
  - ▶ stop at pullout in $\sim$ 0.6 **miles**
  - ▶ continue to parking area another **0.5 miles** down (at signs for restricted entrance)
- *Frenchman Spring Coulee — Optional stops at George* [10 minutes]
  - ▶ follow Silica Road back to **I-90 E**
  - ▶ exit at **George** in 4 miles
  - ▶ **follow** Vic!
- *George — Moses Lake Motel 6* [30 minutes]
  - ▶ return to **I-90 E**
  - ▶ proceed **27 miles** to Moses Lake
  - ▶ **exit 176**, go under insterstate, Motel 6 on the right

Day 5: Tuesday, September 24

- *Moses Lake — West Bark overlook* [1 hour]
  - ▶ **left** out of Motel 6
  - ▶ right onto **I-90 W**
  - ▶ **exit 151** onto **S.R. 281 N** in 24 miles
  - ▶ left in **Quincy** onto **S.R. 28 W** in 9 miles
  - ▶ right onto **Baird Springs Rd.**
  - ▶ pull off on south side of road **between mileposts 21 and 22** just before the guard rail starts
- *West Bar overlook — Moses Coulee stop* [20 minutes]
  - ▶ continue **7 miles, right** turn onto Palisades Rd. (just after power lines; mile post 15 or 16)
  - ▶ stop $\sim$ 5 miles north along the road
- *Moses Coulee — Armour Draw* [1 hour]
  - ▶ **wind along** Moses Coulee, end up headed north on Moses Coulee Rd.
  - ▶ turn **left** (W) onto **U.S. Route 2**
  - ▶ pull off on right in $<$ 1 **mile**
- *Armour Draw - Jameson Lake* [15 minutes]
  - ▶ **U-turn** and head E on U.S. Route 2
  - ▶ left onto **Jameson Lake Rd.**
  - ▶ stop **about 4 miles** in
- *Jameson Lake — Dry Falls* [45 minutes]
  - ▶ return to U.S. **Route 2 E**
  - ▶ turn right onto **S.R. 17 S** in about 15 miles
  - ▶ turn **left** into Dry Falls Interpretive Center parking lot in about **2 miles**

- *Dry Falls — Soap Lake* [30 minutes]
  - ▶ continue S on **S.R. 17** noting an eroded monocline
  - ▶ pull off in ∼ 17 miles, just **before the town** of Soap Lake
- *Soap Lake — Ephrata Fan boulder stop* [15 minutes]
  - ▶ drive through Soap Lake, **staying on S.R. 17**
  - ▶ **right** turn ∼ 4 **miles** (to Rocky Ford Creek)
  - ▶ drive ∼ 1 **mile** to boulder (on left)
- *Boulder — Moses Lake* [30 minutes]
  - ▶ **U-turn** back to S.R. 17
  - ▶ **stay on** S.R. 17 until Moses Lake
  - ▶ exit (right) onto **S.R. 171**
  - ▶ follow S.R. 171 **through town** and turn left into Motel 6

Day 6: Wednesday, September 25

- *Moses Lake — Crab Creek* [45 minutes]
  - ▶ turn **right** onto S.R. 171
  - ▶ turn left onto **J NE in town**
  - ▶ go ∼ 20 **miles** north on J NE
  - ▶ turn **right onto S.R. 28** E to Odessa
  - ▶ *several possible stops* in next 5-10 miles
- *Crab Creek — Ring dikes* [45 minutes]
  - ▶ **continue** on S.R. 28 to the east (20-30 miles)
  - ▶ at **Odessa**, turn **left** onto S.R. 21
  - ▶ after **6 miles** stop in pull out on right for Amphitheater Crater
- *Ring dikes — Marengo Siding* [1 hour]
  - ▶ turn left **(south)** down S.R. 21
  - ▶ drive **23 miles** to I-90
  - ▶ enter **I-90 E** and drive 14 miles to **Ritzville**
  - ▶ **exit 221**, then right turn N (left) note: expect rest stop in Ritzville
  - ▶ turn E **(right)** onto Wellsandt Rd (< 0.5 miles)
  - ▶ go ∼ 5 **miles**, turn S **(right)** onto Hills Rd. (which turns into Urquhart Rd.)
  - ▶ go ∼ 4 **miles**, turn S **(right)** onto Marengo Rd.
  - ▶ cross a **railroad track**, turn right onto Cow Creek Rd.
  - ▶ **Stop** on abandoned railroad grade
- *Marengo — Loess Hills* [30 minutes]
  - ▶ **backtrack** to Urquhart Rd., turn E (right)
  - ▶ Loess hills **5 miles** on left
- *Loess Hills — Williams Lake Gravel Pit* [1 hour, 30 minutes]
  - ▶ continue ∼ 20 **miles** on McCall/Lamont Rd. (same as Urquhart Rd.)
  - ▶ **left** ointo **S.R. 23 N**
  - ▶ drive ∼ 8 **miles** to Sprague
  - ▶ right at **Chevron** station
  - ▶ **left** at Colfax Rd.

- ▶ another **right, left** sequence
- ▶ **right** on First Rd.
- ▶ drive ~ 2.5 **miles**
- ▶ **right** on the Williams Lake Rd. (turns into Martin Dr.)
- ▶ drive ~ 12 **miles** (restrooms at Martin Rd Trailhead)
- ▶ **right** on Mullinix Rd. (after the Marsh, Marsh, Martin house)
- ▶ drive < 0.5 **miles**
- ▶ stop at gravel **pit on left**

- *Williams Lake Gravel Pit — Hole in the Ground* [15 minutes]
  - ▶ continue ~ 2 **miles** on Mullinix Rd.
  - ▶ **left** on Belsby Rd.
  - ▶ enter Hole in the Ground in about **5 miles**
- *Hole in the Ground — Malden Pit* [30 minutes]
  - ▶ **right at** Y-junction after "Hole in the Ground"
  - ▶ drive ~ 4 **miles**
  - ▶ **left** at Stephen Rd.
  - ▶ drive ~ 1 **mile**
  - ▶ **left** at Pine City - Malden Rd.
  - ▶ turn **right** to stay on Pine City - Malden Rd.. (not Pine City North Rd.)
  - ▶ drive ~ 4 **miles**
  - ▶ **left after** 1st **bridge** beyond Malden
  - ▶ drive ~ 1 **mile**
  - ▶ gravel **pit on right**
- *Malden Pit — Spokane* [1 hour, 15 minutes]
  - ▶ **return** to Pine City - Malden Rd.
  - ▶ turn **left** (east) drive ~ 5 **miles**
  - ▶ **left** onto Rosalia Rd.
  - ▶ drive through town (~ 2 **miles**)
  - ▶ get onto **195 N** to Spokane
  - ▶ drive ~ 30 **miles** to I-90
  - ▶ get on **I-90 east**
  - ▶ take **exit 281** (Newport/Colville North)
  - ▶ turn **left** off the off ramp, heading north on Division **two blocks** to Second
  - ▶ Turn **left** on Second, continue for **one block**
  - ▶ turn **left**, (onto Brown) go **two blocks** further, under the freeway, follow curve onto fourth, follow for **two more blocks**
  - ▶ **Hotel** is on the south side of the freeway.

Participants

Drivers: Barnes; Beyer; Radebaugh, Kezstheyi, and Jaeger; Lanagan

⊕ Abromov, Oleg
⊕ Alpert, Adina
★ Baker, Vic
⊕ Barnes, Jason
⊕ Bart, Gwen
⊕ Beyer, Ross
⊕ Bland, Michael
⊕ Burr, Devon
⊕ Chamberlain, Matt
⊘ Ciesla, Fred
⊕ Cooper, Curtis
⊕ Fortney, Jonathan
⊕ House, Sally
⊕ Jaeger, Windy
★ Keszthelyi, Laszlo
⊕ Lanagan, Peter
◯ Lorenz, Ralph
⊕ Mastrapa, Rachel
★ McEwen, Alfred
◯ Melosh, Jay
⊘ Milazzo, Moses
◯ Miyamoto, Dr.
⊕ O'Brien, Dave
⊕ Pasek, Matt
◯ Plassman, Joe
⊕ Preblich, Brandon
⊕ Proctor, Mandy
⊕ Radebaugh, Jani
⊕ Richardson, Jim
◯ Showman, Adam
⊕ Tiscareno, Matt
◯ Turtle, Zibi
⊕ Wasserman, Abigail
⊕ Weirich, John

Key: Earths (⊕) are registered students, gas giants (◯) are those with outside support, and stars (★) are trip leaders, and moons (⊘) are students that dropped out in the last few days.

This page intentionally blank.

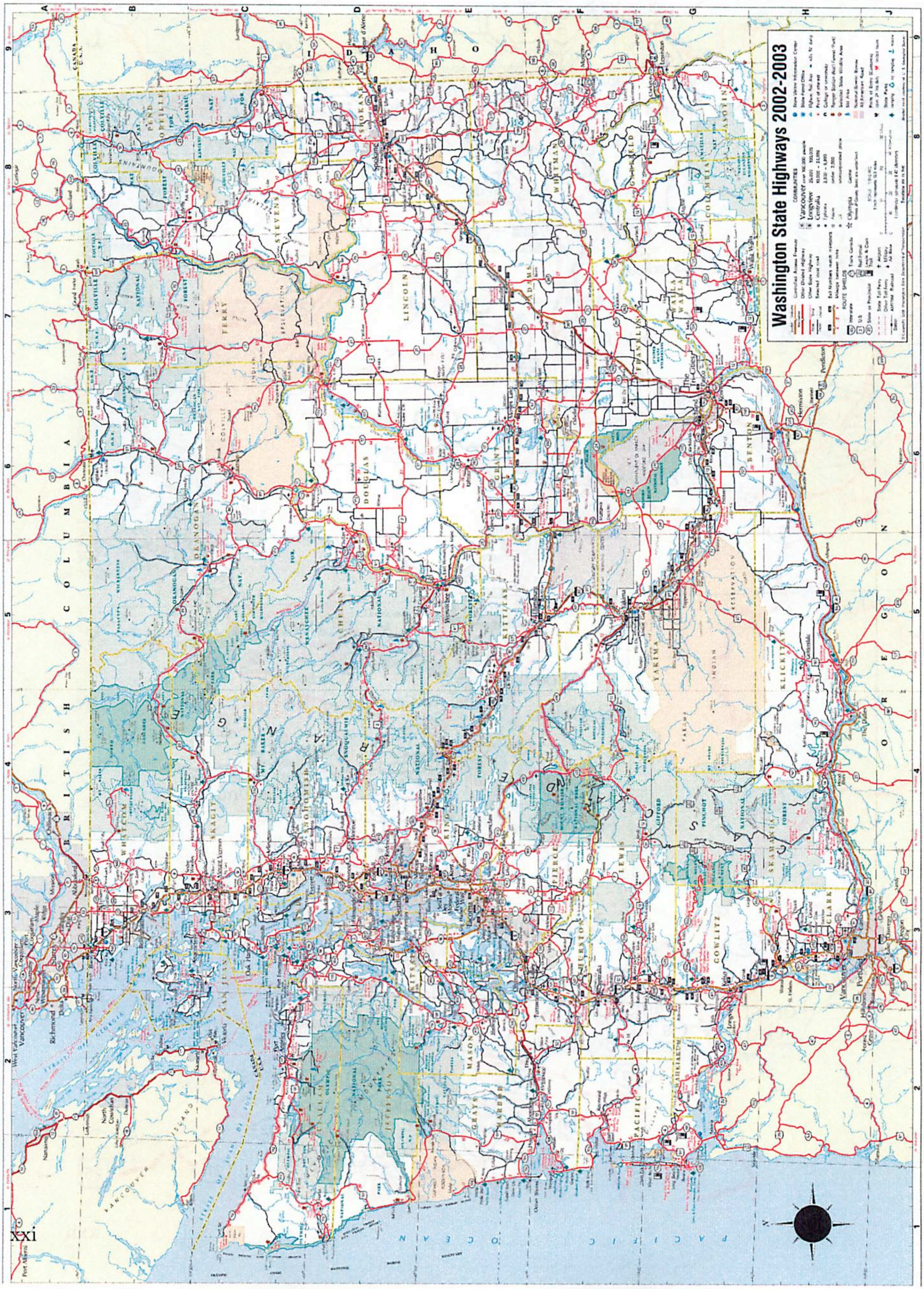
Washington State Highways 2002-2003

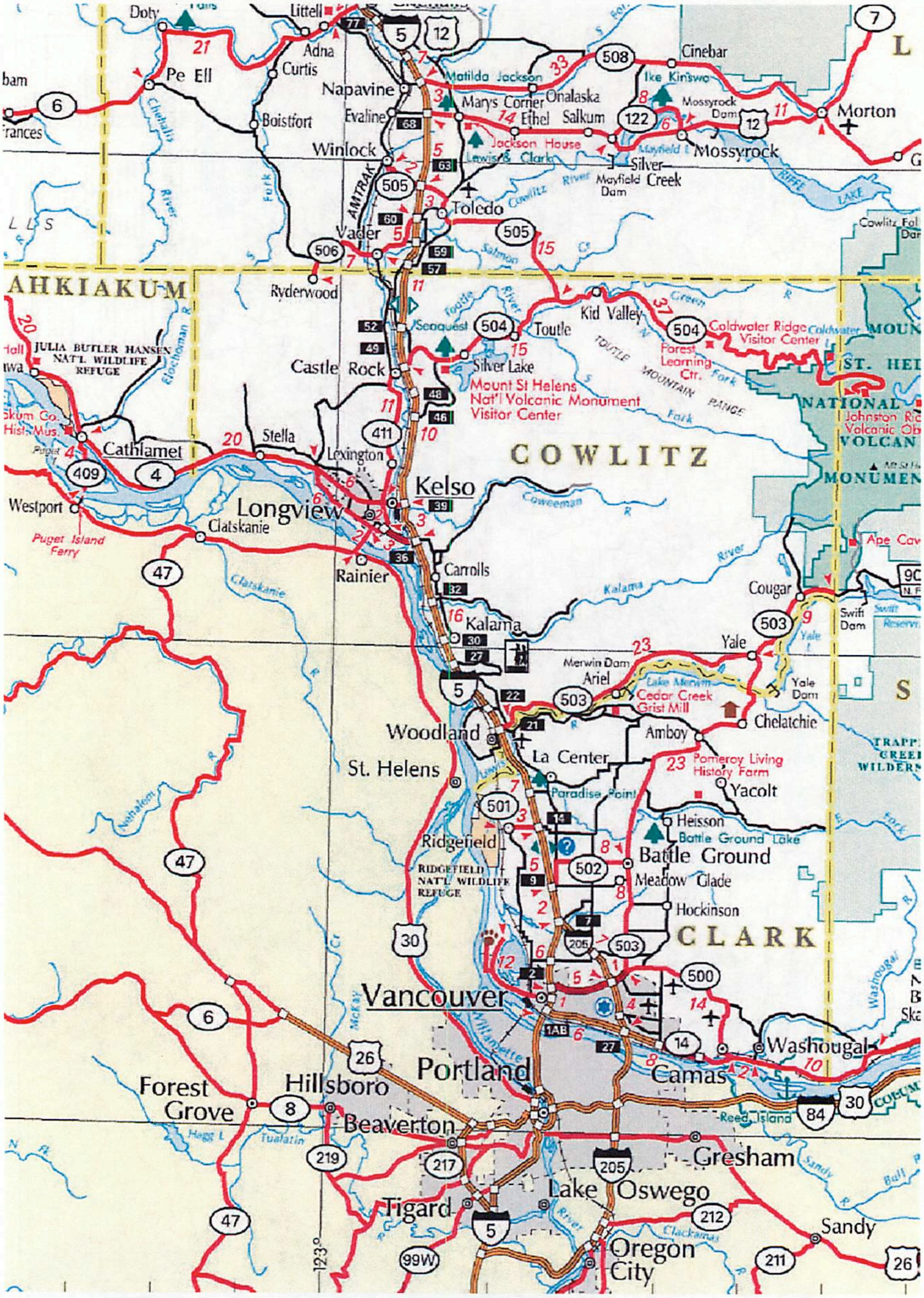
Doty
Pe Ell
Littell
Adna
Curtis
Napavine
Boistfort
Evaline
Winlock
Matilda Jackson
Marys Corner
Onalaska
Ethel
Salkum
Cinebar
Ike Kinswa
Mossyrock
Morton
Jackson House
Lewis & Clark
Silver Creek
Mayfield Dam
Toledo
Vader
Ryderwood
WAHKIAKUM
JULIA BUTLER HANSEN NAT'L WILDLIFE REFUGE
Cathlamet
Stella
Seaquest
Toutle
Kid Valley
Silver Lake
Castle Rock
Coldwater Ridge Visitor Center
Forest Learning Ctr.
Mount St Helens Nat'l Volcanic Monument Visitor Center
TOUTLE MOUNTAIN RANGE
Lexington
Kelso
COWLITZ
Longview
Westport
Clatskanie
Puget Island Ferry
Rainier
Carrolls
Kalama
Cougar
Yale
Swift Dam
Merwin Dam
Ariel
Cedar Creek Grist Mill
Yale Dam
Woodland
Chelatchie
Amboy
La Center
St. Helens
Pomeroy Living History Farm
Yacolt
Paradise Point
Ridgefield
RIDGEFIELD NAT'L WILDLIFE REFUGE
Heisson
Battle Ground Lake
Battle Ground
Meadow Glade
Hockinson
CLARK
Vancouver
Washougal
Portland
Camas
Forest Grove
Hillsboro
Beaverton
Reed Island
Gresham
Lake Oswego
Tigard
Sandy
Oregon City

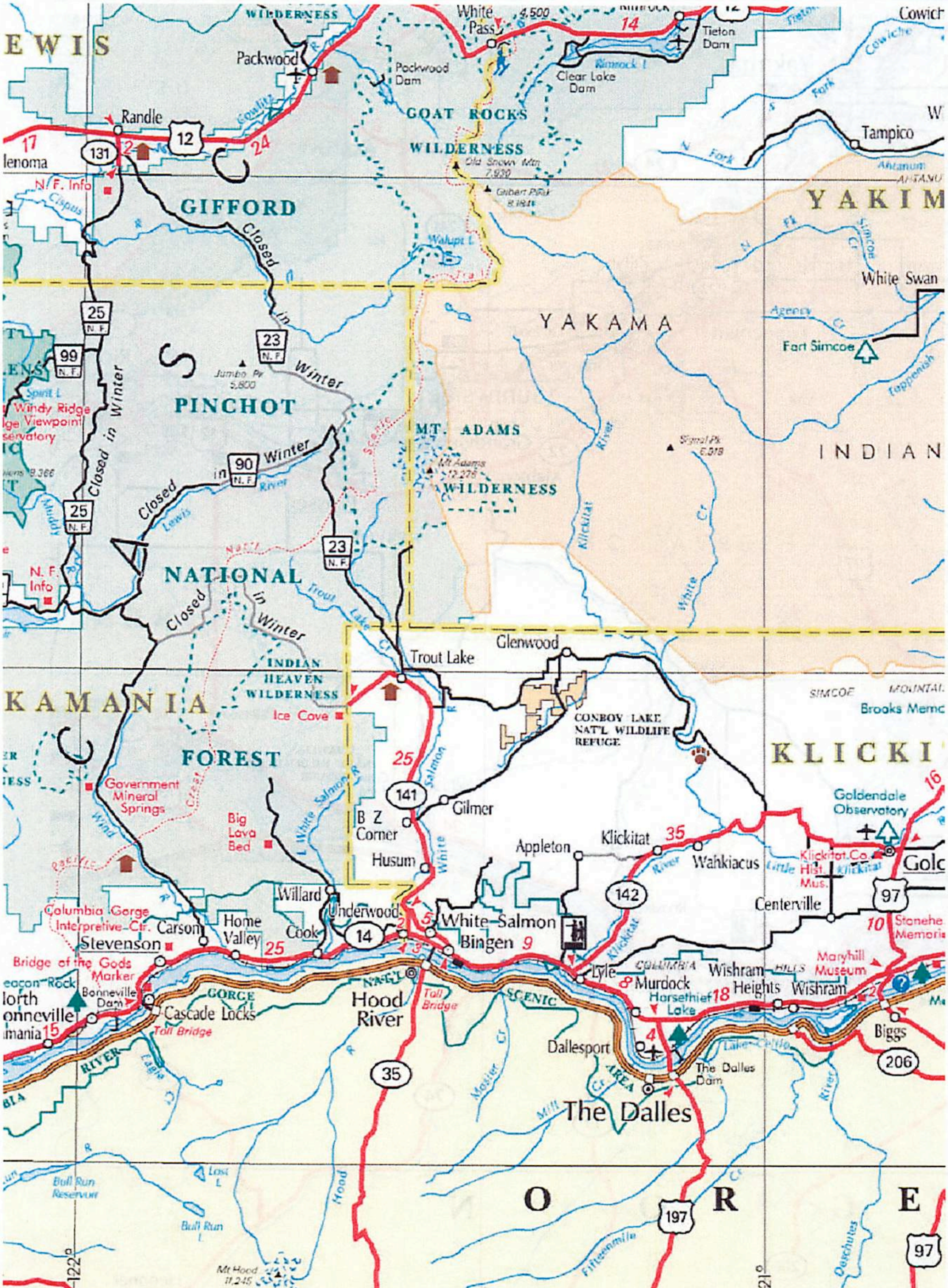

WILDERNESS
White Pass
4,500
14
Tieton Dam
Cowich
EWIS
Packwood
Pockwood Dam
Rimrock L
Clear Lake Dam
GOAT ROCKS
WILDERNESS
Old Snowy Mtn 7,930
Gilbert Peak 8,184
Tampico
Randle
12
17
131
24
lenoma
N. F. Info
Cispus
GIFFORD
Closed in Winter
Walupt L
YAKIM
White Swan
25 N.F.
23 N.F.
Jumbo Pk 5,800
99 N.F.
Spirit L
Windy Ridge Viewpoint
Observatory
PINCHOT
YAKAMA
Agency Cr
Fort Simcoe
Toppenish
MT. ADAMS
Mt Adams 12,276
WILDERNESS
Signal Pk 5,918
INDIAN
Closed in Winter
90 N.F.
Lewis River
25 N.F.
Klickitat River
White Cr
NATIONAL
23 N.F.
N. F. Info
Trout Lake Cr
Closed in Winter
Trout Lake
Glenwood
INDIAN HEAVEN WILDERNESS
KAMANIA
Ice Cove
SIMCOE MOUNTAI
Brooks Memo
CONBOY LAKE NAT'L WILDLIFE REFUGE
KLICKI
FOREST
25
Salmon
Government Mineral Springs
Wind
Crest
141
Gilmer
Goldendale Observatory
16
Big Lava Bed
L White Salmon R
B Z Corner
Appleton
Klickitat
35
Wahkiacus
Husum
White
Klickitat Co. Hist. Mus.
Gold
Willard
Underwood
142
Centerville
97
Columbia Gorge Interpretive Ctr.
Carson
Home Valley
Cook
14
White Salmon
Bingen
9
10
Stonehenge Memorial
Stevenson
25
Bridge of the Gods Marker
Lyle
COLUMBIA HILLS
Wishram Heights
Wishram
Maryhill Museum
Beacon Rock
North Bonneville
Skamania
15
Bonneville Dam
Cascade Locks
Toll Bridge
GORGE
NAT'L
Hood River
Toll Bridge
SCENIC
8 Murdock
Horsethief Lake
18
Biggs
4
Lake Celilo
Dallesport
The Dalles Dam
206
RIVER
AREA
35
Mosier Cr
Mill Cr
The Dalles
Bull Run Reservoir
Lost L
Hood
Bull Run L
O
R
E
197
Fifteenmile
Deschutes
97
Mt Hood 11,245
122°
121°

Yakima
Moxee
Union Gap
Ahtanum
Parker
Wapato
Sawyer
Buena
Zillah
Brownstown
Harrah
Yakama Nation Museum
Toppenish
Outlook
Granger
Sunnyside
Grandview
Mabton
Satus
TOPPENISH NAT'L WILDLIFE REFUGE
Priest Rapids Dam
U. S. DEPARTMENT OF ENERGY HANFORD SITE
HANFORD REACH NATIONAL MONUMENT
Plant 2 Visitor C
Test Facility Visitor Ce
West Richland
Benton City
Kiona
Prosser
Benton Co. Hist. Museum
HEAVEN
HILLS
RATTLESNAKE
RESERVATION
HORSE
BENT
Bickleton
Satus Pass 3,107
Paterson
Plymouth
UMATILLA NAT'L WILDLIFE REFUGE
Crow Butte
Alderdale
Umatill
Boardman
Roosevelt
Arlington
John Day Dam
Columbia
River
G O N
Heppner
120°


Kahlotus
Lyons Ferry
Little Goose Dam
Basin City
Mesa
FRANKLIN
Lower Monumental Dam
Starbuck
JUNIPER DUNES WILDERNESS
Eltopia
Snake
Sheffler
Clyde
WALLA WALLA
The Tri-Cities
Fishhook Park
Eureka
Prescott
Dayton Hist. Depot
Richland
Pasco
Ice Harbor Dam
Waitsburg
Lewis & Trail
Kennewick
McNARY NAT'L WILDLIFE REFUGE
Touchet
Dixie
Fort Walla Walla (US Army) & Museum
Fort Walla Walla Monument (HBC)
Wallula
College Place
Walla Walla Col
Lowden
Walla Walla Comm Col
Whitman Col
Walla Walla
Kooskooskie
WALLULA GAP
WHITMAN MISSION NAT'L HIST. SITE
to Milton-Freewater
AMTRAK
McNary Dam
Lake Wallula
Hermiston
Stanfield
Pendleton
Umatilla River
Butter Cr
Washington Sta
Divided
Undivided
Interchanges
Controlled Access Freeway
Other Divided Highway
Other State Highway
Paved
Gravel
Selected local road
Unpaved
Exit Numbers match mileposts
Mileage between ticks
ROUTE SHIELDS
Interstate
Trans Canada
U.S.
Natl Forest
State or Provincial
Lewis & Clark Trail
State Toll Ferry
Airport
Other Toll Ferry
Military Air Base
AMTRAK Railroad
Station
© Copyright 2002 Washington State Department of Transportation

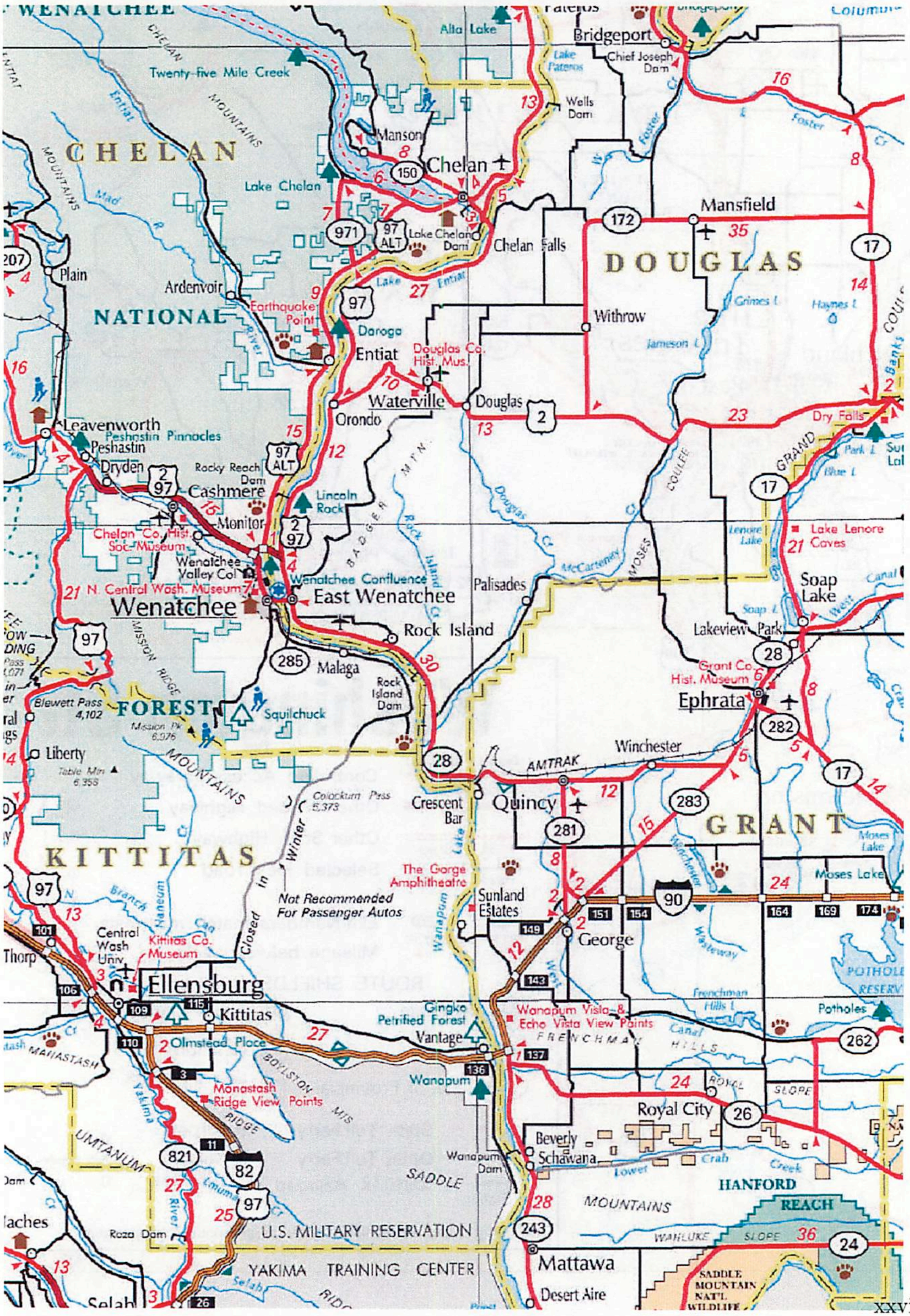
WENATCHEE
CHELAN
NATIONAL
FOREST
KITTITAS
DOUGLAS
GRANT
CHELAN MOUNTAINS
Twenty-five Mile Creek
Alta Lake
Bridgeport
Chief Joseph Dam
Lake Pateros
Wells Dam
Manson
Chelan
Lake Chelan
Lake Chelan Dam
Chelan Falls
Mansfield
Plain
Ardenvoir
Earthquake Point
Daroga
Entiat
Douglas Co. Hist. Mus.
Waterville
Douglas
Withrow
Orondo
Leavenworth
Peshastin Pinnacles
Peshastin
Dryden
Cashmere
Rocky Reach Dam
Lincoln Rock
Monitor
Chelan Co. Hist. Soc. Museum
Wenatchee Valley Col
N. Central Wash. Museum
Wenatchee
Wenatchee Confluence
East Wenatchee
Palisades
Rock Island
Malaga
Rock Island Dam
Dry Falls
Lake Lenore Caves
Soap Lake
Lakeview Park
Grant Co. Hist. Museum
Ephrata
Winchester
Blewett Pass 4,102
Mission Pk 6,976
Squilchuck
Liberty
Table Mtn 6,358
Colockum Pass 5,373
Closed in Winter
Not Recommended For Passenger Autos
MISSION RIDGE
MOUNTAINS
Crescent Bar
Quincy
AMTRAK
The Gorge Amphitheatre
Sunland Estates
George
Moses Lake
Central Wash Univ.
Kittitas Co. Museum
Thorp
Ellensburg
Kittitas
Gingko Petrified Forest
Vantage
Wanapum Vista & Echo Vista View Points
FRENCHMAN HILLS
Potholes
Olmstead Place
Monastash Ridge View Points
MANASTASH
BOYLSTON MTS
Wanapum
Royal City
ROYAL SLOPE
Beverly
Schawana
Wanapum Dam
UMTANUM RIDGE
SADDLE MOUNTAINS
U.S. MILITARY RESERVATION
YAKIMA TRAINING CENTER
Roza Dam
Naches
Selah
Mattawa
Desert Aire
HANFORD REACH
WAHLUKE SLOPE
SADDLE MOUNTAIN NAT'L WILDLIFE
Lower Crab Creek
POTHOLES RESERVOIR

Elmer City
Crown Point
Coulee Dam
Colville Cultural Center
Keller Ferry (Free)
Grand Coulee
Grand Coulee Dam
Electric City
LAKE
Franklin
Steamboat Rock
Lake
SPOKANE
INDIA
RESERVATION
Fort Spokane
Porcupine Bay
Wellpinit
Seven Bays
Lincoln
Little Falls Dam
Spokane
Hawk
Wilbur
Creston
Hartline
Almira
Davenport
Reardan
Lincoln Co. Hist. Museum
Dry Falls Dam
Coulee City
LINCOLN
Twin Lakes
AMTRAK
Summer Falls
Billy Clapp L
Harrington
Coffeepot L
Rock Cr
Pinto Dam
Wilson Creek
Krupp (Marlin P.O.)
Stratford
Pacific L
Duck Cr
Lamona
Mohler
Crab
Irby
Odessa
Coal Cr
Sylvan L
Creek
Sprague
Odessa Hist. Museum
Sprague L
Bunting L
Low Canal
Batum
Burroughs Wheatland Museum
Ritzville
Lamont
Big Bend Comm Col
Wheeler
Moses Lake
ADAMS
Cow Cr
O'Sullivan Dam
Warden
Ralston
Soda L
Goose L
Lind
East
Benge
COLUMBIA NTL WILDLIFE REFUGE
Cunningham
Othello
Hatton
Canal
Washtucna
Hooper
Scooteney Reservoir
Eagle Lakes
Connell
Palouse Falls
Alkali

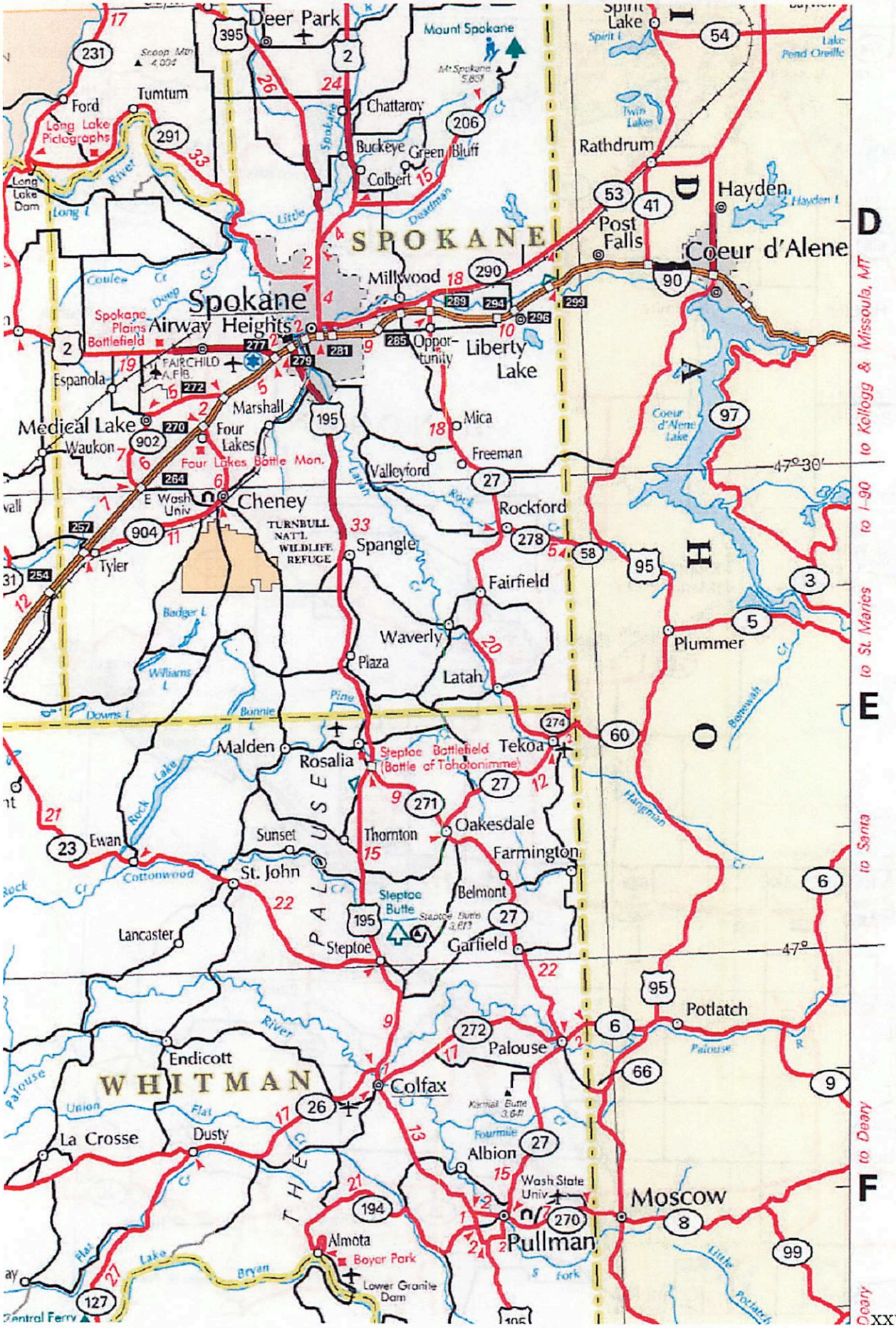
Deer Park
Mount Spokane
Spirit Lake
Lake Pend Oreille
Ford
Tumtum
Long Lake Pictographs
Chattaroy
Buckeye
Green Bluff
Colbert
Rathdrum
Hayden
Hayden L
Post Falls
Coeur d'Alene
SPOKANE
Millwood
Spokane
Airway Heights
Spokane Plains Battlefield
FAIRCHILD A.F.B.
Opportunity
Liberty Lake
Espanola
Medical Lake
Waukon
Four Lakes
Four Lakes Battle Mon.
Marshall
Mica
Freeman
Valleyford
Coeur d'Alene Lake
47°30'
Cheney
E Wash Univ
TURNBULL NAT'L WILDLIFE REFUGE
Rockford
Spangle
Fairfield
Tyler
Badger L
Waverly
Plummer
Plaza
Latah
Williams L
Downs L
Malden
Rosalia
Steptoe Battlefield (Battle of Tohotonimme)
Tekoa
Hangman Cr
Ewan
Sunset
Thornton
Oakesdale
Farmington
St. John
Cottonwood Cr
Belmont
Steptoe Butte
Steptoe
Garfield
Lancaster
47°
Potlatch
Palouse
Endicott
WHITMAN
Colfax
Union Flat Cr
La Crosse
Dusty
Albion
Wash State Univ
Moscow
Pullman
Almota
Boyer Park
Lower Granite Dam
Central Ferry
Bryan Flat
S Fork Palouse R
Little Potlatch Cr
to Kellogg & Missoula, MT
to I-90
to St. Maries
to Santa
to Deary
D
E
F

0.2 Landsat Overview Maps

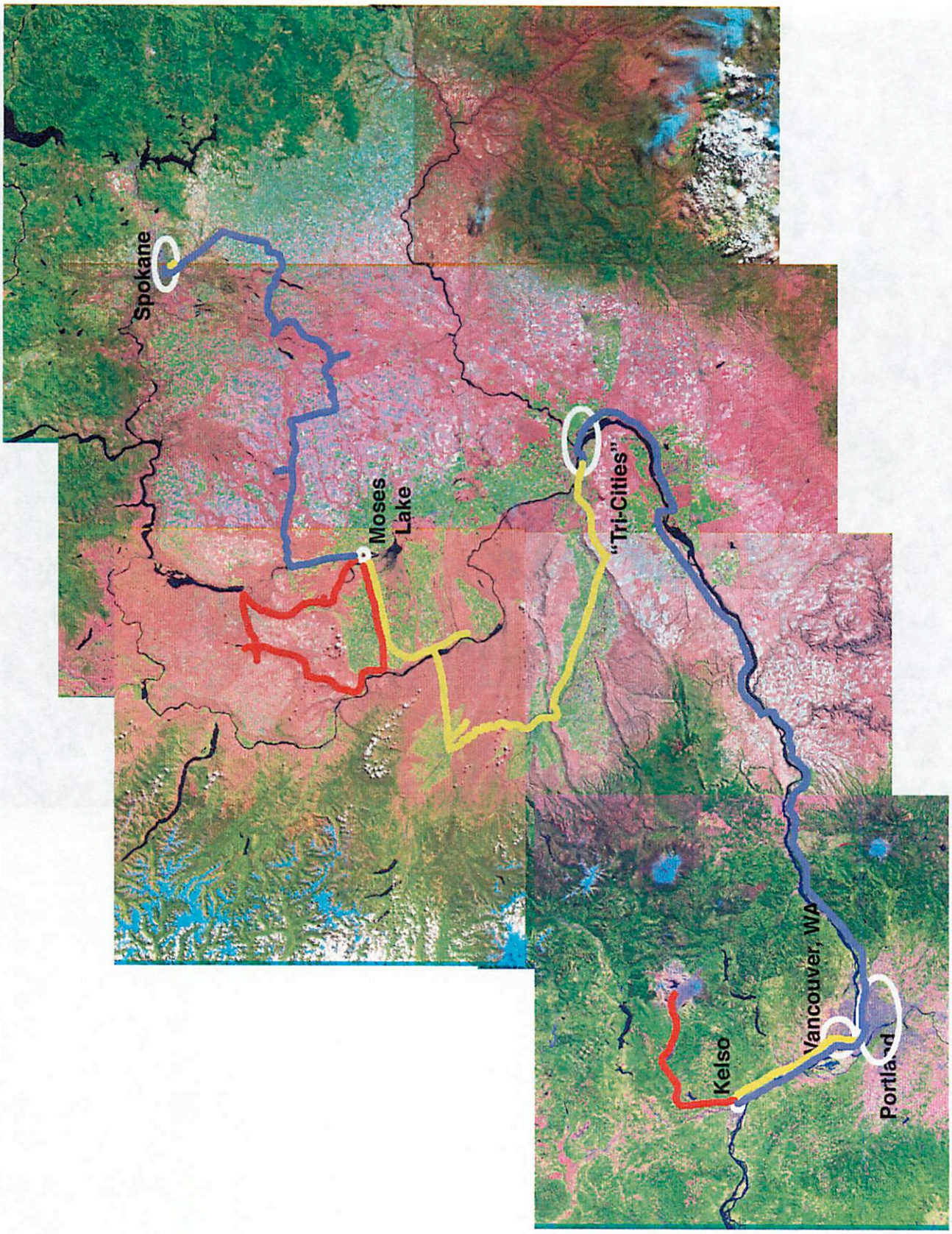

Day 2 Landsat

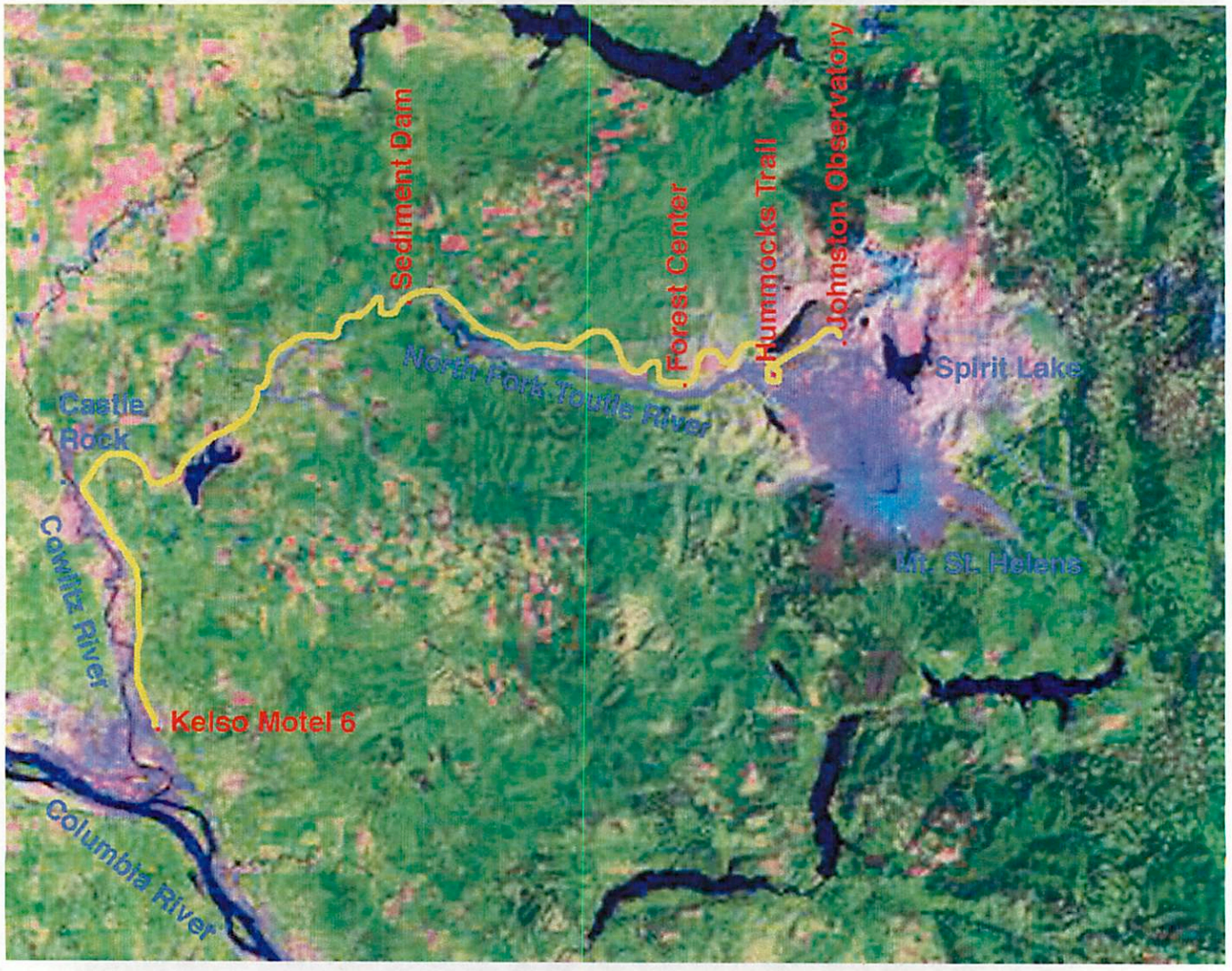

Day 3 Landsat

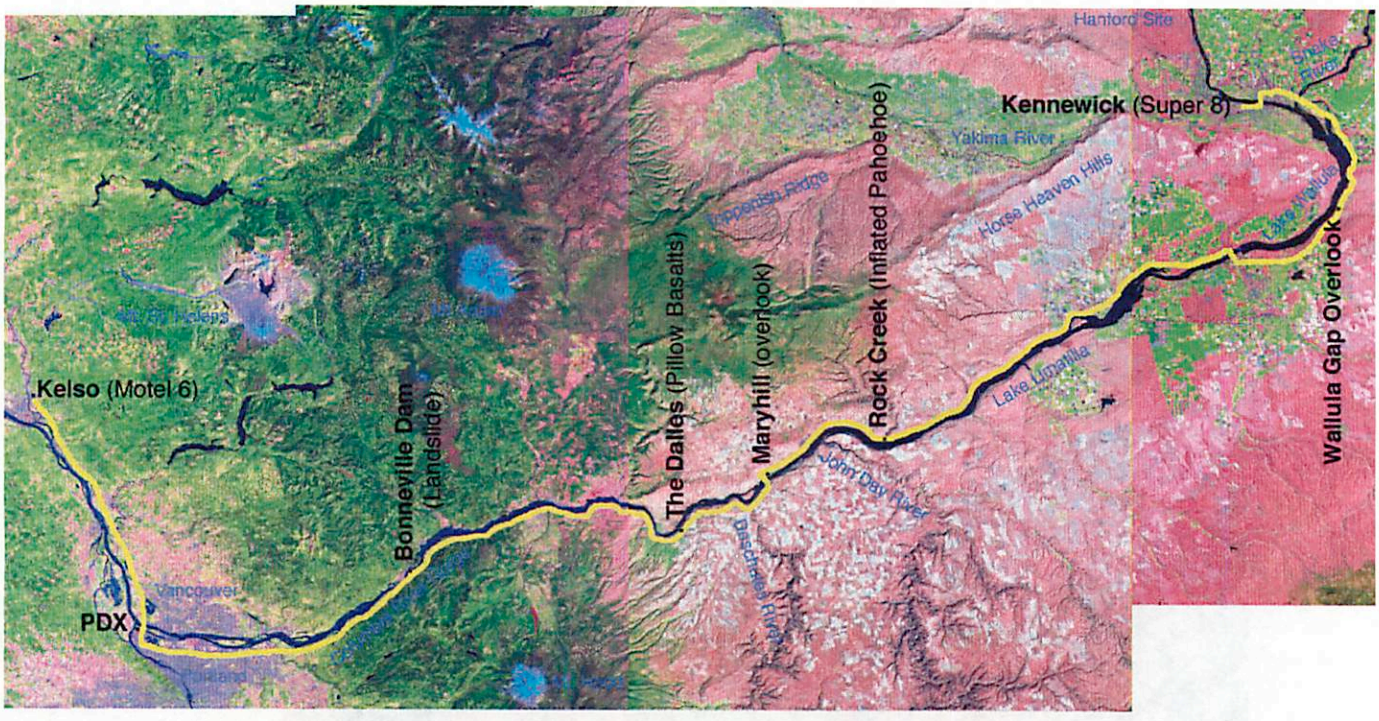

Day 4 Landsat

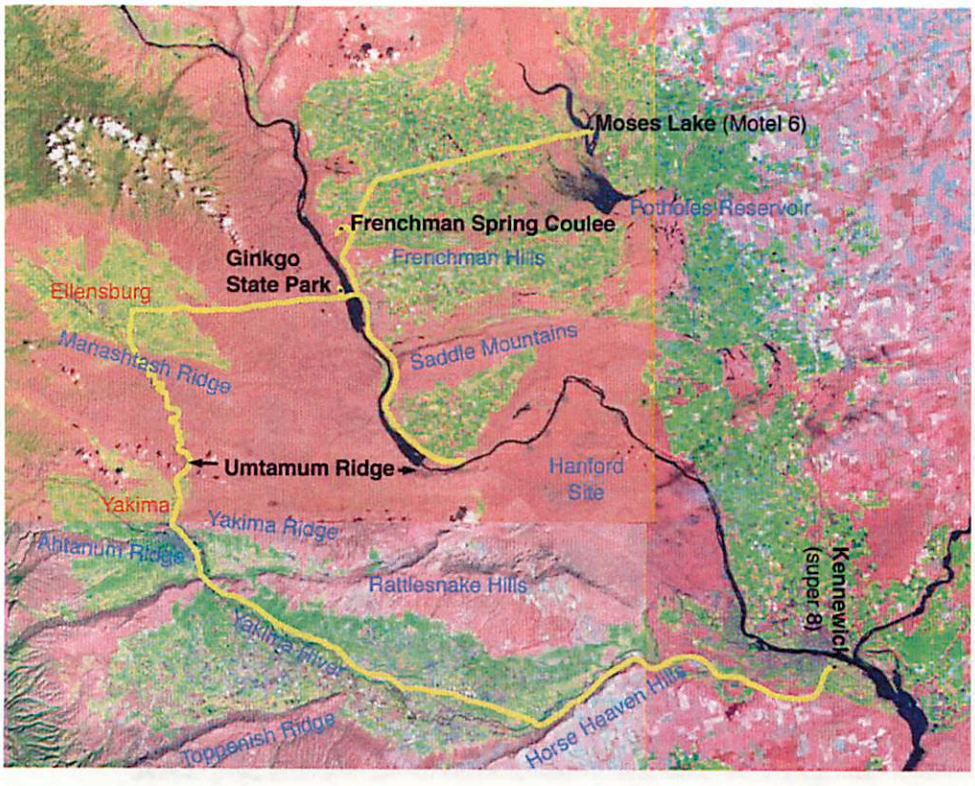

Day 5 Landsat

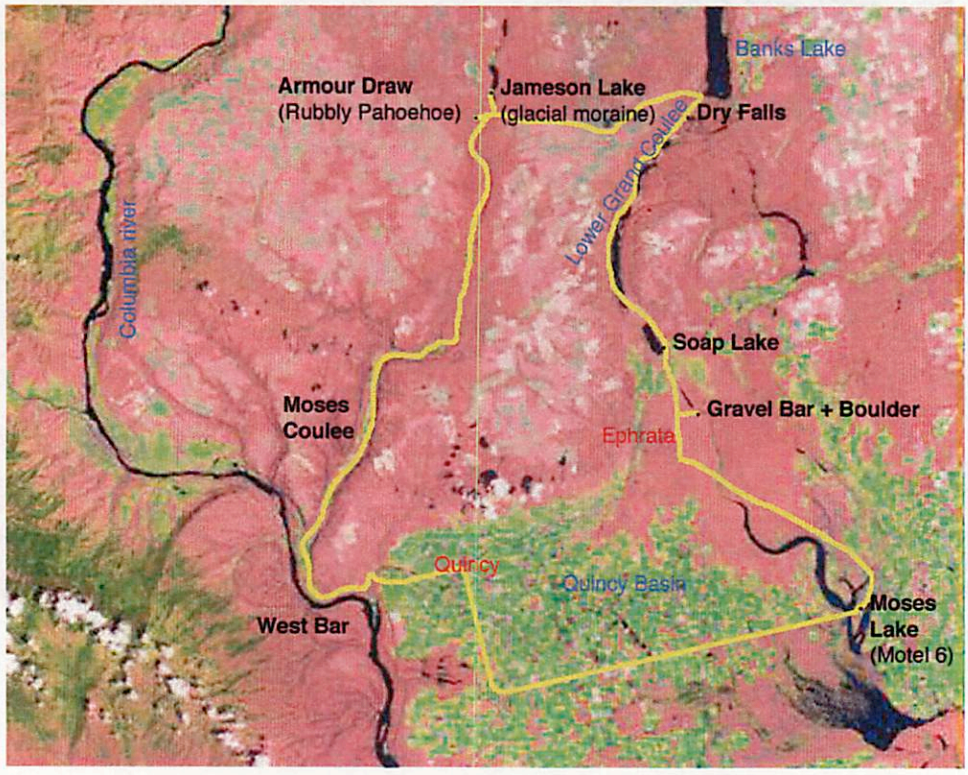

Day 6 Landsat

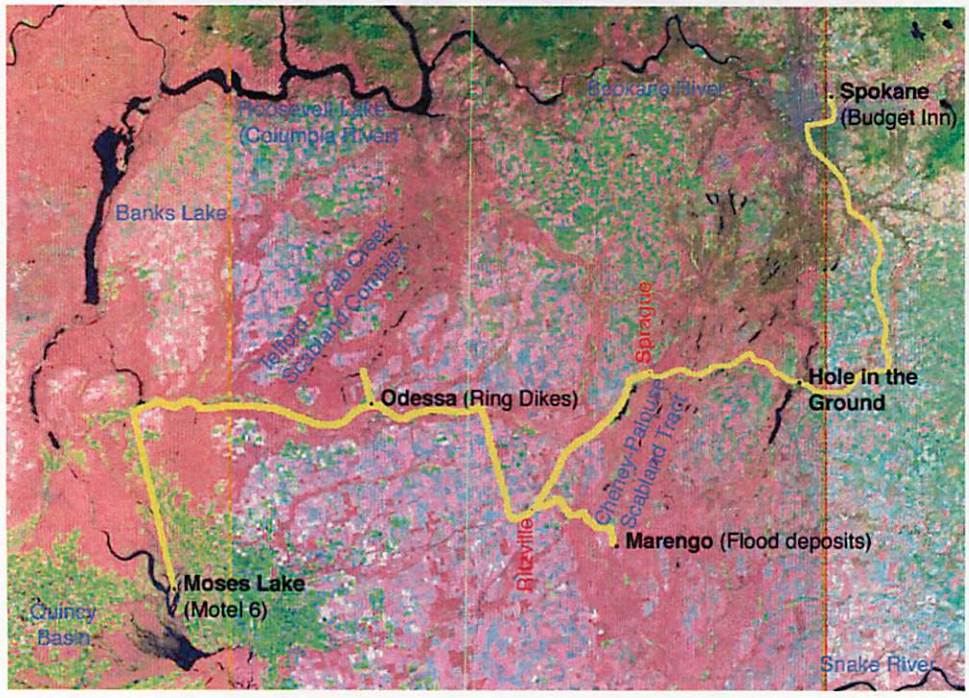

0.3 Other Maps

Northwest Shaded Relief Map

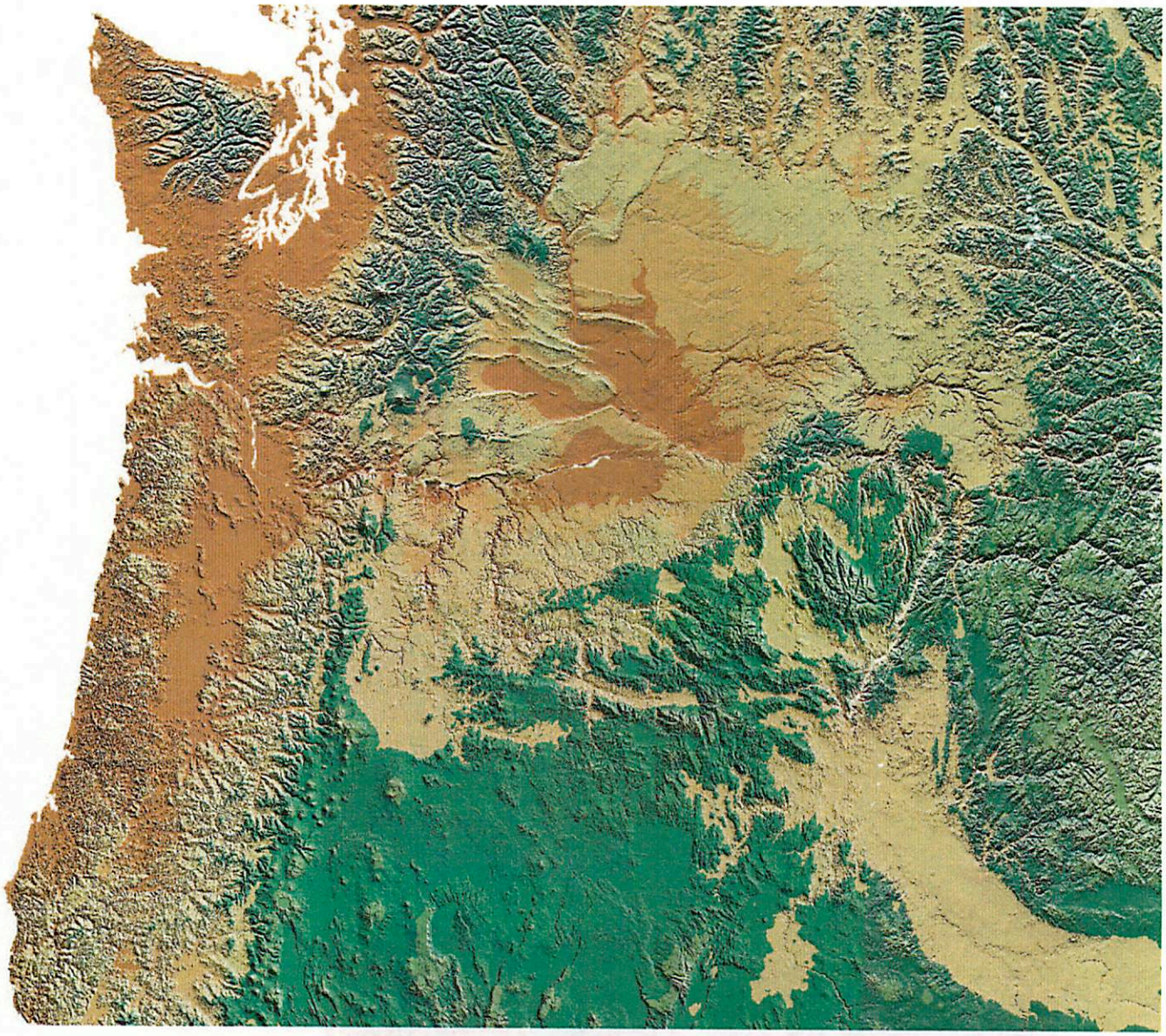

Geologic Age Map

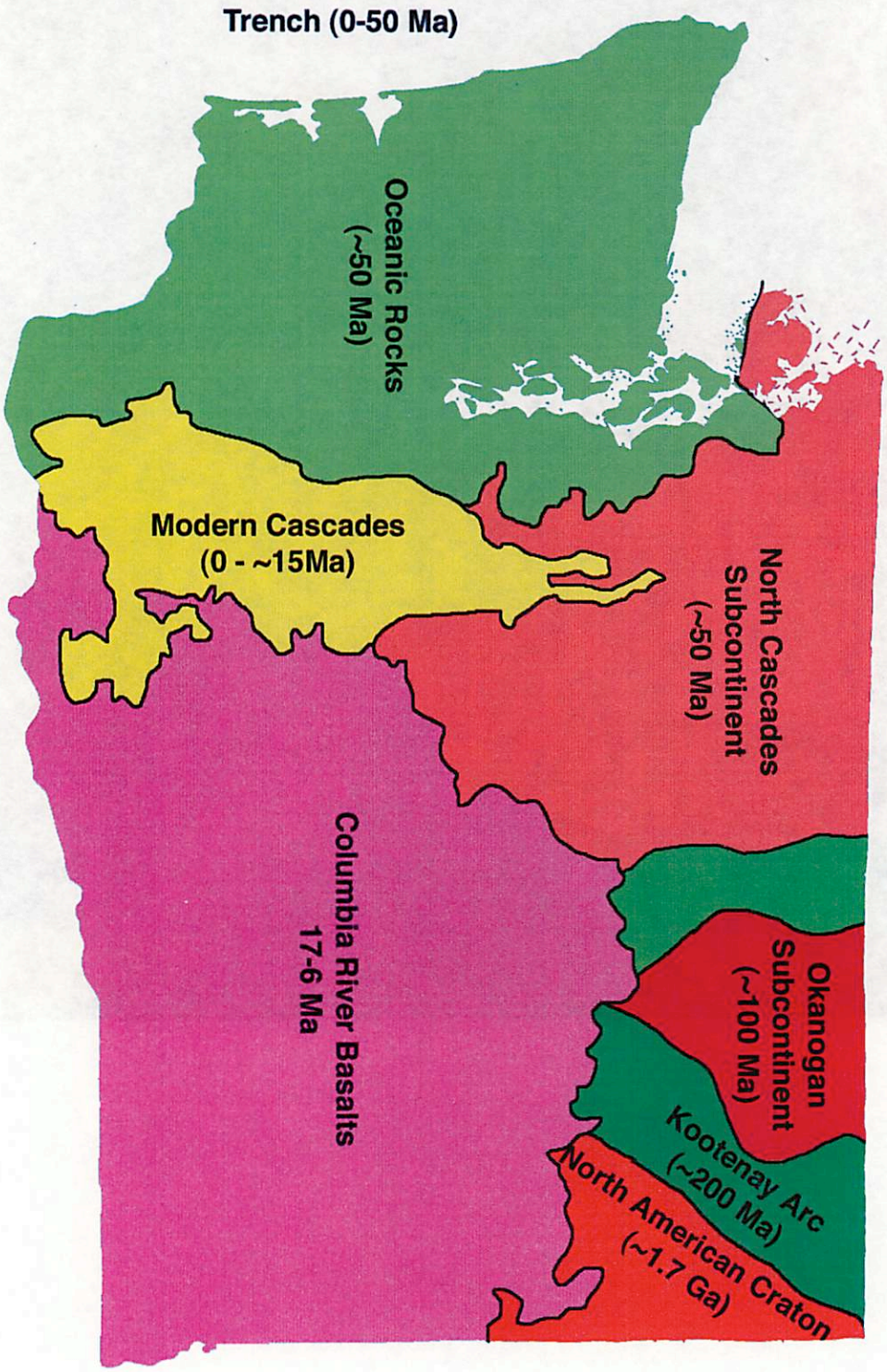

Uniform Time Scale	Subdivisions Based on Strata/*Time*			Radiometric Dates (millions of years ago)	Outstanding Events	
		Systems/*Periods*	Series/*Epochs*		In Physical History	In Evolution of Living Things
0				0		
PHANEROZOIC	CENZOIC	Quaternary	Recent or Holocene Pleistocene		Several glacial ages Making of the Great Lakes; Missouri and Ohio Rivers	*Homo sapiens*
				2?		
		Tertiary	Pliocene			Later hominids
				6	Beginning of Colorado River	Primitive hominids
			Miocene			Grasses; grazing mammals
				22	Creation of mountain ranges and basins in Nevada	
			Oligocene			
				36		
			Eocene		Beginning of volcanic activity at Yellowstone Park	Primitive horses
				58		
			Paleocene			
				65	Beginning of making of Rocky Mountains	Spreading of mammals Dinosaurs extinct
	MESOZOIC	Cretaceous	Many		Beginning of lower Mississippi River	Flowering plants
				145		Climax of dinosaurs
		Jurassic				Birds
				210		
		Triassic			Beginning of Atlantic Ocean	Conifers, cycads, primitive mammals Dinosaurs
	PALEOZOIC			250	Climax of making of Appalachian Mountains	
		Permian				Mammal-like reptiles
				290		
		Pennsylvanian (Upper Carboniferous)				Coal forests, insects, amphibians, reptiles
				340		
		Mississippian (Lower Carboniferous)				
				365		Amphibians
		Devonian			Earliest economic coal deposits	
				415		
		Silurian				Land plants and land animals
				465		
		Ordovician			Beginning of making of Appalachian Mountains	Primitive fishes
				510		
		Cambrian			Earliest oil and gas fields	Marine animals abundant
575				575		
PRECAMBRIAN	PRECAMBRIAN (Mainly igneous and metamorphic rocks; no worldwide subdivisions.)			1,000		Primitive marine animals Green algae
				2,000		
				3,000		Bacteria, blue-green algae
~4,650	Birth of Planet Earth			4,650	Oldest dated rocks	

Flint & Skinner, "Physical Geology" 2 ed (1977)

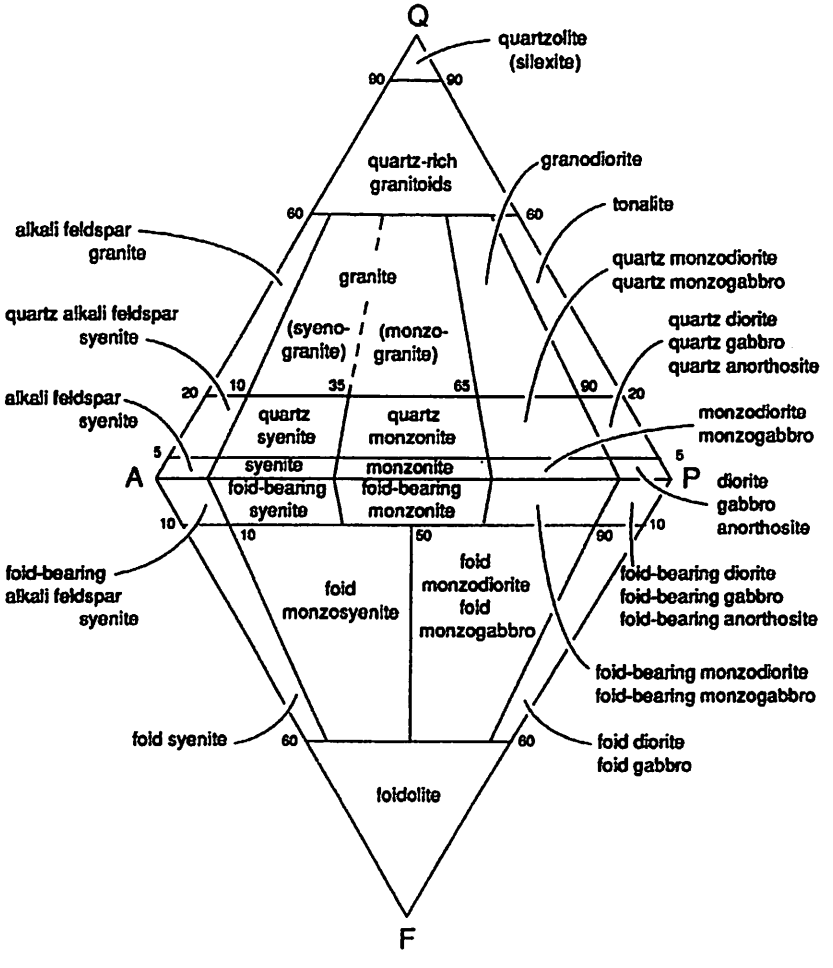

Fig. B.4. Classification and nomenclature of plutonic rocks according to their modal mineral contents using the QAPF diagram (based on Streckeisen, 1976, Fig. 1a). The corners of the double triangle are Q = quartz, A = alkali feldspar, P = plagioclase and F = feldspathoid. However, for more detailed definitions refer to section B.2. This diagram must not be used for rocks in which the mafic mineral content, M, is greater than 90%.

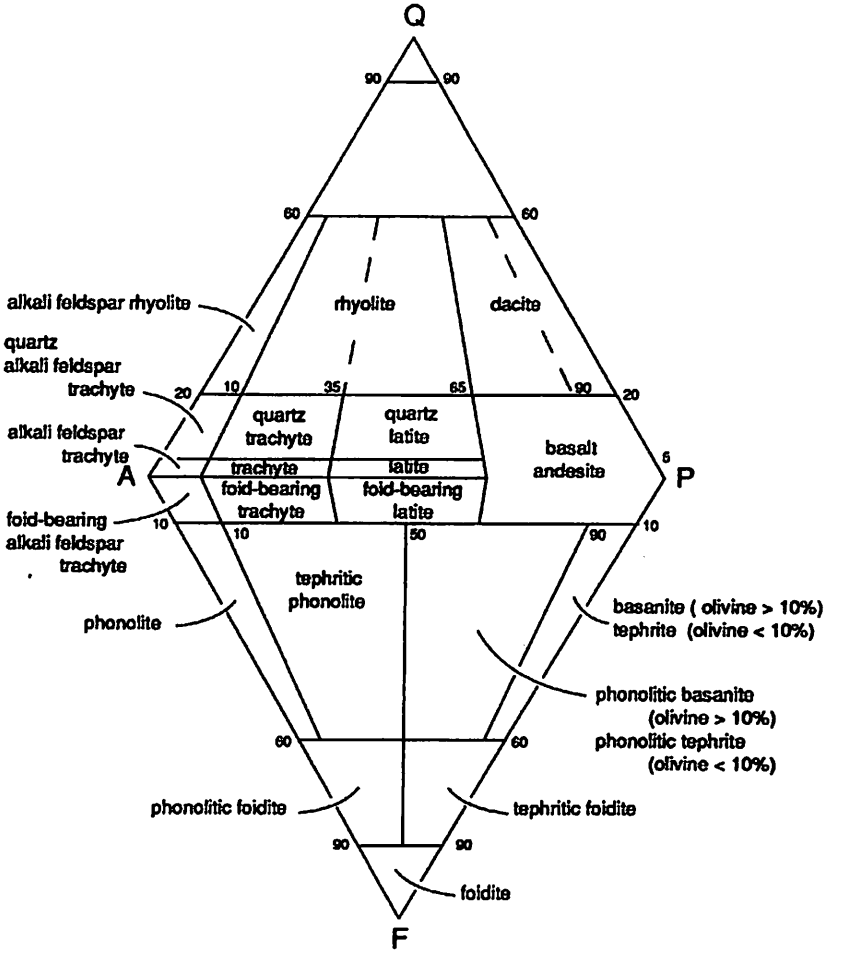

Fig. B.10. Classification and nomenclature of volcanic rocks according to their modal mineral contents using the QAPF diagram (based on Streckeisen, 1978, Fig. 1). The corners of the double triangle are Q = quartz, A = alkali feldspar, P = plagioclase and F = feldspathoid. However, for more detailed definitions refer to section B.2.

"Classification of Igneous Rocks and Glossary of Terms", Le Maitre, ed. xxxvi Blackwell Scientific Publications (1989)

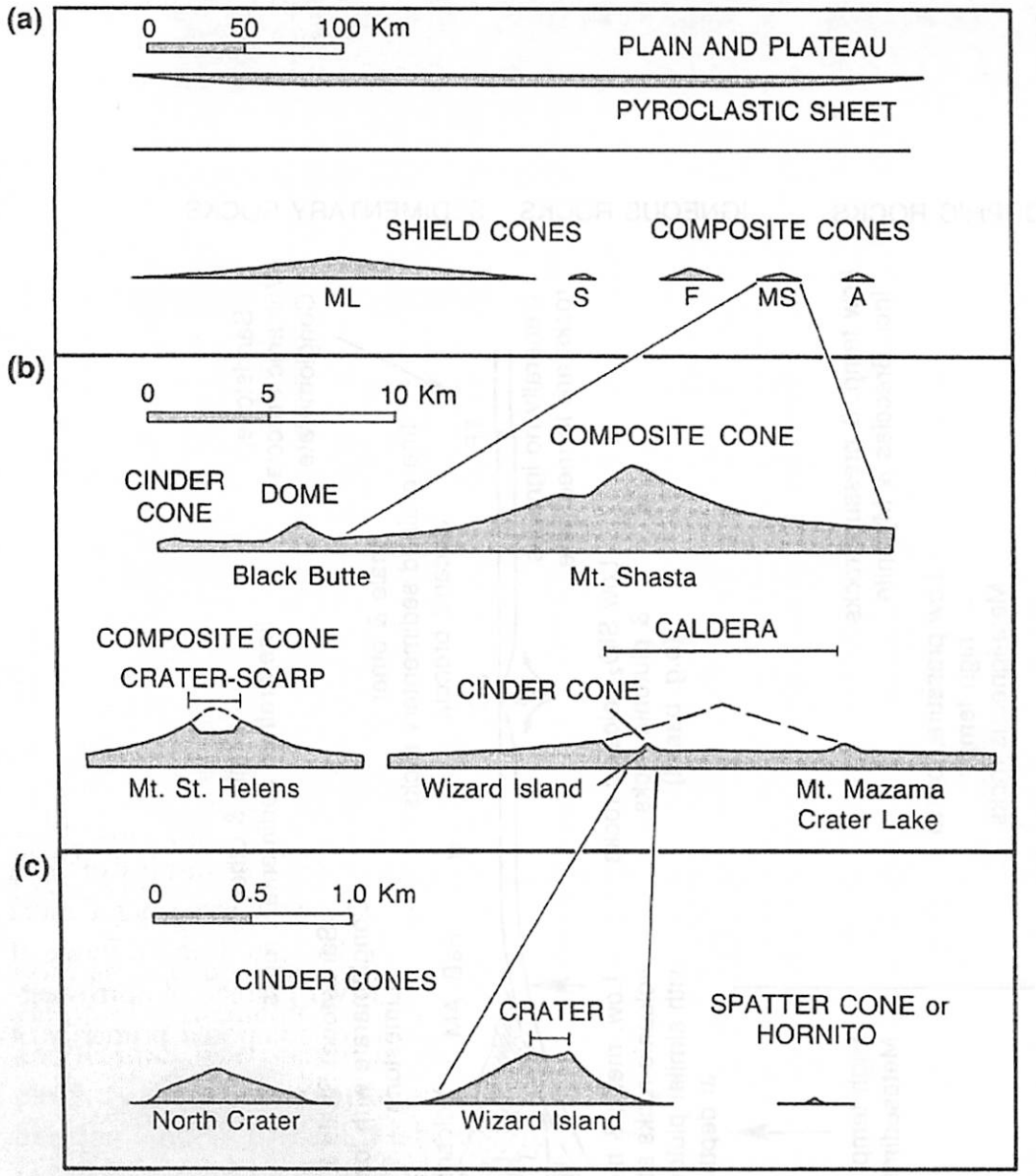

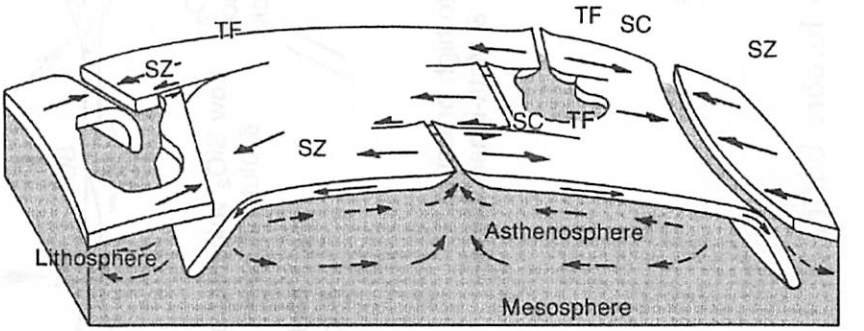

Figure 1.3 Schematic block diagram showing the three types of plate boundaries—spreading centers (SC), subduction zones (SZ), and transform faults (TF).
(Modified from Isacks et al., 1968.)

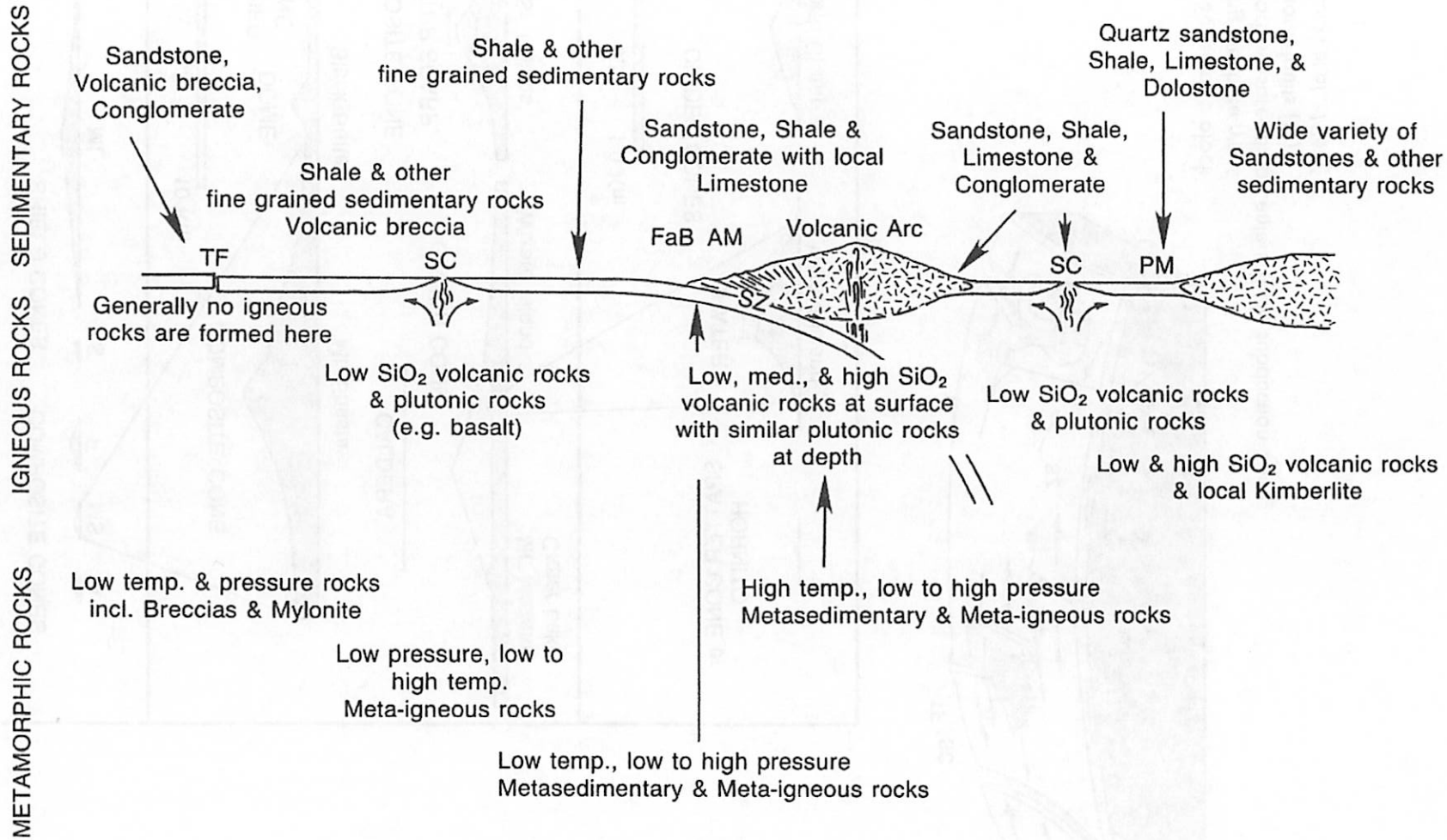

Figure 1.4 Diagram showing petrotectonic assemblages at various sites. FaB = forearc basin, SC = spreading center, SZ = subduction zone, TF = transform fault, AM = active margin, PM = passive margin.

Aerial Photos and Diagrams

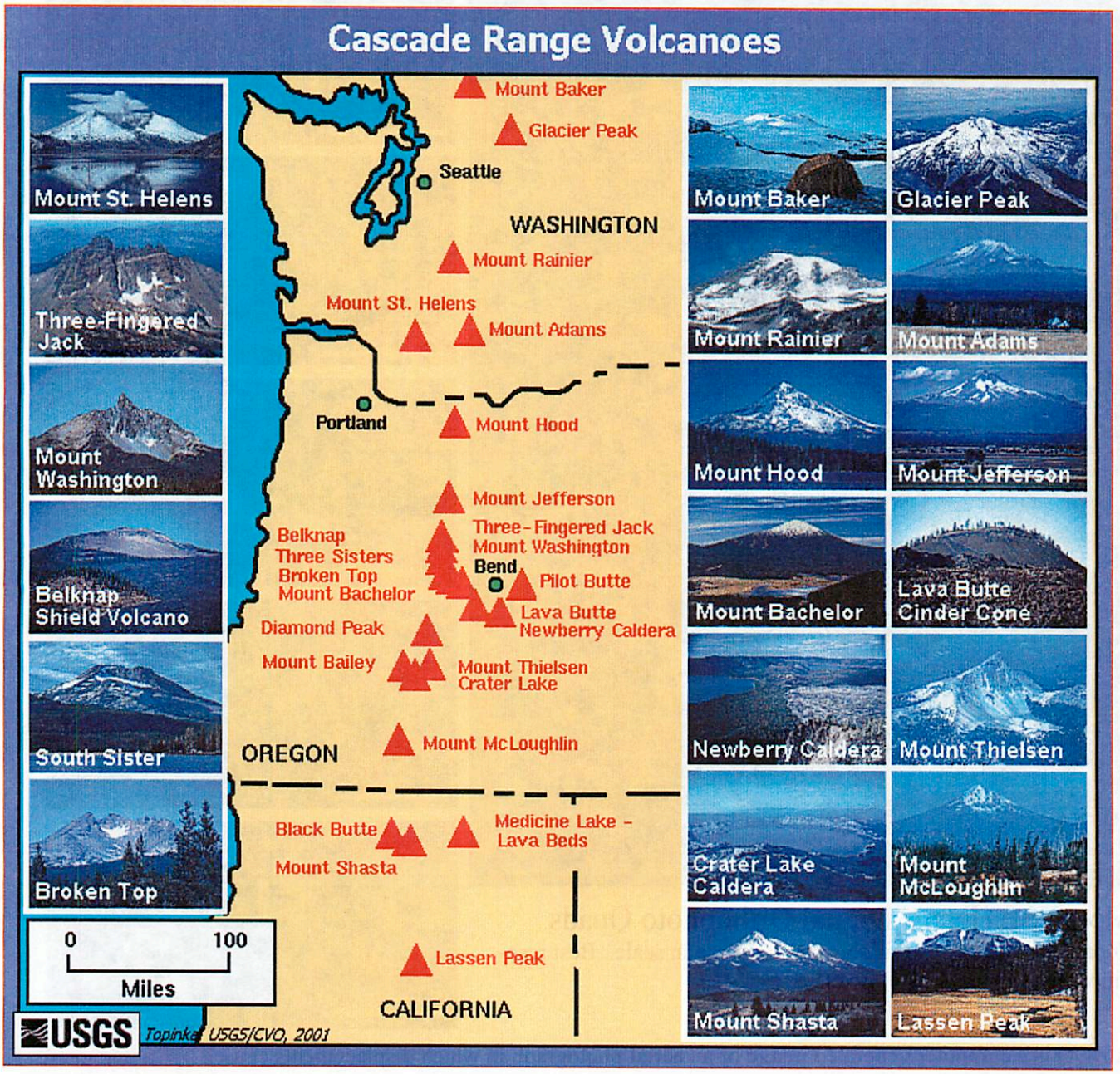

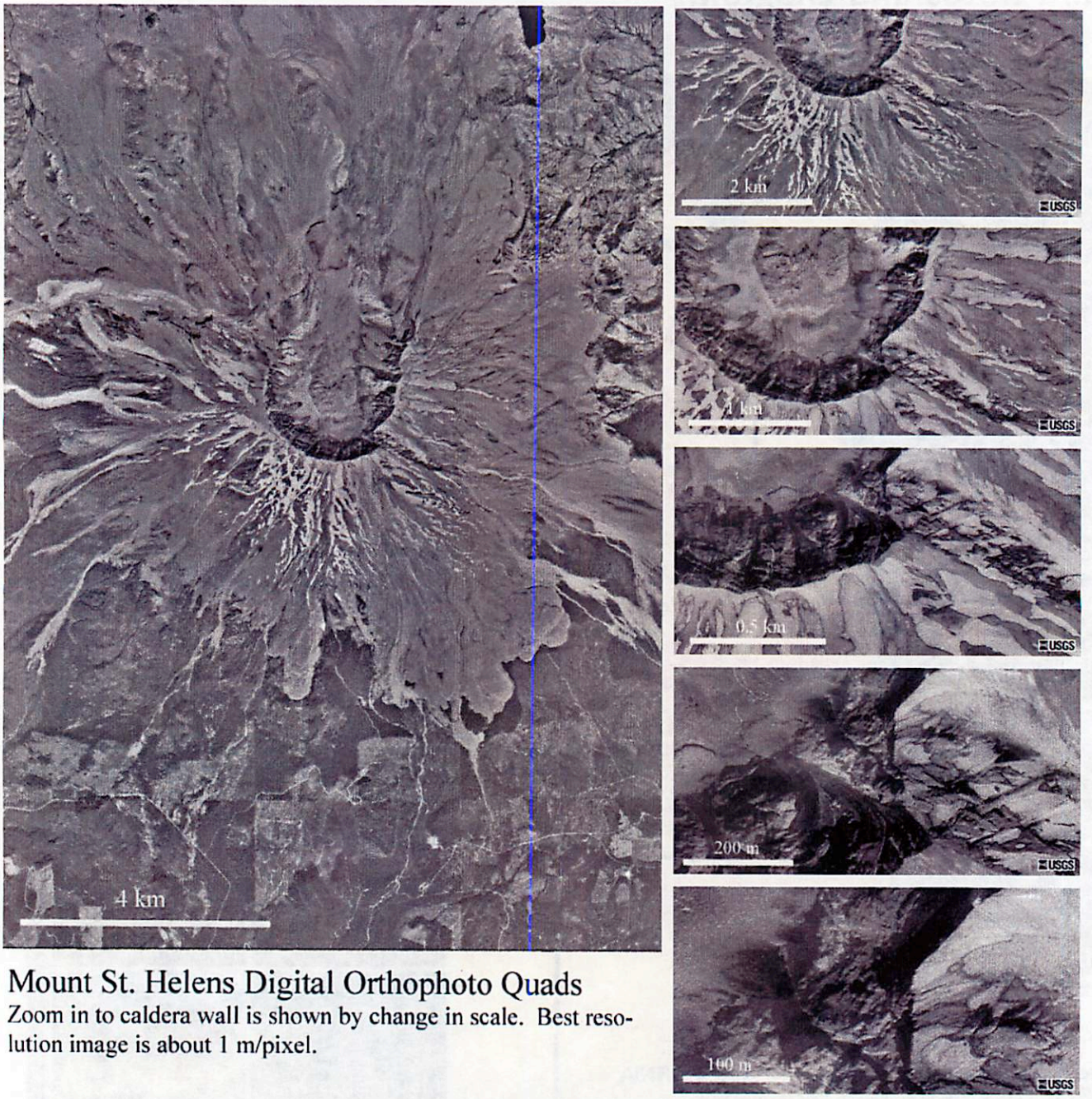

Mount St. Helens Digital Orthophoto Quads

Zoom in to caldera wall is shown by change in scale. Best resolution image is about 1 m/pixel.

A DOQ is a computer generated image of an aerial photograph in which displacements caused by camera orientation and terrain have been removed. Unlike a standard aerial photograph, relief displacement in orthophotos has been removed so that ground features are displayed in their true ground position. This allows for the direct measurement of distance, areas, angles, and positions. Also, an orthophoto displays features that may be omitted or generalized on maps.

From http://mapping.usgs.gov/www/ndop/
and http://terraserver.homeadvisor.msn.com

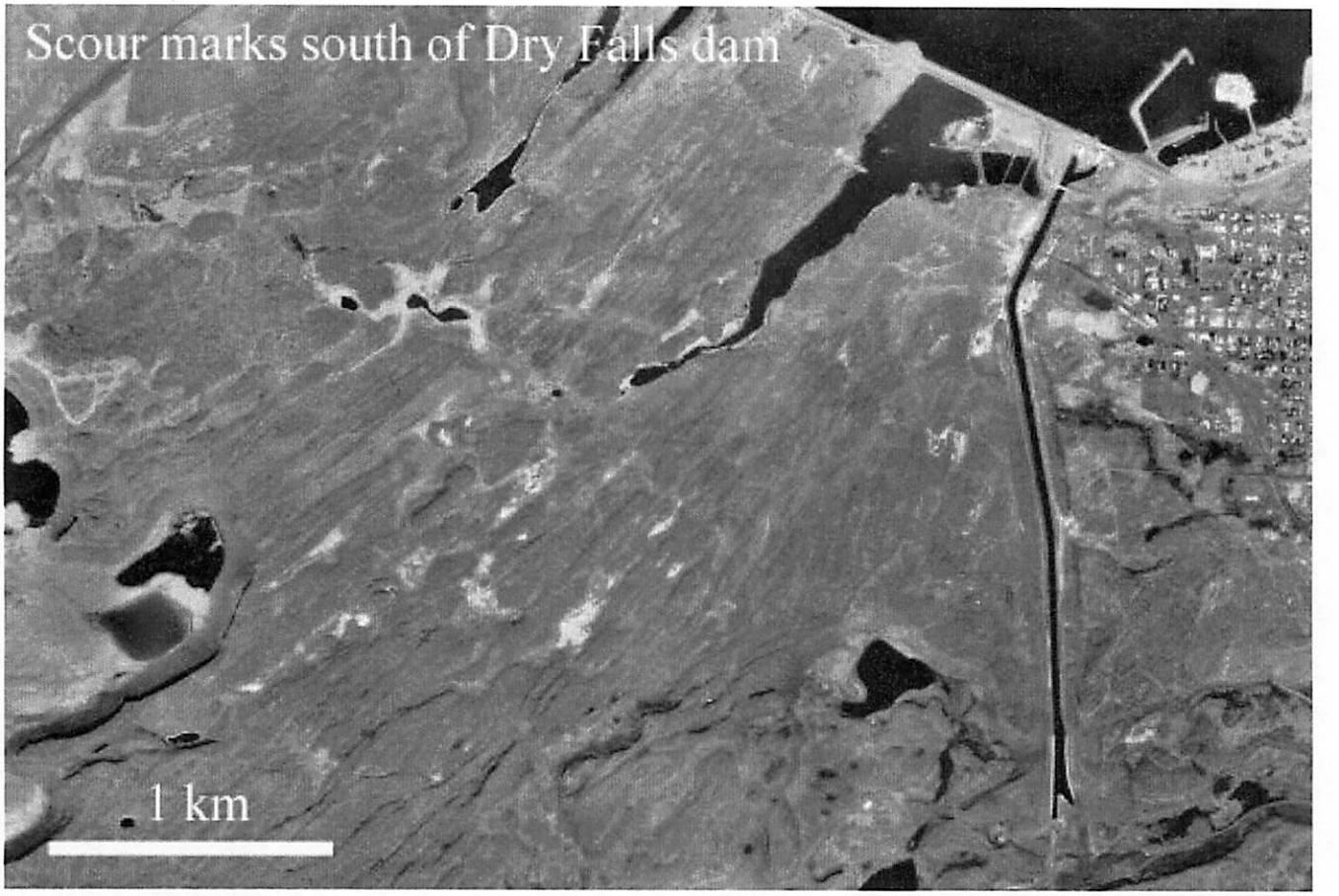
Scour marks south of Dry Falls dam
1 km

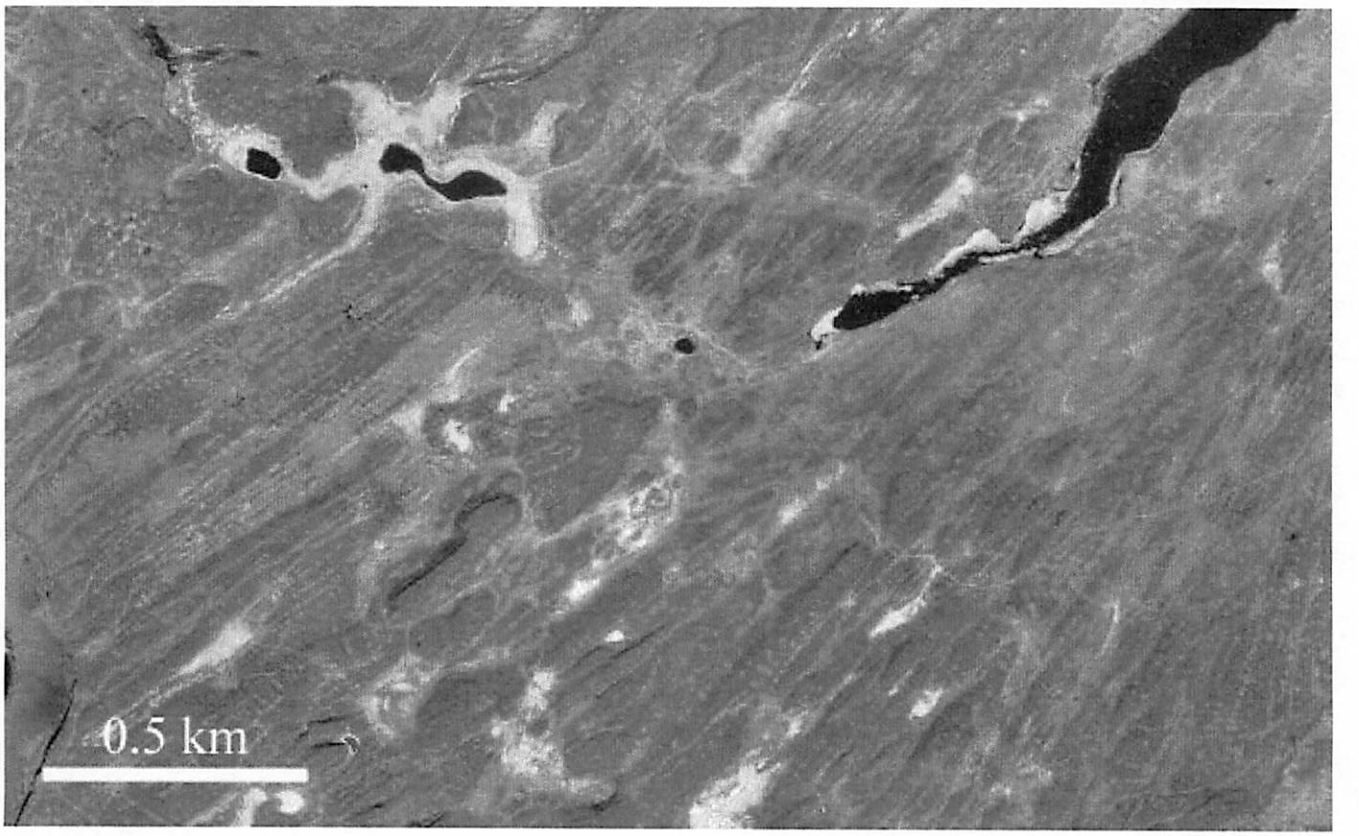
0.5 km

1 Post-Eruption Ecology of Mt. St. Helens: A Succession Experiment

by JASON W. BARNES

According to conventional ecological succession theory, after the biota of an area are wiped out the ecology recovers in stages. Pioneering species such as grasses and hardy weed-like plants colonize the area first. After these have suitably altered the soil chemistry and shade environment, larger forms such as bushes take hold. Lastly, smaller trees and then large, hardy trees begin to grow and return the area to mature, old-growth forest on timescales of centuries. Ecologists looked forward to studying this process in detail after the eruption of Mt. St. Helens in 1980.

To their surprise, this isn't what happened at all.

All the trees were downed in a 600 km^2 area surrounding the mountain, and other areas were covered by many tens of cm of ash, mud, and/or pumice. The whole area appeared sterile. However, instead of recovering in orderly succession from the edges of the blast zone, late-successional plant species began to recolonize the area from within.

In some areas, trees that were formerly rooted in the ground tipped over, exposing old plants and seedlings from below the volcanic deposits. Dead trees began to decay, attracting insects and birds that fed on the insects. In areas entirely covered by pumice, instead of hardy pioneering lichens and small plants taking hold first, whatever seeds found moisture and purchase grew with abandon.

Larger animals have returned much more quickly than predicted as well. Because the lakes in the area were covered by 30 cm of ice at the time of the eruption, amphibians such as frogs and salamanders survived the blast, and almost unbelievably, have expanded their range across kilometers of barren terrain to colonize previously uninhabited ponds. Small rodents and mammals migrated to habitat islands among young forests also across kilometers of wasteland.

In short, ecological recovery at Mt. St. Helens has not been dominated by the average, typical area — it has been dominated by the exceptions.

This result has application to ecological recovery in a planetary sense, as well. Several mass-extinctions (e.g., Permian-Triassic, Cretacious-Tertiary) have driven large fraction of the Earth's species extinct from a single, violent event much like the Mt. St. Helens eruption. What planetary scientists should take away from this is how quickly the biology has flourished after such an event. In order for a asteroid impact, or climate change, or massive volcanic eruptions to wipe out a large fraction of species they must sterilize not only the average area, but rather must be so effective as to totally sterilize even protected areas, such that nothing at all survives to pioneer the recovery. In this context, the scale of destruction that must have brought about these mass-extinctions is sobering.

Source: Lovett, Richard A. Mt. St. Helens Revisited, *Science* 2000 288: 1578-1579.

Figure 1.1: *There's no ecology left right after the eruption.*

Figure 1.2: *Late-successional species grow in a previously devastated area near Mt. St. Helens.*

2 Lahars of Mount St. Helens and Possible Planetary Analogs

by MIKE BLAND

Lahars: General Info

The term lahar is an Indonesian word for a mudflow that is associated with a volcanic eruption. Such a mudflow is generally distinguished from a debris flow in that they are less course and more cohesive. As such, lahars can travel tens to hundreds of kilometers from a volcano disrupting pre-eruption drainages for thousands of square kilometers (Brantley, 1985).

While lahars, by definition, range from a few centimeters to a few hundred meters wide, most interest has focused on the large, eruption activated lahars. Such lahars can be initiated by several eruptive processes. Landslides of saturated debris, sudden melting of snow and ice pack by pyroclastic flows, ballistic showers of hot debris, break out of crater lakes, and melting of snow and ice by radiant heating of a lava dome are a few of the most common sources of lahars (Pierson, 1983).

The Mount St. Helens Eruption: Description of Lahars

The May 18th eruption of Mount St. Helens created a number of large lahars, which traveled down the flanks of the mountain into three of the four major drainages in the Mount St. Helens area (Figure 2.1). Mudflows on the south flank of the river moved into the smith creek, muddy river and pine creek drainage system and continued into the Swift Reservoir (Figure 2.2) (Haeni, 1981). Upon reaching the reservoir, however, flow velocity rapidly decreased and deposition of most of the mudflows sediment load occurred. The reservoir, which had been lowered for the very purpose of accommodating a large debris flow, was able to hold the influx of water and sediment and the mudflow terminated there. It is estimated that the lahar deposited 18 million cubic yards of sediment into the reservoir (Tilling, 1990).

Further mudflows originating at the summit of the crater moved west off the flanks of the volcano and into the drainage of the South Toutle River (Figure 2.2). This lahar was most likely caused by the melting of glaciers and snow and ice pack on the upper slopes of Mount St. Helens. It is estimated that 70% of the volume of glacial ice was removed from the mountain during the eruption (Brugman, 1981). Despite this, the lahar that moved into the South Toutle drainage was relatively small.

The collapse of the north flank of the volcano created a debris avalanche which deposited approximately three billion cubic yards of rock, ash, pumice, snow and ice into the upper seventeen miles of the North fork of the Toutle river. This deposition created the most destructive of the eruption's three major mudflows (figure 2.2). On the upper reaches of the mountain it is estimated that mudflow velocities were in excess of 100 km/h (actual estimates vary greatly). As the mudflow moved down stream and reached the broader portions of the Toutle drainage the flow velocity decreased sharply to four or five kilometers per hour, but the volume of the flow continued to increase. With the decrease in flow velocity, the lahar left sediment deposits twenty five to ninety feet deep

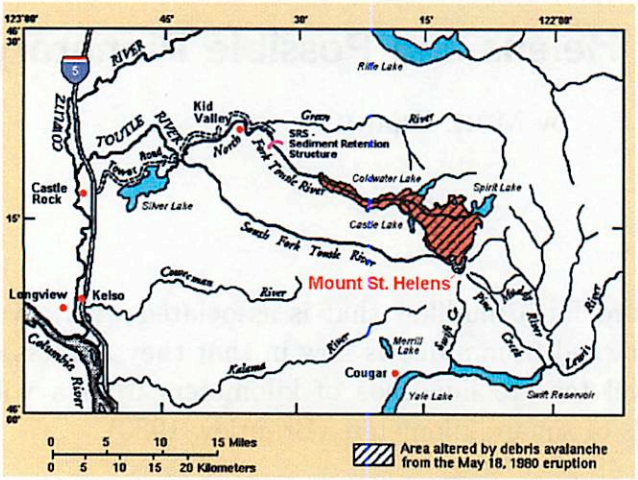

Figure 2.1: *Map of Mount St. Helens drainages. Debris avalanche is marked by striped fill. Three major lahars were produced by the eruption. The largest of which extended down the North Fork Toutle River to the confluence of the Cowlitz and Columbia Rivers. (Image with permission of USGS).*

along the flood plain of the North Toutle River (Figure 3). However, the flow carried the bulk of its sediment down to the lower Cowlitz and Columbia Rivers where it was subsequently deposited into the two river channels (Cumming, 1981).

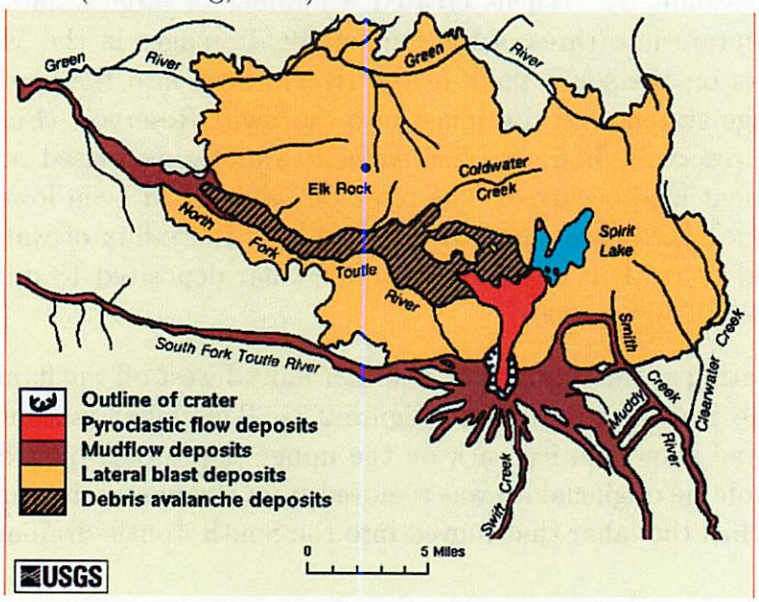

Figure 2.2: *Zoomed in map of Mount St. Helens devastation area showing three major mudflows emanating from the crater and debris flow (dark solid fill). The largest of these lahars was in North Fork Toutle River. (Image with permission of USGS). .*

The lahar on the North and South Toutle Rivers had a profound effect on the hydrology of the lower Cowlitz and Columbia rivers. It is estimated that 35.6 million cubic yards of material was deposited along a nine mile stretch of the Columbia River. In general, the deposition occurred two

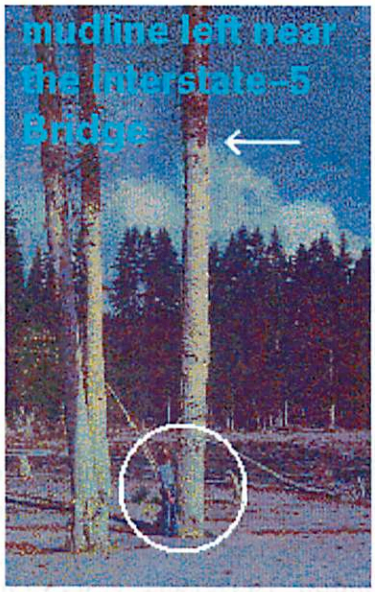

Figure 2.3: *Mudline left on tree near the confluence of the North Toutle and Cowlitz Rivers. Lahars deposits along the North Fork Toutle River were 25 to 90 ft deep. Note person for scale. (Image with permission of USGS)..*

miles downstream and seven miles upstream of the confluence of the two rivers. This surprising depositional pattern was most likely due to a twice daily, tidal driven flow reversal of the Columbia River, which created a backwater environment at the mouth of the Cowlitz River (Haeni, 1981).

The deposition of the mudflow sediments into the Columbia reduced the depth of the commercial channel from forty feet to fourteen feet, effectively cutting of ocean bound travel through the channel. Furthermore, strong evidence suggests scouring of the lower Cowlitz River and redeposition into the Columbia. This is evidence by the apparent increase in depth of the lower Cowlitz River after the Lahars. Despite this the overall water carrying capacity of the river was decreased by 85 percent (Haeni, 1981).

Planetary Analogs

It is hard to image many planetary analog for current lahar processes in the solar system since they require large amount of liquid water to be present. However, there is currently some evidence to suggest that volcanism has played a role in the formation of fretted channels on Mars. Several fretted channels in the Ismeniae Fossae region of Mars have been linked to volcanism. It is suggested that ground ice, concentrated in previously existing fractures, is melted by nearby volcanic activity and channel formation commences. Unlike a lahar, however, most of the water movement is below the Martian surface and any water reaching the surface is likely to sublimate into the atmosphere. Later, mass wasting events are thought to widen the channels (Carruthers, 1997).

References

Brantly, Powers, Report from the U.S. Geological survey's Cascade Volcano Observatory at Vancouver, Washington: Earthquake Information Bulletin, v.17, n.1, January-February 1985, p.20, 1985.

Brugman, M. M., Post, A., Effects of volcanism on the glaciers of Mount St. Helens, Geo survey Circular 850 D, 1981.

Caruthers, M. W. and McGill, G. E., Evidence for volacnism associated with Ismeniae Fossae fretted channels, *Conference on Early Mars: geologic and hydrologic evolution, physical and chemical environments and implications for life*, LPI, Housten, TX, 1997.

Cummings, J., Mudflows resulting from May 18, 1980 eruption of Mount St. Helens, Geo Survey Circular 850 B, 1981.

Haeni, F. P., Sediment deposition in the Columbia and lower Cowlitz Rivers, Washington-Oregon caused by the May 18, 1980 eruption of Mount St. Helens, Geo survey Circular 850 k, 1981.

Pierson, Waitt, Dome collapse, rockslides, and multiple sediment-water flows generated by a small explosive eruption Feb 23, 1983, *Hydrologic consequences of hot-rock/snowpack interactions at Mount St. Helens Volcano, Washington*, 1992-1994, USGS Open File Report 96-179.

Tilling, Topinka, Swanson, Eruptions of Mount St. Helens: past, present and future, USGS Special Interest Publication, 1990.

3 A Whole Lot of Shaking Going On: Seismology of Mount St. Helens

by ®

A Crash Course in Seismology

Seismology - "the study of the passage of elastic waves through the earth" These elastic waves are produced by a variety of activities including earthquakes, volcanic explosions, and really big bombs.

Body Waves

Body waves travel through the "body" of the Earth, that is they travel through the deep regions, as opposed to surface waves that travel on the surface (easy, isn't it?) The two kinds of body waves are P and S.

P-waves - also knows as pressure, push-pull, or primary, P-waves are compressional like a spring. The particle motion within a P-waves is longitudinal, so usually in the same plane that the wave travel.

S-waves - also known as shear, shake, or secondary, the particle motion in an S-wave is mostly perpendicular to the direction of travel, more like waves in the ocean.

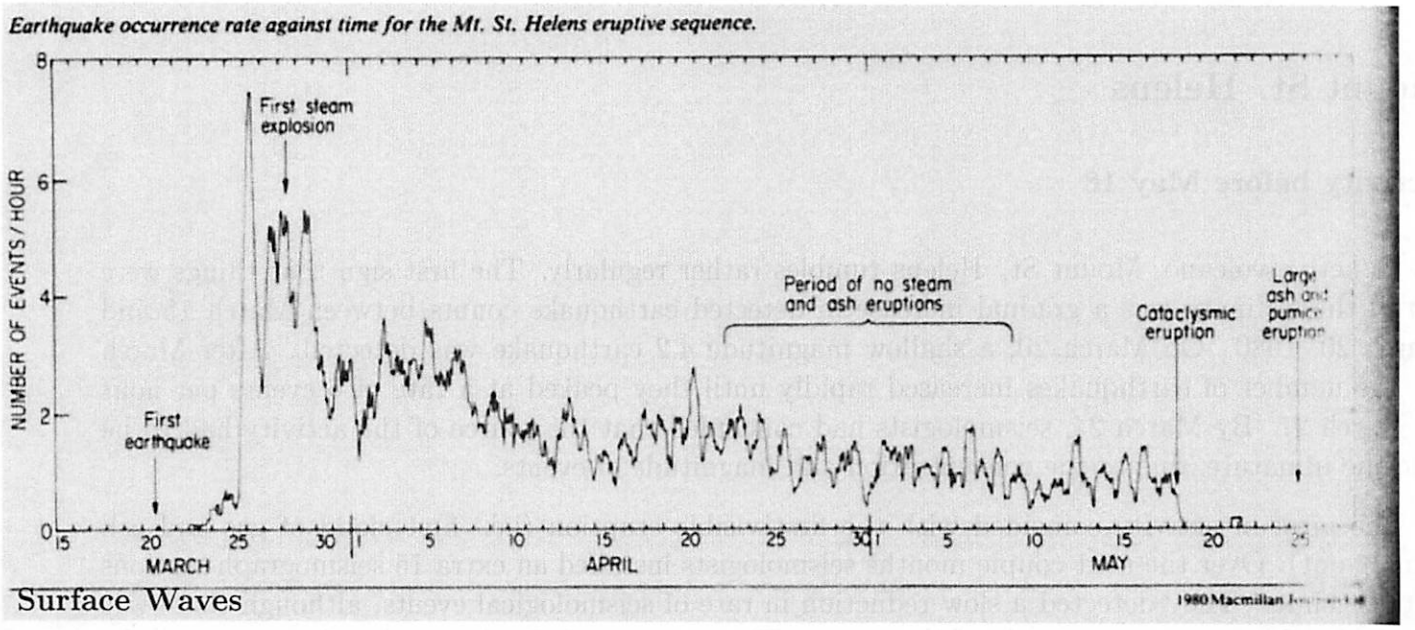

Surface Waves

Surface waves travel at the surface of the Earth, or very close to the surface. They are slower than body waves, so they are usually detected after the body waves arrive. The difference in time

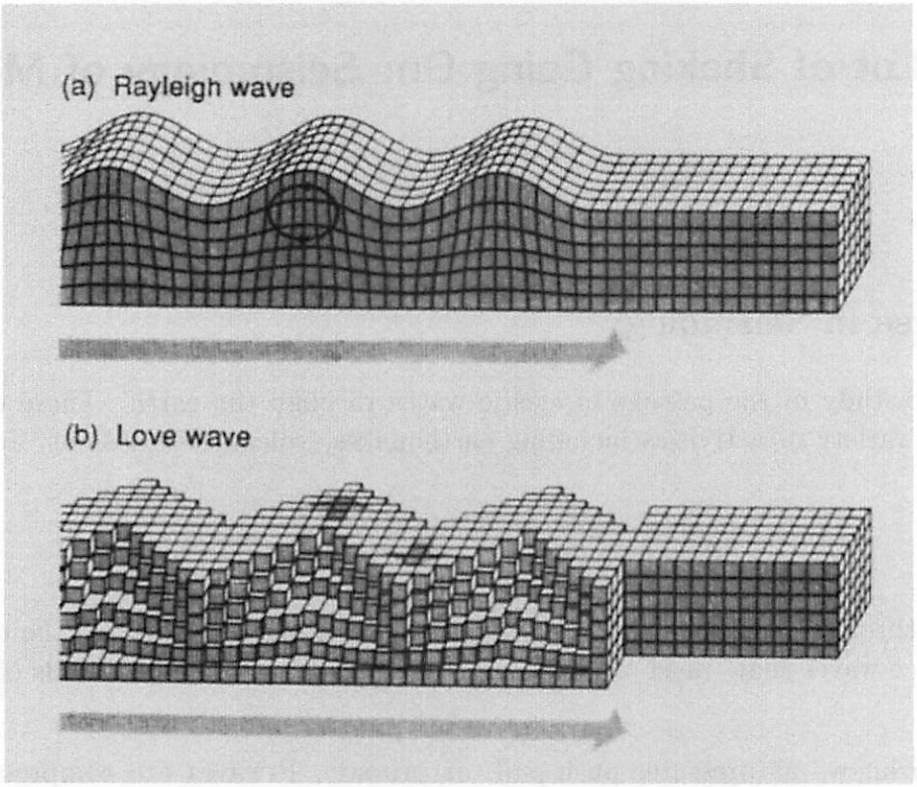

between the arrival of the body and surface waves can tell you how far away the event occurred from the detector. There are two types of surface waves **Rayleigh** and **Love** both named after dead guys. They take a couple paragraphs to describe, so just look at the Figure 1.

The main thing to remember about surface waves is that they are good for detecting shallow seismological activity, which Mount St Helens was.

Mount St. Helens

Activity before May 18

As an active volcano, Mount St. Helens rumbles rather regularly. The first sign that things were out of the ordinary was a gradual increase in detected earthquake counts between March 15 and March 20, 1980. On March 20, a shallow magnitude 4.2 earthquake was detected. After March 20, the number of earthquakes increased rapidly until they peaked at a rate of 6 events per hour on March 27. By March 24, seismologists had concluded that the source of the activity had to be volcanic in nature, due to the concentration and magnitude of events.

The peak in activity coincided with the first visible eruption (i.e. first cloud of gas and ash coming out). Over the next couple months seismologists installed an extra 15 seismograph stations in the vicinity. They detected a slow reduction in rate of seismological events, although there was an increase in average magnitude of the events. The new array helped pinpoint the sources of the events to be about 2 km north of the volcano summit, at depths varying from 0 to 5 km below the surface (this is what seismologists call "shallow").

May 18, 1980

At 0832 PDT, a magnitude 5.1 earthquake occurred at a depth of 3 km. It is believed that this event triggered the landslide and subsequent explosion that removed the northern flank of the volcano. After this large event, the seismographs detected only small events until 1140 PDT when the number of events started increasing until 1530 PDT when the stations within 100 km were saturated. At 1730, the amount of earthquake activity decreased rapidly.

Body waves detected on May 18 detected 2 distinct events of predominantly vertical force, representing the eruption of the volcano. These two events were two minutes apart and lasted 25 seconds.

Analysis of surface waves detected during the event showed a variety of activity lasting about 250 seconds. The initial pulse was resolved as being almost completely horizontal and pointing South, the opposite of the direction of the landslide. Later pulses track the direction change in the landslide and the vertical motion caused by the explosions.

Combining the analysis of both surface and body waves, seismologists were able to construct a schedule of events for the Mount St. Helens eruption, Figure 2.

Activity May 18, 1980 - present

The amount of earthquake activity continued to decrease over the months following the eruption, until the remaining events were only detectable by the stations still operating on the surviving flanks of the volcano.

Hazard Prediction

The eruption at Mount St. Helens followed a pattern that had been seen before at Kamchatka in 1956. The pattern goes as follows: 1) a period of volcanic earthquake activity 2) ash eruptions 3) declining earthquake activity 4) a cataclysmic explosion 5) a slow return to normal seismic activity (see Figure 3). This has become the pattern that seismologists use to identify an earthquake hazard. Note that there were no particular signs in the days or weeks before the large eruption that anything was out of the ordinary. Pin-pointing a large event to a day is very difficult, but a pattern of activity over the timescale of months to a year can predict whether there will be a large explosive event.

Planetary Connection

The methods used to detect earthquakes are also useful in telling you something about the medium that they travelled through. Therefore, exploration of any rocky bodies in the system will need to include a seismological study. A set of seismic detectors on Europa could easily settle the ocean question. The moon already has a set of seismic detectors on the surface, but sadly only on the near side, so the interior is still poorly understood.

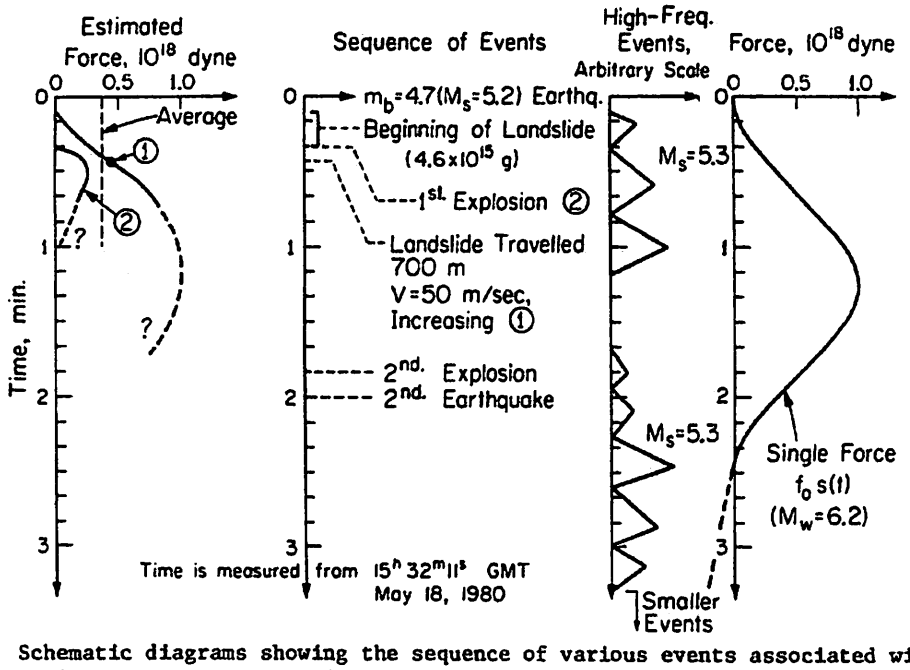

Fig. 8. Schematic diagrams showing the sequence of various events associated with the Mount St. Helens eruption. Time is taken positive downward. The time history of the single force determined from surface waves is shown on the right, and the magnitude and the time history of the force estimated from the reported sequence are shown on the left. References are Voight et al. [1982], Glicken et al. [1981], Moore [1981], Moore and Rice [1981], Malone et al. [1982], and Kieffer [1981a, b].

References

Seismology Review section* was lifted from The Solid Earth by C. M. R. Fowler.

A good chunk was taken from USGS PP 1250. The other papers are in my office. Drop by if you care.

4 The May 1980 Mount St. Helens Rockslide-Debris Avalanche

by JIM RICHARDSON

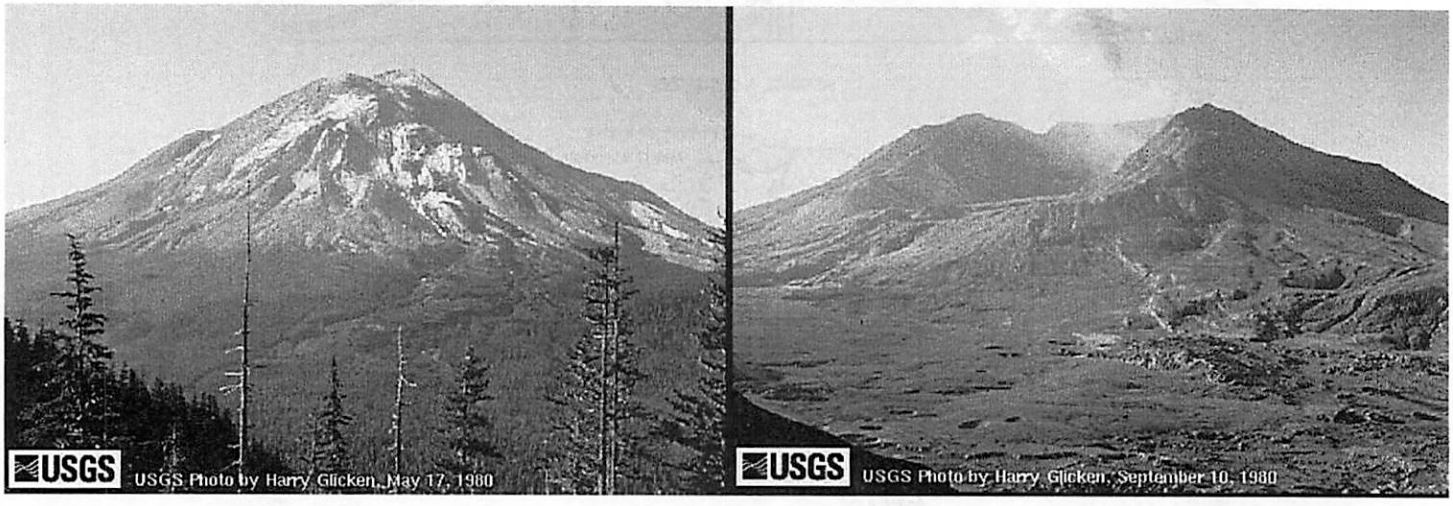

Figure 4.1: Mount St. Helens as photographed from Johnston Ridge: (*left*) just prior to the eruption on May 18, 1980, and (*right*) a few months after the eruption, showing the decapitated mountain and large debris flow in the foreground, which has replaced the forest pictured on the left. (USGS photographs)

Introduction

The rockslide-debris avalanche associated with the May 18, 1980 eruption of Mount St. Helens in Washington state is cited as being one of the largest debris avalanches in recorded history, consisting of what was nearly the entire upper portion of Mount St. Helens, and having a volume of about 2.5 km^3. The initial rockslide was triggered by a magnitude 5.1 earthquake which occurred following a period of bulge formation on Mount St. Helens in the few months prior the slide. This initial slide unroofed a forming magma chamber below, causing a tremendous pyroclastic blast, sustained eruption, and further collapse of the mountain.

The debris flow traveled a distance of 24-26 km at its distal end, dropping in altitude a distance of about 2.4 km (7900 ft), and thus has a H/L ratio of 0.096 (slope of 5.5°) – classifying this flow as a long-runout landslide. The flow filled a long portion of the North Fork Toutle River valley with unconsolidated rock debris, covering an area of about 60 km^2. The average depth of the deposit is about 45 m, but is locally as deep as 180 m. Additionally, levees as high as 30 m occur along the margins of the deposit against the valley walls. According to the USGS report by Harry Glicken, the most conspicuous feature of the deposit is its hummocky chaotic surface morphology, with individual hummocks and ridges as high as 70 m, separated by low-lying areas and closed depressions, many of which now form ponds.

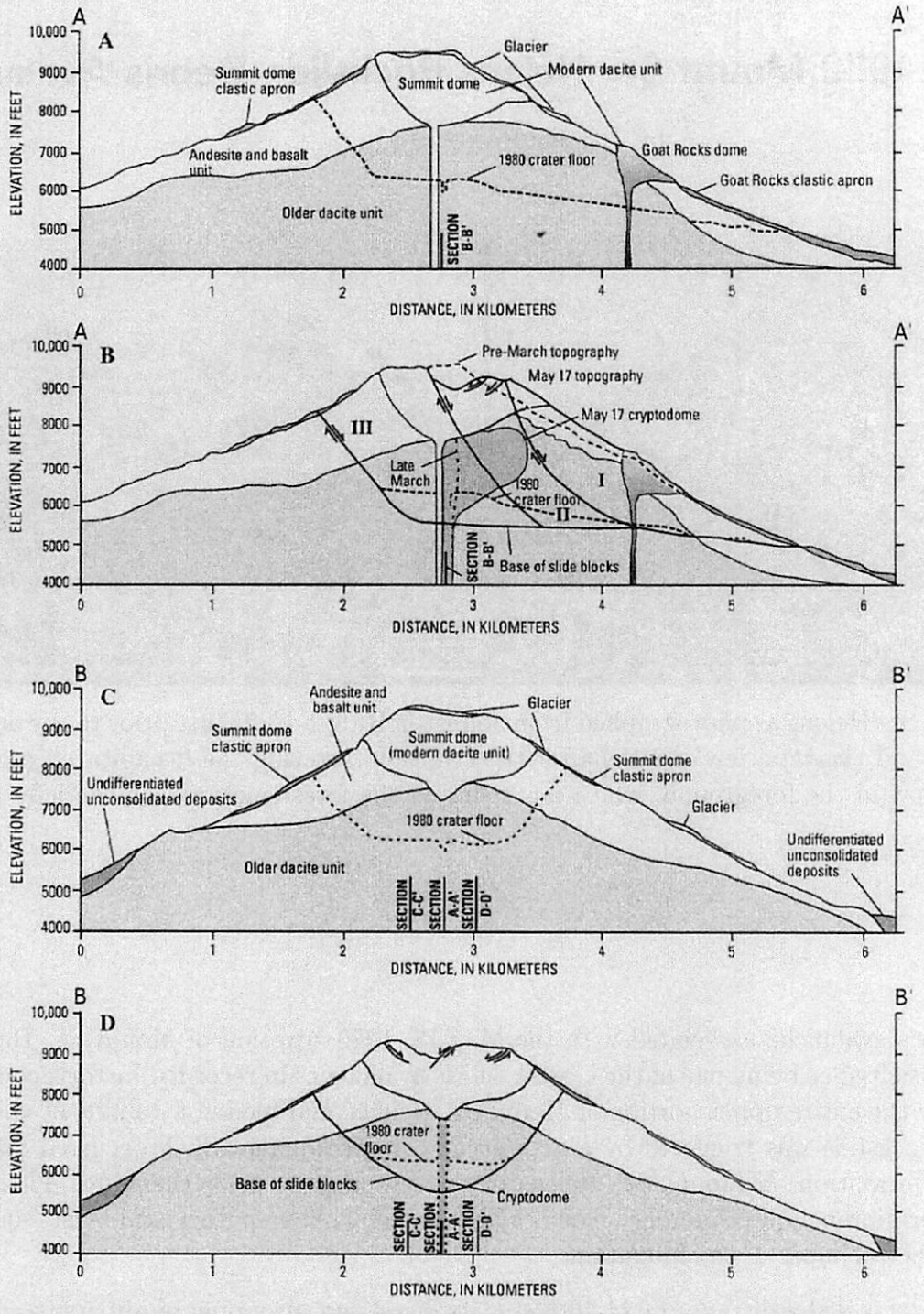

Figure 2. Cross sections of Mount St. Helens. I,II,III are slide blocks. Locations on figure 1. A, *A- A'* pre-March 1980. B, *A-A'* at time of failure, 8:32 a.m., May 18, 1980. C, *B-B'* pre-March 1980. D, *B-B'* at time of failure. E, *C-C'* pre-March 1980. F, *C-C'* at time of failure. G, *D-D'* pre-March 1980. H. *D-D'* at time of failure.

Figure 4.2: Cross-sections of Mount St. Helens, before and just prior to the rockslide and eruption. The slide can be divided into three major blocks (labelled I, II, and III), which broke loose in succession following the initial earthquake. Note the basic geological structure of the mountain, consisting of an old dacite base, an andesite/basalt upper layer, two younger dacite domes (Summit and Goat Rock), along with the newly intruded dacite cryptodome. (from Glicken, 1996)

Pre-slide Geologic Structure

Figure 4.2 displays the geological structure of Mount St. Helens prior to the May 1980 eruption, dividing the mountain into four basic extrusive volcanic rock types as follows (listed in order of age);

- *Old Dacite Unit:* A lightly colored hornblende-hypersthene Dacite (an intermediate stage between Rhyolite and Andesite), characterized by abundant large ($> 2\ mm$ length) phenocrysts of plagioclase and hornblende. This unit forms the bulk of what is known as "Old Mount St. Helens" and rests on a Tertiary aged bedrock of slightly metamorphosed igneous rocks. The older dacite unit ranges from about 40,000 years old at the mountain's base to 2500 years old in the current crater exposures (late Pleistocene / Holocene epochs). This unit is frequently cut by dikes of younger material, described below.

- *Andesite and Basalt Unit:* A darkly colored andesite and basalt unit rests on the Old Dacite Unit, and appears in both flow and scoriaceous tephra forms. These flows are from about 2200 to 350 years in age, contain small phenocrysts of plagioclase, and show some red aqueous alterations in addition to their generally black to dark grey coloration.

- *Modern Dacite Unit:* A lightly colored augite-hornblende-hypersthene dacite comprising the pre-1980 Summit Dome and Goat Rock dome. These rocks differ in appearance from the Old Dacite Unit in that they contain only very small phenocrysts (of hornblende, pyroxene, or plagioclase) and appear almost aphyric in hand samples. The Summit Dome portion of this unit is about 350 years old, while the Goat Rock dome portion was dated as being emplaced between 123 and 180 years before the 1980 eruption.

- *Cyrptodome Unit:* This unit is composed of the dacite magma body which rose up inside of the mountain just prior to May 18, 1980, and is the primary constituent of the pyroclastic blast/flow deposits. This material is a distinctive gray, microvesicular to subpumiceous hypersthene-hornblende dacite.

Rockslide-Debris Avalanche Sequence of Events

Details of the rockslide event were revealed in eyewitness photographs and show three individual slide blocks in the rockslide movement. The motion of slide block I was triggered by a magnitude 5.1 earthquake at 8:32 a.m. Pacific Daylight Time, with motion of the block beginning about 10 seconds later. This unroofed the magmatic cryptodome below, and triggered a pyroclastic explosion which burst through slide block II to produce the "blast surge." This blast surge overtook slide block I in its northward movement down the mountain, flattening trees and laying down a veneer of deposits underneath the advancing debris flow. By the time slide block I reached Johnston Ridge, it had reached an estimated speed of 50-70 m/s (110-160 mi/hr). As shown Figure 4.3, slide block I primarily moved north into Spirit Lake and against Johnston Ridge. In Spirit Lake, up to 240

ft of bottom deposits were emplaced, producing a large seiche and mud-flows in the lake area, and raising the final level of the lake by about 200 ft. The flow against Johnston Ridge moved up and over, scouring the 1100 ft high ridge of plant life and soil, and emplacing a ramp of material (a runup) called the "Spillover." Some material made it over and around the ridge into a branch of Coldwater Creek further to the north. Remaining portions of this block moved west into the North Fork Toutle River valley.

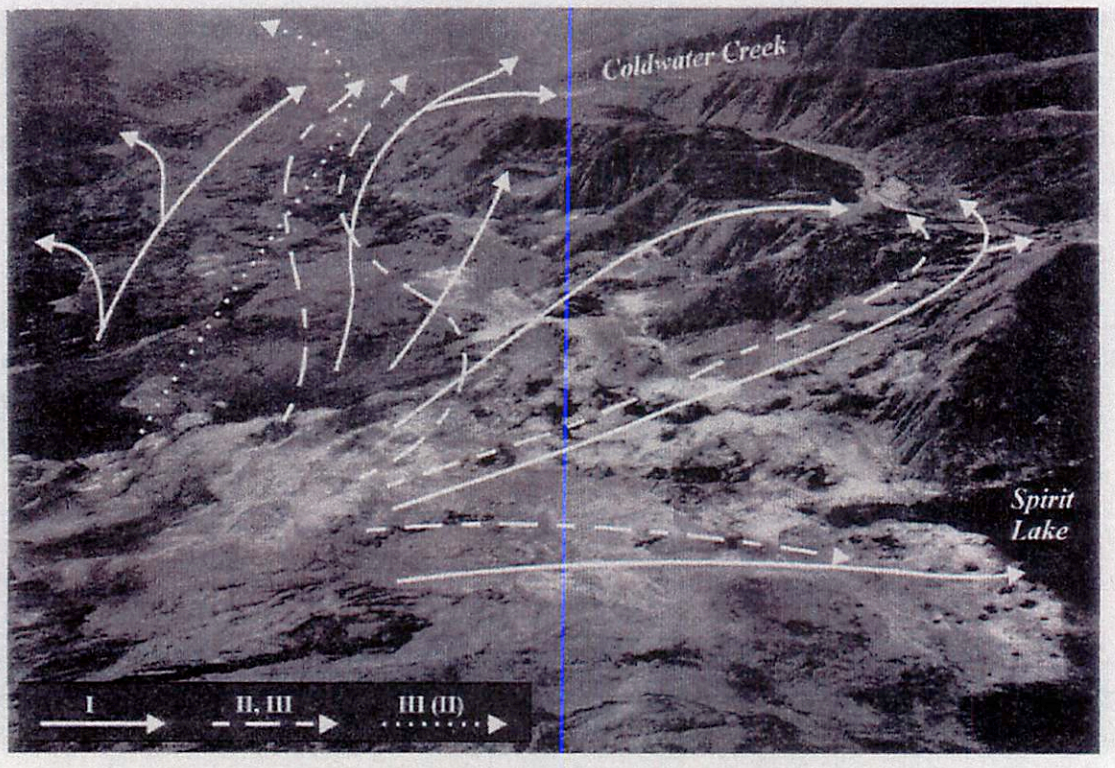

Figure 62. Oblique aerial photograph, looking west from Spirit Lake. Arrows show interpreted paths of slide blocks. Dotted line shows trace of slide block III, deposited first, and slide block II, deposited over slide block III material. Photograph by Austin Post, U.S. Geological Survey, June 4, 1980.

Figure 4.3: Photograph showing the general directions of motion for the debris flow, as designated by slide blocks. Note that slide block I primarily moved north into Spirit Lake and against Jonston Ridge, while slide blocks II and III primarily moved west into the North Fork Toutle River valley. (from Glicken, 1996)

Following the initial pyroclastic explosion, slide block II followed quickly on the heels of slide block I, while slide block III consisted of many discrete failures that occurred during the continuing pyroclastic currents generated from the exploding cryptodome. The cryptodome continued to depressurize after the loss of slide block III, producing a blast deposit that rests on top of the debris avalanche deposit. As these blocks broke up and transitioned from rockslide to debris-avalanche, they primarily proceeded west into the North Fork Toutle River valley (also carrying the remainder of slide block I) over a distance of 24 km and producing the bulk of the debris deposits. As the debris flow advanced down the river valley, it formed levees which blocked several entering streams and creeks. The two most prominent of these, Coldwater Creek to the north and Castle Creek to the south now contain lakes wich are held in place by fragile debris dams.

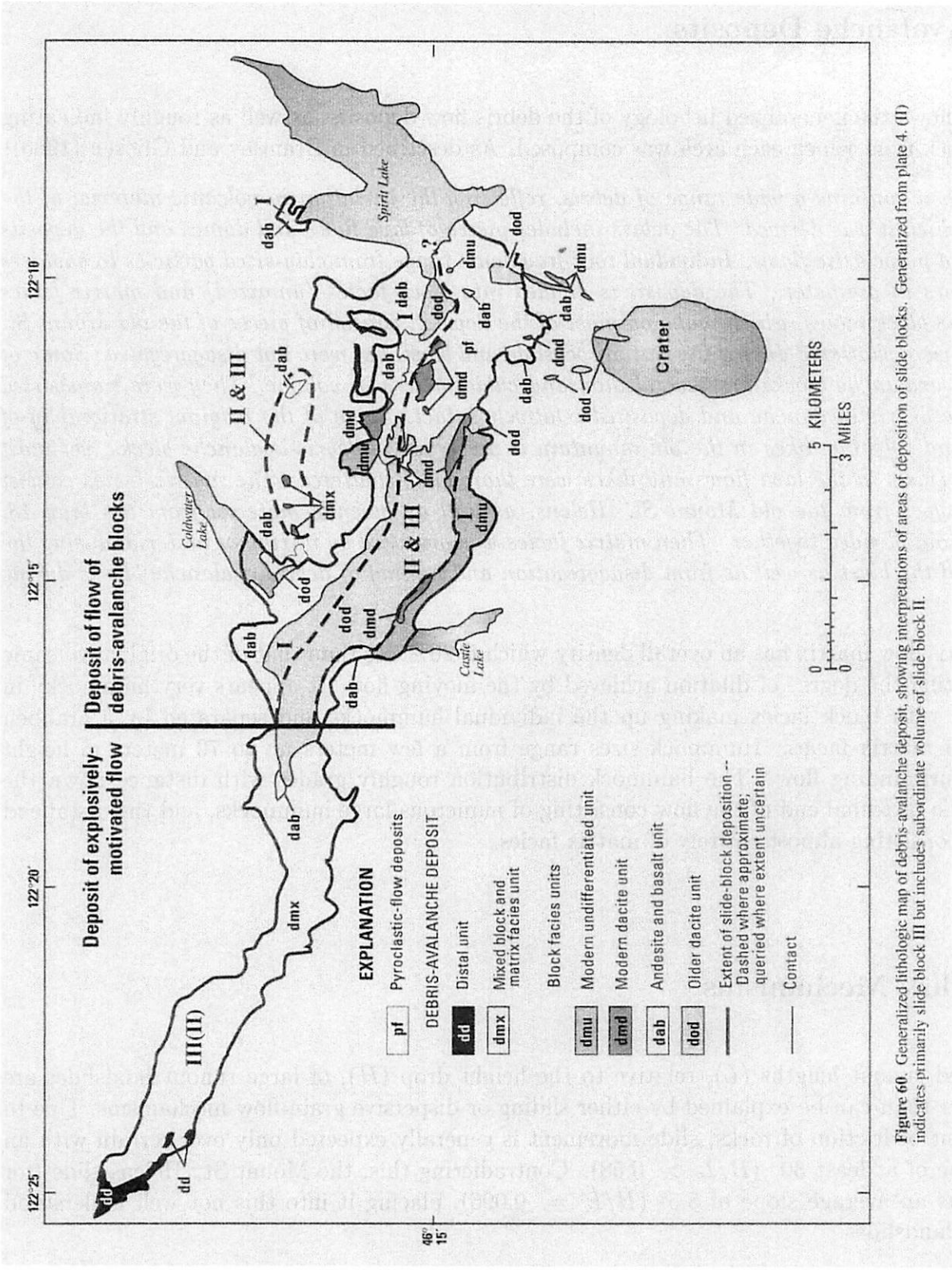

Figure 60. Generalized lithologic map of debris-avalanche deposit, showing interpretations of areas of deposition of slide blocks. Generalized from plate 4. (II) indicates primarily slide block III but includes subordinate volume of slide block II.

Figure 4.4: A map of the May 18, 1980 rockslide-debris avalanche, showing the final emplacement of remnants of the three initial slide blocks (labelled I, II, and III) as well as the primary volcanic rock unit comprising each area. (from Glicken, 1996)

Debris Avalanche Deposits

Figure 4.4 shows the generalized lithology of the debris flow deposits, as well as roughly indicating the slide block from which each area was composed. As described in Brantley and Glicken (1986):

The deposit contains a wide range of debris, reflecting the variation in volcanic material of the cone from which it was derived. The debris includes pieces of lava flows and domes and the deposits of lahars and pyroclastic flows. Individual rock fragments range from clay-sized particles to boulders several meters in diameter. The deposit is divided into block facies (unmixed) and matrix facies (mixed). The block facies, which make up most of the deposit, consist of pieces of the old Mount St. Helens that were shattered during the initial rockslide and blast, but were not disaggregated. Some of these debris-avalanche blocks are several thousand cubic meters in volume. They were transported gently in the debris avalanche and deposited relatively intact. Some of the original stratigraphy of lava flows and volcanic dikes in the old mountain is preserved in debris-avalanche blocks, yet most of the large clasts in the lava flows and dikes were thoroughly shattered. The matrix facies consist of all rock types from the old Mount St. Helens, as well as juvenile material from the May 18, 1980, eruption, blended together. Then matrix facies was produced by mixing of material during the explosions of the blast as well as from disaggregation and mining of debris-avalanche blocks during transport.

The debris flow matrix has an overall density which is 20% less than that of the original volcanic rock, indicating the degree of dilation achieved by the moving flow. It appears very hummocky in appearance, with block facies making up the individual hummocks and separated by a grabben composed of matrix facies. Hummock sizes range from a few meters up to 70 meters in height above the surrounding flow. The hummock distribution roughly grades with distance down the flow, with the proximal end of the flow consisting of numerous large hummocks, and the distal end of the flow consisting almost entirely of matrix facies.

Debris Flow Mechanisms

The observed runout lengths (L), relative to the height drop (H), of large runout landslides are much greater than can be explained by either sliding or dispersive grain-flow mechanisms. Due to the coefficient of friction of rocks, slide movement is generally expected only over terrain with an average slope of at least 30° ($H/L > 0.58$). Contradicting this, the Mount St. Helens slide (for example) has an average slope of 5.5° ($H/L = 0.096$), placing it into this not well understood catagory of landslides.

The mechanism for the long-runout landslide is a long-standing problem in geophysics, and remains controversial and under investigation. Some of the more notable theories include (taken from McEwen, 1989) fluidization by air (Kent, 1966), frictionless support on a layer of trapped and compressed air (Shreve, 1966-68), inertial grain flow or mechanical fluidization (Davis, 1982), and grain support by acoustic energy (Melosh, 1979, 1987).

The Planetary Science Connection

Landslides and slumps are a common feature on non-terrestrial terrain having a high degree of surface relief, occurring in connection with impact craters, fault scarps, volcanic activity, and channel scarps (Mars). Other bodies upon which we have imaged slides or slumps in one form or another include the Moon, Venus, Mars, Phobos, Eros, and the Galilean satellites. Long-runout landslides have been studied on Venus and Mars (and perhaps Phobos), including a study performed by Alfred McEwen on slides in the Valles Marineris area (shown in Figure 4.5), in which the effects of a lower gravity field and lack of atmosphere (along the with a lack of water) on these slides were investigated.

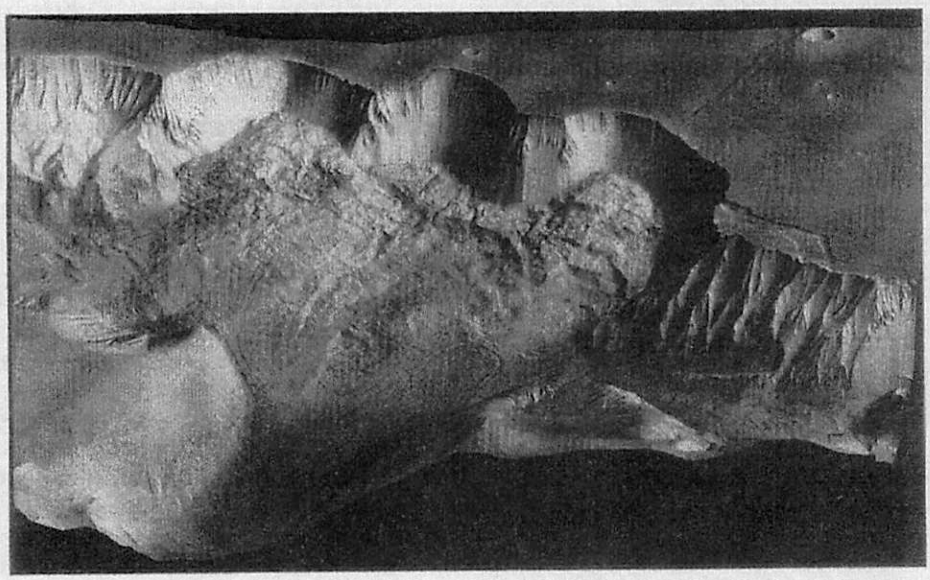

Figure 2. Synthetic oblique view from south of landslides in Ophir Chasma, Mars. Observer is 25° above horizon. Three large landslide slump scars occur in center of scene, and part of fourth slump scar is visible at right margin. Slopes in landslide scars are near 30°, whereas older slopes (with gully and ridge morphology) are near 20°. Vertical exaggeration 2×. Width of scene is 120 km, and maximum vertical relief (from low area in front to plateau surface) is 9.4 km. Oblique view produced by orthographic rotation using two data sets: digital mosaic of area and digital elevation model produced from 1:500 000-scale topographic map.

Figure 4.5: A series of long-runout landslides asssociated with a channel scarp on Mars (see caption above for details). (from McEwen, 1989)

References

Glicken, Harry (1996). *Rockslide-Debris Avalanche of May 18, 1980, Mount St. Helens Volcano.* Washington: USGS Open-File Report 96-677.

Brantley, and Glicken (1986). *Volcanic Debris Avalanches: Earthquakes & Volcanoes*, v.18, n.5.

McEwen, Alfred (1989). Mobility of Large Rock Avalanches: Evidence from Valles Marineris, Mars. *Geology*, v.17, p.1111-1114.

5 Lateral Blast of Mount St Helens

by JOHN WEIRICH

1. Intrusion of Magma
    (a) General increase in pressure bulged the north side of Mt. St. Helens (average of 5 meters per day). (Fig. 5.1)
    (b) This bulge deformed the magma body. (Fig. 5.2)
2. The landslide occurred and carried a large portion of the magma body and exposed it to the atmosphere.
3. Eruption
    (a) Water saturated magma, initially at 12.5 MPa and 600K, vaporized when exposed to the atmosphere.
    (b) Vaporization process carried $\sim 0.25 \times 10^15$ g of mass into the air at speeds ~100 m/s creating a heated "dust" cloud.
    (c) Multi-phase expansion caused by heated particles accelerated the blast to ~320 m/s.
    (Note: this speed is sub-sonic when compared to the surrounding "enhanced" density of the atmosphere)
4. Destruction path (Fig. 5.3)
    (a) Directed Blast Zone: path in which the blast was not deflected by topographic features.
        i. Speed of blast in this zone greater than Mach 1.
        ii. Irregular tree blowdown patterns.
    (b) Channelized Blast Zone: path in which the blast was deflected by topographic features.
    (c) Seared Zone: Trees were burned but still standing.

i. The temperature of the blast had only dropped by about 20% due to heating by the included solids.

ii. The blast expanded until the density was smaller than that of the surroundings, at which point it lifted away from the ground. This left a very small seared area compared to the blast.

iii. Areas sloping upward had larger seared zones, whereas downward sloping areas had smaller seared areas. This was due to the vertical rise of the blast.

5. Factoids of blast

   (a) Zone of silence due to super-sonic blast.

   (b) Lateral blast deposited a very thin layer of material, leaving no "fingerprint" on a geological time scale.

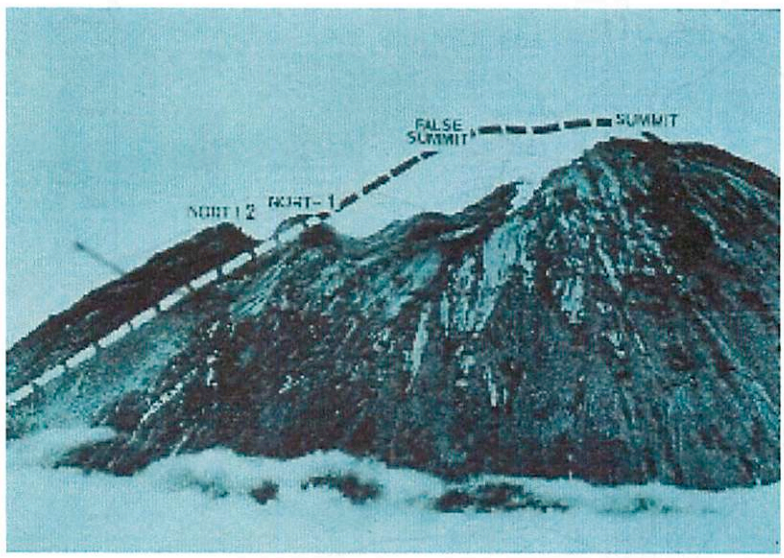

Figure 5.1: *Mount St Helens from the west in early May. Dashed line indicates pre-1980 profile. (USGS photo)*

Works Cited

1) Lipman, Peter W. and Mullineaus, Donat Ray. The 1980 Eruptions of Mount St. Helens, Washington. U.S. Dept. of the Interior, U.S. Geological Survey ; Washington, D.C., 1982.

2) Mount St. Helens, Washington. September 15, 2002.
USGS/Cascades Volcano Observatory, Vancouver, Washington. August 26, 2002 `http://vulcan.wr.usgs.`

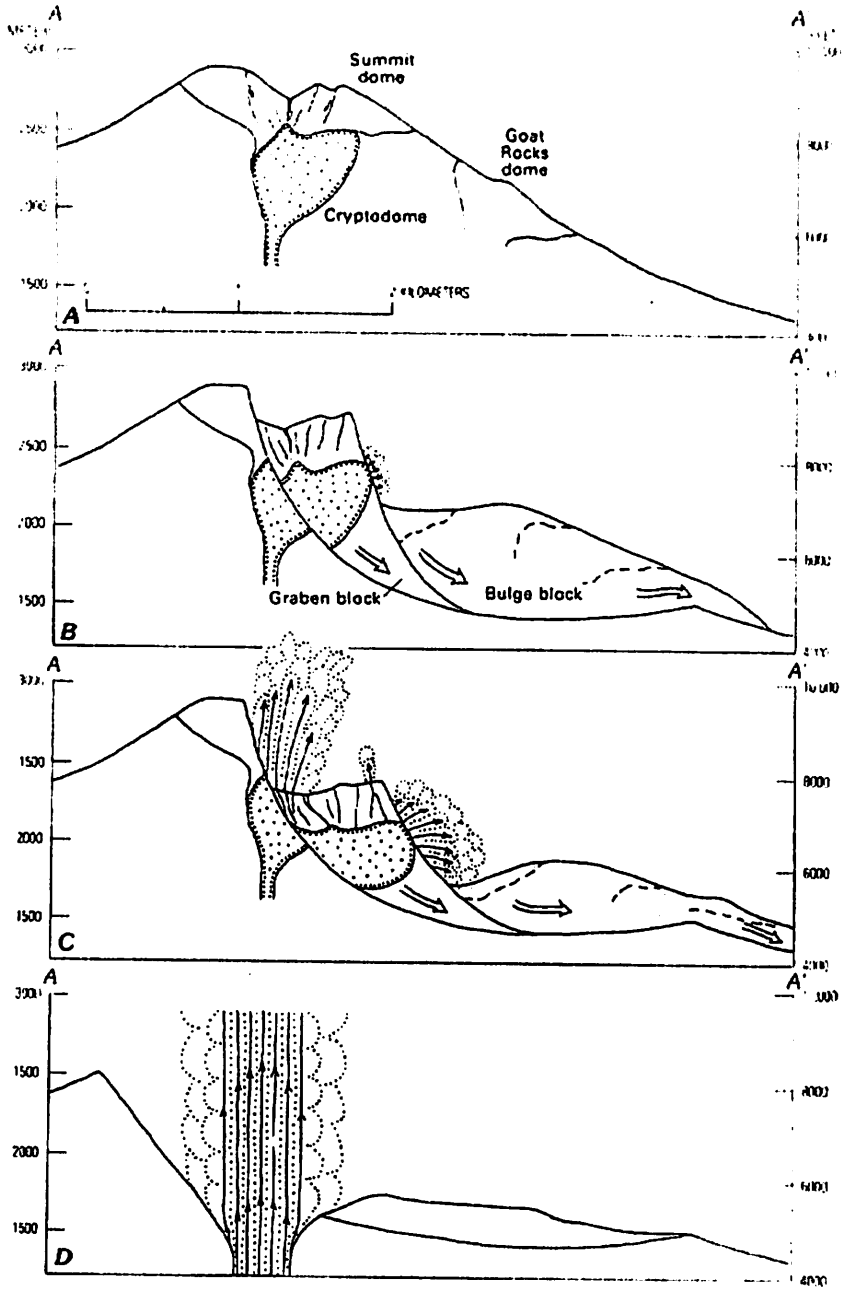

Figure 5.2: *Changes in profile of Mount St. Helens during morning of May 18, 1980. A, Before eruption showing intrusion of cryptodome (heavy dotted pattern). B, About 20s after landsliding began showing development of bulge and graben landslide blocks; explosions have begun on headwall of bulge block where cryptdome is exposed in graben block.. C, About 30s after landsliding began, showing massive explosions form side and top of fractured graben block. D, After landsliding has exposed the main volcanic conduit from which a vertical eruption column rises to more than 20 km.*

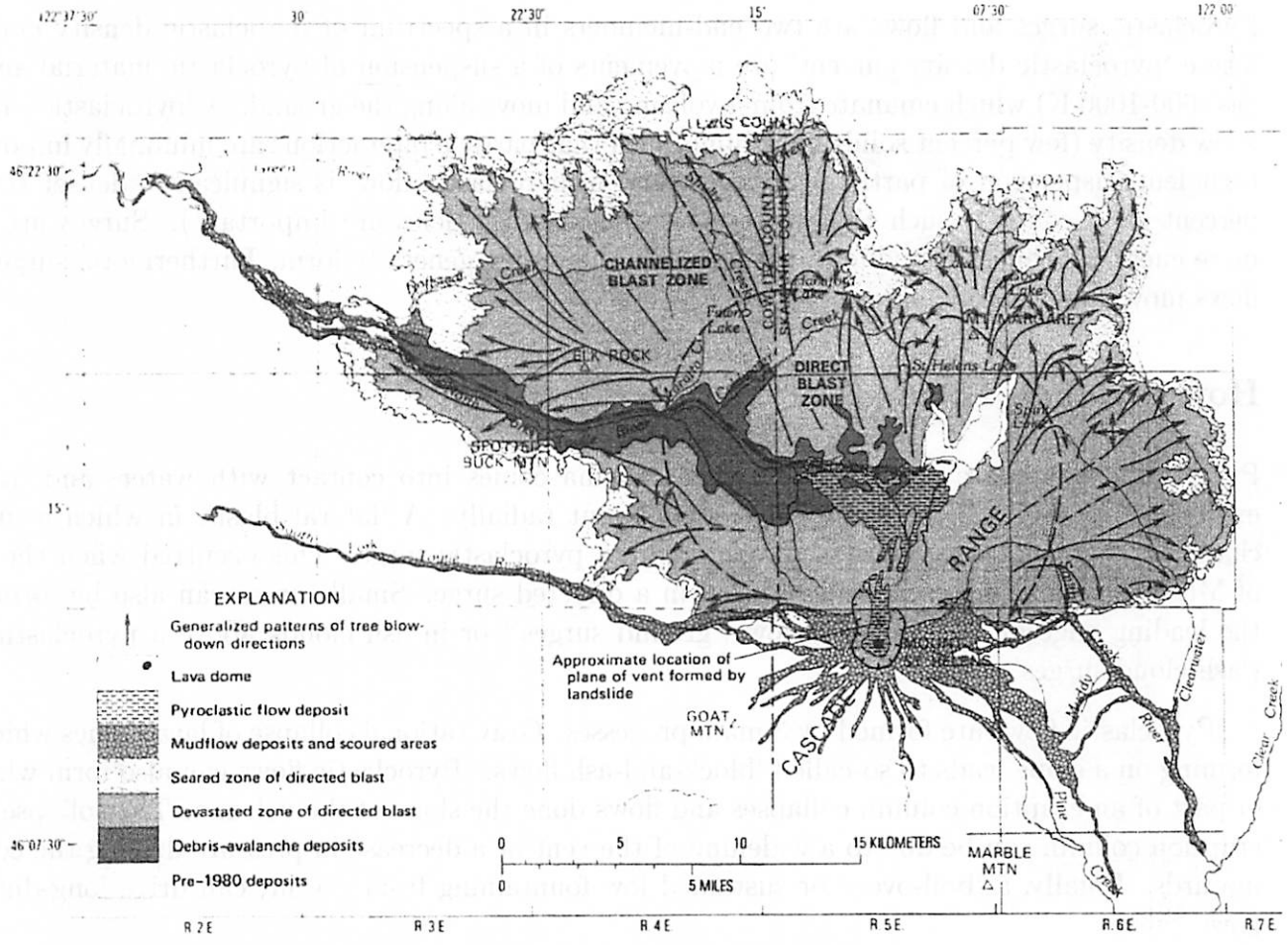

Figure 5.3: *Schematic map of devastated area and generalized directions of streamlines of the blast flow, as indicated by directions of alignment of fallen trees. Streamline arrows are dashed where information is lacking, Devastated area is divided into two zones (dashed line), the inner direct blast zone and the outer channelized blast zone. Note that near new vent (approximate location indicated by X), margin of blast zone lies south of vent in spite of the fact that flow emerged to north; however, at a distance of 10 to 20 km, margins have been deflected to northeast and northwest. Note also that singed zone is narrow compared to devastated area, and is wider where blast approached rising terrain (as in the northwest) and narrower where the blast approached falling terrain (as in the east) at its outer limits.*

6 The Physics of Pyroclastic Surges and Flows

by DAVE O'BRIEN

Description

Pyroclastic surges and flows are two end-members in a spectrum of pyroclastic density currents. These 'pyroclastic density current' are movements of a suspension of pyroclastic material and hot gas (600-1000 K) which emanate from a volcano and move along the ground. A 'pyroclastic surge' is a low density (few percent solids by volume, such that particle interactions are minimally important) turbulent suspension of particles in a gas, and a 'pyroclastic flow' is significantly denser (tens of percent solid content, such that interactions between particles are important). Surges are often more energetic than flows, due to differences in how they generally form. Furthermore, surges and flows move and deposit material differently.

How are they Formed?

Pyroclastic surges are often formed when magma comes into contact with water, and literally explodes, creating a 'base surge' that spreads out radially. A 'lateral blast', in which a magma chamber is suddenly decompressed, can create a pyroclastic surge. This occurred when the flank of Mt. St. Helens collapsed, and resulted in a directed surge. Small surges can also be formed at the leading edge of a pyroclastic flow ('ground surges') or in ash clouds above a pyroclastic flow ('ash-cloud surges').

Pyroclastic flows are formed by 3 main processes. Gravitational collapse of lava domes which are forming on a slope leads to so-called 'block-and-ash flows.' Pyroclastic flows can also form when all or part of an eruption column collapses and flows done the slope of the volcano. The collapse of an eruption column can be due to a widening of the vent or a decrease in pressure driving the column upwards. Finally, a 'boil-over,' or sustained low fountaining from a vent, can drive long-duration flows.

How do they move?

Flows can travel 100-200 km/hr, and surges can exceed 500 km/hr. Due to their higher energy and lower density, surges can move over topography, while flows tent to follow pre-existing topography, such as valleys. Surges can travel up to about 25 km from their source volcano (further if they are ground surges or ash-cloud surges associated with a flow), and pyroclastic flows can travel over 100 km from their source. When the momentum driving the flow or surge outwards from its source decays, the surge or flow may loft into the air as a 'phoenix plume' which can stop the flow or slow it somewhat.

How do they deposit stuff?

Both surges and flows can transport and deposit thousands of km^3 of material. Surges tend to give a relatively uniform thickness deposit, while flows tend to preferentially fill in topographic lows. Surges tend to form sorted, finely bedded deposits, while flows generally give massive, poorly sorted deposits consistent with deposition from a dense suspension. Flows can carry larger particles due to their higher density, and can transport particles tens of centimeters or more in size.

The planetary connection

Pyroclastic flows and surges are expected to occur in association with volcanism on other planets. I'll let the Mars and Io people talk about that. In addition, 'cryoclastic' flows and surges could form where there is icy volcanism (i. e. on Europa or other icy satellites). It has been hypothesized that the depressurization of CO_2 reservoirs on Mars could lead to cryoclastic flows that could explain flow features without having to invoke liquid water.

References

[1] Dobran, F. *Volcanic Processes.* Kluwer Avademic, New York (2001).

[2] Druitt, D. H. 1998. Pyroclastic density currents. In: Gilbert, J. S. and Sparks, R. S. J. (eds) *The Physics of Explosive Volcanic Eruptions.* Geological Society, London, Special Publications, **145**, 145-182.

[3] Fisher, R. V. and H. U. Schmincke. *Pyroclastic Rocks.* Springer-Verlag, New York (1984).

[4] Hoffman, N. 2000. White Mars: A New Model for Mars' Surface and Atmosphere Based on CO_2. *Icarus* **146**, 326-342.

7 Physics of Plinian Plumes and Ash Deposition from the 1980 Mount St. Helens Eruption

by Mandy Proctor

Definition: A Plinian Plume is a sustained, explosive eruption which generates a high-altitude plume. These plumes occur when the discharge from the vent occurs over timescales much larger than the ascent time of the erupted material.

Three parts to the plume: (See Figures 7.1, 7.2, 7.3)
- Base: gas thrust region (extends from a few meters to several kilometers)
  - Pyroclasts and hot gas are ejected at speeds of up to 600 m/s.
  - Has diameter of orders of tens of meters.
  - Outer air around the jet is entrained and heated
  - The density becomes less than that of the surrounding air if enough heating and entrainment.
- Column: convective region (can extend for several kilometers)
  - Our plume will increase in width as it rises because of entrainment and heating, this will also make the plume buoyant.
  - In this region the vertical velocities increase with height, until they eventually reach a peak near the top of the column.
- Top: umbrella region
  - Stops rising when plume density equals that of the atmosphere.
  - The plume will then spread out laterally.
  - System can be treated as a large expanding gravity current.
  - Sedimentation occurs from the base of the cloud.

Four major types of ash deposited from the eruption: (See Figure 7.5)
- Largest: deposited at base of plume in the gas thrust region.
- Large: deposited in the convective region as materials are swirled around.
- Small: deposited at the base of umbrella, just at atmosphere and plume densities equal.
- Smallest: deposited from umbrella cloud. Fall from cloud as it spreads out.

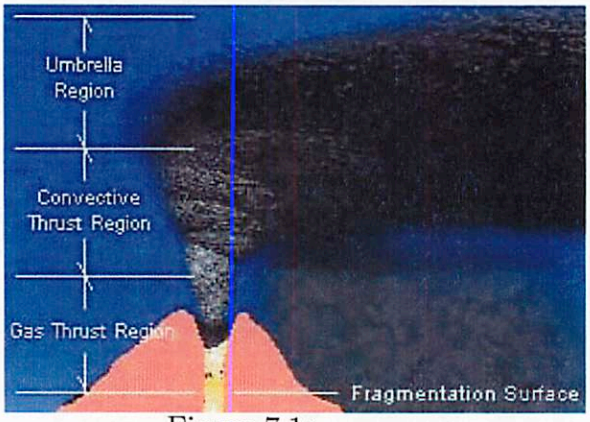

Figure 7.1:

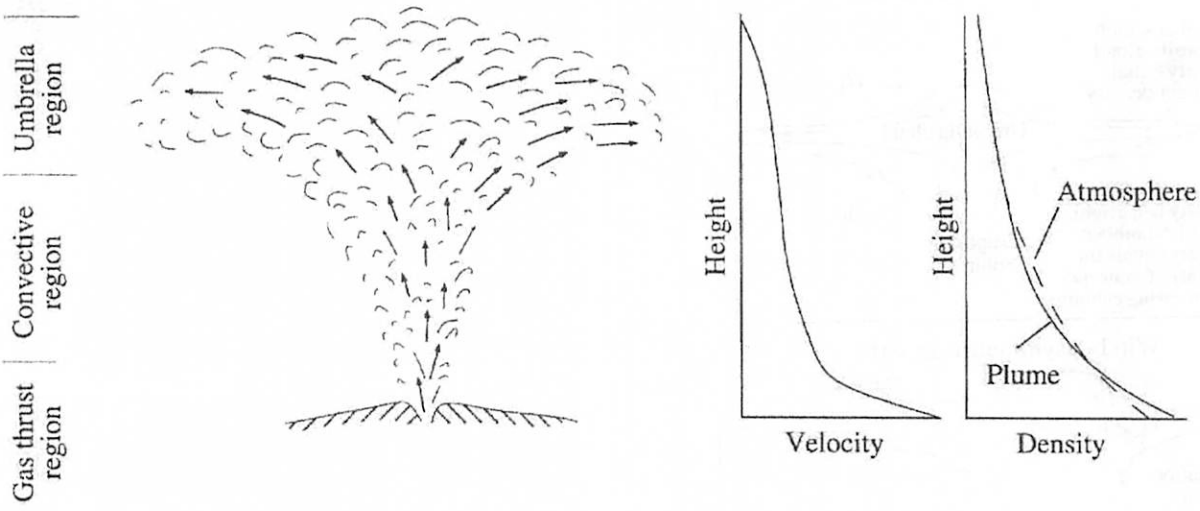

Figure 7.2:

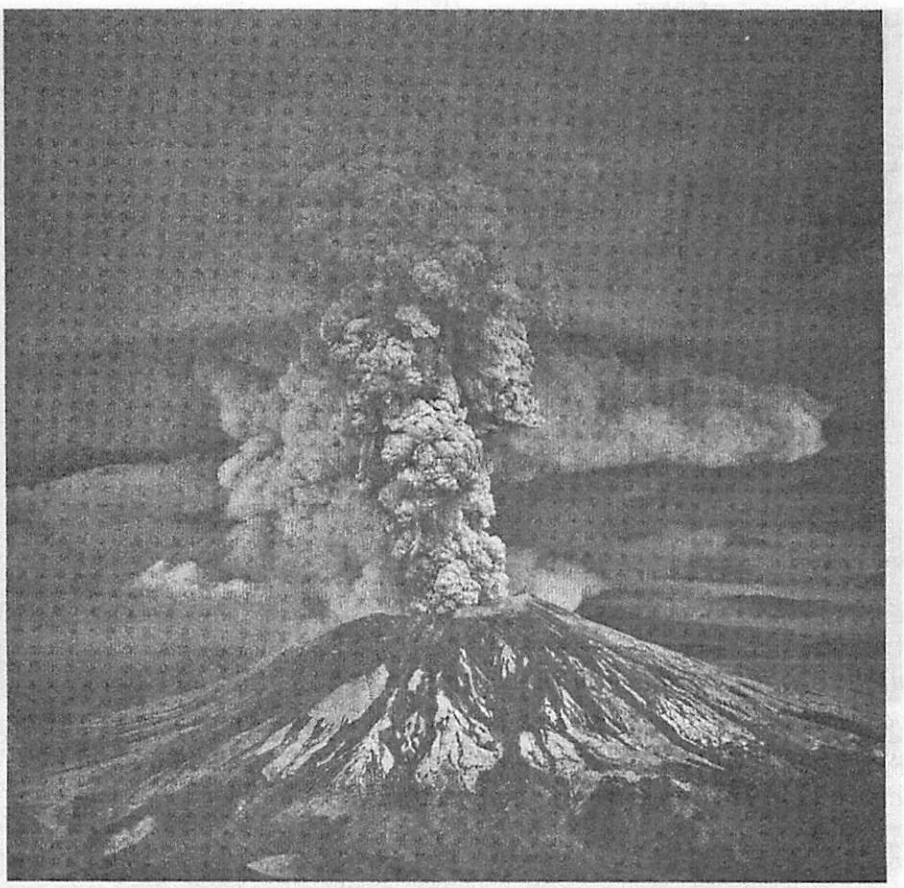

Figure 7.3: *Plinian eruption column developed over Mount St Helens during the May 18, 1980 eruption. (Courtesy of the US Geological Survey.)*

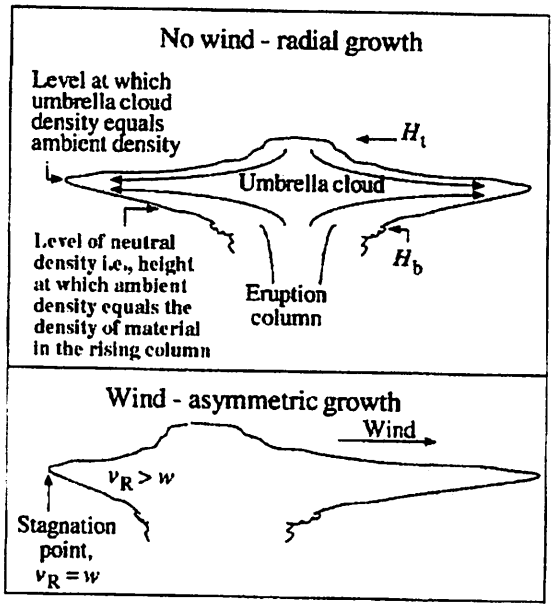

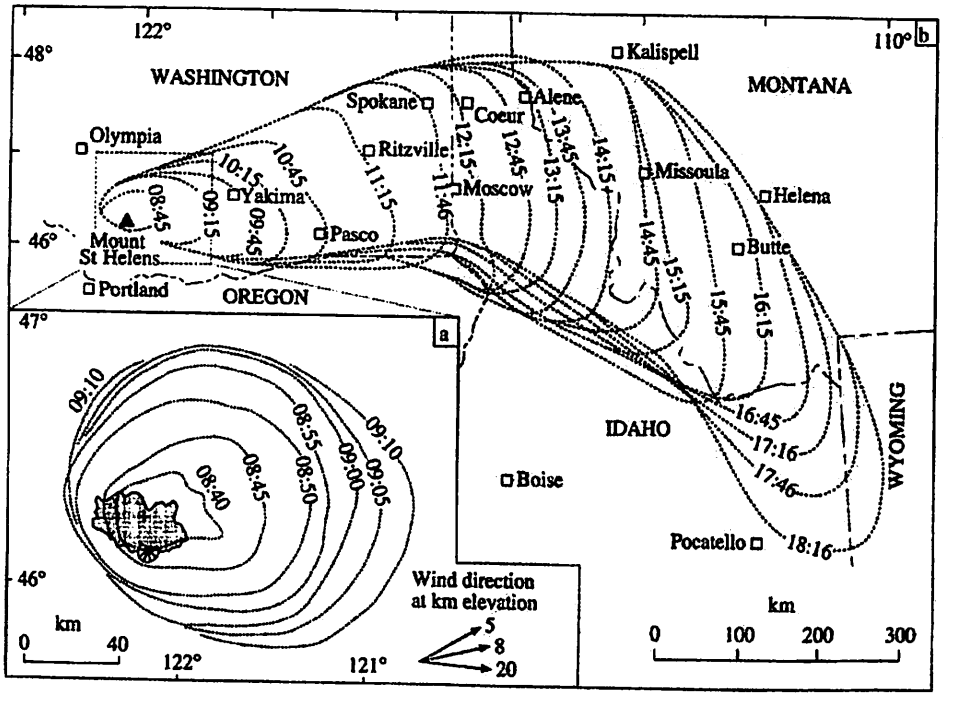

Figure 7.4: *(a) Map traced from satellite imagery showing the initial growth of the giant umbrella cloud of Mount St Helens (from Sparks et al. 1986). Contours are in five minute intervals labelled with local time in hours and minutes. (b) Map traced from satellite imagery showing the later growth of the May 18, 1980 Mount St Helens plume (redrawn from Sarna-Wojcicki et al. 1981)*

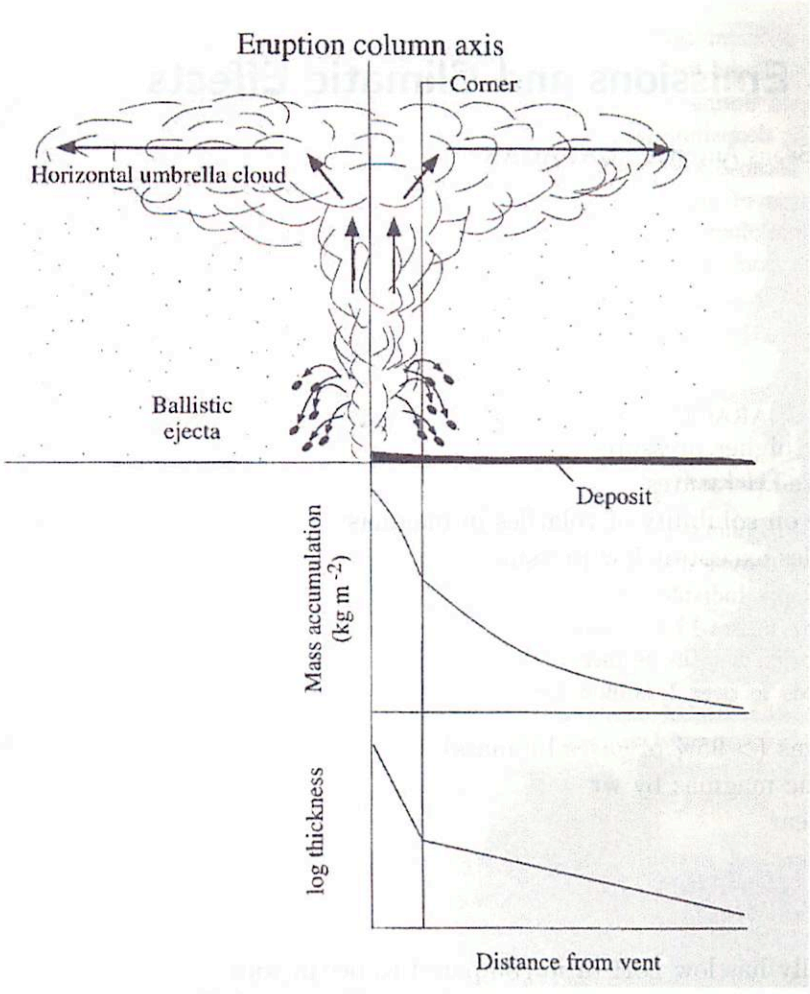

Figure 7.5:

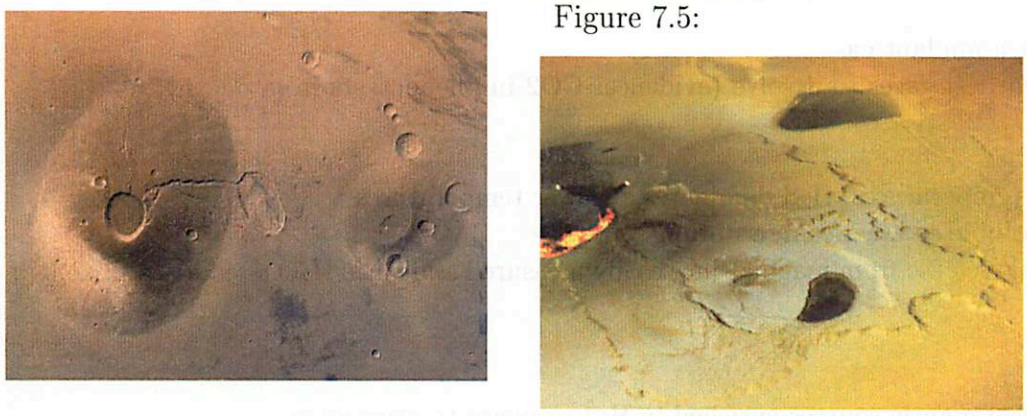

Figure 7.6: *(left) Mars — No Plinian Plumes. (right) Io — No Plinian Plumes.*

References

Mitchell, K.L., L. Wilson, L.S. Glaze, S.M. Baloga. (2002) Influence of Climate on Martian Magmatic Eruptions. Lunar and Planetary Science XXXIII.

Sparks, R.S.J., M.I. Bursik, S.N. Carey, J.S. Gilbert, L.S. Glaze, H. Sigurdsson, A.W. Woods. (1997) Volcanic Plumes. John Wiley and Sons. New York.

8 Mt. St. Helens 1980 Gas Emissions and Climatic Effects

by PETE "Beans Anyone?" LANAGAN

Background (Macdonald, 1972)

General Behavior of Gases in Melts

- volatiles are more soluble in magmas under higher pressure
- volatiles more soluble in magmas at lower temperatures
- pressure more important than temperature on solubility of volatiles in magmas
- magmas generally undersaturated in volatiles except at low pressures

Important Volcanic Gases

- **H_2O**
  - almost always most abundant volcanic gas (> 95% of gases by mass)
  - more soluble in silicic magmas than mafic magmas by wt
  - Problem in measurement — source unclear
    - magmatic?
    - meteoric?
    - phreatic (groundwater)?
  - useful identifier: magmatic water typically has low D:H ratio compared to ocean water
- **Carbon**
  - CO2 typically 2nd most abundant gas
  - Low solubility: one of earliest gases to exsolve (evidence: CO2 in phenocrysts from depth)
- **Sulfur Species**
  - include H_2S, S_2, SO_2
  - SO_2 dominates at high temperatures, H_2S dominates at lower temperatures
  - At high fO_2, SO_2 less soluble so escapes in eruption
  - used to determine volatile release from magma since easily measured and since H_2O does weird things (like go into glasses)
- **Other gases**
  - Noble gases
    - He: magmas from deep mantle sources enriched in He^3 compare to atmosphere
    - Ar: magmas from deep mantle sources enriched in Ar-36 compare to atmosphere
      - Suggests deep mantle not degassed early in earth history
  - Halogens and Friends
    - Cl, F, HCl, HF more abundant in continental rather than oceanic settings
    - Link b/t Cl and H_2O: more H_2O in magma, the sooner vapor saturation reached and sooner Cl evolved from magma
  - Hydrocarbons
    - plant material entrained in lava flows decompose
    - released hydrocarbons may ignite

Notable Historic Climatic Effects of Eruptions (as reviewed by Rampino et al., 1988; Rampino, 2002)

- Tambora: haze over troposphere noted over northern US; aerosol enhancement noted in Greenland ice core data for this period
- Laki: aerosols created "dry fog" over much of Europe; lower temps. in winter; destruction of Icelandic crops led to famine

Climatic Effects of the 1980 Eruption

- global effects: minimal
- Robock (1981) energy-balance model
  - stratospheric volcanic dust + gas-to-particle (mostly S compounds) contributes to cooling
  - models indicate maximum temperature amplitude due to MSH eruption $< 0.1°C$
  - (much less than standard deviation of temperature in region: 2.5°C in winter, 1°C in summer)

The Planetary (Other Than Earth) Connection

Mars

- Plescia (1993) proposed volatiles released from Cerberus Plains volcanism could have climatic effects
  - H_2O: local precipitation from flows may have had fluvial effects
  - CO_2: double CO_2 atmospheric mass
  - S species: warming due to greenhouse effect followed by cooling due to aerosol formation
  - Halides: contribute to duricrust (with sulfur compounds)
  - Issue: assumes volatiles released all at once, which is probably not the case

Venus

- presence of H_2S and H_2O in disequilibrium in Venusian clouds
  - used to argue for recent volcanism on Venus
    - within 1.9 Ma (Fegley and Prinn, 1989)
    - within 20-50 Ma (Bullock and Grinspoon 2001)

References

- Bullock, M. A. and D. H. Grinspoon 2001. The Recent Evolution of Climate on Venus. Icarus **150**, 19-37.
- Fegley, B. and R.G. Prinn 1989. Estimation of the rate of volcanism on Venus from reaction rate measurements. *Nature* **337**, 55-58.
- Macdonald, G.A. 1972 Volcanoes. Prentence-Hall Inc. Engelwood. pp 44-54.
- Plescia, J.B. 1993. An Assessment of Volatile Release from Recent Volcanism in Elysium, Mars. *Icarus* **104**, 20-32.
- Rampino, M.R. 2002. Supereruptions as a Threat to Civilizations on Earth-like Planets. *Icarus* **156**, 562-569.
- Rampino, M.R., S. Self, and R.B. Strothers 1988. Volcanic Winters. *Ann. Rev. Earth Planet Sci.* **16**, 73-99.
- Robock, A. 1981. The Mount St. Helens Volcanic Eruption of 18 May 1980: Minimal Climatic Effect. *Science*, 212, 1383-1384.

TABLE 1. Mount St. Helens Emissions

Emitted Species	Principal Physical and Chemical Roles	Relative and Total Abundances[1]					
		Ambient Air[2]		Fumarolic[3] Vapor		Stratospheric Plume[4]	
Ash	Light Scattering and Absorption, Sites for Condensation, Surface Chemistry	———		$\sim 10^{-2}$ - 10^{-3}	($\sim 8 \times 10^{8}$)	$\sim 10^{-5}$	($\sim 1 \times 10^{8}$)[5]
H_2O	Cloud Formation, Initiate HO_x Chemistry, Washout of SO_4^{2-}, Cl^- and NO_3^-	$2-4 \times 10^{-6}$	($\sim 2 \times 10^{9}$)	$\sim 10^{-2}$	($> 4 \times 10^{7}$)	$\sim 10^{-4}$	($\geq 1 \times 10^{7}$)
H_2	———	$\sim 4 \times 10^{-8}$	($\sim 2 \times 10^{7}$)		($\geq 5 \times 10^{3}$)[6]	———	
SO_2, H_2S	Precursors of Sulfate Aerosols.	$\sim 1 \times 10^{-10}$, $\ll 10^{-9}$	($\sim 1 \times 10^{5}$)	10^{-5} - 10^{-2}, 10^{-5} - 10^{-2} [7]	($> 2 \times 10^{5}$ tons S)[8]	$\sim 10^{-7}$, $< 10^{-9}$?	($\leq 1 \times 10^{6}$)
OCS, CS_2	Consume OH Radicals	$\sim 1 \times 10^{-9}$, $\leq 10^{-12}$	($\sim 5 \times 10^{5}$)	$< 10^{-4}$, $< 5 \times 10^{-6}$		$\sim 10^{-9}$, $\leq 10^{-10}$	($\sim 1 \times 10^{4}$)
SO_4^{2-}	Aerosol Light Scattering	$\sim 10^{-9}$	($\sim 5 \times 10^{5}$)		($\sim 10^{5}$)[9]	$\leq 10^{-8}$	($< 10^{5}$)[10]
HCl, CH_3Cl	Ozone Catalysis	$\sim 1 \times 10^{-9}$, $\sim 5 \times 10^{-10}$	($\sim 5 \times 10^{5}$), ($\sim 3 \times 10^{5}$)	———	($\geq 8 \times 10^{5}$ tons Cl)	$\sim 10^{-9}$, $\sim 10^{-9}$	($\leq 1 \times 10^{5}$), ($\sim 1 \times 10^{5}$)
Cl^-	Sink for Gaseous Chlorine	$\leq 10^{-11}$	($\leq 1 \times 10^{4}$)		($< 10^{6}$)[11]	$\sim 3 \times 10^{-10}$	($\leq 10^{4}$)[12]
S/Cl[13]	———	$\sim 0.1 - 1$		~ 1		1 - 100	
CO_2	Infrared Transmission	3.4×10^{-4}	($\sim 3 \times 10^{11}$)	3.4×10^{-4}	($\geq 1 \times 10^{7}$)[14]	3.4×10^{-4}	($\leq 1 \times 10^{7}$)[14]
CO	Tracer of OH	$\sim 1 \times 10^{-8}$	($\sim 1 \times 10^{7}$)	$< 5 \times 10^{-6}$	($\geq 4 \times 10^{4}$)[15]	$\sim 10^{-7}$[16]	($\leq 4 \times 10^{4}$)
CH_4	Source of H_2O, Smog Chemistry	$\sim 1 \times 10^{-6}$	($\sim 5 \times 10^{8}$)	$\sim 10^{-5}$		———	
NO_x	Active in Ozone Cycles	$\sim 1 \times 10^{-8}$	($\sim 1 \times 10^{7}$)		($\geq 3 \times 10^{2}$)[17]	———	
N_2O	Precursor of NO_x	5×10^{-7}	($\sim 3 \times 10^{8}$)	———		$\sim 5 \times 10^{-7}$	
NO_3^-	Sink for NO_x	$< 10^{-11}$	($< 10^{4}$)		($\leq 10^{4}$)[18]	$\sim 10^{-9}$[19]	

1. Estimates of relative abundances are expressed as mass mixing fractions. Total abundances, in brackets, are expressed in metric tons (10^6 g).
2. Air in the lower stratosphere. The sources of information are Hudson and Reed (1979) and WMO (1981). The total stratospheric burdens in metric tons are shown in brackets.
3. Primarily clouds near the volcano, although measurements taken in active fumaroles and vents were used to determine relative concentrations. Total abundances emitted during the May 18 eruption and subsequent major outbreaks are given in brackets. Data sources are surveyed in the text (also see the Mount St. Helens workshop report by Newell et al., 1982).
4. A discussion of the stratospheric data sources is presented in the text. Estimates of the total abundances of materials injected into the stratosphere are enclosed in brackets (values are based mainly on measurements in stabilized eruption clouds which have aged one day or more).
5. The quantity of ash remaining in the stratosphere more than a few days would be much smaller, perhaps $\sim 10^6$ tons.
6. A crude estimate based on the data of Evans et al. (1981) for the molar ratio, $CO_2/H_2 \sim 7 - 11$.
7. Values correspond to a wide range of conditions including active vents and cracks (Casadevall and Greenland, 1981; Evans et al., 1981).
8. Casadevall et al. (1981) measured total sulfur emissions of $\sim 1 \times 10^5$ tons S during quiescent periods at Mount St. Helens between May 25 and December, 1980.
9. Estimated using a lower limit for the sulfate found on ashfall particles of 100 ppm by mass (Taylor and Lichte, 1980; Stoiber et al., 1980; Newell, 1982). Phelan et al. (1982) found only ~ 5% of the total sulfur in one stable plume as particulates. Gas-to-particle conversion exaggerates the importance of primary sulfate emission.
10. Based on samples collected by Gandrud and Lazrus (1981) in clouds ~ 1 day old. Vossler et al. (1981) found condensed soluble sulfur to comprise ~ 0.1% of the ash mass in the same samples.
11. Chloride on ash samples ranged from ~ 1 - 1000 ppmm (Taylor and Lichte, 1980; Stoiber et al., 1980), much of which may have been scavenged from the gas phase.
12. Based on analyses of samples taken in one-day-old stratospheric clouds (Gandrud and Lazrus, 1981; Vossler et al., 1981).
13. Molar ratio, for total gaseous plus condensed materials.
14. The CO_2 emissions may be connected with SO_2 emissions using molar ratio data from: Harris et al. (1981), $CO_2/SO_2 \sim 9 - 12$, Casadevall and Greenland (1981), ~ 8 - 20, and Evans et al. (1981), ~ 30 - 144; average, ~ 30. Other data suggest the ratio could be as low as 1 - 10 (Newell et al., 1982).
15. The CO emissions are estimated using molar ratios relative to CO_2 measured in vapors from cracks and fumaroles: Casadevall and Greenland (1981), CO_2/CO ~ 130 - 220; Evans et al. (1981), ~ 140 - 190; average, ~ 170.
16. Enhancements in stratospheric CO were localized.
17. Using an NO/S molar gas ratio of 1.6×10^{-3} (Friend et al., 1982), neglecting NO_2 and other nitrogen oxides.
18. From measurements showing the nitrate composition of ash to be ≤ 10 ppmm (Taylor and Lichte, 1980; Fruchter et al., 1980). One sample yielded 100 ppmm of NO_3^-.
19. Average concentrations near the tropopause (Lezberg et al., 1982). Occasional patches with total (gaseous plus particulate) NO_3^- mixing ratios of 10^{-8} or greater were also seen (Inn et al., 1981).

Figure 8.1: *Gas Emissions from Mt. St. Helens - General Observations, from Turco et al., 1983.*

■ Turco, R.P., O.B. Toon, R.C. Whitten, P. Hamill, and R.G. Keesee 1983. The 1980 Eruptions of Mount St. Helens: Physical and Chemical Processes in the Stratospheric Clouds. *JGR* **88**, 5299-5319.

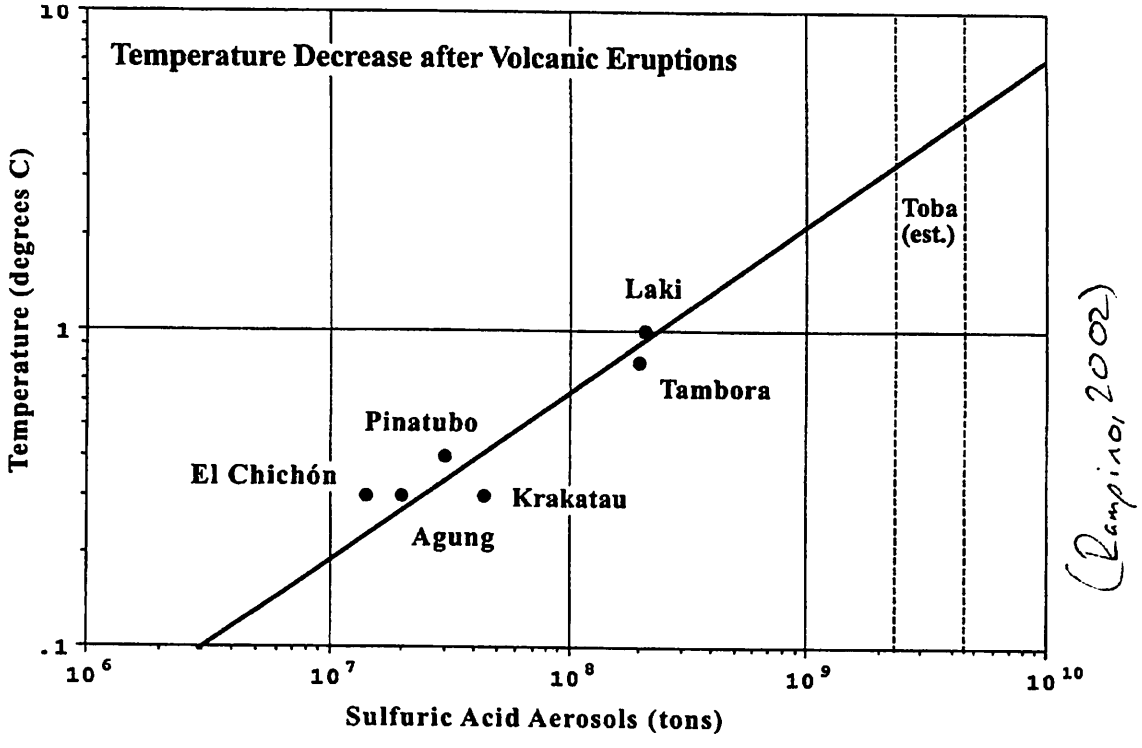

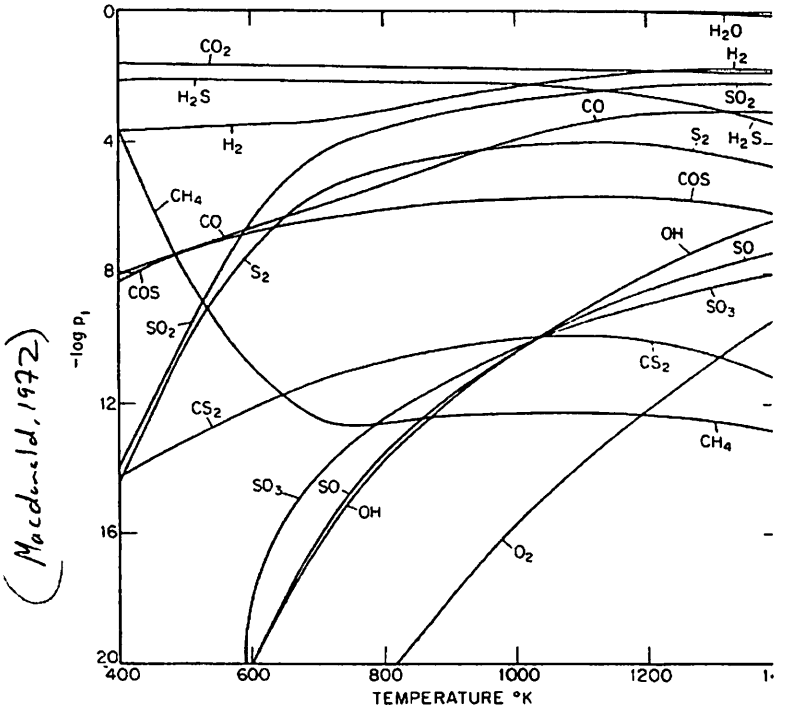

9 Magma Chemistry and Andesitic Volcanism

by MATT PASEK

Important Definitions

Magma "Molten rock" or a mixture of silicate melts, crystals, as well as fluids and gases

Lava Magma that has been extruded onto the surface of a planet

Fractional crystallization As a rock cools, crystals form. Fractional crystallization is the progressive removal of these crystals, and which results in differences between the crystals and the melt

Mafic A rock composed generally of magnesian minerals, such as olivine and pyroxene

Felsic A rock composed generally of feldspar and quartz (silica)

Intrusive A magma body that stays subsurface, and cools slowly. Coarse-grained

Extrusive A magma body that erupts as lava on the surface, cools rapidly, resulting in a fine-grained texture

Simplified View of Igneous Rock Types

	Mafic	Intermediate	Felsic
Intrusive	Gabbro	Diorite	Granite
Extrusive	Basalt	**Andesite**	Rhyolite

Chemistry of the Earth

Element	Earth[a]	Oxide	Mantle[a]	Oceanic crust[b]	Continental crust[c]
Fe	31	SiO_2	45.2	49.4	60.3
O	30	TiO_2	0.71	1.4	1.0
Si	18	Al_2O_3	3.54	15.4	15.6
Mg	16	FeO[d]	8.48	10.1	7.2
Ni	1.7	MnO	0.14	0.3	0.1
Ca	1.8	MgO	37.48	7.6	3.9
Al	1.4	CaO	3.08	12.5	5.8
Na	0.9	Na_2O	0.57	2.6	3.2
		K_2O	0.13	0.3	2.5
		P_2O_5	—	0.2	0.2

(a) Ringwood (1975). (b) Ronov and Yaroshevskiy (1976). (c) Taylor (1964). (d) Total iron oxide ($FeO + Fe_2O_3$). — Igneous rocks generally have compositions similar to Oceanic or Continental crust, and in rare cases, the mantle.

How do you get andesite?

Fractionation and Bowen's reaction series:
Progressive removal of crystallized rock from a melt results in enrichment of minerals that have low crystallization temperatures like quartz and Na-feldspar

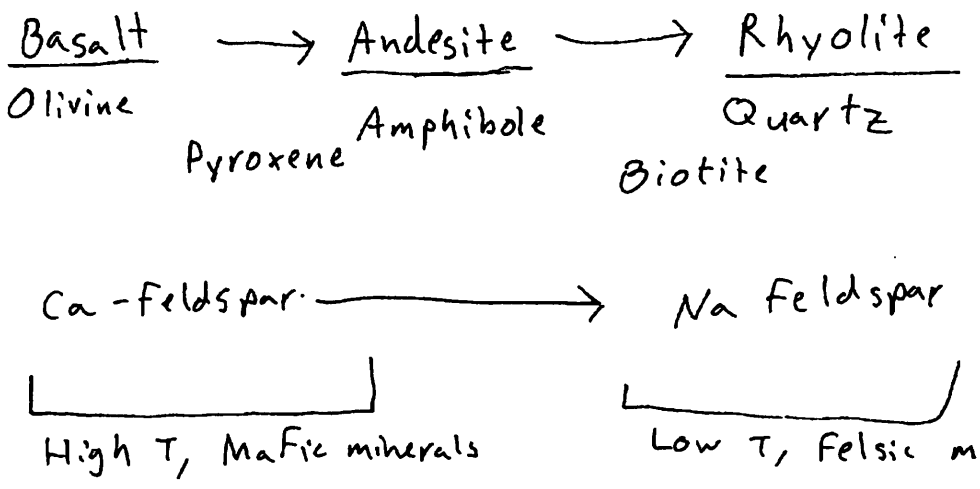

Fractional crystallization is seen in many volcanic settings, and probably also occurs here at Mt, St. Helens.

Mount St. Helens is composed of mainly andesite and dacite (which is more silicic than andesite). However, basalt and rhyolite can both be found in the stratigraphy of Mount St. Helens.

Magnesium, iron, calcium, and aluminum are removed from the magma through the crystallization of minerals containing these elements. Elements which have not been removed end up enriched.

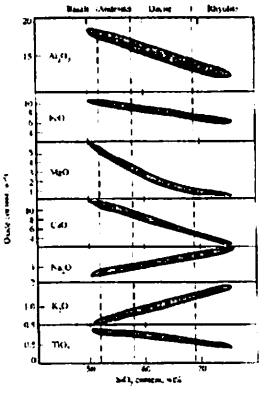

Crustal Mixing

Fractional crystallization is applicable to many volcanic systems. However, it is difficult to get a large volume of felsic magma from a mafic magma, especially on the scale seen in most continental environments. Some other process must be at work.

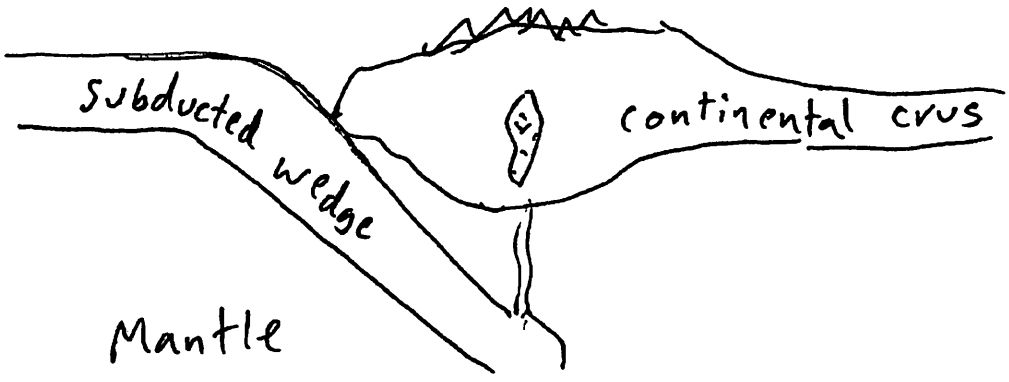

Dangerous Chemistry

The viscosity of liquid rock is roughly dependent on its silica content. SiO_4 tetrahedra can link together, forming a polymer or network. Cations such as Mg_2^+, Fe_2^+, Ca_2^+ and K^+ prevent this linkage, breaking the network. Thus rocks with lower silica and higher cation concentrations (like basalts) are less polymerized and therefore less viscous.

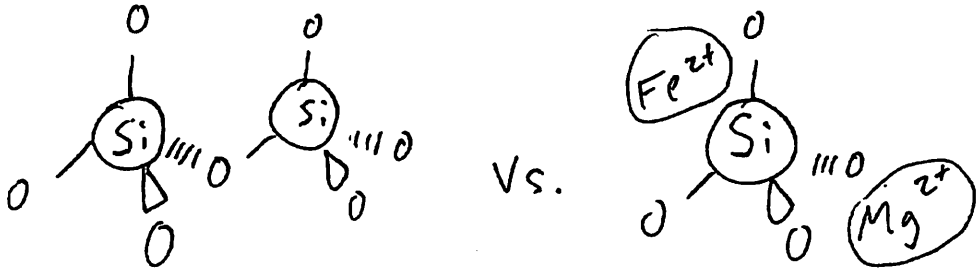

Also, magma that must travel through the crust tends to pick up a fair bit of water. As a result, continental volcanic eruptions tend to be much more violent and explosive due to the release of this gas than do drier magma bodies. As an example, think of the style of eruptions that take place in Hawai'i and compare them to what happened at Mt. St. Helens.

Why is andesite important for the Earth?

- Indicates active tectonics
- The continental crust has an overall composition similar to andesite
- The continental crust was formed through the generation of andesite at convergent plate boundaries
- No andesite, no land!

What about Mars?

The Mars Pathfinder/Sojourner mission investigated the composition of some of the rocks nearby its landing site. It found a $Na_2O + K_2O$ value of $\sim$ 4 wt. %, and a SiO2 content of $\sim$ 58 wt. (McSween, 2002). What rock type do these values correspond to?

What might this imply?
The controversy: As a basalt rock weathers, a silica-rich rind may form. Perhaps this is what the Pathfinder mission found. No conclusive evidence pointing one way or another has been found (Wyatt & McSween, 2002).

References

Blatt, H. and Tracy, R.J., 1996, Petrology: Igneous, sedimentary, and metamorphic. New York: W. H. Freeman and Company.

Ewart, A., 1982, The mineralogy and petrology of Tertiary-Recent orogenic volcanic rocks: With special reference to the andesite-basalt compositional range. In Andesites, ed. R.S. Thorpe. New York: Wiley, p. 25-95.

McSween, H.Y., 2002, The rocks of Mars, from far and near. Meteoritics & Planetary Science, v. 37, p. 7- 25.

Ringwood, A.E., 1975, Composition and Petrology of the Earth's Mantle. New York: McGraw-Hill.

Ronov, A.B., and Yaroshevsky, A.A., 1969, Chemical composition of the earth's crust. American Geophysical Union, Monograph 13, p. 37-57.

Taylor, S.R., and McLennan, S.M., 1985, The Continental Crust: Its Composition and Evolution. Oxford: Blackwell.

Wyatt, M.B., and McSween, H. Y., 2002, Spectral evidence for weathered basalt as an alternative to andesite in the northern lowlands of Mars, Nature v. 417, p. 263-266.

10 Landslides Damming the Columbia River

by SALLY HOUSE

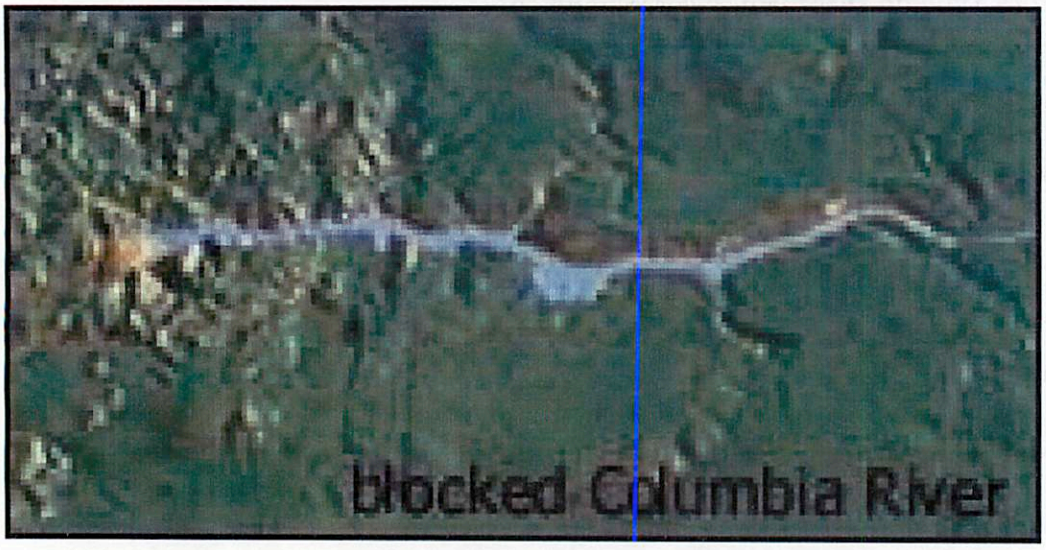

Figure 10.1: http://www2.opb.org/ofg/1105/bridge/geology.htm

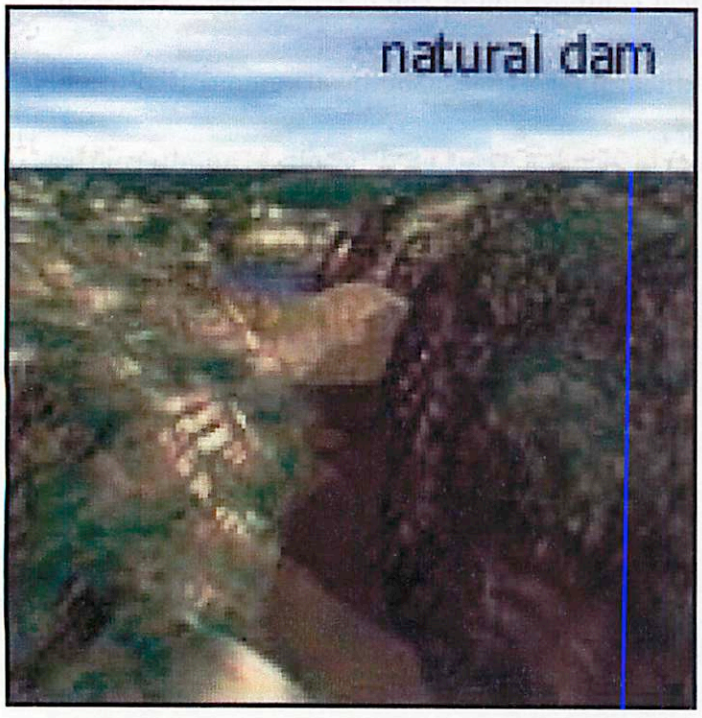

Figure 10.2: http://www2.opb.org/ofg/1105/bridge/geology.htm

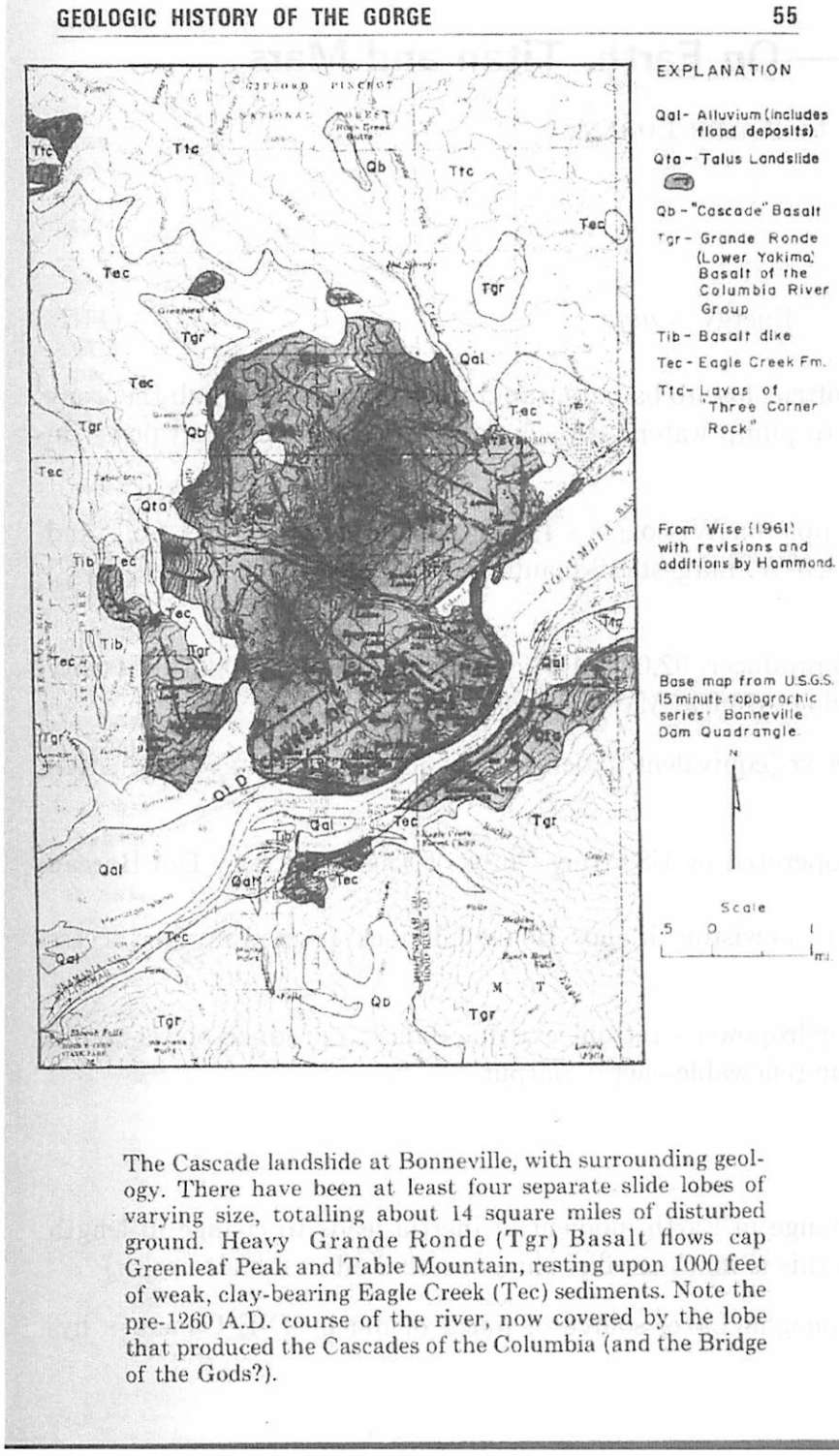

The Cascade landslide at Bonneville, with surrounding geology. There have been at least four separate slide lobes of varying size, totalling about 14 square miles of disturbed ground. Heavy Grande Ronde (Tgr) Basalt flows cap Greenleaf Peak and Table Mountain, resting upon 1000 feet of weak, clay-bearing Eagle Creek (Tec) sediments. Note the pre-1260 A.D. course of the river, now covered by the lobe that produced the Cascades of the Columbia (and the Bridge of the Gods?).

Figure 10.3: *The Magnificent Gateway* by John Eliot Allen Timber Press, Forest Grove, Oregon 1979

11 Hydroelectric Power — On Earth, Titan and Mars

by RALPH LORENZ

Hydropower

$$\text{Energy} = mgh \tag{11.1}$$

Hydroelectric power is useful - 'green', often close to bauxite, rapid start-up, reversible (nb the irony - original steam engines' function was to pump water. also common application of wind power in USA and solar power in e.g. Egypt)

First hydroelectric power plant 1882 Appleton Wisconsin - 12.5 kW (lighting two paper mills and a home) Modern plants typically $10^5 - 10^9$W. Largest US plant Grand Coulee - 10,080 MW. (cf 13 GW plant in Brazil)

In 1998 USA was world's leading hydro producer, 92,000 MW - supplying 9% of national electricity (49% of all renewable energy). Worldwide, 675,000 MW (24% of world electricity).

Bonneville Dam — 5 Billion kWh per yr (equivalent to demands of 500,000 homes) = production cost of 1.2 cents/kWh.

29 dams in Columbia River Basin -21 operated by US Army Corps of Engineers, 8 by DoI Bureau of Reclamation
Dams allow goods to travel 465 miles to Lewiston, Idaho. Bonneville lock granted upriver access to 11 million tons of goods in 1997.

Only 2,400 of US's 80,000 dams have hydropower - retrofit existing dams to produce power would be a modest-cost route to increasing the renewable-energy output.

Planetary Connections

Dams redistribute terrestrial mass. Change in Earth moment of Inertia leads to change in length of day of - few microseconds (although this is much smaller than seasonal effects due to snow)

another planetary connection - Manicouagan Lake, source of much of much ofNE Canada's hydropower, is an impact crater.

Hydroelectric Power - Generation of Potential Energy by atmosphere

Rainfall in a greenhouse world - a global increase since increasing optical depth forces tigher vertical convective flux? But distribution almost certainly different.

	Earth	Mars	Titan
Insolation $Wm^{-}2$	340	150	3.7
Convective Flux $Wm^{-}2$	~ 90	~ 10	~ 0.04
Surface Temperature K	290	200	94
$\Delta T(T_{surf} - Teff)$ K (=greenhouse)	40	2	10
Atmospheric Work $(F\ \Delta T/T)Wm^{-2}$)	13	1.5	~ 0.005
Average Annual Rainfall (cm) (Convective Flux/Latent Heat)	100	~ 10	~ 1

GCM simulations of a warm, wet Mars show precipitation fluxes of $\sim 50Wm^{-2}$ ($\sim$ 50cm/yr) poleward of 60 degrees latitude: equatorial regions get dried out. In the case of an oblique, warm, wet Mars (i.e. obliquity $\sim 60°$) the polar fluxes are the same, but there is additionally $\sim 100Wm^{-2}$ in a narrow midlatitude band. A warm, wet mars could .nly have been a factor ~ 2 less wet (in terms of rainfall) than present-day Earth.

Note even though energy fluxes are $\sim$ 1000 times lower on Titan than Earth, rainfall is only $\sim$ 100 times smaller there, largely through the lower latent heat of methane compared to water — we are reminded of Huygens' remark,

> *"But since 'tis certain that the Earth and Jupiter have their Water and Clouds, there is no reason why the other Planets should be without them.] can't say they are exactly of the same nature with our Water,. but that they should be liquid their use requires, as their beauty does that they be clear. For this Water of ours, in Jupiter or Saturn, would be frozen up instantly by reason of the vast distance of the sun. Every Planet therefore must have its waters of such a temper, as to be proportion'dto its heat: Jupiter's and Saturn's must be of such a nature as not to be liable to Frost..."*
> — Christiaan Huygens, The Celestial Worlds Discover'd, 1698

refs

`http://www.nrel.gov/lab/pao/hydroelectric.html`
Lorenz and Renno: Work Output of Planetary Atmospheres: Dissipation as Clouds and Rain, GRL, Vol.29, 10.1029/2001GL013771,2002 (####ing AGU numbering scheme!)
Abe, Y and Namaguchi, A. 2001. Water Circulation on a Land Planet: An Implication for Paleo-Mars, Lunar and Planetary Science Converence, Houston, TX. XXXII Abstract number 1551
`dgfi2.dgfi.badw-muenchen.de/dgfi/DOC/poster_99_seite12.pdf` (earth rotation)

Salmon

Chinook salmon (*Oncirhynchus tsawytscha*) have been recorded to dash as fast as 7 m/s, corresponding to a $\sim$ 2.5m jump (this would be $\sim$ 5m on Mars!) Salmon leaping is, as with most choices in nature, a selection of efficiency. Leaping becomes the most efficient way of ascending an elevation difference of more than 1-2 feet. studies of sockeye salmon (*Oncorhynchus nerka*) at a 1m Alaskan waterfall found that leaps were 11% successful (i.e. need to make 9 attempts to succeed.)

Note that as with bird migration, both salmon swimming and leaping exploit natural perturbations in the environment — in particular salmon swimming upstream must exploit eddies in the stream to avoid fighting uphill all the way. Leaping salmon are observed to attempt their jumps from specific locations along wide waterfalls — usually from the prow of a standing wave at the base of the fall. (This route selection in turn may be exploited by hungry and clever bears)

Salmon migration on the Stuart River in Canada (640miles) was observed to take $\sim$ 20 days, requiring a mean progress of 1.3 mph (0.6 m/s). Since the mean river speed is 1.5 m/s, the salmon would need to swim at 2 m/s.

(Salmon need clear, flowing water — high oxygen content to support energetic swim. Salmon typically lose $\sim$ 20% body mass (3/4 of that as fat, the rest protein, although much replaced by water) during migration. Also need to tolerate dramatic change in salinity.

Dams clearly present an obstacle to fish migration. Usual mitigation approach is salmon ladders. In reversible hydroelectric plants, careful pump design can reduce (but not completely eliminate) mortality. A bigger concern is that Salmon require gravel beds to spawn — gravel ultimately from landslides etc. (Thus salmon rely on tectonic and erosional processes, as well as the flow of water). Dams may prevent the gravel transport, both directly, and by reducing flow such that stream meander in flood plains is eliminated.

refs

www2.kenyon.edu/projects/dams/bec03wilsona.html
www-heb.pac.dfo-mpo. gc.ca/ congress/2000/migration.migration.pdf
J R Bett, The Swimming Energetics of Salmon, Scientific American, August 1965

12 Jointing in Basalts: Colonnade and Entablature in the CRB

by ROSS A. BEYER

joint A fracture on which any shear displacement is too small to be visible to the unaided eye.

colonnade A volcanic layer with columnar jointing which is regular and vertical.

entablature A volcanic layer with fanlike joints, commonly alternating with colonnades.

As lava cools, joints develop in the resulting rock mass. The joints form due to the contraction of the lava as it solidifies. These joints are generally observed to be perpendicular to a cooling lava surface, and are thought to form perpendicular to cooling fronts that move through the lava. The spacing of joints in a lava flow are indicative of how long the lava took to cool. The larger the spacing of the joints, the longer it took for the lava to cool.

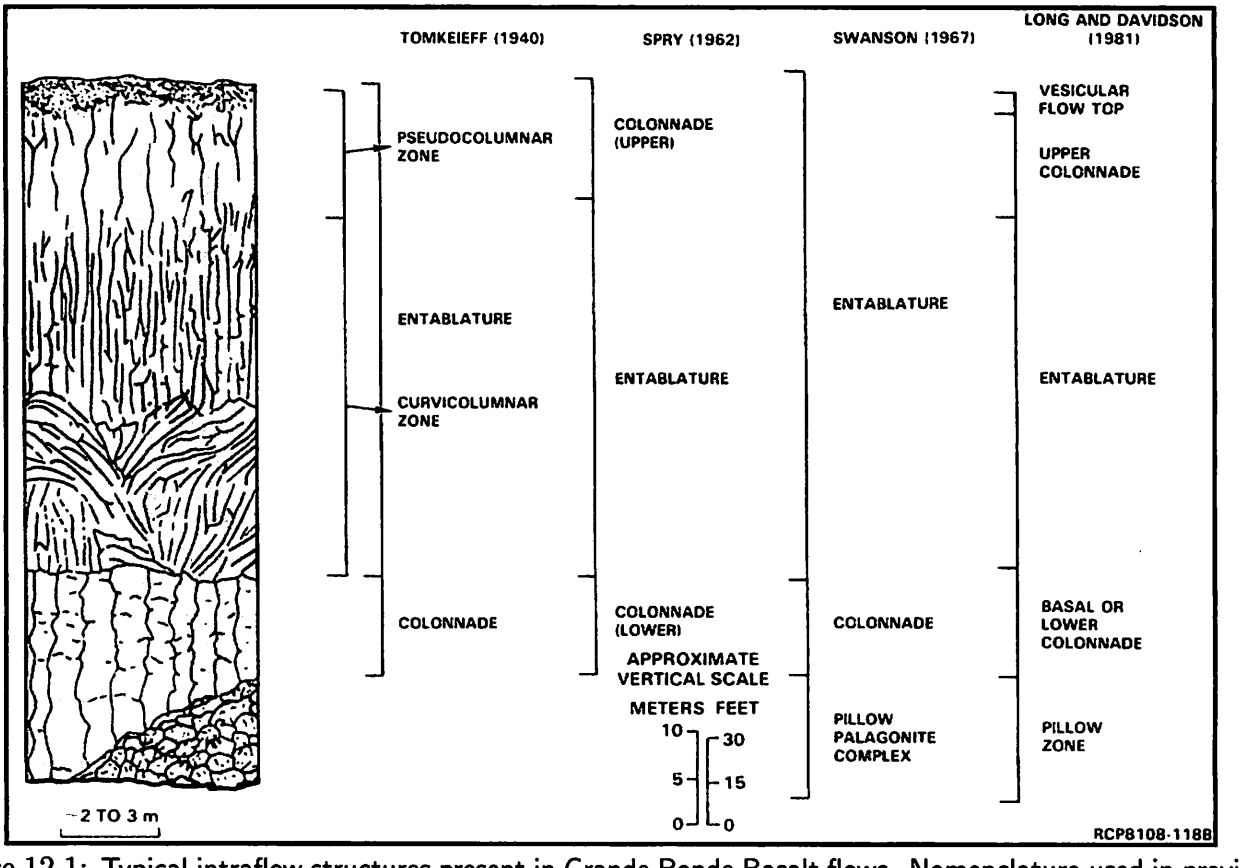

Figure 12.1: Typical intraflow structures present in Grande Ronde Basalt flows. Nomenclature used in previous studies is compared. Fractures in this figure and others are represented in a stylized manner; fracture widths not to scale. This figure taken from Long & Wood 1986.

Jointing in solidified lava is further broken down into two broad subtypes, colonnade and entablature. Colonnade is the more common type of jointing. Often entire flows consist of only colonnade, but when entablature occurs, the colonnade pattern is generally found on the upper and lower flow margins. Consisting of well-formed basalt columns with a regular spacing of ~0.3–2m. They are usually perpendicular to the base of the flow. Entablature generally either overlies the basal colonnade or occupies the interior of the flow. It consists of small irregular to hackly columns of ~0.2–0.5m in diameter. Entablature often forms radiating patterns or other patterns which are not perpendicular to the base of the flow.

Entablature has been found in a number of localities, like interglacial and post glacial lavas in Iceland; Giant's Causeway in Ireland ; near Melbourne, Australia ; the Deccan Traps in India; the Columbia Plateau in the United States; and one example near Hilo, Hawaii. The Grande Ronde basalts of the Columbia Plateau are a good place to study entablature because it is present in 60% of the exposed flows in this area. A much higher occurrence than other flood basalt provinces.

Long (1978), classified flows into three general types. Type I flows consist of an irregular colonnade and lack an entablature. Type II flows have repeated colonnade and entablature tiers. Type III flows have a lower colonnade, a single well-defined entablature, and often have a crude colonnade that caps the entablature.

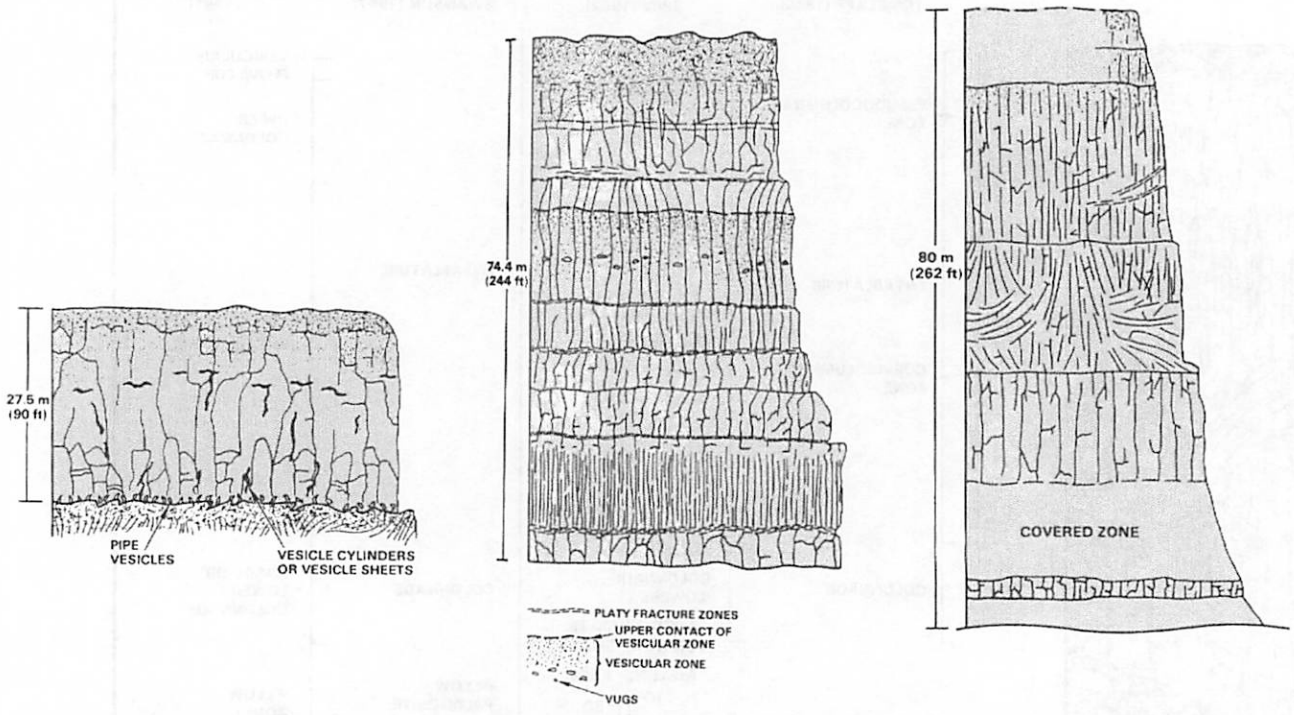

Figure 12.2: Intraflow structures in Type I, Type II, and Type III flows, respectively. These figures are adapted from Long & Wood 1986.

The existence of entablature (which is indicative of quick cooling) sandwiched between colonnade (slow cooling) is the reverse of what one might expect. Generally the outer margins of a flow would cool quickly (hence the glassy surface texture on most flows), but the interiors of a flow would cool more slowly. How does the core of a flow become quenched to form entablature (once in the case of Type III flows, multiple times in the case of Type II flows)?

Long & Wood (1986) argue that flooding or extensive rainfall is responsible. At some point after the lava is emplaced, a deluge of water inundates the cooling flow, seeping down the pore spaces of the outer colonnade down into the core of the flow, quenching and cooling it to form the entablature. This explains the Type III flow, and the Type II flow of repeated colonnade and entablature tiers can be achieved by multiple slow cooling and flooding episodes.

It is important to note that despite the heavy rainfall in the Hawaiian islands, entablature occurs in only one locality there. This indicates that if rainfall were involved in creating entablature, it would have to be much greater than the 250 cm/yr that Kilauea Iki sees.

Amongst the extensive lavas of the solar system we should certainly expect to see colonnade joint patterns. However, no remote sensing instrument has yet had the ability to resolve features on that length scale. If we manage to observe entablature on other planets, then the case can be made for some kind of quenching event, most likely inundation by water. This may help pin down the geologic sequence of events in those localities, or constrain the volume and duration of flooding.

References

Kearey, P. (1996) New Penguin Dictionary of Geology. *Penguin Books.*

Long, P.E. (1978) Characterization and recognition of intraflow structures, Grande Ronde Basalt. Rockwell Hanford Operations, Richland Washington. RHO-BWI-LD-10. 74 p.

Long, P.E. & Wood, B.J. (1986) Structures, textures, and cooling histories of Columbia River basalt flows. *Geological Society of America Bulletin.* v. 97, pp. 1144–1155.

13 Palagonite on Earth and Mars

by JANI RADEBAUGH

What is Palagonite?

Palagonite is a fine-grained, yellowish-to-brownish altered basaltic glass. It is formed by the effusion of magma into subaqueous environments. This leads to the explosive fragmentation of the lava, the solidification of the fragments into glass (called hyaloclastites), and the subsequent interaction between the glass fragments and water. The main reactions that occur are hydration and ion exchange. Picture from L. Fantane, web ref below.

Will we see it in Washington?

Palagonites are found wherever there is substantial interaction between basaltic glasses and water. Therefore, we see a lot of palagonite in Hawaii, because lava has often been erupted into sea water or onto marshy terrain or into riverbeds. We also see palagonite in Iceland, because there are many sub-glacial basaltic eruptions. Many of the Columbia River flood basalt lavas flowed into large basins or depressions, which at the time were filled with water, since we see pillow basalts (formed when basalt erupts under water) in many locations. These areas will be good regions in which to look for palagonites.

Palagonite on Mars?

Extremely dry conditions and massive global dust storms on Mars lead to a ubiquitous surficial dust coating that can be a fraction to several mm in thickness. This makes it difficult to obtain an accurate dust-free spectral measurement of rocks and minerals in the visible and thermal IR range.

The Viking Lander X-ray Spectrometer gave possible evidence for clays and palagonite in the martian soil. In addition, the best match to Martian spectra is obtained with terrestrial palagonites which contain poorly crystalline iron oxides (e.g. limonite, hematite).

Several groups have undertaken to observe and model the spectra of various dust coatings (such as palagonite and loess) on different rocks (mostly basalt and basaltic andesite).

The figures are from a PGG project by the USGS Astrogeology group in Flagstaff.

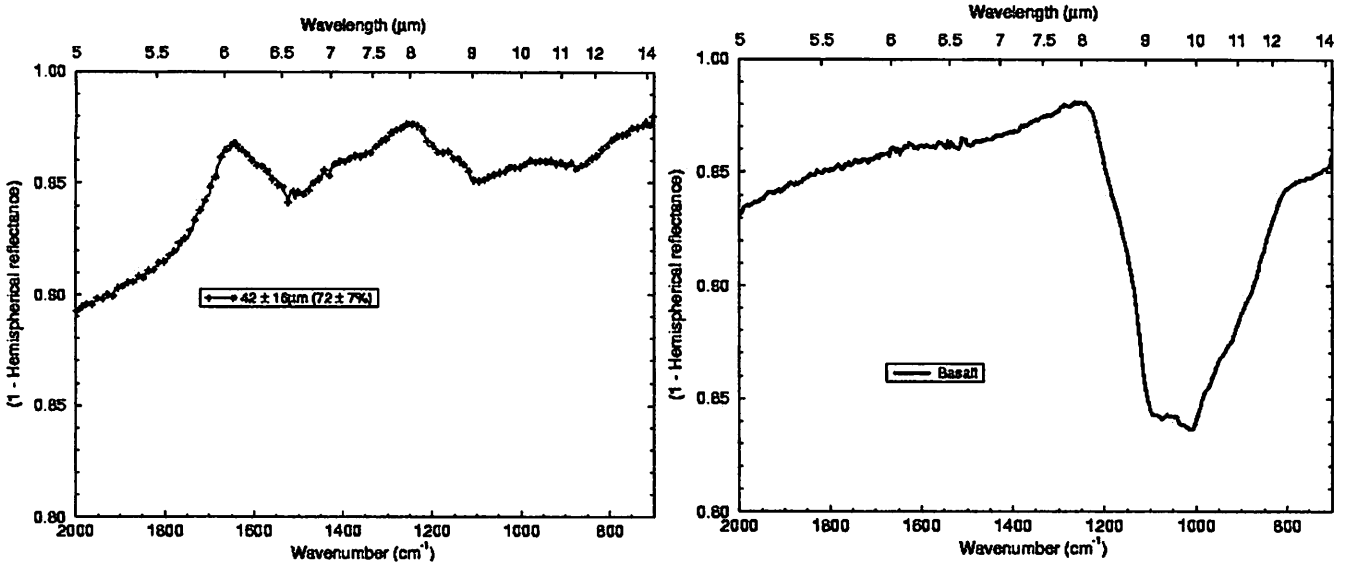

Figure 13.1: *Left: Graph of the reflectance spectra for a San Francisco volcanic field basalt. Right is the spectra of the same basalt, coated with a 42 um layer of Hawaiian palagonite. The difference is pretty extreme!.*

Projects like this, in which spectra of substances, such as palagonite dust, are compiled and models are created to account for all situations not individually measureable will lead to an understanding of the compositions of the dust as well as underlying rocks.

References

USGS project: Jeffrey R. Johnson, Friedrich Horz, Philip R. Christensen, Paul G. Lucey, Will Grundy. `http://astrogeology.usgs.gov/Projects/Spectroscopy/`

Johnson, J. and W. Grundy, 2001, Visible/Near-Infrared Spectra and Two-Layer Modeling of Palagonite-Coated Basalts, GRL 28, 2101_2104.

Stoker, C. R., J. L. Gooding, T. Roush, A. Banin, D. M. Burt, B. C. Clark, G. Flynn, O. E. Gwynne, 1993, The physical and chemical properties and resource potential of Martian surface soils. In, Resources of near_Earth space., eds. J. S. Lewis, M. S. Matthews, M. L. Guerrieri, p. 659-707.

`http://www.turismo.catania.it/allegati/Palagonia/natura_territorio/palagonite.htm` L. Fantane picture

14 Other Terrestrial Flood Basalts

by MATT CHAMBERLAIN

Introduction

The Columbia River Basalt (CRB) may be one of the most recent flood basalt provinces, and certainly the most studied, but that doesn't mean that it is the only one or the biggest. The CRB is just one example of a number of flood basalts around the world, flood basalts are just one form of Large Igneous Province (LIP). Other forms of LIPs are passive volcanic margins, oceanic plateaus and seamounts chains.

The Siberian and Deccan Traps are the largest known continental flood basalts. See the table below for other examples. (The term "Traps" comes the Swedish work for stairs.) Some of the LIPs listed formed primarily over oceanic crust. Consequently they have not been as well studied as their continental counterparts. Several lines of evidence suggest that in most instances the greatest number of individual eruptions and the largest volumes of lava probably occurred within a million years or less.

Province	Age (Myr)	Volume ($10^6 km^3$)	Paleolatitude	Duration (Myr)
Columbia River	16 ± 1	0.25	$45°N$	~ 1 (for 90%)
Ethiopia	31 ± 1	~ 1.0	$10°N$	~ 1
North Atlantic	57 ± 1	> 1.0	$65°N$	~ 1
Deccan	66 ± 1	> 2.0	$20°S$	~ 1
Madagascar	88 ± 1	?	$45°S$	~ 6?
Rajmahal	116 ± 1	?	$50°S$	~ 2
Serra Geral/Etendeka	132 ± 1	> 1.0	$40°S$	~ 1 or ~ 5?
Antarctica	176 ± 1	> 0.5	$50 - 60°S$	~ 1?
Karoo	183 ± 1	> 2.0	$45°S$	$0.5 - 1$
Newark	201 ± 1	> 1.0?	$30°N$	~ 0.6
Siberian	249 ± 1	> 2.0	$45°N$?	~ 1

Table 1: Estimated dates of flood basalts over the last 250 million years.
`http://www.geolsoc.org.uk/template.cfm?name=fbasalts`

Deccan Traps and Association of Flood Basalts with Rifting

The flood basalts of the Deccan Traps are located in west central India, east of the city of Bombay. The Deccan Traps were emplaced around 66 million years ago. In places the flows of basalts have formed a stack 2000 m thick. The present outcropping area is 500,000 km2 though the original area could have been three times this.

Below the basalt flows of the Deccan Traps are a series of sandstones and conglomerates from the Cretaceous, the Bagh sediments (Gwalani 1981). Below these sediments is a basement of schist. This sequence matches a scenario of flood basalt initiated by rifting of a continent. In reality, Deccan Traps are just half of the original LIP that was formed. The other part of the original province is now in the middle of the Indian Ocean, in the Seychelles (see Figure 14.1).

Other Examples

Other examples of flood basalts that have been associated with rifting are in the North Atlantic. Basalts in the North Atlantic are found from Baffin Island, across Greenland and Iceland, all the way to the British Isles. The

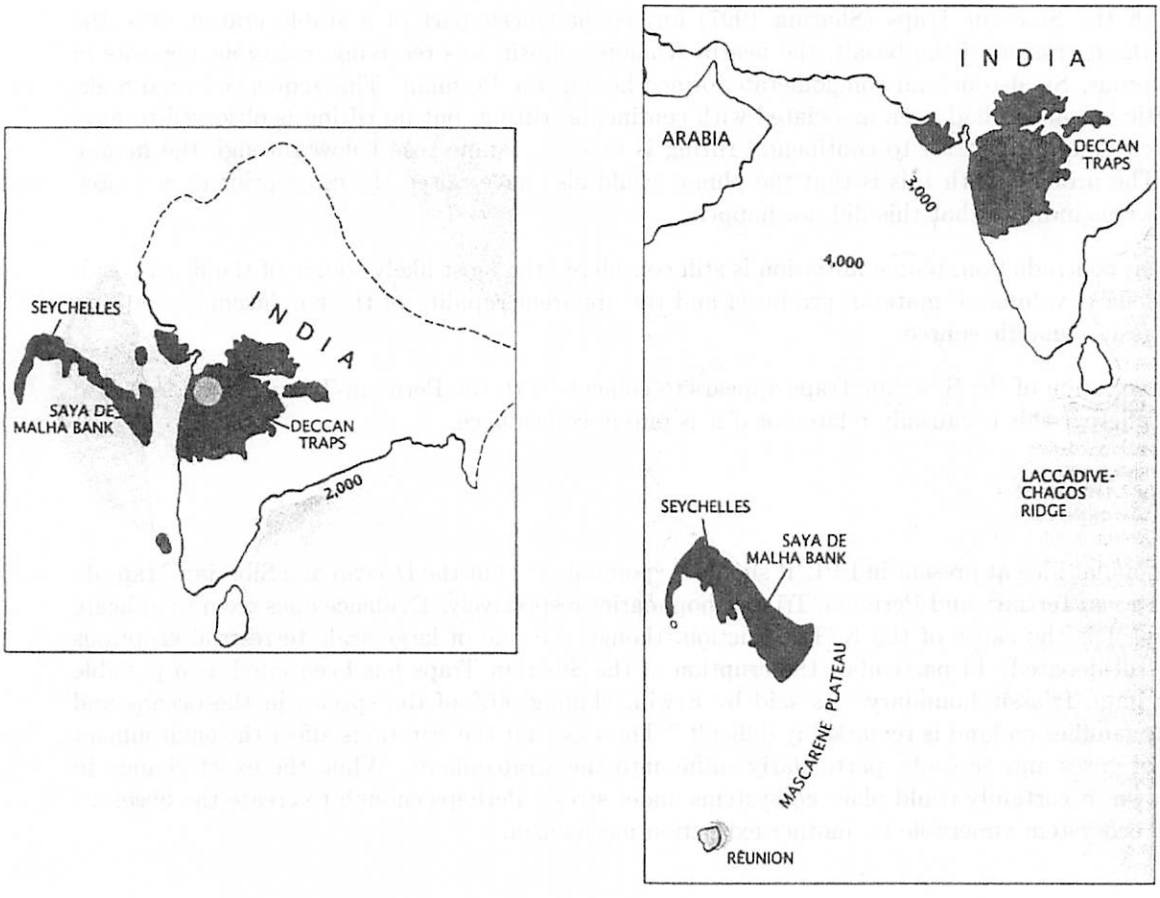

Figure 14.1: *Position of the Deccan Traps and the Seychelles at the time of the estrusive volcanism and the present day. The Deccan Traps is a good example of a flood basalt associated with rifting. The flood basalt is thought to correspond to arrival of the plume head, followed by a hot spot formed by the plume tail.*

initial flood basalts were cotemporaneous with the Deccan Traps, and the following rifting has produced the present wide geographic distribution. Iceland is believed be sitting over the top of the tail of the same plume that initiated the first basaltic flood.

This LIP in the North Atlantic is nearly an exact copy of what happened in the South Atlantic, though it occurred some 70 million years earlier. Today basalts can be found on the South American and African continents that formed as these two land masses pulled apart. Trailing from each basaltic region on either side South Atlantic is a tail of volcanism pointing to the present location of the hot spot that, at least, coincided with the initial rifting.

The basaltic volcanism around the Red Sea occurred around 30 million years ago and coincided with the beginning of rifting apart of the Red Sea.

Siberian Traps

The Siberian Traps, like the Columbia River Basalt, is an atypical example of the flood basalts that are found on earth. Most flood basalts are associated with rifting of continents though this did not occur for either of these provinces. Though there could be an important association between the CRB and the extension of the southwestern US.

The region in which the Siberian Traps (Sharma 1997) formed had been part of a stable craton since the precambrian. Prior to the extrusion of the basalt, the nearby Tunguska Basin was receiving, calcerous deposits in the Devonian/Carboniferous. Sandstone and conglomerate formed here in the Permian. This sequence would make sense if the flood basaltic volcanism had been associated with continental rifting, but no rifting is observed to have taken place. The conventional alternative to continental rifting is to say a plume rose below through the mantle to initiate volcanism. The problem with this is that the plume would also have raised the crust prior to eruption. Nearby sedimentation seems indicate that this did not happen.

Despite this apparent contradiction, plume initiation is still considered the most likely source of the flood basalt volcanism based on the sheer volume of material produced and the apparent rapidity of the emplacement. A high $^3He/^4He$ ratio also suggests a mantle source.

The timing of the formation of the Siberian Traps appears to coincide with the Permain-Triassic boundary, and it is still under debate whether this is causally related or if it is purely coincidence.

Mass Extinctions

While this may not be popular idea at present in LPL, it should be pointed out that the Deccan and Siberian Traps do coincide with the Cretaceous/Tertiary and Permian/Triassic boundaries respectively. Evidence does seem to indicate that the Chicxulub impact is the cause of the K/T extinction, though the role of large scale terrestrial eruptions in mass extinctions is still debated. In particular, the eruption of the Siberian Traps has been cited as a possible mechanism for the Permain/Triassic boundary. As said by Erwin, "killing 90% of the species in the oceans and about 70% of vertebrate families on land is remarkably difficult." The way that the eruptions affect the environment is through the release of gases and aerosols, particularly sulfur into the stratosphere. While the exact change to climate may not be known, it certainly could place ecosystems under stress. Perhaps enough to create the observed extinction, or make the ecosystem vunerable to another extinction mechanism.

Mantle Plumes and Flood Basalts

The ideas at the moment are that flood basalts, whether continental or oceanic, form as the head of a plume arrives at the base of the lithosphere. The delivery of heat to the lithosphere is sufficient to partially melt the lithosphere and create the flood basalt volcanism. In the case of flood basalt forming at rift margin, it is thought that the location of the plume and the rifting center could be a coincidence. The extra heat provided by the plume is sufficient to change the eruption from a typical mid ocean ridge type setting to a more interesting flood basalt province (White and McKenzie 1989).

Once the plume head has a arrived and the plume and hot spot have developed, eruptions decrease in volume. There can be a change in composition as well, explained in part by the changing depth of melting. Other composition characteristics are determined by the degree of contamination of the produced melt en route to the surface.

The formation of flood basalts seems to occur every 32 million years, suggesting a periodicity in the mantle plume circulation (Rampino 1988). There is also evidence that the eruption at the Deccan and Sieran Traps occurred just after a period of less mantle activity, as evidenced by pole wander and pole reversals. The size of these particularly large LIP could be related to this restarting of plume activity after a period of quiescence.

Old Relics

Relatively young flood basalts are easier to recognize than their older cousins. The flood basalts that are still exposed today are essentially those that were formed since the last continental break up, 250 million years ago.

There is evidence that flood basalts were still formed before this time, though erosion has done its best to hide the evidence. The last features to be removed are the dykes that were the feeder dykes during the basaltic volcanism. One such province is to be found in Northern Australia, the Kalkarinji Basalts currently outcrop for 35 000 km^2

though they are estimated to have been ten times this size originally (Clark and Cook 1986). These basalts were formed around 510 million years ago, in the Late Cambrian (Glass 2001).

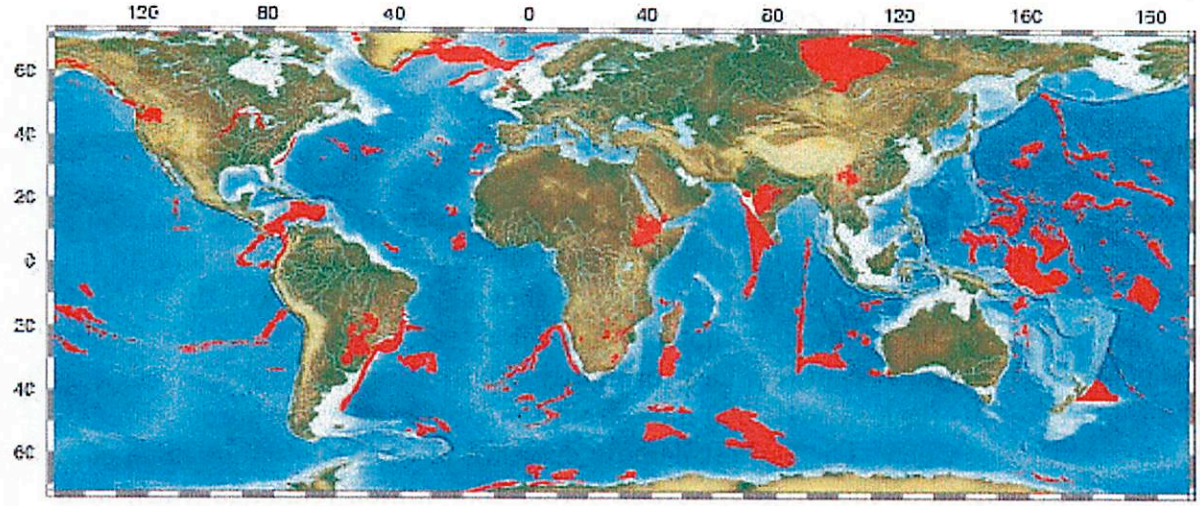

Figure 14.2: *Global distribution of recent large igneous provinces. Mahoney and Coffin 1997..*

References

Clark, I. F. and B. J. Cook, 1986. Perspectives of the Earth, Australia Academy of Science, Canberra.

Courtillot, V. and J. Besse 1987. Magnetic field reversals, polar wander, and core-mantle coupling, Science **237**, 1140-1147.

Erwin , D. H. 1994. The Permo-Triassic extinction. Nature **367**, p 231-236.

Glass, L. M. and D. Phillips 2001. A precise Ar-Ar age for the Kalkarinji low-Ti Continental Flood Basalt Province of northern Australia, Petrochemistry and Experimental Petrology Annual Report 2001http://wwwrses.anu.edu.au/pep/annualr

Gwalani, L. G. 1981. Petrology of Deccan Traps and Bagh Beds of Dugdha-Naswadi, Gujarat. Somaiya Publications, Bombay.

Mahoney, J. J. and M. F. Coffin 1997. Large igneous provinces: continental, oceanic and planetary flood volcanism. American Geophysical Union, Washington DC.

Rampino, M R and R B. Stothers 1988. Flood basalt volcanism during the past 250 million years. Science, **241**, p. 663-668.

Sharma M. 1997. Siberian Traps, in Large igneous provinces: continental, oceanic and planetary flood volcanism, Ed.s Mahoney and Coffin. American Geophysical Union, Washington DC.

White, R S & D. McKenzie 1989. Volcanism at rifts. Scientific American, **260**, 62-71.

15 The Yellowstone Hotspot

by GWEN D. BART

Path of the plume

The Yellowstone hotspot is currently the driving force of the geology in Yellowstone National Park. Yellowstone itself emits 30-40 times the average heat emitted from North America because of the hotspot underneath it. Because the North American plate is moving southwest over the hotspot at the rate of one inch per year, the Yellowstone hotspot has left a trail of more than 100 caldera eruptions in its wake. These caldera eruptions have primarily occurred at 7-13 volcanic centers, leaving a path (figure 15.1). This path extends 500 miles from the Oregon/Nevada border through the Snake River plain to Yellowst one. The earliest definite evidence of the Yellowstone hotspot is the calder a eruption that occurred at the Oregon/Nevada border 16.5 million years ago (Ma), with the most recent eruption having occurred 630,000 years ago in Yellowstone. The hotspot has left the Snake River valley in its wake and is being preceded by a parabola shape of mountains around the current location of the active hotspot.

How the hotspot works

First, a review of the structure of the Earth is in order. The crust of the Earth comprises the upper 60 km or so, beneath which is the more dense, iron-rich rock mantle. The mantle continues to a depth of 2890 km, beneath which is Earth's iron-rich core. The lithosphere is the crust and upper part of the mantle, which together form the brittle plates that drift about on the asthenosphere, where rocks are weaker and behave more like fluids.

Most hotspots form when a plume of molten rock from the core/mantle boundary rises through the solid rock of the mantle (due to the molten plume's lower density). Indeed, seismic evidence shows warmer or molten rock beneath the location of most hotspots on Earth, down to the core/mantle boundary. The plumes may form because of variations in rock temperature and density at the core/mantle boundary. Because these plumes begin so deep in the Earth, their location is not affected by topography on the surface.

The Yellowstone plume is different because seismic evidence shows that the plume started only 200 km below the surface. In this case it is likely that the hotspot has taken advantage of the local Basin and Range extension of the North American plate. The extension has resulted in weaknesses in the lithosphere, and the plume may have taken advantage of these weaknesses to push its way to the surface.

Caldera eruptions associated with the Yellowstone hotspot generally occur in three stages. (Elements of these stages can be seen in figure 15.2.) In the first stage, a 80 km wide plume of basaltic lava rises from 200 km up to the bottom of the North American tectonic plate where it forms a 500 km wide pool of iron rich basalt. This lava plume causes the surface above to bulge upward by about 500 m over the 500 km wide pool.

In the second stage, molten blobs of basalt move upward and form a magma chamber (known as a pluton) which is about 16 km in diameter and 5-12 km underground. In this magma chamber, silica-rich crustal granite melts. The melted granite is known as rhyolite. Rhyolite is thick and viscous (compared to basaltic magma). As the magma presses upward, faults form in the surface. When these faults intersect the magma chamber, the eruption occurs. Because the rhyolite is so viscous, and because rhyolite carries lots of gas, the eruption is quite explosive and voluminous. (See figure 15.3 for a comparison of the volume of the Yellowstone caldera eruptions to the volume of other volcanic eruptions such as Mount St. Helens.) When the magma chamber is drained, the above ground sinks down into the chamber, creating the caldera. Caldera eruptions can occur repeatedly as long as the hotspot is still there feeding it magma.

The third stage is after the connection from the caldera to the hotspot is cut off. The rhyolite cools and allows the basaltic magma deeper down to erupt. The basalt is less viscous and has less gas and therefore the eruptions are significantly less explosive. As the hotspot leaves the area, the crust cools and the bulge sinks back down.

Connection to the Columbia River flood basalts

The connection of the Yellowstone hotspot to the Columbia River flood basalts (CRFB) seems to be somewhat in debate. It has been proposed that 17-14 Ma, the head of the Yellowstone plume may have spread northwest under the lithosphere and erupted to form the CRFB. This theory is supported because of the coincidental timing of three events: the CRFB eruption 17-14 Ma, the Yellowstone hotspot's first eruption 16.5 Ma near the Oregon/Nevada border, and the speedup of the Basin and Range extension of the West 17 Ma. However, other scientists argue that the CRFB were just formed by the same forces that formed the Cascade Range volcanoes - the subduction and melting of the Pacific Ocean plate beneath the Pacific Northwest.

Planetary connection

The surfaces of many planetary bodies in our solar system show evidence of having been shaped by hotspots. Mars' famous Tharsis volcanoes may have been formed from a large hotspot plume which raised the summit of Olympus Mons to 85,000 feet above the surrounding terrain.

Venus has no plate tectonics as the Earth does, but shows numerous circular features known as coronae with diameters of up to 200 km. Since chains of these coronae have been observed, and since Venus has no lithospheric plates to move over the hotspot, this would imply that perhaps the hotspots themselves are moving underneath the surface of Venus.

Tidal heating in two of the moons of Jupiter may be sufficient to produce hotspots on those bodies. At least 30 hotspots have been observed on Io by the Galileo spacecraft, with temperatures reaching as high as 1550C. The rocky core of Europa may have hotspots contributing heat to preserve a liquid water ocean under Europa's brittle outer ice shell.

References

Smith, R. B. and Siegel, L., 2000, Windows into the Earth: The Geologic Story of Yellowstone and Grand Teton National Parks, Oxford University Press, New York.

`http://volcanoes.usgs.gov/yvo/index.html`

Christiansen, R.L., 1984, Yellowstone magmatic evolution: Its bearing on understanding large-volume explosive volcanism, in Explosive volcanism: its inception, evolution, and hazards, National Research Council Studies in Geophysics, National Academy Press, Washington D.C., p. 84-95.

Christiansen, R. L., 2001, Quaternary and Pliocene volcanism of the Yellowstone Plateau region of Wyoming, Idaho, and Montana: U.S. Geological Survey Professional Paper 729-G, p. 145.

Dzursin, D., Savage, J.C., and Fournier, R.O., 1990, Recent crustal subsidence at Yellowstone Caldera, Wyoming: Bulletin of Volcanology, v. 52, p. 247-270.

Smith, R. B., and Braile, L. W., 1994, The Yellowstone Hotspot: Journal of Volcanology and Geothermal Research, eds. Hill, D.P., Gasparini P., McNutt S., and H. Rymer, H., v. 61, p. 121-188.

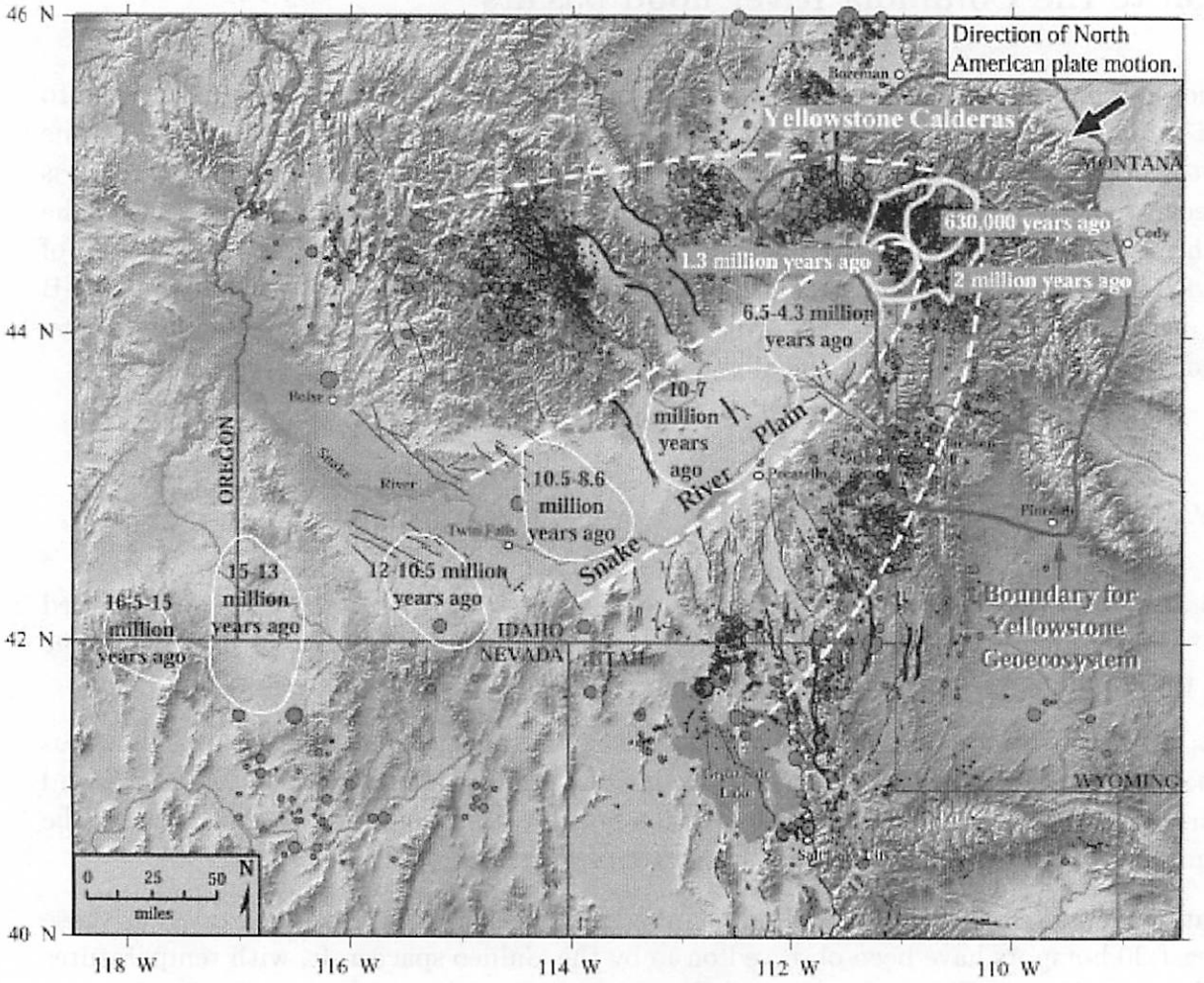

Figure 15.1: *Path of the Yellowstone hotspot*

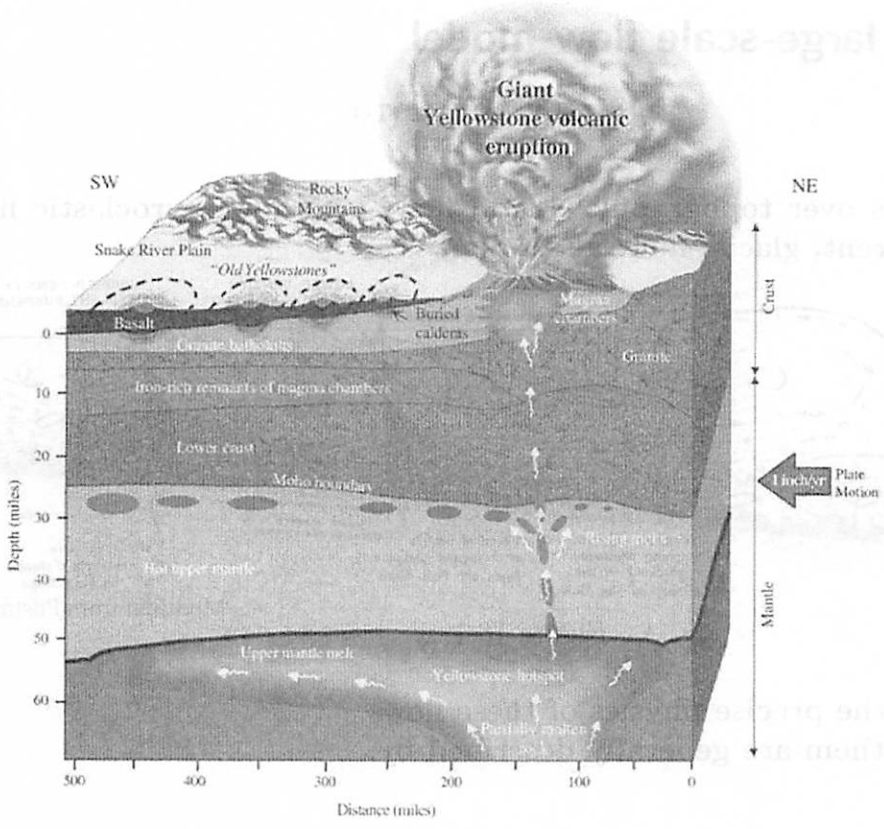

Figure 15.2: *Cross section showing relationship of Yellowstone and the Sanke River Plain to the Yellowstone hotspot and surrounding mountains.*

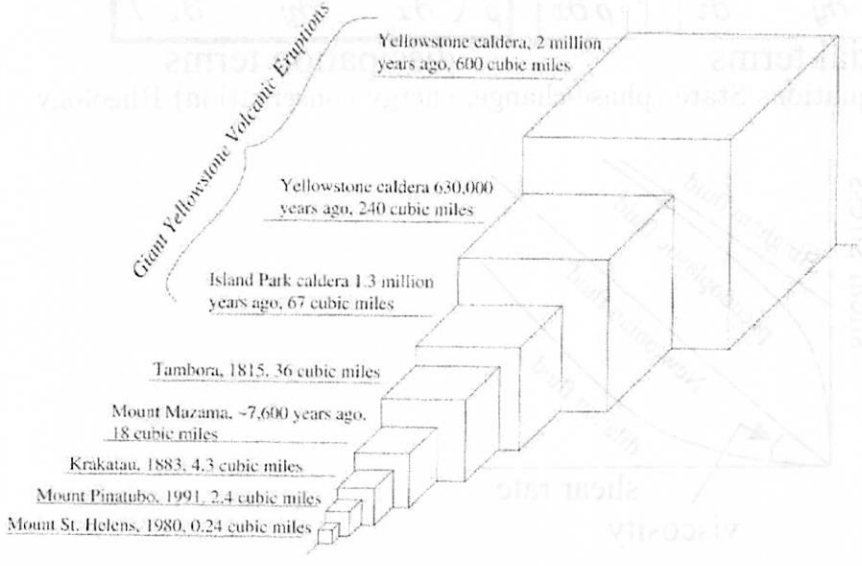

Figure 15.3: *Volumes of Yellowstone's giant volcanic eruptions compared with volumes of other major eruptions.*

16 Note on a large-scale flow model

by HIRDY MIYAMOTO

Large-scale flows over topography: Flood flow, lava flow, pyroclastic flow, debris flow, Turbidity current, glacial flow, and so on.

Something like this?

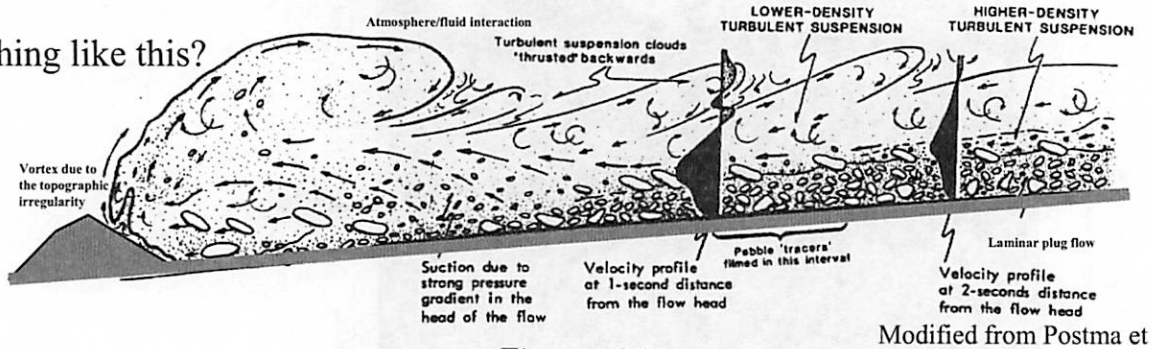

Modified from Postma et al. [1988]

Figure 16.1: .

We don't know the precise physics of these flows.
But movements of them are generally described by:

1. Mass conservation equation(s)

2. Momentum conservation equation(s) Navier-Stokes equation

acceleration driving force

$$\boxed{\frac{\partial u}{\partial t}} + \boxed{u\frac{\partial u}{\partial x} + v\frac{\partial u}{\partial y} + w\frac{\partial u}{\partial z}} = \boxed{-\frac{1}{\rho}\frac{\partial p}{\partial x}} + \boxed{\frac{1}{\rho}\left(\frac{\partial \tau_{xx}}{\partial x} + \frac{\partial \tau_{yx}}{\partial y} + \frac{\partial \tau_{zx}}{\partial z}\right)}$$

inertial terms dissipation terms

3. Constitutive equations State (phase-change, energy conservation) Rheology

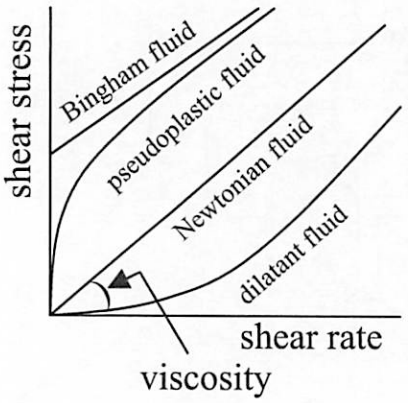

Laminar/turbulence Raynolds number $\frac{\rho U H}{\eta}$
Inclusion (bubble, sediments, crusts, etc) Dispersive pressure, Buoyancy
Base effects friction, erosion, ...
other sedimentation, etc

Too complicated to be solved even numerically
A simplification is important.

Three approaches to the Scabland flood.

- Neglect one or two dimensions (and/or time variation)

Manning equation
Chezy equation
General velocity equation $->$ the peak discharge rate [e.g., Bretz, 1925; Baker, 1973]

- Integrate in time $->$ Energy

Bernoulli's energy equation
Step-Backwater Model (HEC-2) [Feldman, 1981] $->$ the geologically-based estimation of the peak discharge rates [e.g., O'Connor and Baker, 1992]

[O'Connor and Webb, 1988]

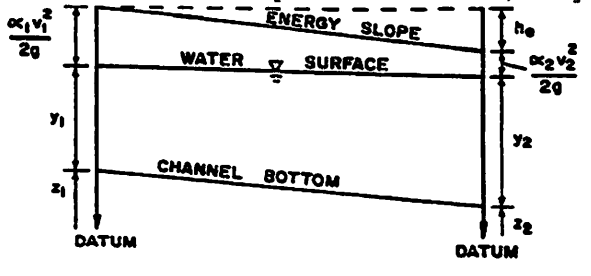

Figure 16.2: .

- Integrate in depth $->$ Mass flux

Shallow water long wave approximation
Saint-Venant equation [e.g., Woolhiser and Liggett, 1967]

$$\frac{\partial \bar{u}}{\partial t} + \bar{u}\frac{\partial \bar{u}}{\partial x} = -g\frac{\partial h}{\partial x} + g\frac{1}{\rho g h}\int_0^h \frac{\partial \tau_{zx}}{\partial z} dz \tag{16.1}$$

$\bar{u}$:vertically averaged velocity accerelation(+inertia)=gravity - resistance

viscous model:

$$\tau_{zx} = \eta\frac{\partial u}{\partial z} \tag{16.2}$$

fully-developed turbulent:

$$\tau_{zx} \sim pl^2 \left(\frac{\partial u}{\partial z}\right)^2 \tag{16.3}$$

Chezy model:

$$g\frac{1}{\rho g h}\int_0^h \frac{\partial \tau_{zx}}{\partial z} dz = -\frac{\bar{u}^2}{C^2 h} \tag{16.4}$$

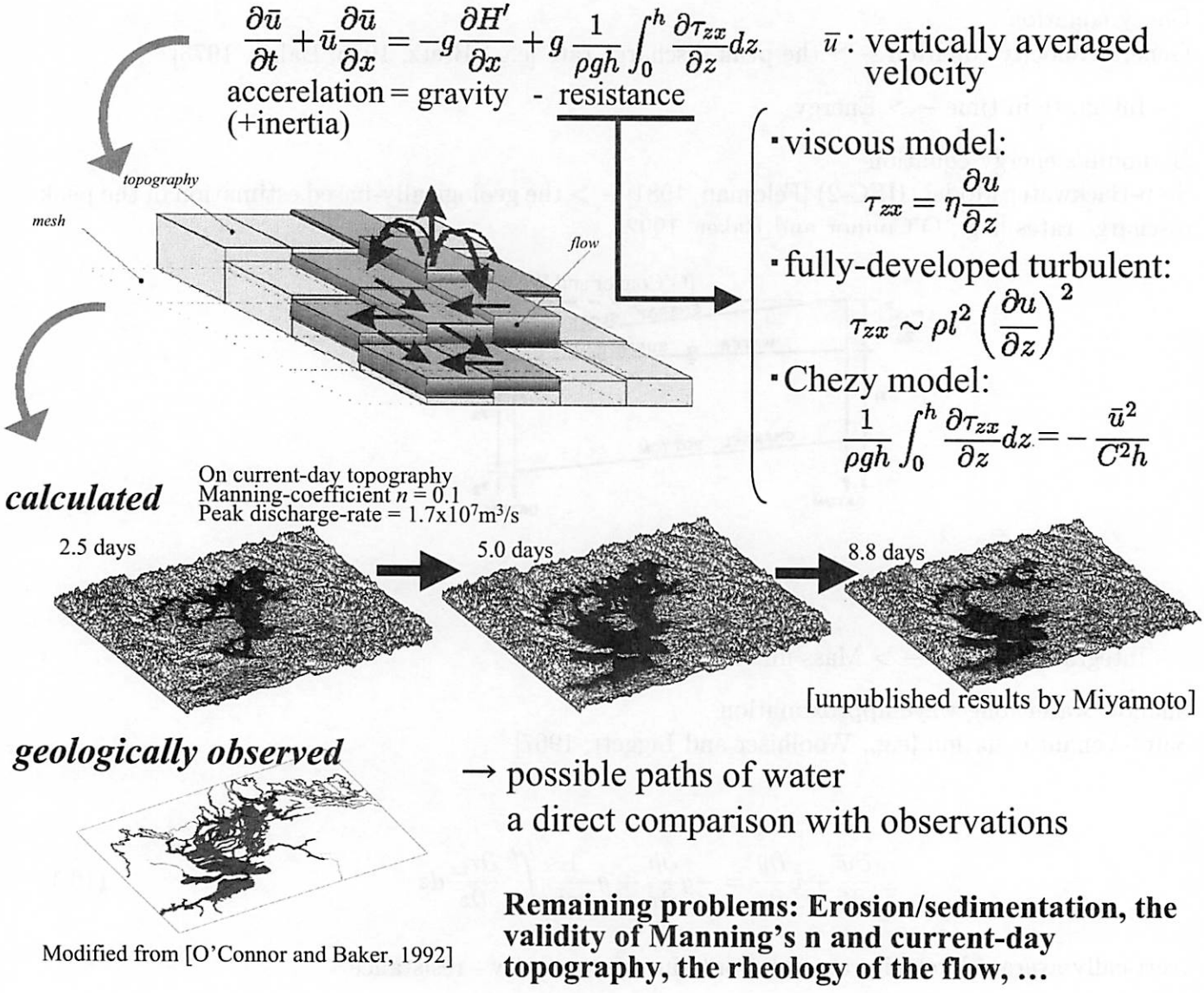

Figure 16.3: .

THE YAKIMA FOLD BELT: STRUCTURE, FORMATION, AND ORIGIN

Windy L. Jaeger

The Yakima fold belt is characterized by a series of generally E-W trending narrow, sinuous anticlinal ridges separated by broad, flat-floored synclinal valleys. The folding has primarily occurred in the Columbia River Basalt Group (CRBG), which was emplaced ~17 to 14 Ma ago, during the Miocene epoch. The CRBG is underlain by Tertiary continental sedimentary rocks and overlain by late Tertiary and Quaternary fluvial and eolian sediments.

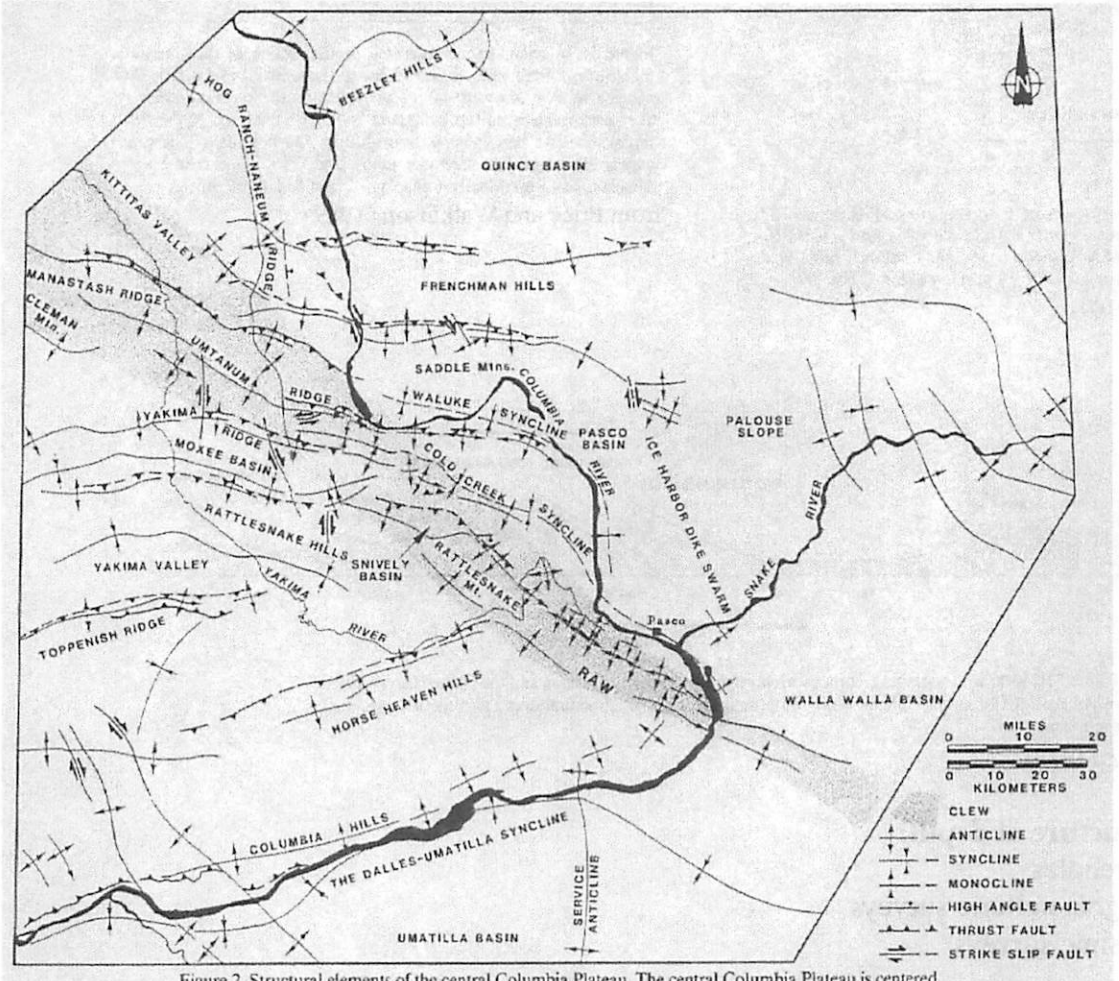

Figure 2. Structural elements of the central Columbia Plateau. The central Columbia Plateau is centered on the Pasco Basin but includes a major portion of the Yakima fold belt and Palouse slope. Also shown are the Cle Elum–Wallula deformed zone (CLEW) and Rattlesnake–Wallula alignment (RAW).

from Reidel *et al.* (1989)

Typical Ridge Dimensions	
Length	~10 km to >100 km
Width (between anticlinal fold axes)	~20 km
Relief	<600 m

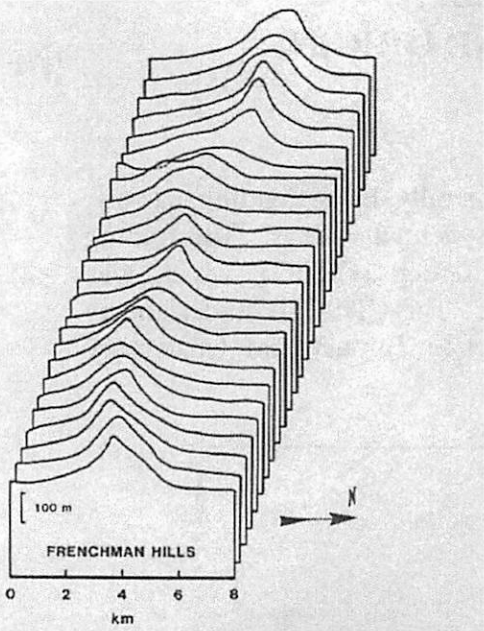

Figure 2. Topographic profiles of a portion of the Frenchman Hills anticline. Cross sections are spaced at 1-km intervals with a roughly 10× vertical exaggeration. Measurements were made from the Priest Rapids Quadrangle, U.S. Geological Survey, topographic map, 1:100,000.

from Watters (1989)

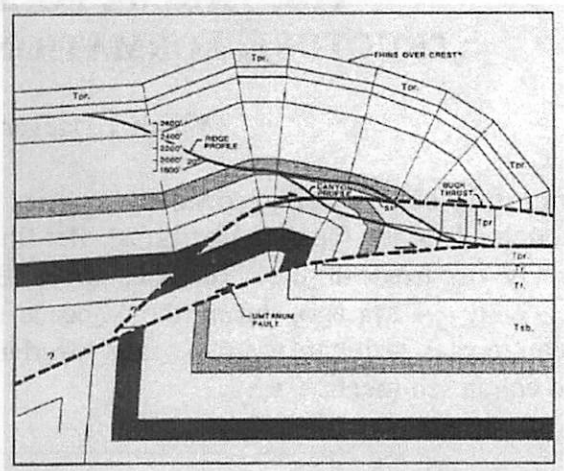

Figure 16. A balanced reconstructed profile section of the Umtanum fold. Straight limb sections were fitted to the mapped fold profile. The hanging-wall cut-offs were used as a template for the foot-wall geometry, after back-rotation on the Umtanum fault. The thickness of the flows represented is a best estimate from drilling and field data. The stratigraphy shown is: Tsb - Sentinel Bluffs Unit, Tf - Frenchman Springs Member, Tr - Rosa Member, and Tpr - Priest Rapids Member.

from Price and Watkinson (1989)

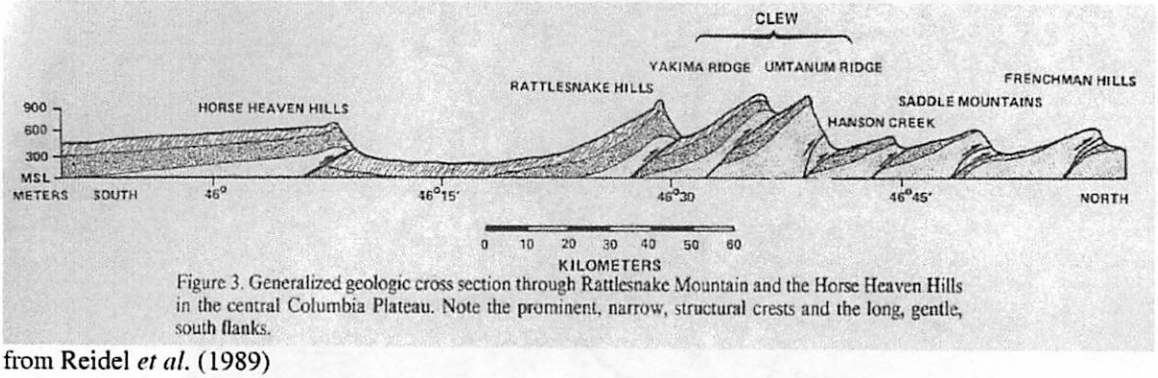

Figure 3. Generalized geologic cross section through Rattlesnake Mountain and the Horse Heaven Hills in the central Columbia Plateau. Note the prominent, narrow, structural crests and the long, gentle, south flanks.

from Reidel *et al.* (1989)

Inferring structure at depth:

1) Boreholes
2) Magnetotelluric surveys
3) Seismic surveys

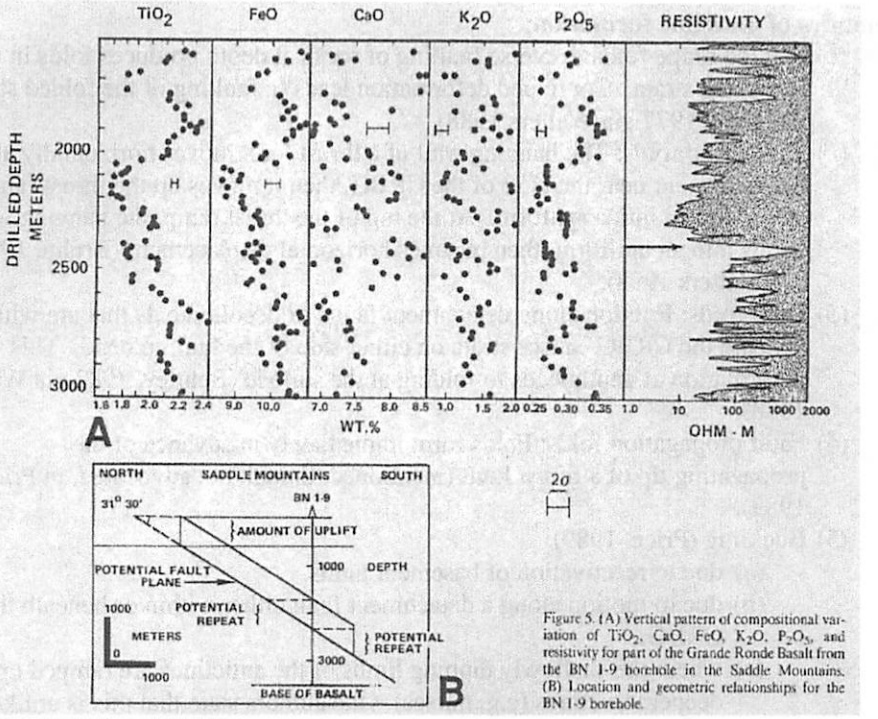

Figure 5. (A) Vertical pattern of compositional variation of TiO_2, CaO, FeO, K_2O, P_2O_5, and resistivity for part of the Grande Ronde Basalt from the BN 1-9 borehole in the Saddle Mountains. (B) Location and geometric relationships for the BN 1-9 borehole.

from Reidel *et al.* (1989)

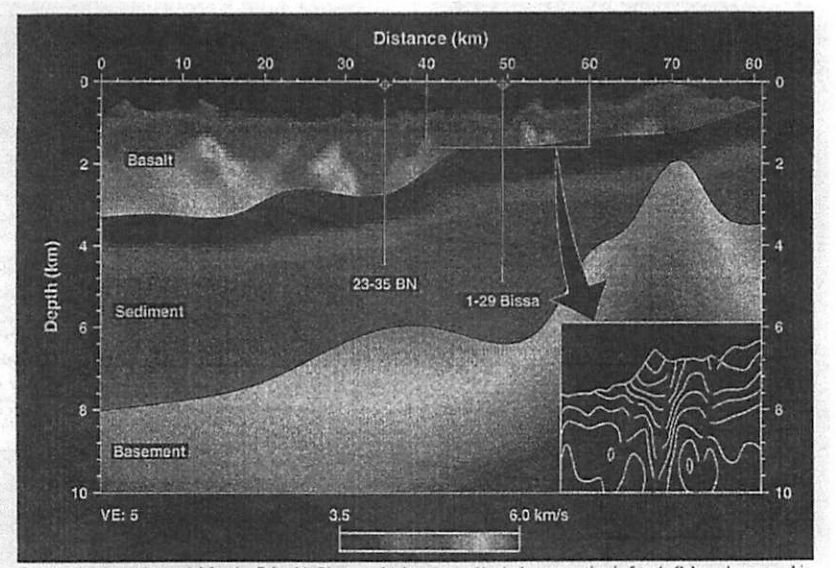

FIG. 13. Final velocity model for the Columbia Plateau seismic program Vertical exaggeration is 5 to 1. Color scheme used is the standard "rainbow" palette. Blues correspond to low velocities (~3.0 km/s), greens and yellows to progressively higher velocities, and red is used for the highest velocities (~6.0 km/s). North is to the right and south is to the left. The location and total depth of the two well ties are shown (23-35 BN was drilled on top of Boylston Mountain and 1-29 Bissa was drilled on top of Whiskey Dick anticline). Note (1) low-velocity zones beneath Whiskey Dick anticline and Boylston Mountain, (2) large variation in base-of-basalt depth, (3) thick sediments to the south, and (4) approximately 6 km of relief on the sediment-basement interface, including a basement high to the north. (inset) Isovelocity contours in the vicinity of Whiskey Dick anticline with superimposed interpreted fault geometries (red lines). Vertical exaggeration is 10 to 1.

from Jarchow et al. (1994)

Kinematics of anticline formation:

(1) Faulted drape folds: Reverse faulting of rocks at depth produces folds in the overlying strata. Continued deformation leads to faulting of the folded strata (Bentley, 1977 via Watters 1988).

(2) Fault-bend folds: The hanging wall of a thrust fault moves horizontally along a *décollement* near the base of the CRBG, then it moves up the thrust ramp and is flexed into a synform. At the top of the thrust ramp, the hanging wall bends into an antiform, then resumes horizontal displacement (Bruhn, 1981 via Watters 1988).

(3) Drag folds: Friction along detachment faults or décollements that are within or beneath the CRBG causes strata on either side of the fault to bend. This deformation at depth leads to folding at the surface (Bentley, 1982 via Watters 1988).

(4) Fault propagation folds: Folds form immediately in advance of the propagating tip of a thrust fault (mentioned, though not advocated, in Price, 1989).

(5) Buckling (Price, 1989):
   (a) due to reactivation of basement faults.
   (b) due to motion along a detachment fault either within or beneath the CRBG.
   (c) where the shallowly dipping limbs of the anticlines are ramped up over deeper structures (e.g. horses) – the authors state that this is unlikely.

(6) Combination of fault-bend fold and drag fold.

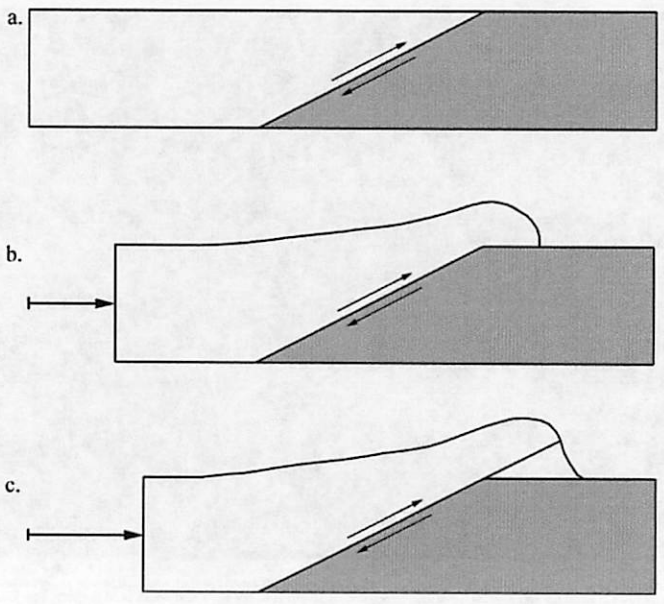

Driving mechanism:

(1) Oblique subduction of the Juan de Fuca plate in the Pacific Northwest (Reidel, 1989).

(a) The coincidence in the timing of subsidence, CRBG emplacement, and ridge formation and in the rate of basalt emplacement and fold growth suggests a common cause.

(b) Subsidence apparently started before the volcanism.

(2) The Yellowstone plume (Suppe, 1975).

(a) Plume head uplift beginning in the south and spreading northward (Pierce *et al.*, 2000).

(b) Thermal subsidence (Mège and Ernst, 2001).

(3) Mascon tectonics (Mège and Ernst, 2001).

References & Bibliography:

Bentley, R.D. (1977) Stratigraphy of the Yakima basalts and structural evolution of the Yakima Ridges in the western Columbia Plateau, in *Geology Excursions in the Pacific Northwest*, edited by E.H. Brown and R.C. Ellis, pp. 339-389, Western Washington University, Bellingham.

Bentley, R.D. (1982) Later Tertiary thin skin deformation of the Columbia Plateau, Washington-Oregon. *EOS Trans. AGU* 63, 173.

Bruhn, R.L. (1981) Preliminary analysis of deformation in part of the Yakima Fold Belt – South central Washington. Wash. Public Power Supply Syst., Richland, pp. 27.

Campbell, N.P. (1989) Structural and stratigraphic interpretation of rocks under the Yakima fold belt, Columbia Basin, based on recent surface mapping and well data. GSA Spec. Pap. 239, pp. 209-222.

Jarchow, C.M., Catchings, R.D., and Lutter, W.J. (1994) Large-explosive source, wide-recording aperture, seismic profiling on the Columbia Plateau, Washington. *Geophysics 59*, 259-271.

Lutter, W.J., Catchings, R.D., and Jarchow, C.M. (1994) An image of the Columbia Plateau from inversion of high-resolution seismic data. *Geophysics 59*, 1278-1289.

Mège, D. and Ernst, R.E. (2001) Contractional effects of mantle plumes on Earth, Mars, and Venus. GSA Spec. Pap. 352, pp. 103-140.

Mège, D. and Reidel, S.P. (2001) A method for estimating 2D wrinkle ridge strain from application of fault displacement scaling to the Yakima folds, Washington. *GRL 28*, 3545-3548.

Pierce, K.L., Morgan, L.A., and Saltus, R.W. (2000) Yellowstone plume head: Postulated tectonic relations to the Vancouver slab, continental boundaries, and climate. USGS Open-file report 00-498, pp. 39.

Price, E.H. and Watkinson, A.J. (1989) Structural geometry and strain distribution within eastern Umtanum fold ridge, south-central Washington. GSA Spec. Pap. 239, pp. 265-281.

Reidel, S.P., Fecht, K.R., Hagood, M.C., and Tolan, T.L. (1989) The geologic evolution of the central Columbia Plateau. GSA Spec. Pap. 239, pp. 247-264.

Suppe, J., Powell, C., and Berry, R. (1975) Regional topography, seismicity, Quaternary volcanicm, and the present-day tectonics of the western United States. *Am. J. Sci. 275-A*, 397-436.

Watters, T.R. (1988) Wrinkle ridge assemblages on the terrestrial planets. *J. Geophys. Res. 93*, 10236-10254.

Watters, T.R. (1989) Periodically spaced anticlines of the Columbia Plateau. GSA Spec. Pap. 239, pp. 283-292.

18 Planetary Wrinkle Ridges

by ZIBI TURTLE

Wrinkle ridges are long, relatively narrow, segmented, strongly asymmetric (in cross section) features that are frequently observed on volcanic plains on the Moon, Mars, Mercury, and Venus (Figures 18.1 and 18.2). They often cap or flank arches, broad rises which are also asymmetric in cross section. Ridges are typically classified, by size, into primary (first-order) ridges or secondary (second and even third-order) ridges which are often associated with the larger ones. The primary ridges are generally several hundred meters to a few kilometers across and a few to several hundred meters high (Figure 3). The amount of shortening accomodated by wrinkle ridges depends on the formation mechanism, several of which have been proposed (e.g., Figures 4 and 5). Watters (1988) estimates the shortening for ridges on the Moon, Mercury, and Mars as well as on the Columbia Plateau on Earth to be 0.01 - 0.2 depending on the subsurface geometry.

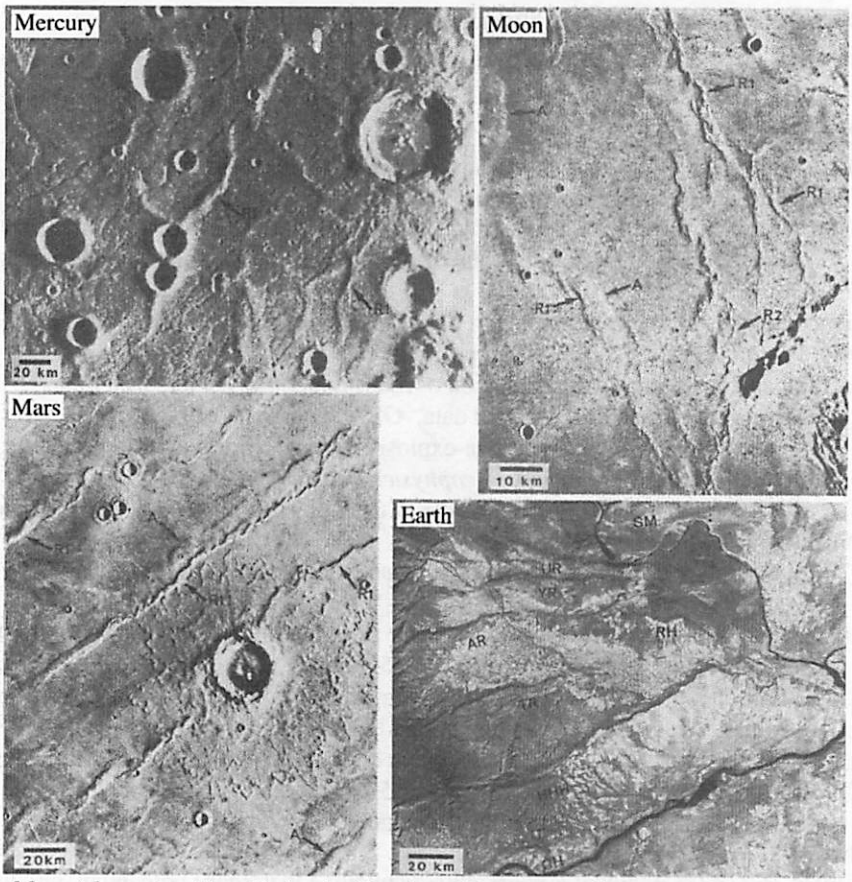

Figure 18.1: *Wrinkle ridges in the Caloris Basin, Mercury; Oceanus Procellarum, Moon; Coprates region of Tharsis Plateau, Mars; and the western Columbia Plateau, Earth. For Mercury, Moon and Mars, (A) denotes arches and (R1, R2, R3) first, second, and third order order ridges, respectively. For Earth, CH=Columbia Hills, HHH=Horse Heaven Hills, TR=Toppenish Ridge, AR=Ahtanum Ridge, YR=Yakima Ridge, UR=Umtanum Ridge, SM=Saddle Mountains, and RR=Rattlesnake Ridge. (From Watters, 1998)*

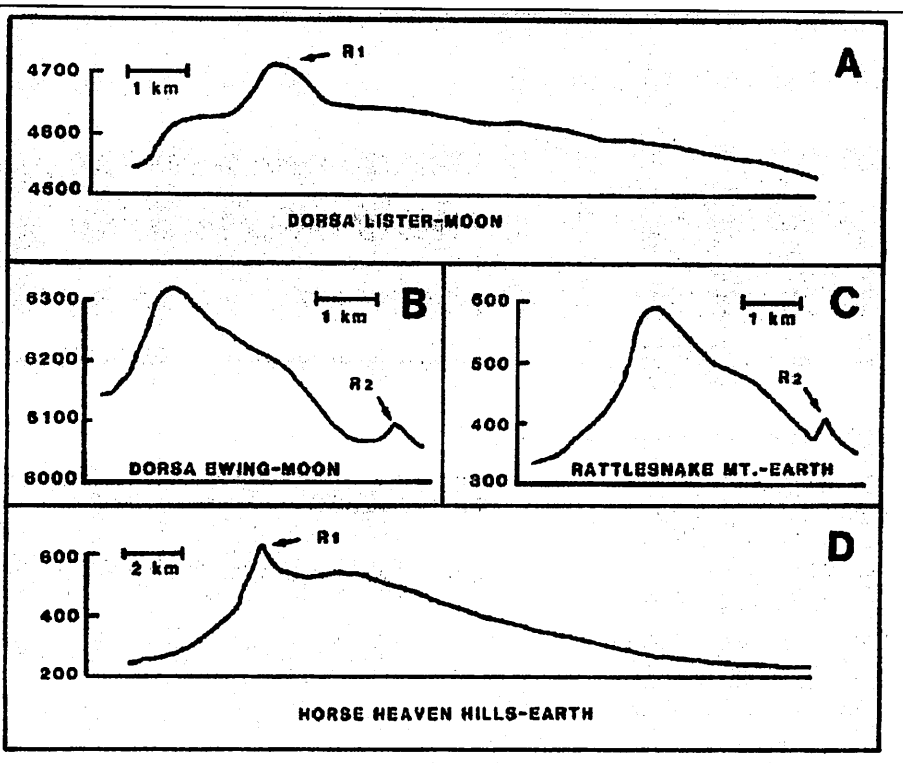

Figure 18.2: *Topographic cross sections of first (A-D) and second-order (R2 in C and D) ridges (A and D) and arches on the Earth and Moon. (From Watters, 1998)*

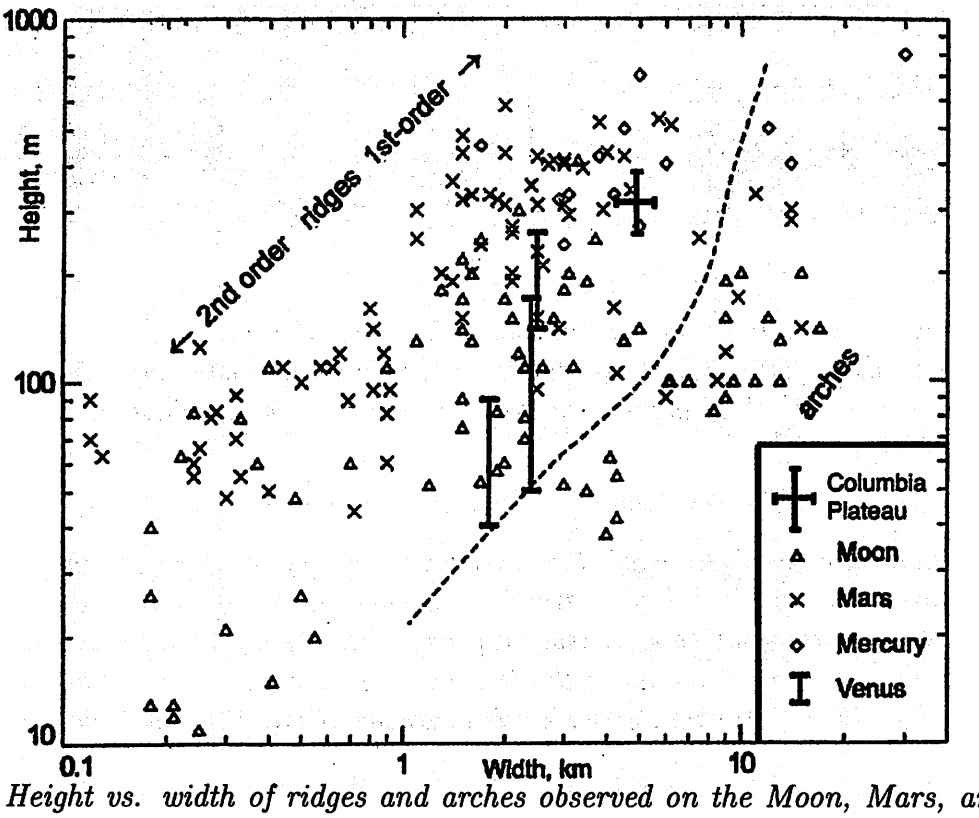

Figure 18.3: *Height vs. width of ridges and arches observed on the Moon, Mars, and Mercury as well as a few examples from Venus and Earth. (After Kreslavsky and Basilevsky, 1998 and Watters, 1988)*

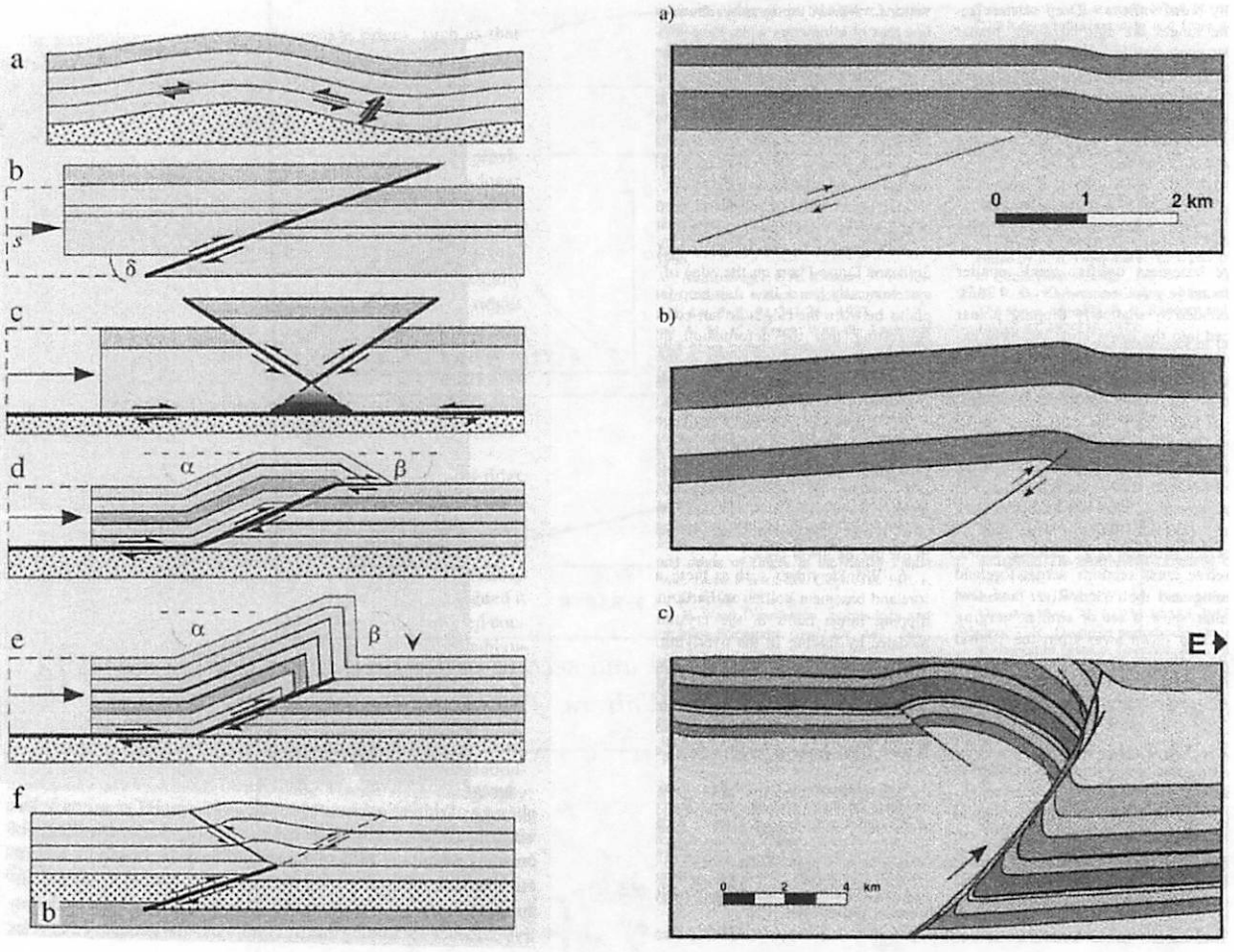

Figure 18.4: *(left) Proposed structural models: (a) buckle-fold showing nucleation of thrust faults within oversteepened concentric folds; (b) thrust fault; (c) conjugate thrust faults; (d) fault-bend fold; (e) fault-propagation fold; (f) blind thrust fault beneath flexural slip anticline with back thrust fault. (After Schultz, 2000)*

Figure 18.5: *(right) Structural cross sections of other possible terrestrial analogs: (a) interpretation of a seismic reflection profile of the Black Hollow trend, Colorado indicating folding in sedimentary rocks overlying a basement thrust fault (no vertical exaggeration); (b) cross section of a clay experiment illustrating foreland basement uplifts in the Rockies, e.g. that in (a); (c) schematic cross section of the Oregon basin thrust, Wyoming (no vertical exaggeration). (From Golombek et al., 2001)*

References:

Golombek M.P., Anderson F.S., and Zuber M.T., Martian wrinkle ridge topography: Evidence for subsurface faults from MOLA. *JGR, 106*, pp. 23,811-23,821, 2001.

Kreslavsky M.A., and Basilevsky A.T., Morphometry of wrinkle ridges on Venus: Comparison with other planets. *JGR, 103*, pp. 11,103-11,111, 1998.

Schultz R.A., Localization of bedding plane slip and backthrust faults above blind thrust faults: Keys to wrinkle ridge structure. *JGR, 105*, pp. 12,035-12,052, 2000.

Watters T.R., Wrinkle Ridge Assemblages on the Terrestrial Planets. *JGR, 93*, pp. 10,236-10,254, 1988.

19 A Brief History of Hanford

by JOE PLASSMANN

Why does Hanford exist in the first place?

During WWII the Manhattan Project was busy trying to create an atom bomb, with the original purpose of bringing an end to the war with Germany. However, by the time of Germany's surrender, the bomb was not ready. Japan was not so lucky. In August of 1945, two bombs, one a uranium bomb, the other plutonium, were used on Japan. Nuclear weapons development has continued, in varous stages of earnestness, since then.

Hanford's part in this story is the manufacture of plutonium. Early in the 20th century, it was discovered that with the addition of a neutron to normally non-fissile U^{238} an entirely new, and fissile metal - Pu^{239} was created [1]. It was recognized that if a strategically significant supply of plutonium could be created, it would greatly increase the number of bombs that could be manufactured. In addition, it wasn't known how well a uranium bomb would work. With the parallel development of a plutonium bomb, the odds of success were greatly increased. There were several plants in the United States that were tasked with creating fissile materials. One, in Oak Ridge, Tennessee, was built to enrich natural uranium (which is mostly unusable U^{238}), and Hanford, Washington, tasked with the production of Pu^{239} from heavy uranium. Since Pu^{239} is created by neutron bombardment of U^{238}, the easiest way to create large quantities of Pu^{239} is to use the neutron flux from the fission of natural uranium^{235} in an enriched mixture of the two isotopes. After the nuclear reaction is complete, the Pu^{239} is chemically extracted [1]. The first reactor at Hanford started operation in September of 1944. Three reactors and two processing plants were in operation by war's end, and by 1955 eight reactors were in operation. The reactors were sited along the Columbia river (100 area [8], see figure), and used river water as coolant [4]. The processing plants were located in the 200 areas, and the fuel fabrication and support buildings were in the 300 area [8].

Plutonium production continued at Hanford from 1944 to 1973, then again starting in 1984, [2]. In the mid 1980's the reactors and processing plants were shut down for the last time [4].

In the 1970's the focus at Hanford changed towards developing non-military uses for nuclear energy. Some of the non-nuclear research programs included solar, geothermal, and advanced systems(?), fossil energy, national security, conservation, energy policy analysis, and resource assessment [8].

There are a whole series of health and environmental concerns with running the reaction and chemical extraction of plutonium. Plutonium itself, while only an alpha emitter (radiation from it can be stopped by a piece of paper), tends to settle in bone marrow, making it dangerous even if ingested in very small quantities. In addition, there are a series of reactor byproducts - short-lived radioactive iodine^{131}, for example, has figured prominently at Hanford. Other metals included plutonium, ruthenium, strontium and cesium [4], and other non-radioactive but toxic metals.

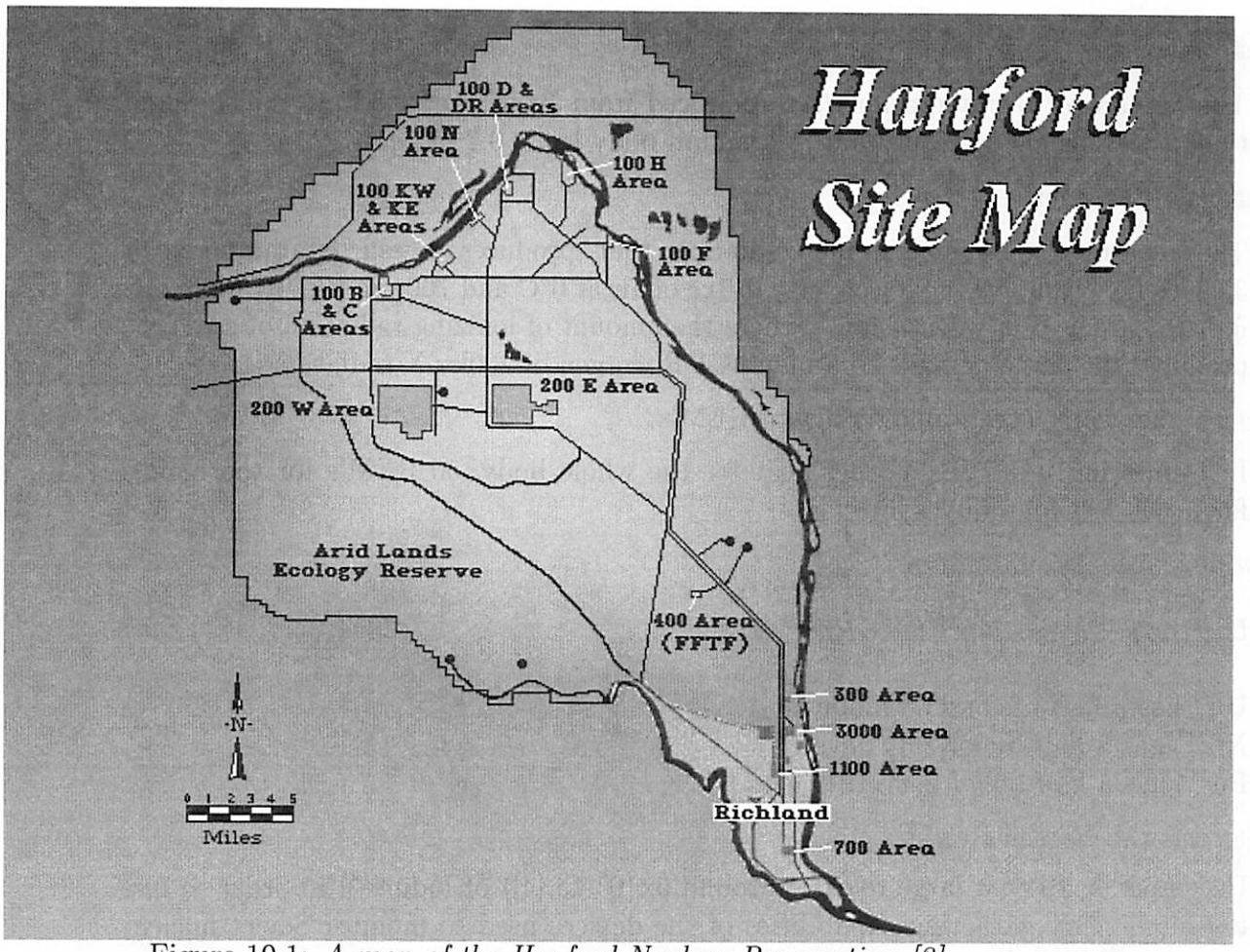

Figure 19.1: *A map of the Hanford Nuclear Reservation [3].*

Some of the environmental challenges at Hanford today:

Storage tanks of toxic materials in the 200 areas (64 were built during WWII alone [8]).

Trenches of low-level radioactive waste (buried up until the 1970's [8]).

Partially lined vaults and surface trenches of contaminated material (post 1970's [8]).

Contaminated groundwater plumes (see *Questions*).

1,391 locations containing contaminated materials are listed at Hanford, including drums, boxes, and bags. There are contaminated locations at the 100, 200, 300, 400 and 600 areas [8].

Since 1989, Hanford has been under the direction of the Office of Environmental Management. As a federally funded Superfund site, The focus now is remediation and cleanup, including processing and storing radioactive and hazardous waste, managing spent nuclear fuels and nuclear material, decontaminating and decommissioning facilities that are no longer needed, and developing technologies to clean up Hanford and other contaminated sites. Hanford contains some 2/3 of the nation's stored weapons-related radioactive waste [8].

Related Questions, in no particular order

What is a Curie (Ci)?

The amount of disintegrations/sec produced from 1g of Ra^{226}, $3.7x10^{10}$ disintegrations/sec, half life of 1620 years. Maximum body load: 0.2 μCi [1].

What is a Roentgen?

The measure of X or gamma radiation that produces 1 esu (statampere, or $3.2256x10^{-10}$ amperes) of electricity in 1cc of air at 0°C and 760mm Hg. REM stands for "Roentgen Equivalent Man", where the amount of ionizing radiation of any type produces the same damage to a man as 1 Roentgen of 200kv X radiation [1].

What is the yearly acceptable dosage of REM's?

In California, it's 5 REM's per year for the whole body, 50 REM's for the hands, forearms, feet and ankles [6].

How do you make plutonium?

$U^{238}(n\gamma)U^{239} \xrightarrow{\beta} Np^{239} \xrightarrow{\beta} Pu^{239}$ [1]

U^{239} has a half-life of 23.5 minutes
Np^{239} has a half-life of 2.35 days
Pu^{239} has a half-life of $2.44x10^4$ years [7].

What was the "Green Run"?

December 2, 1949, a large release (around $5x10^5$ Ci [4]) of $Iodine^{131}$ in order to test the intelligence gathering capabilities of the devices used to monitor Soviet nuclear weapons facilites [2].

Who are the "Downwinders"?

People living downwind of the Hanford reservation when intential or unintentional releases of radioactive materials occurred.

What is the half-life of $Iodine^{131}$?

8 days. [1]

How much radiation was released at the Three Mile Island accident (for comparison)?

About 20 Ci [4].

How many kilograms of U^{235} is needed to create a critical mass?

Little Boy was 64Kg U^{235}, with 1.38% efficiency, 0.9Kg of material fissioned for a yield of 15Kt. [5], so at least this much material is needed.

How many kilograms of Pu^{239} is needed to create a critical mass?

Fat man was 6.2 Kg of Pu^{239}, with beryllium and polonium added to increase neutron production. 1 Kg was converted to energy for a 21Kt yield - about 13% efficiency [5]. So, at least this much material is needed.

When were the bombs dropped on Japan?

Hiroshima, August 6, 1945, Little Boy, a uranium gun-type bomb [5].
Nagasaki, August 9, 1945, Fat Man, a plutonium implosion-type bomb [5].

When was the Trinity test?

July 16, 1945. Plutonium implosion-type bomb [5].

When was it discovered that you could make plutonium out of U^{238}?

In 1940, Seaborg, McMillan, Kennedy, and Wahl created Pu^{238} from U^{238} in the 60 in. Cyclotron at Berkeley. No information on Pu^{239} [1].

What are some of the radioactive and non-radioactive byproducts of breeding plutonium?

There's a lot. The important and dangerous radioactive byproducts (caused by the fission of U^{235}) include cesium^{137} and strontium^{90} (with half-lives of around 30 years), plus iodine^{131} (8 day half-life). Some non-radioactive byproducts include cerium^{140} and zirconium^{94} [7].

What's the toxicity of plutonium?

Permissible quarterly intake: [1]
Pu^{238}: $1.1x10^{-3}\mu Ci$
Pu^{239}: $2.4x10^{-2}\mu Ci$

What was done at Savannah River, Ga?

Plutonium extraction, tritium production.

What else was done at Hanford besides plutonium production?

Research reactors and facilities mostly dealing with improving plutonium production - until the 1970's when the Hanford site branched out into many other science and research areas. See text.

What's the inventory of toxic materials at Hanford?

See text. Also great information here [8].

What's the percentage of U^{235} in natural uranium?

About .7% [7].

How much energy is in Pu^{239}?

1 Kg = 22 GW/hrs of energy = 20Ktons explosive power.

How much contaminated groundwater at Hanford is there, and how big is the contaminated area?

440 billion gallons of contaminated liquids were pumped into the ground. There is approximately 200 square miles of contaminated groundwater [4] [8]. There are 11 contaminants, including tritium, carbon tetrachloride, chromium, nitrates, cobalt, strontium, cesium, technetium, iodine, plutonium, and uranium that exceed drinking water standards at various locations on the site [8].

Bibliography

[1] Handbook of Chemistry and Physics, 65th Edition, *CRC Press*, 1984

[2] Thomas, James P., *Bulletin of the Atomic Scientists*, November/December 2000 Vol. 56, No. 6, pp. 40-41

[3] DOE Hanford Site, *www.hanford.gov*

[4] Short Cressman and Burgess, *The Downwinders Home Page, www.downwinders.com*, Oct 22, 2001

[5] *Society for the Preservation of the Manhattan Project, www.childrenofthemanhattanproject.org*, Sep 10, 2002

[6] EH&S Radiation Safety Training Manual *Office of Environmental Health and Safety, University of California, San Francisco* 1998

[7] C.R. Nave *Hyperphysics* 2002

[8] *U.S. Department of Energy Office of Environmental Management*

20 Fossil Trees and a Fossil.Rhinoceros?! The Ginkgo Petrified Forest State Park and The Blue Lake Rhinoceros Mold

by Abigail Sheffer

What is a fossil?

The remains of a once living organism, including skeletons, tracks, impressions, trails, molds, and casts. A mold is a cavity that retains the shape of the organism, and a cast is when the cavity has been filled by a secondary rock or mineral.

What is petrified wood?

Petrified wood is a fossil cast where minerals, usually silica, have filled in the mold of woody parts of a tree. Casts of small branches, leaves, and fruit are extremely rare.

The Ginkgo Petrified Forest State Park

During the Miocene (20 million years ago), this area had a tropical climate - very wet with a lush forest of mixed deciduous trees (including rare ginkgo) and conifers. It is believed that a large lake formed at Vantage when the Columbia River was temporarily blocked. The river system carried logs to the lake where they gathered in large rafts on both the lake's surface and bottom.

When the lava flows flooded the area and filled the lake at Vantage, the water-saturated logs were entombed rather than burned. For a fossil to form the plant must be quickly buried in an anoxic environment, most often lake bottom sediments or volcanic ash (the combo is also seen). The method of preservation at Vantage is somewhat unusual because the fossils are found directly in the lava itself. More evidence for the fossil logs having been formed in a water-rich environment includes finding pillow basalts directly with the fossils. Few branches, bark, or roots have been found, consistent with them having been stripped as the logs were carried downstream to the lake.

Once the wood was inside the basalt, the water in and around the wood dissolved silica minerals from the basalt. These minerals were carried into the wood and deposited inside its structure. The wood is then said to be silicified. Some question exists about how exactly the silica minerals and the organic structure interact. Different sources state that the organics are replaced by minerals - molecule for molecule or atom for atom. In either case, there seems to be a problem of volume. Although Si and C are chemically similar, Si atoms are larger than C atoms. Other sources say that it is a gradual dissolving of the organics and replacement by minerals. This kind of replacement would not have the problem of volume. Either would completely preserve the structure of the fossil. The other possible process is permineralization, where minerals fill in the pore spaces in the structure or fill in the spaces where the organics have decayed. This may not preserve the cell structure, just the general shape of the wood.

The varied colors of the petrified wood are caused by small amounts of other minerals carried into the wood with the silica.

Silica - white, clear, or grey
Chromium, Copper, Cobalt - green or blue

Manganese Oxides - black, blue, purple, or pink
Iron Oxides - red, orange, yellow, or brown

The last step to get what we see today is erosion - a combination of regular erosion over millions of years and erosion from catastrophic flooding has uncovered the fossils from their basalt tombs.

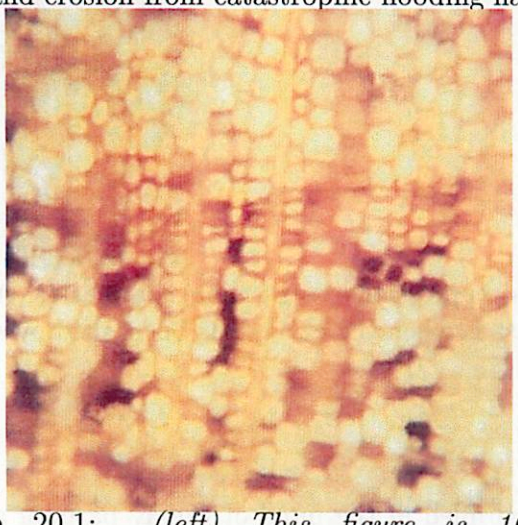

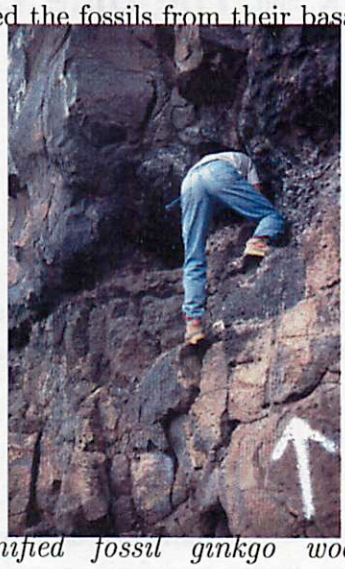

Figure 20.1: *(left) This figure is 100x magnified fossil ginkgo wood. The structure of the cells is used to determine the tree species. From: Strauss, E. (2002)* `http://www.mashell.com/ estrauss/Gink.htm`

The Blue Lake Rhinoceros Mold

In 1935, petrified wood hunters found a body-sized cavity in the basalt of Jasper Canyon on the northeast side of Blue Lake. Climbing inside, they found bone fragments and a jawbone with teeth. In 1948, a plaster cast was made of the inside and the bones identified - it was an early Miocene rhinoceros, Diceratheriom anneciens. The rhino mold was found in a layer of pillow basalt on top of a thin section of sandy sediments. As mentioned before, this area had been very wet with many lakes and streams. The rhino probably died in or was carried to a lake and was still intact when the basalt flows arrived. The water protected the bloated rhino from being completely burned, and the lava cooled quickly around it. Most of the organic material decayed away, leaving just a few bones. According to one visitor, skin textures are visible on the inside of the mold, along with the complete body shape of the rhino, horn and all. The above picture (courtesy of Laszlo) shows the entrance from the rear of the rhino. Sitting inside the mold has been described as a sensation of "rhinowrapping."

The Planetary Connection - indirectly

If Mars (or other planets) once had water and life, especially woody or bony life, then evidence might be preserved in lava flows. There's no way to know unless we go there.

References

Dillhoff, T., 2002, Fossil Forests of Eastern Washington.
`http://www.evolvingearth.org/learnearthscience/sciencearticles0501fossilforest.htm`
Fire, Faults, and Floods, M Mueller and T Mueller, 1997, University of Idaho Press, Moscow ID, 288 pp.
Raynolds, B., 1999, Rhino Revelation.
`http://www.fossilnews.com/1999/rhino.html`
Roadside Geology of Washington, DD Alt and DW Hyndman. 1984, Mountain Press Publishing Co., Missoula, MT 288 pp.
Strauss, E., 2001, Petrified Wood from Western Washington.
`http://www.mashell.com/ estrauss/pwoodfx.html`

21 Vortex Scouring and Scabland Formation

by MATT TISCARENO

Glossary

Basalt Entablature – Top layer of basalt, generally more resistant to erosion than *colonnade.*
Basalt Colonnade – Lower layers of basalt, fractured by *columnar jointing.*
Columnar Jointing – When igneous rocks cool below the surface, the associated contraction can cause vertical fractures that divide the basalt mass into columns.
Kolk – A vertical vortex with tremendous sucking power. Kolks play an important role in macroturbulent erosion, including plucking and scouring.

Scabland Formation

The characteristic topography known as **scabland** is the result of the erosion of bare basalt surfaces by macroturbulent flow. Three major erosional stages of scabland formation (see Figure 21.1):

1. After any overlying loess has been removed, erosion of the *entablature* begins with **Longitudinal Grooving**. Average grooves are 50 meters wide, 5 meters deep. Can be kilometers long. Figure 21.2 shows grooves above Dry Falls.
2. Once *kolks* begin to penetrate through the *entablature*, they begin to erode vertically into the *colonnade* by **plucking** out large blocks of basalt. The results of this are **Potholes** and **Butte-and-Basin Topography**. An example of this is seen in Figure 21.3.
3. The end stage of erosion is the formation of a **Deep Inner Channel**.

Vortex Scouring

Another erosional form associated with macroturbulent flow is **vortex scouring**, formed by to increased pressure caused by the deflection of fluid around an obstacle. Think of erosion you feel when you place your foot in receding surf, although patterns are somewhat different when flow is turbulent. Two separate processes form scouring features, one upstream of the obstacle, the other downstream.

Upstream of the obstacle, vortices roll ahead of the obstacle and around it, forming a "horseshoe vortex." The result is a crescent-shaped scour hole immediately upstream of the obstacle. Downstream of the obstacle, vortices peel off the obstacle and migrate down, in a "wake vortex." In less-intense turbulent regimes, flow velocities in the wake are low, resulting in an elliptical depositional feature known as a pendant bar. As turbulent increases, the wake vorticesdevelop into *kolks*, forming a large elliptical scour hole in the lee of the obstacle.

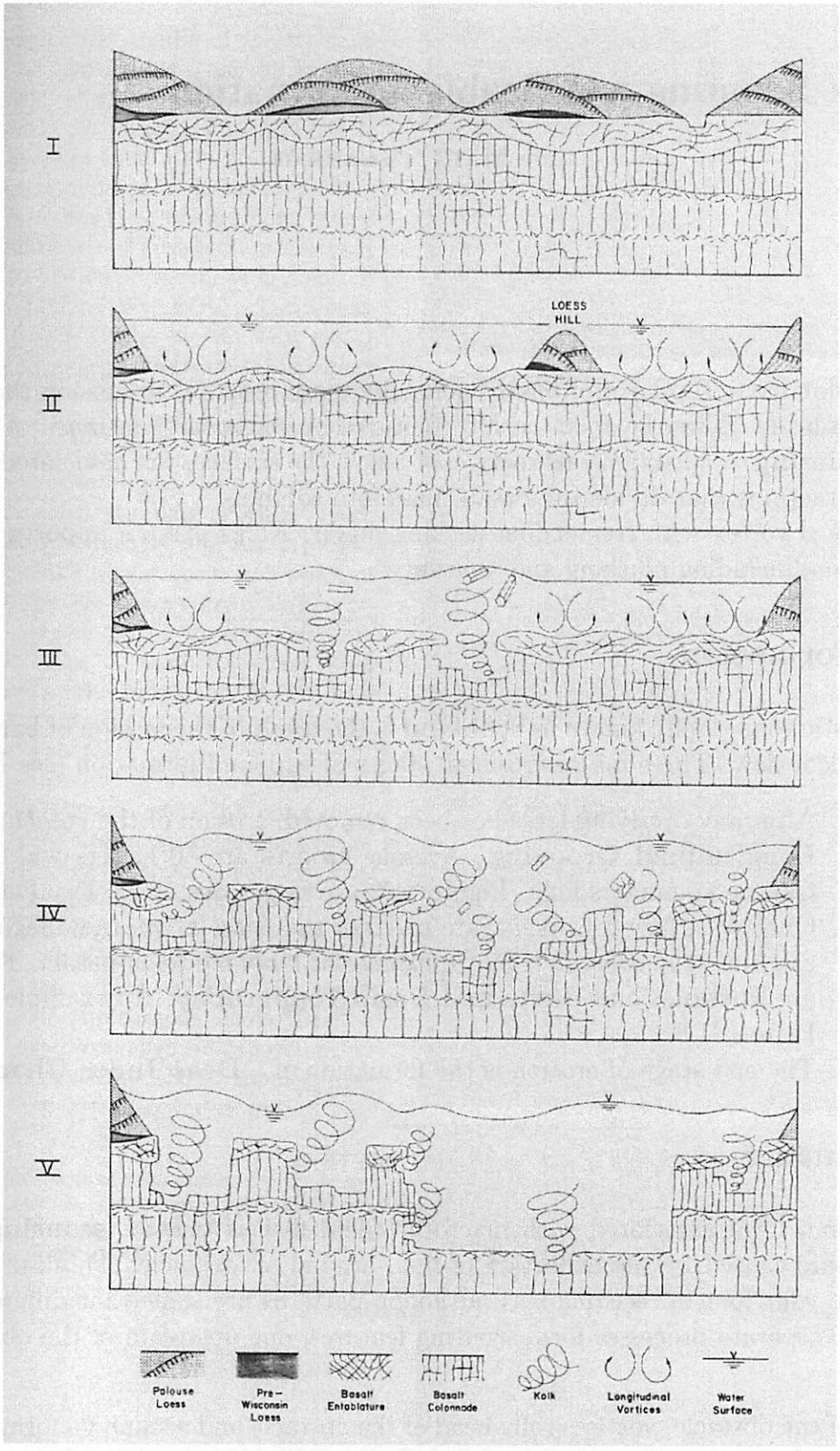

Figure 21.1: Hypothetical sequence of flood erosion for a typical scabland divide crossing. From Figure 5.32 of Baker (1978).

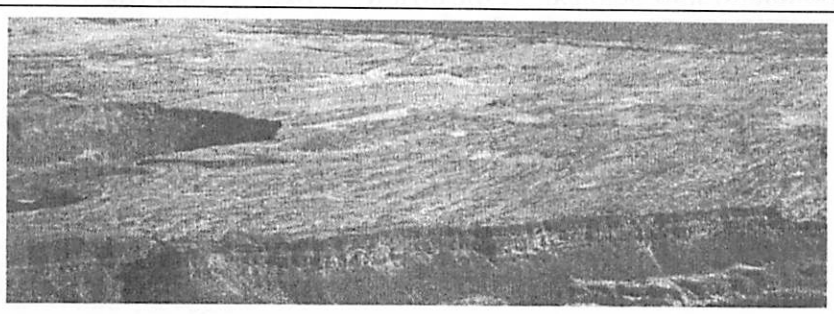

Figure 21.2: Longitudinal grooving near Dry Falls, WA. Dry Falls itself is on the left. From Figure 5.23a of Baker (1978).

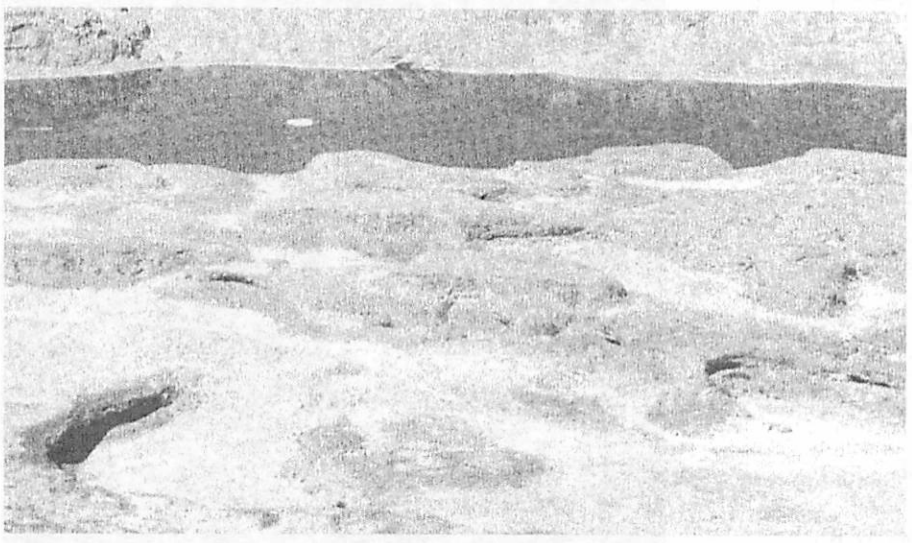

Figure 21.3: Butte-and-basin topography near Blue Lake, WA. From Figure 5.30b of Baker (1978).

Macroturbulent Erosional Forms on Mars

Burr *et. al.* (2002) report longitudinal grooves on Mars (Figure 21.4), as one of many pieces of evidence for high-volume floods in the Cerberus Plains. The Martian grooves are 100 meters wide and 10 meters deep. Some evidence may exist for vortex scouring features on Mars (D. Burr, pers. comm.), although they are on the cusp of visibility for MOC and MOLA. The presence or absence of vortex scouring could provide a constraint for flow velocities of Martian floods.

References

Baker, V. R. 1978. "Large-Scale Erosional and Depositional Features of the Channeled Scabland" in *The Channeled Scabland* (V. R. Baker and D. Nummedal, Eds.), pp.81-115. NASA, Washington.

Burr, D. M., A. S. McEwen, and S. E. H. Sakimoto 2002. Recent aqueous floods from the Cerberus Fossae, Mars. *Geophys. Res. Lett.* **29** (1), 10.1029/2001GL013345.

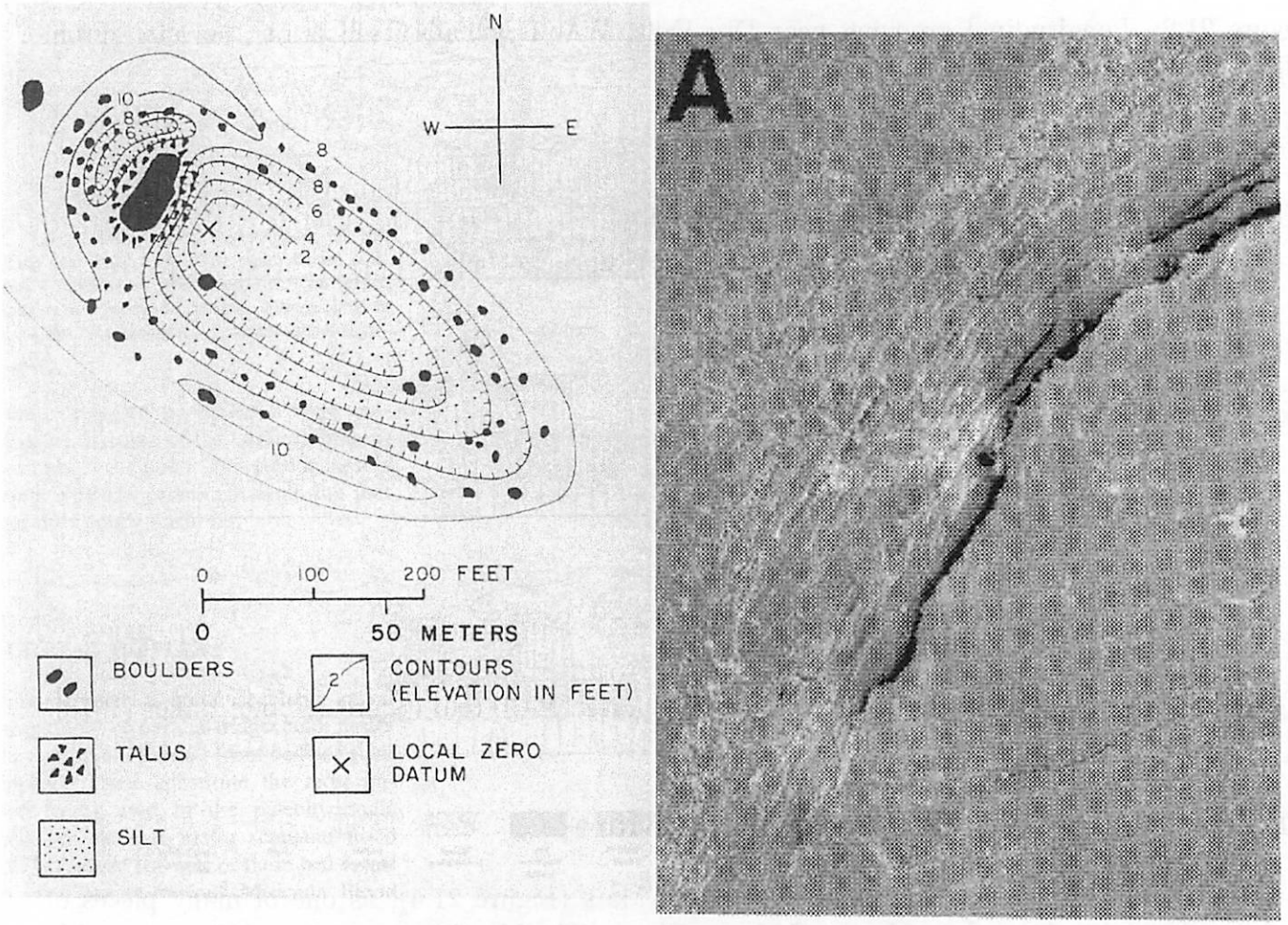

Figure 21.4: *(a) Longitudinal grooving in Athabasca Valles on Mars. From Figure 1a of Burr et. al. 2002. (b) Scour hole development near an* $18x11x8$ *m boulder. From Figure 5.33b of Baker (1978).*

22 Giant Current Ripples

by ADINA ALPERT

Background

"Giant current ripples" are parallel ridges found atop depositional gravel bars formed by the Lake Missoula floods (Fig 22.1). They were identified and named by Bretz, Smith, and Neff in their 1956 GSA paper. Detailed aerial photographic surveying have revealed over 100 trains of these bed forms in the Channeled Scabland (Baker 1978).

Figure 22.1: *Giant current ripples on a gravel bar.*

Morphology

The giant current ripples have an asymmetric profile, with the downstream-facing slopes (lee sides) averaging $\sim 18-20°$, and the upstream-facing slopes (stoss sides) averaging $\sim 6-8°$ (Fig 22.2, left). The plan view form can be classified as transverse catenary and out of phase, with cuspate troughs on the lee slopes (Fig 22.2, right). Chord lengths (wavelengths) generally range from 20 to 200 m, and heights range from 1 to 15 m (Baker 1978). The heights have probably been reduced slightly by waning flood stages and post-flood modification (in some areas, the post-flood loess deposition has completely buried giant current ripples).

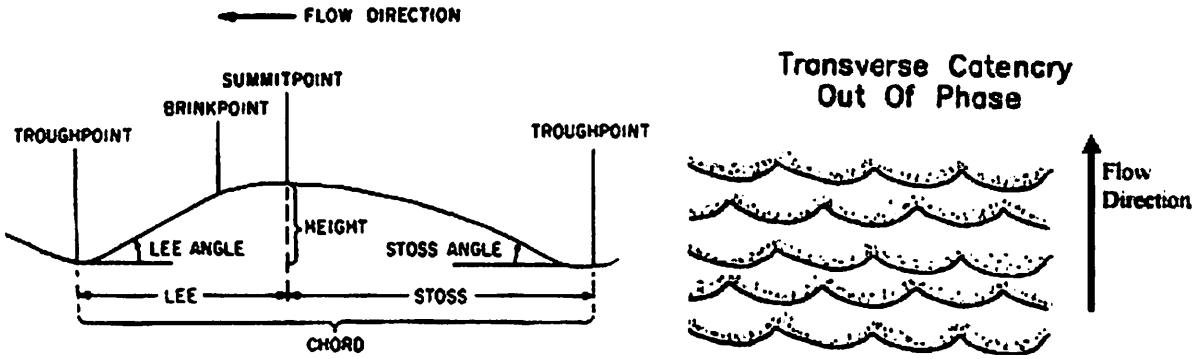

Figure 22.2: *(left) Features of a giant current ripple viewed in profile (Baker 1973). (right) Sediment ripple form of the giant current ripples (modified from Allen 1968).*

The sediment comprising the giant current ripples is some of the coarsest known to occur in large-scale depositional bed forms. The largest particles are 1.5 m or greater in diameter.

Hydraulic Parameters

The hydraulic factors that determine ripple form can include (1) water depth, (2) slope, (3) particle size and shape, (4) particle sorting, (5) specific gravity of the grains, (6) density and viscosity of the water-sediment mixture, and (7) cross-sectional shape of the channel (Harms & Fahnestock 1965).

Baker (1973 & 1978) used ripple height and chord data from 40 scabland ripple trains to find their correlation to these hydraulic factors in order to evaluate the hydraulic environment which resulted in these giant current ripples. The following includes the results from the ripple chords only, since they are believed to be a more general indicator of maximum flow conditions than ripple height.

- **Mean ripple chord** ($\bar{B}$, in feet) vs. **Maximum flow depth** (D, in feet)
  * $\bar{B} = 37.8 \cdot D^{0.348}$
  * correlation coefficient = 0.758

- **Mean ripple chord** vs. **"Depth-slope"** product (DS)
- "Depth-slope" represents a maximum shear stress achieved by the passage of the flood through the reach containing the giant current ripples. Its importance is its influence on the critical interactive force necessary to initiate bed-load movement.
- $DS = \tau/\gamma$, where D = depth, S = Slope, τ = shear stress, γ = specific weight (65 lbs/ft^2 for cold water with 20,000 ppm suspended sediment)
  * $\bar{B} = 393.5(DS)^{0.66}$
  * correlation coefficient = 0.945
- Since critical shear stress is related to the maximum grain size moved in traction, ripple chord should also be related to the maximum grain size, and it is (correlation coefficient = 0.930).
- **Mean ripple chord** vs. **Mean flow velocity** ($\bar{V}$, in feet/second)
  * $B = 8.24 \cdot \bar{V}^{0.870}$
  * correlation coefficient = 0.81
- The relatively low correlation may arise from the fact that the mean velocity in deep flows lies considerably above the mobile bed. The bed forms, like boulder movement, actually respond to

velocities close to the bed.

- Mean ripple chord vs. Stream power (ω)
  - Stream power is commonly used to predict certain bed forms.
  - $\omega = \tau\bar{V} = \gamma(DS)\bar{V}$
    * $B = 8.65\omega^{0.458}$ (Fig 22.3)
    * correlation coefficient = 0.977: highest of any parameter!
- **Froude number** (F)

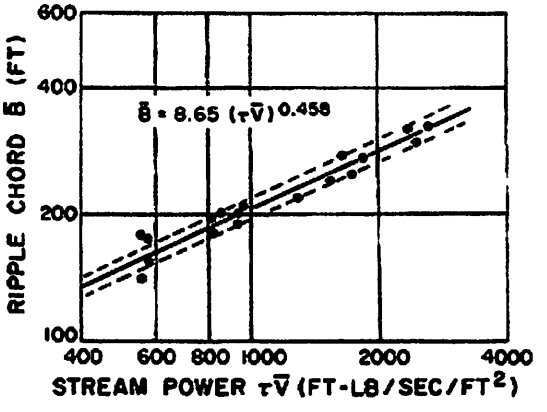

Figure 22.3: *Mean ripple chord as a function of stream power. The dashed lines represent one standard error..*

  - ranges from 0.5 to 0.9
  - $F < 1$ is sub-critical flow.
  - These bed forms are formed within the tranquil range.
  - This Froude numbers reinforce the concept that scabland giant current ripples are the large-scale, coarse-grained analogs of dunes. Thus, despite their name, "giant current ripples are not true ripples, which are only responsive to boundary conditions, but sub-aqueous dunes, which *are* responsive to the hydraulic flow.

Summary of the Hydraulic Environment

- Flow depths ranging from 40 to 500 feet
- Water-surface slopes ranging from 0.0014 (7 feet/mile) to 0.0057 (30 feet/mile)
- Mean flow velocities of 30-60 feet/second, while Froude numbers indicate the maintenace of tranquil flow
- Subrounded basaltic bed-load ranging in size from granule and pebble gravel to boulders 5 feet in diameter
- A cold, turbid transporting fluid with a probably specific weight of 65 lbs/ft^2

Giant Current Ripples may be the most convincing evidence that the Channeled Scabland formed by a massive flood!

Giant Current Ripples on Mars

MOC has imaged features that may be "giant current ripples" in Athabasca Vallis (Fig 5). Burr et al. (2002) describe these features as slightly sinuous or barchanoid in plan view and have chord lengths averaging approximately 50 m, similar to the giant current ripples in the Channeled Scabland. So far, only one MOC image shows features such as these. Possible explanations for the rare occurrence of giant current ripples on Mars include that the hydraulic or sedimentary conditions on Mars may not have been generally conducive to the formation of such features, or perhaps MOC coverage may under-represent their true abundance (Burr et al. 2002). Nevertheless, the presence of the features in Athabasca Vallis provide geomorphic evidence for large-scale aqueous flooding on Mars.

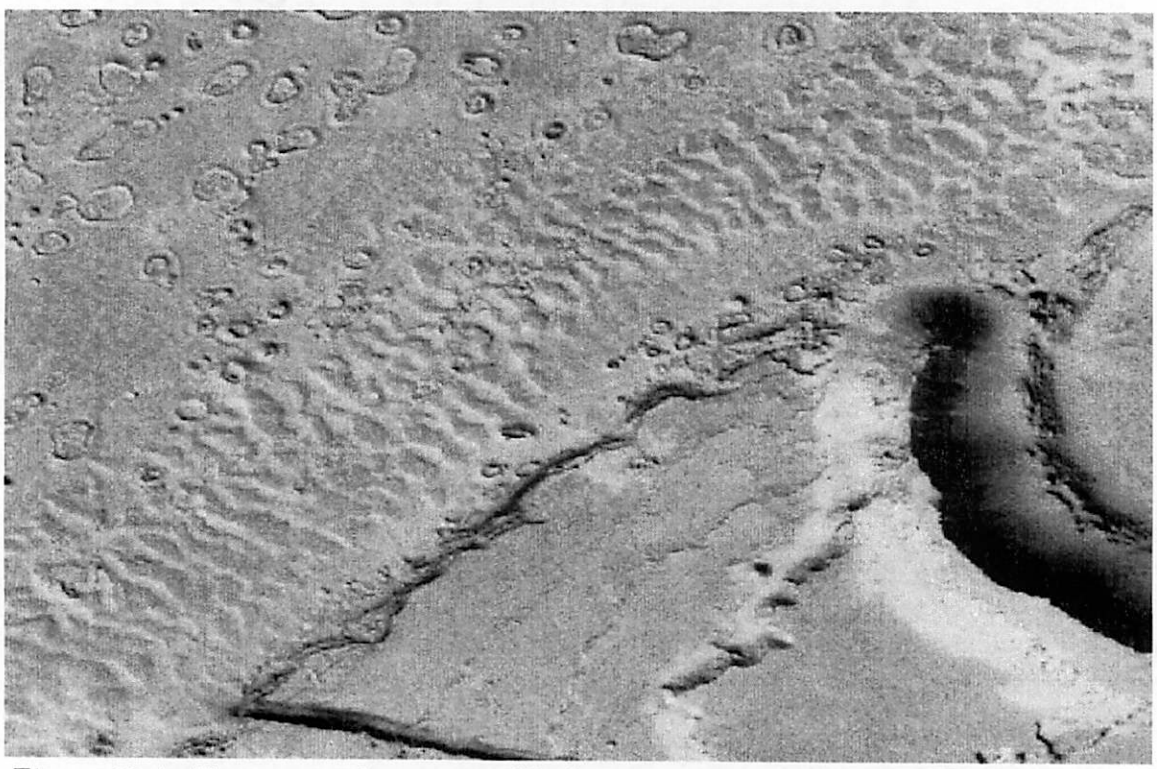

Figure 22.4: *Transverse dunes, possibly "giant current ripples" in Athabasca Vallis, Mars..*

References

Allen, J. R. L., 1968, Current Ripples: Their Relation to Patterns of Water and Sediment Movement, Amsterdam, Netherlands.

Baker, V. R., 1973, Paleohydrology and sedimentology of Lake Missoula flooding in eastern Washington, Geol. Soc. Am. Spec. Paper 144, 79 pp.

Baker, V. R., 1978, Large-scale erosional and depositional features of the Channeled Scabland, in *The Channeled Scabland*, V. R. Baker and D. Nummedal (eds.), NASA, Washington, DC, pp. 81-115.

Bretz, J. H., Smith, H. T. U., and Neff, G. E., 1956, Channeled Scablands of Washington: New data and interpretations: Geol. Soc. Am. Bull., 67, pp. 957-1049.

Burr, D. M., Grier, J. A., McEwen, A. S., and Keszthelyi, L. P., 2002, Repeated aqueous flooding from the Cerberus Fossae: Evidence for very recently extant, deep groundwater on Mars, *Icarus* 159, 53-73.

Harms, J. C., and Fahnestock, R. K., 1965, Stratification, bed forms, and flow phenomena (with an example from the Rio Grande), Soc. Econ. Paleontologists and Mineralogists Spec. Pub. 12, pp. 84-115.

23 Hanging Valleys and other Glacial Features

by BRANDON PREBLICH

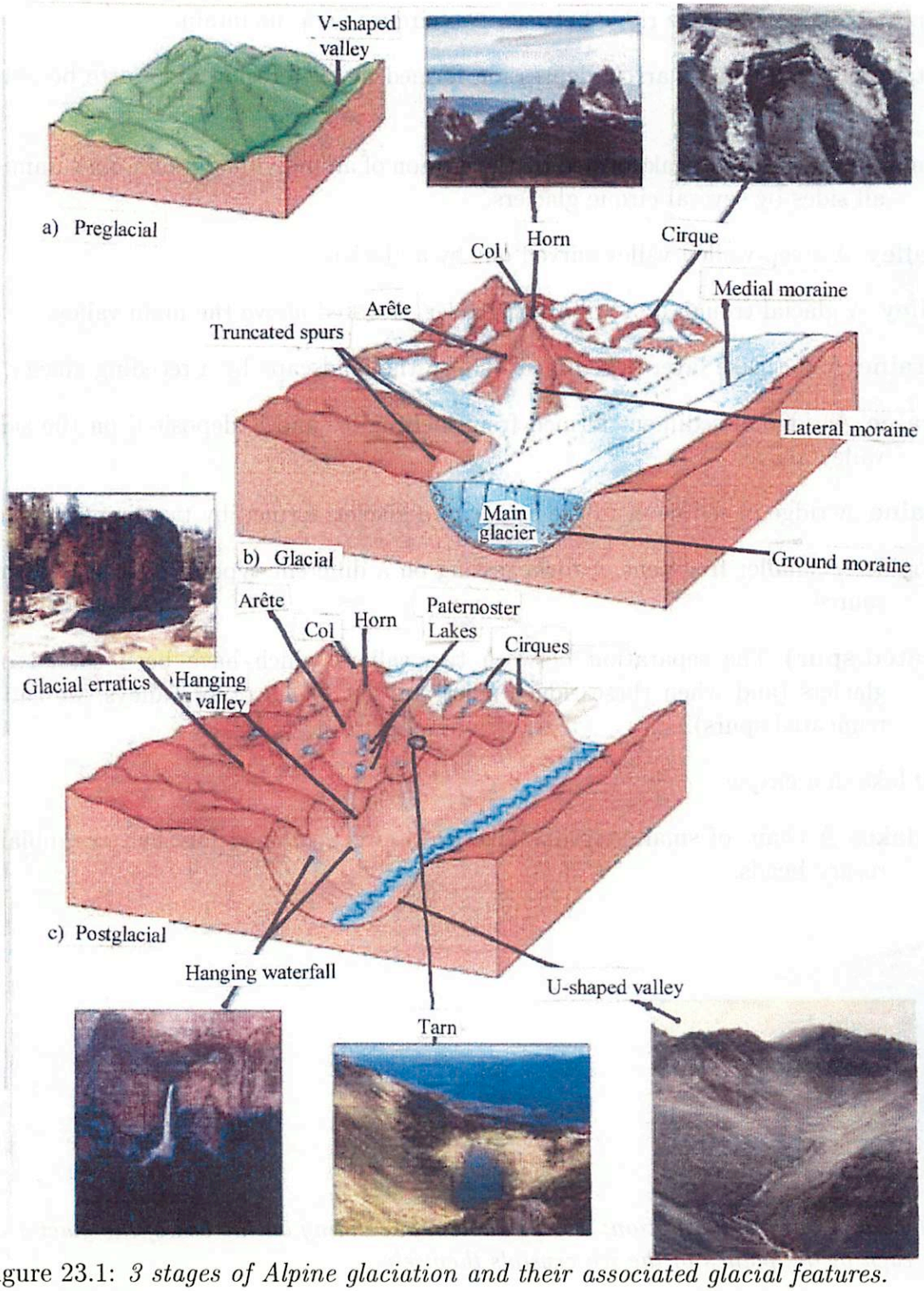

Figure 23.1: *3 stages of Alpine glaciation and their associated glacial features.*

Glacial Features

V-shaped valley A valley carved out by a river running though it.

Cirque A bowl-shaped depression at the top of a mountain slope, formed by a glacier.

Arte A sharp, serrated, knife-edge ridge between two cirques on a mountain.

Col A mountain pass/saddlelike narrow depression formed by the erosion of an arte between two adjacent cirques.

Horn A pyramidal, steep-sided peak formed by the erosion of an individual mountain summit from all sides by several cirque glaciers.

U-shaped valley A steep-walled valley carved out by a glacier.

Hanging valley A glacial trough of a tributary glacier, elevated above the main valley.

Ground moraine A sheetlike layer of sediment left on the landscape by a receding glacier.

Lateral moraine A ridge of sediment formed from melting ice and is deposited on the side of a valley glacier.

Medial moraine A ridge of sediment in the center of a glacier, formed by two merging glaciers.

Erratic A boulder / smaller fragment of rock, resting on a different type of bedrock far from its source.

Spur (truncated spur) The separation between two valleys which have been carved out by glaciers (and when these ridged spurs are cut off by other valleys, we call them truncated spurs).

Tarn A small lake in a cirque.

Paternoster lakes A chain of small step-like lakes in a cirque, named for their resemblance to rosary beads.

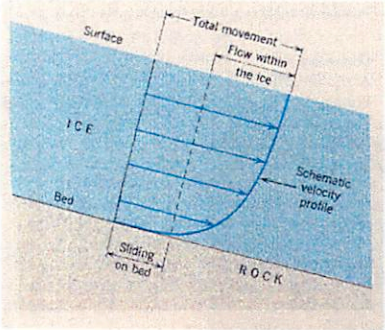

Figure 23.2: *Two types of glacial motion: 1. the whole mass sliding on the bed of the glacier and 2. slipping along each of the planes of the ice crystals themselves.*

Figure 23.3: *A hanging valley (the U-shaped valley on the right with the waterfall flowing down from it).*

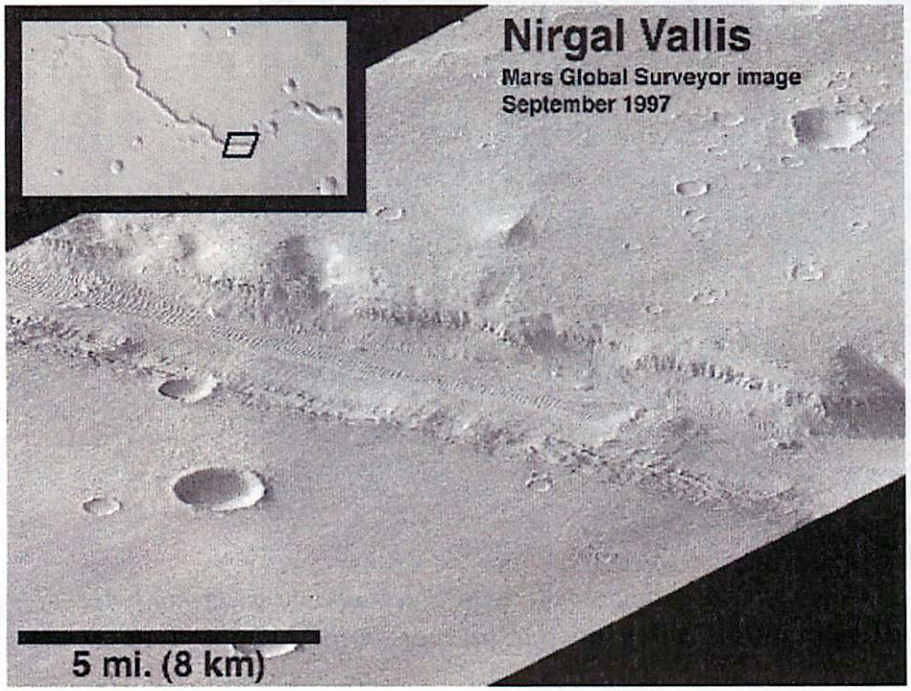

Figure 23.4: *Overview of Nirgal Vallis (see the below figures for details).*

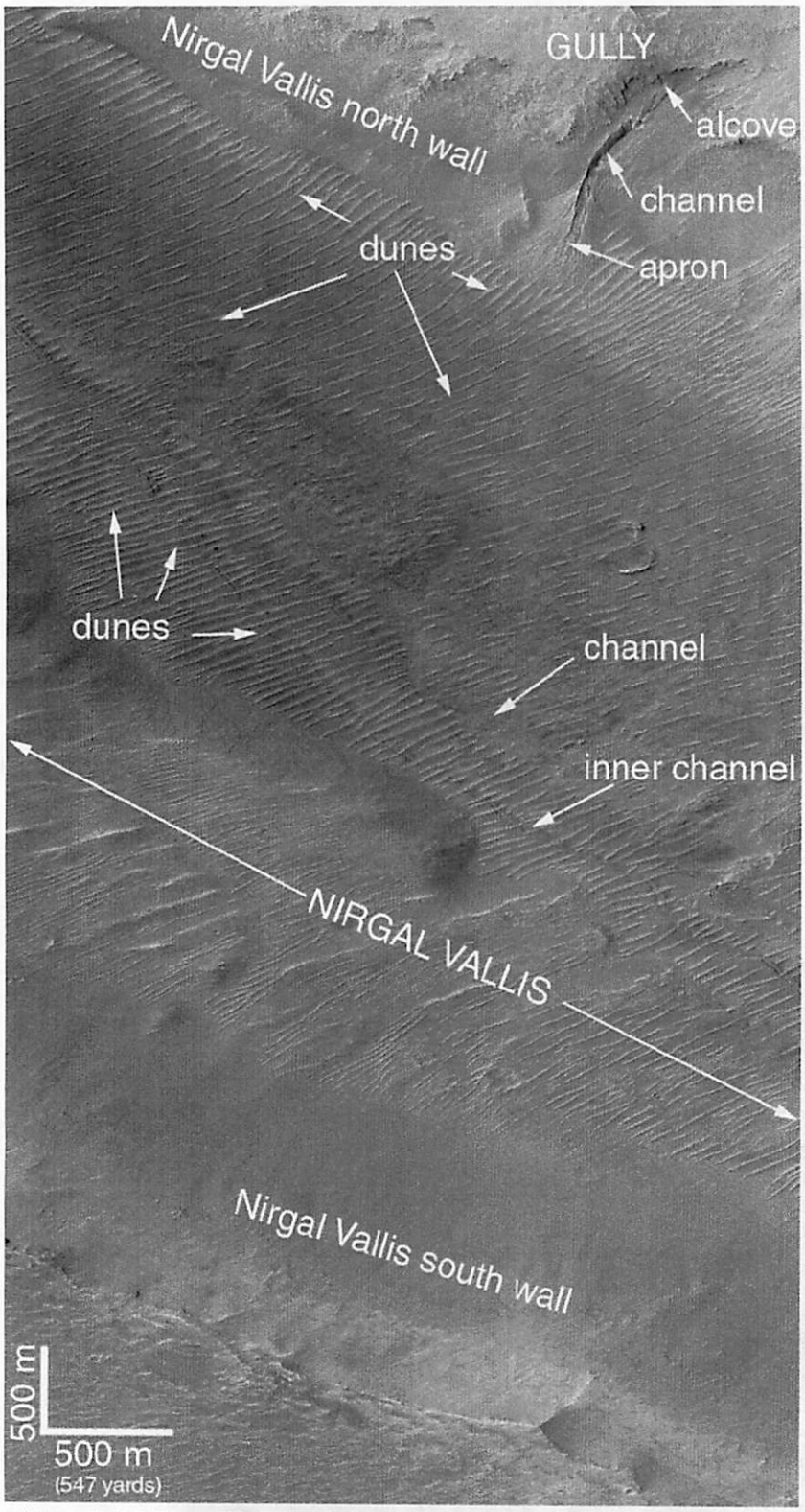

Figure 23.5: *Nirgal Vallis. View of the valley itself, with channels showing evidence of running fluid, below an alcove formed by material collapsing due to undermining by the fluid (see last image for close up view of channels).*

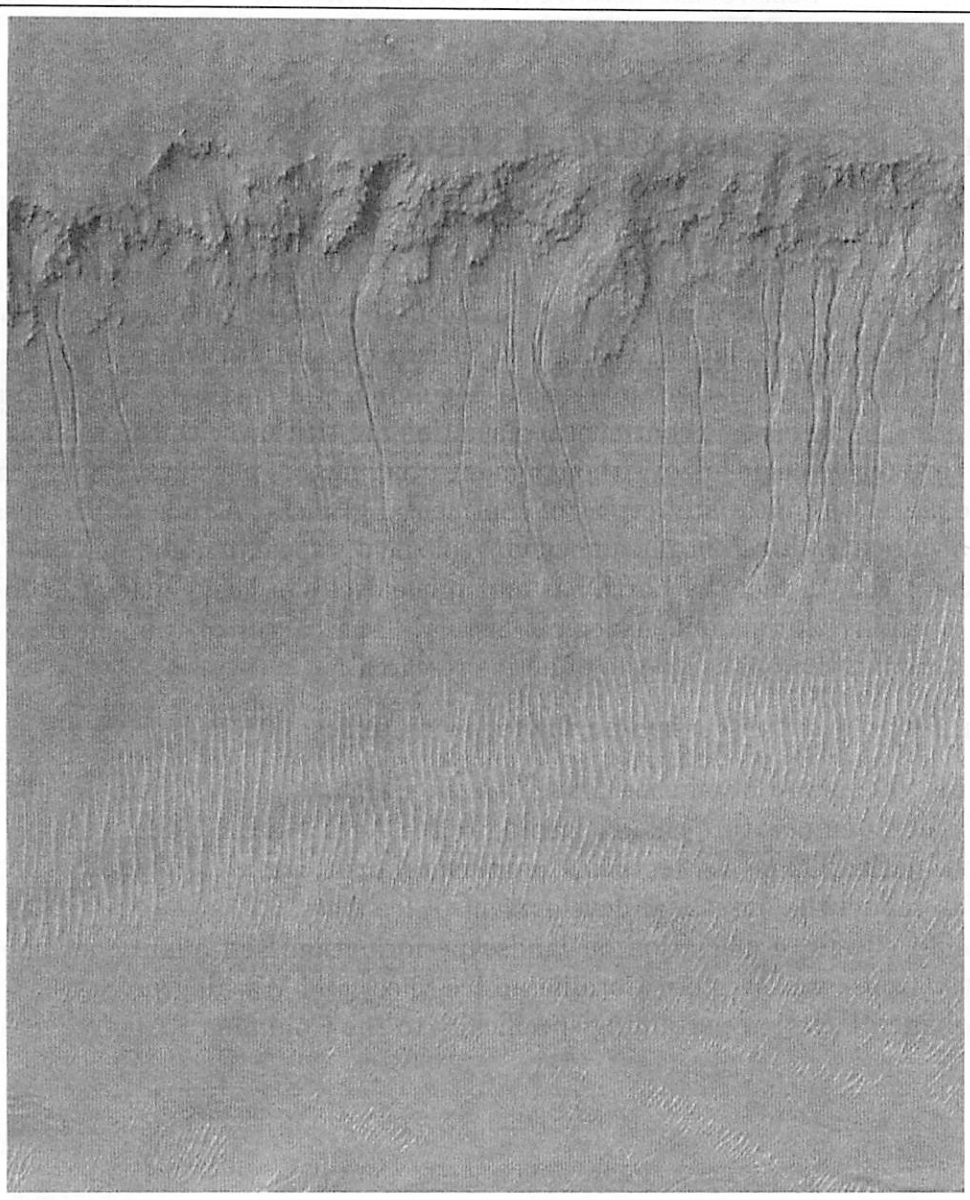

Figure 23.6: *Nirgal Vallis. Close up view of the south-facing valley wall (on the inside of the valley). The channels all start at roughly the same position near the top of the wall, leading to an idea that at the time these channels formed, there was a fluid layer which intersected the valley in this area. This is an analog to a hanging valley because the main valley (going left-right in the image) eroded (most likely by water) and is lower than the layer out of which the fluid is flowing.*

References

Busch, R. M., and Tasa, D. (1993). Laboratory Manual in Physical Geology. Macmillan Publishing Company.
Christopherson, R.W. (2000). Geosystems. Prentice Hall.
Flint, R.F., and Skinner, B.J. (1977). Physical Geology. John Wiley & Sons.
Jakosky, B. (2000). Unearthing Seeps and Springs on Mars, The Planetary Report, Sept/Oct 2000.
Marshak, S. (2001). Earth; Portrait of a Planet. W.W. Norton & Company, Inc.
Read, H.H., and Watson, J. (1972). Beginning Geology. Macmillan & Company, LTD.
TES NEWS: `http://emma.la.asu.edu/TESNEWS`
JPL: `http://masr.jpl.nasa.gov`
About.com: `http://geology.about.com`

24 Pleistocene Climate and Glacial History

by CURTIS S. COOPER

The recurring advance and retreat of vast glacial ice sheets into North America are associated with a general cooling of the global climate during the Pleistocene period, which began roughly 1.8 Ma ago.[1] Each advance of the glaciers marks the beginning of a small Ice Age during this geologic period. The causes of large-scale continental glaciation are tied up with the general global temperature variation through geologic history, though many other factors play a role in determining the cycle of growth, advance, and ultimate retreat of continental glaciers. Although Ice Ages were previously thought to be a relatively recent phenomenon, geologically speaking, new evidence points to the alternate hypothesis that in fact the Earth has undergone cycles of heavy glaciation followed by periods of general warming throughout geological history. The causes of the general climate variation of the Earth through time are subjects of active research.

In my presentation, I will lead a discussion on the following topics:

Evidence for the history of climate change on the Earth.
Causes of global temperature change leading to Ice Ages.
Correlations with CO2 levels, tectonics, continental drift, etc.
Attempts to model the onset and development of Ice Ages.
The profound effects of glaciation on landscape formation, soil quality, sediment deposits, extinctions, etc. Western Cordilleran Ice Sheet and Washington State.
Issues involving glaciation pertaining specifically to the Columbia River.

References

[1] **The Physical Geography of North America**, Edited by A.R. Orme, Oxford University Press, Oxford, 2002.

[2] **Glacial Geology and Geomorphology of North America**, American Geophysical Union, Washington, D.C., 1989.

[3] `http://www.scotese.com`

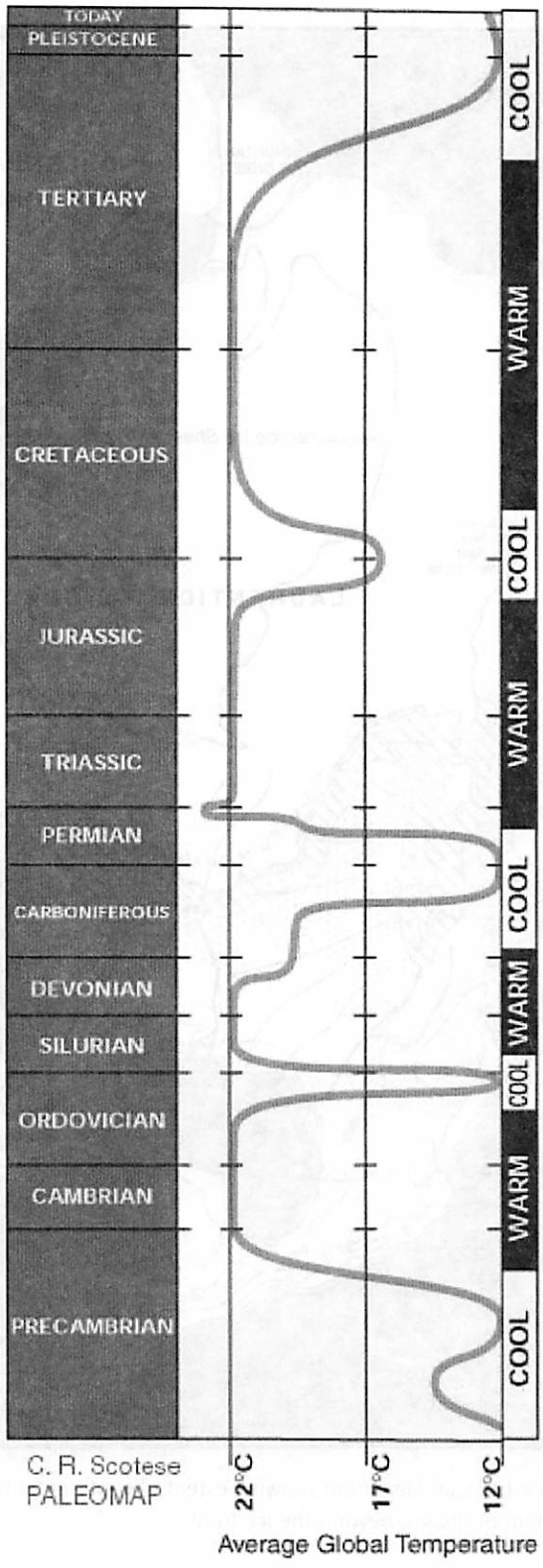
TODAY
PLEISTOCENE
TERTIARY
CRETACEOUS
JURASSIC
TRIASSIC
PERMIAN
CARBONIFEROUS
DEVONIAN
SILURIAN
ORDOVICIAN
CAMBRIAN
PRECAMBRIAN
COOL
WARM
COOL
WARM
COOL
WARM
COOL
WARM
COOL
C. R. Scotese
PALEOMAP
22°C
17°C
12°C
Average Global Temperature

Figure 24.1:

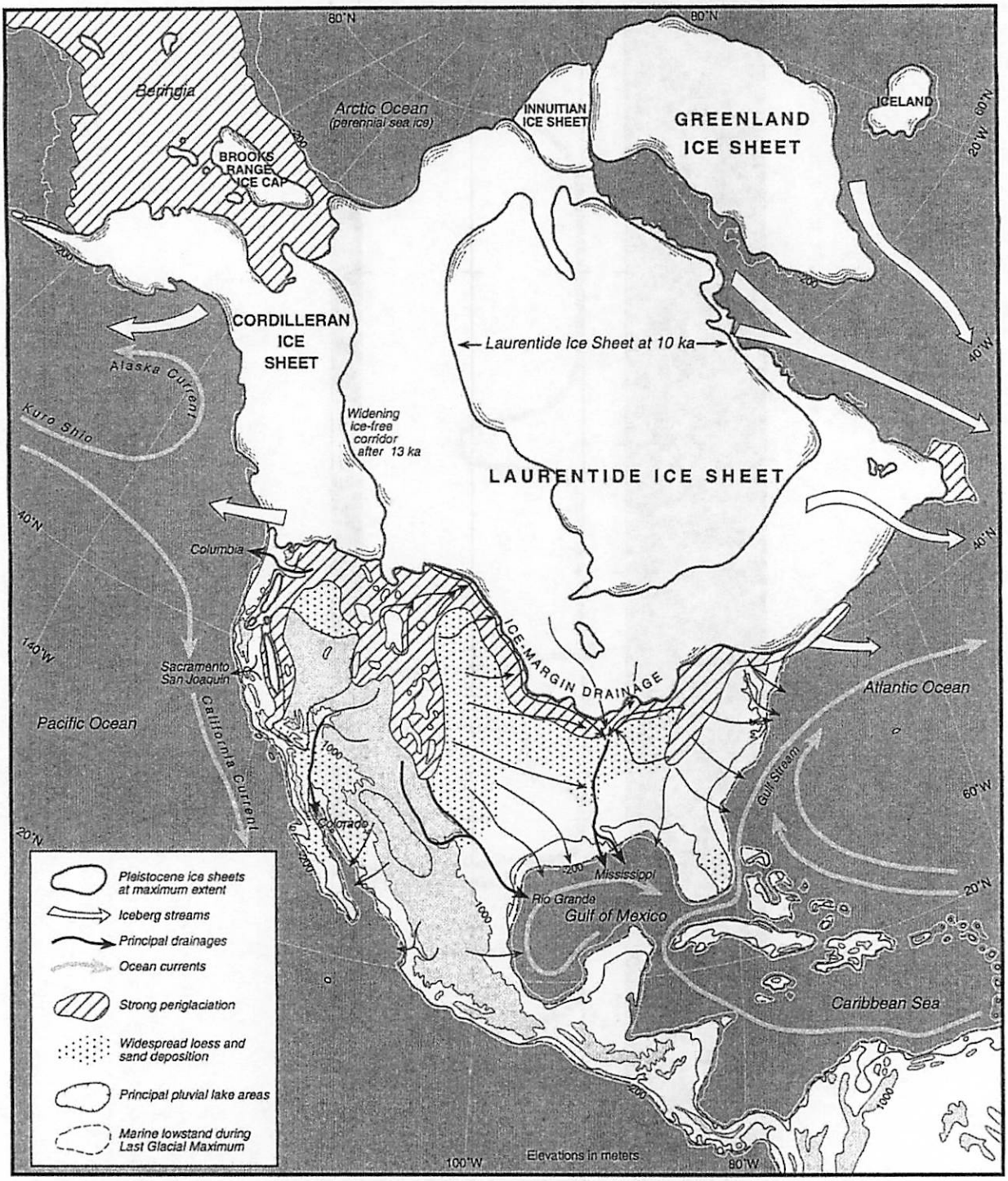

Figure 3.1 North America during the Last Glacial Maximum showing extent of continental ice sheets, larger ice caps, periglacial and aeolian activity, and main drainages beyond the ice front.

Figure 24.2:

'able 2.2 Correlation of Quaternary Glaciations in Canada and the United States of America (modified from Bowen et al., 1986)

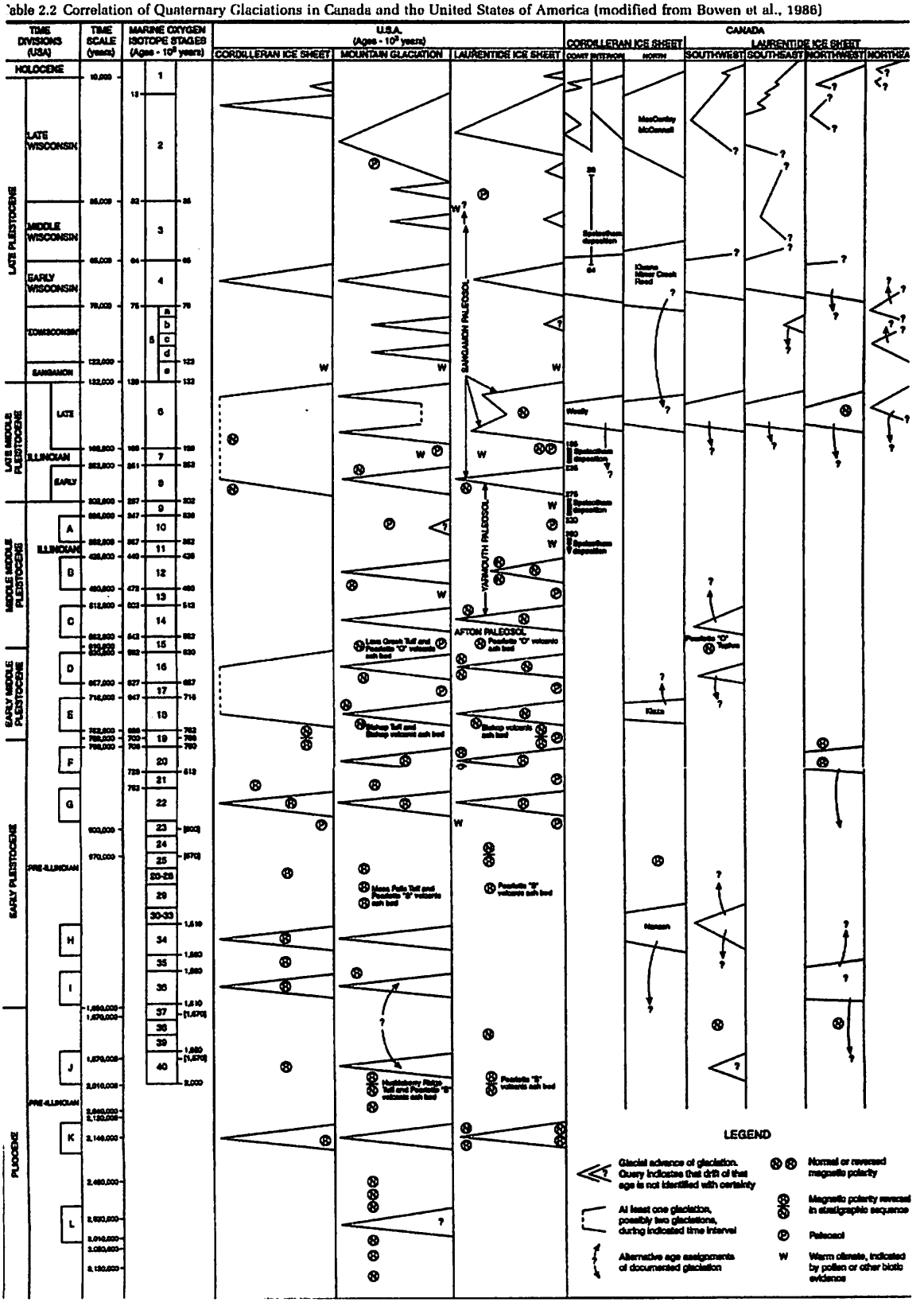

Figure 24.3:

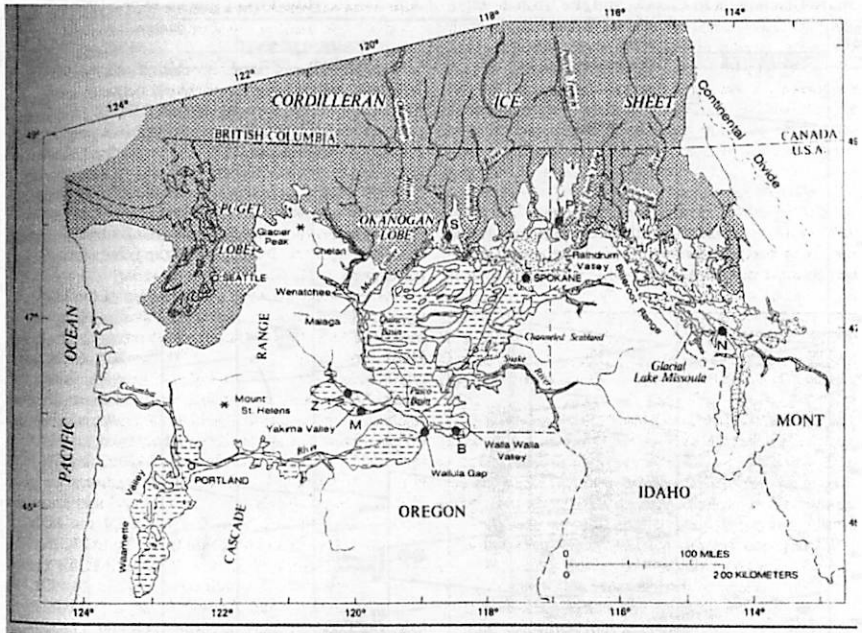

Figure 1 Map of Columbia River valley and tributaries. Irregular small-dot pattern shows maximum area of glac Lake Missoula east of Purcell Trench ice lobe and maximum extent of glacial Lake Columbia east of Okanogan lot Dashed-line pattern shows area that, in addition to these lakes, was swept by the Missoula floods. Late Wiscons Cordilleran icesheet margin (heavy-dot pattern) is from Waitt and Thorson (1983, Fig. 3-1). Large dots indicate sit of bedded flood sediment mentioned text or figures: B, Burlingame Canyon; L, Latah Creek; M, Mabton; N, Ninem Creek; P, Priest valley; S, Sanpoil valley; Z, Zillah. From Waitt (1985, Fig. 1).

Figure 24.4:

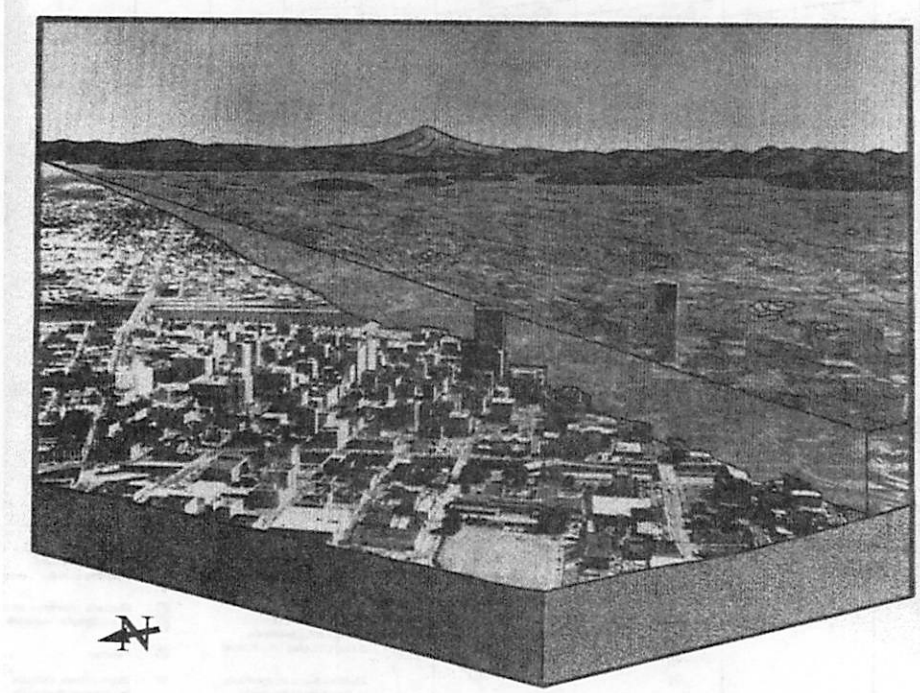

Cover Portland, Oregon under a Pleistocene Missoula flood.

Figure 24.5:

DRY FALLS GEOLOGY AND HISTORY

Fall 2002 Mega Trip

Jonathan Fortney

- Falls width: 5.5 km (3.5 x Niagara Falls!)
- Falls height: 120 m (2.4 x Niagara Falls!)

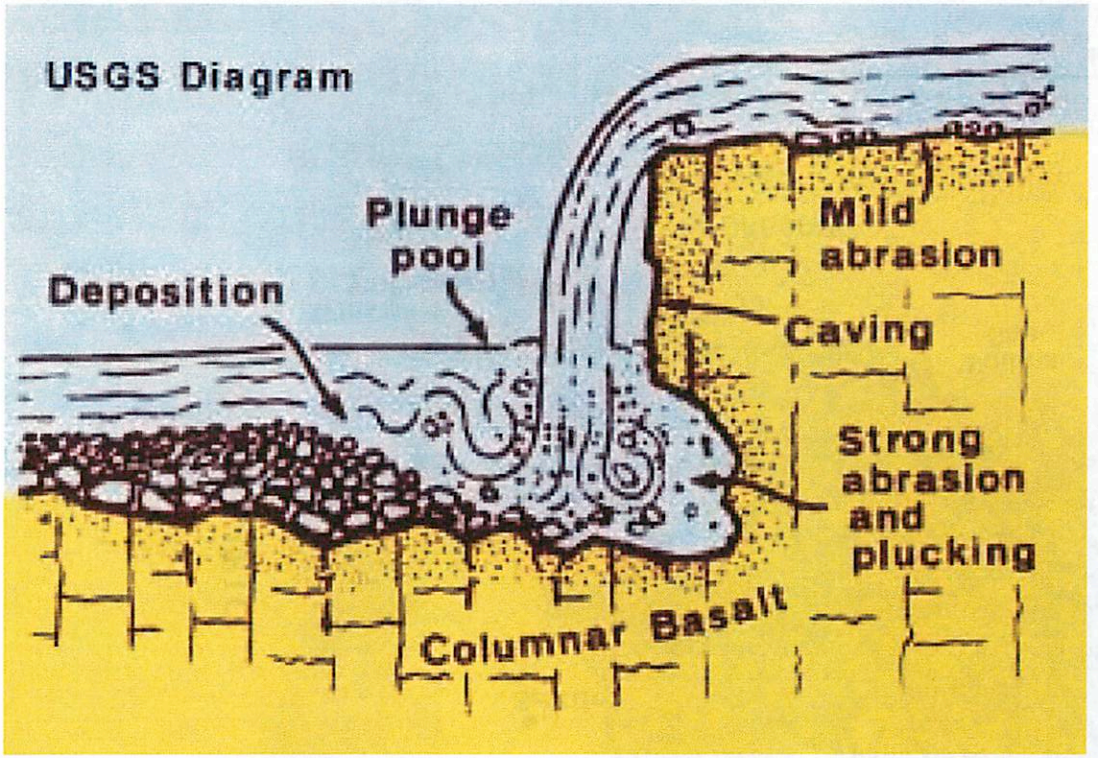

Diagram of a waterfall

Dry Falls are a cataract, a waterfall with a single, sheer drop, usually with a large volume of water flowing over the falls. Cataracts have horseshoe-shaped headcuts and large, enclosed depressions at their bases.

The location of the falls appears to have moved upstream 25-30 km since their creation, due to erosion as depicted at left.

The flooding was episodic, happening perhaps ~ 60 times (or more) over the course of history 12,000 to 20,000 years ago.

Lake Missoula held ~ ½ the water of Lake Michigan, and drained in several days. Water volume over the falls may have been so high that the falls itself were under ~ 100m of water.

Notice the accumulation of large basaltic boulders downstream of plunge pools.

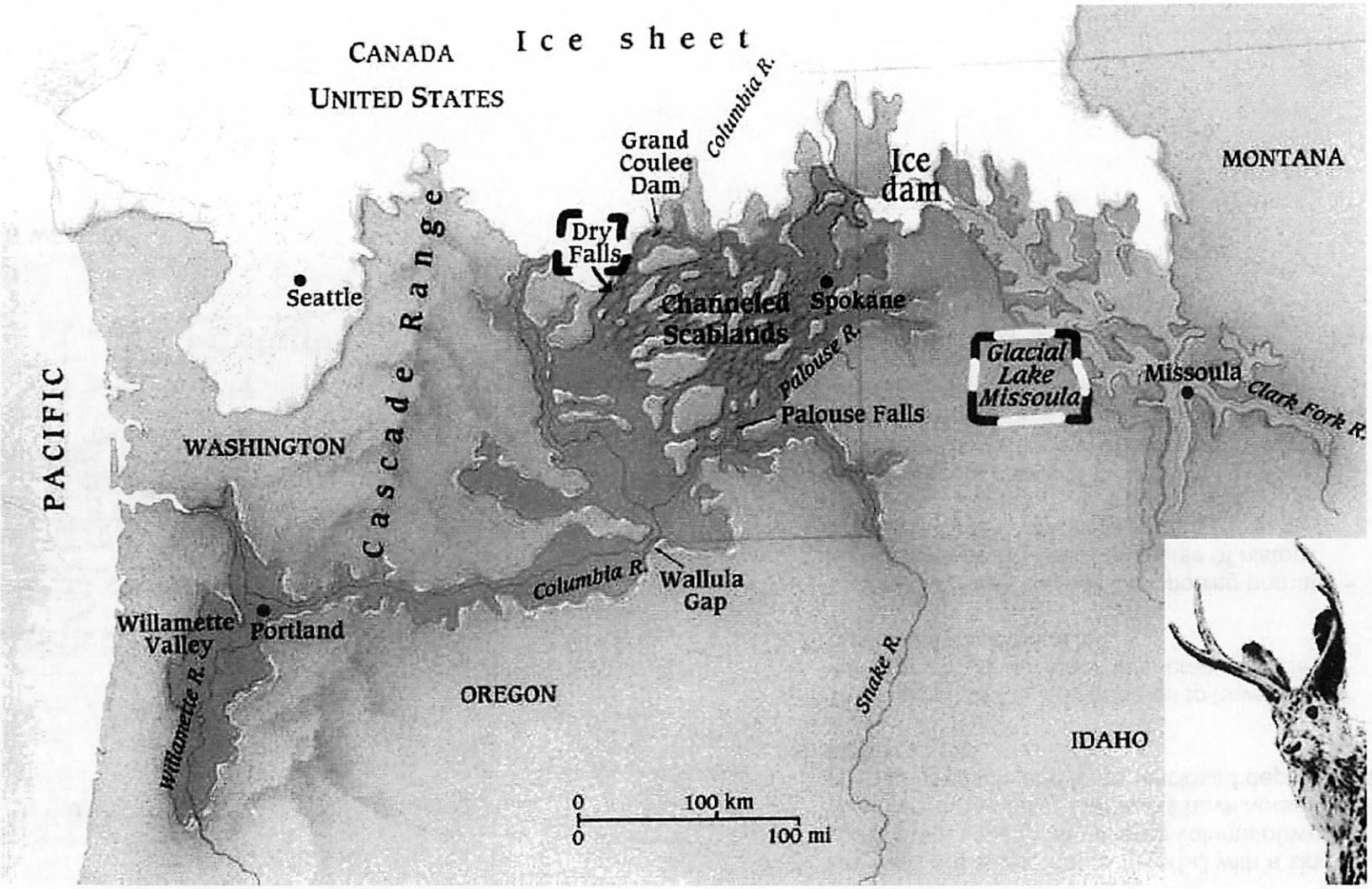

Map of the Northwest US, ~ 12,000 years ago

JÖKULHLAUPS is a flood created when a body of water held by a glacial dam breaks through the confining walls. The Missoula Floods were a jökulhlaups.

26 Extremophiles in Soap Lake: Implications for Life on Mars

by OLEG ABRAMOV

Soap Lake Introduction

Soap Lake, a small body of water with a surface area of about 7 km^2, was created by the Glacial Missoula Floods over 10,000 years ago. Chemically, it is saline, extremely alkaline, and lacks significant amounts of oxygen. It also has high concentrations of sulfides, which are considered toxic for most forms of life. The lake is permanently stratified, with the upper layer being much less salty and less dense than the lower layer. These two layers have not mixed for at least 2000 years, making it the longest documented stratification of any lake on Earth. In spite of the extreme chemistry of this environment, the lake is dominated by microorganisms, supporting thriving communities of algae, zooplankton, and bacteria.

Extremophiles

Extremophiles are microorganisms that thrive in the Earth's most hostile environments. Examples include hydrothermal vents, deep within the lithosphere, high-radiation environments, and severe chemical environments, such as saline lakes and ponds at pH 10.

Soap Lake is easily classified as an extreme chemical environment, as it contains 25 to 125 grams per liter total dissolved solids depending on depth, and has a pH of 10. It is known to support thriving populations of extremophilic microorganisms, particularly halo-alkaliphiles, which are bacteria that flourish in high salt and high pH environments.

Martian connection

As the climate of ancient Mars became colder and drier with time, open bodies of water would have entered a regime in which evaporation exceeded input from precipitation or runoff. This would have resulted in increases in salinity and perhaps pH. The last open water on Mars was most likely found in alkaline hypersaline lakes, and these lakes would have been the last surface aquatic habitats for life on Mars. It follows, then, that the biomarkers most likely to be found in ancient sedimentary basins on Mars are those left by organisms adapted to high salt and high pH habitats. Thus, Soap Lake can be used as a terrestrial analog to study the nature of biological diversity of extremophiles and their adaptation to these types of extreme environments, as well as the potential of these environments for biomarker preservation.

The recently funded Soap Lake Microbial Observatory will serve as a model for studying interactions of the anaerobic communities in haloalkaline environments similar to those proposed on early Mars. Results generated by this project will supplement data available for the search for biological activity on Mars and extra-solar terrestrial environments, and will augment the Virtual Planet Laboratory Program (which aims to simulate the environments of extrasolar planets) being developed at the Jet Propulsion Laboratory.

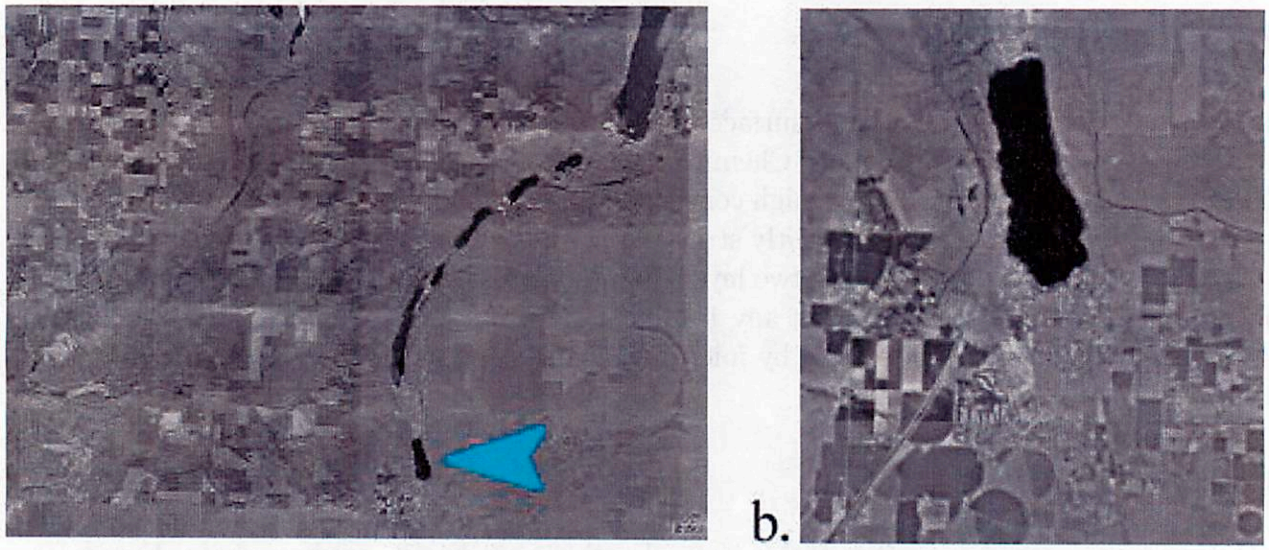

Figure 26.1: .

References

1. International Society for Salt Lake Research, `http://www.isslr.org/`

2. The Soap Lake Conservancy, `http://www.thelake.org`

3. McDonald, G.D., A. I. Tsapin, M. C. Storrie-Lombardi, K. H. Nealson, K. L. F. Brinton, H. Sun, K. Venkateswaren, I. Tsapin, J. Melack, and R. Jellison 1999. Alkaline Hypersaline Lakes as Analogs for Ancient Microbial Habitats on Mars. *The Fifth International Conference on Mars*, 6136.

4. Kempe, A. and J. Kazmierczak 1997. A terrestrial model for an alkaline Martian hydrosphere. *Planet. Space Sci.*, **45**, 1493 - 1499

5. Mills, A.A. and M. R. Sims 1995. pH of the Martian surface. *Planet. Space Sci.*, *43*, 695 - 696

27 The Ephrata Gravel Fan

by ADINA ALPERT

(or, "How 'Earth is the most Mars-like planet in the Solar System'")

(above quotation by Jeff Moore, NASA Ames)

Introduction

Exactly 7 years ago this week, more than 60 engineers, scientists, and educators gathered right here for the Mars Pathfinder Landing Site Workshop and Field Trips in the Channeled Scabland of Washington. The September 24-30, 1995 excursion allowed Mars Pathfinder scientists and engineers to prepare for the Mars landing by studying and evaluating a real, Mars-analog terrain. In addition, it was an excellent education and public outreach opportunity to involve K-12 educators in the process.

The Channeled Scabland is considered to be the best terrestrial analog to Ares Vallis, Mars, the landing site of Pathfinder. The Ares Vallis site was picked because it is an area where massive floods have deposited sediment. The hope was that these sediments would include a large variety of different types of rock brought from various locations upstream. The Ephrata Gravel Fan, here in the Scabland, was thought to especially resemble the vast flood deposit that Pathfinder would encounter (Edgett 1995).

Ephrata Gravel Fan

The Ephrata Fan system is an extensive coarse gravel unit deposited as flood waters from the lower Grand Coulee expanded into the wide Quincy Basin after leaving the last coulee constriction at Soap Lake (Fig 27.1). The deposit is thought to have been built as a subfluvial bar, not as a common alluvial fan on which the active channels constantly change location but never submerge the entire fan at one time. Evidence for being a subfluvial bar is that there is a steep adverse slope (0.01) going from the bottom of Soap Lake to the area of the highest deposits near the town of Ephrata downstream (Nummedal 1978).

The flood gravel is typically poorly sorted. The deposit is dominated by basalt fragments that were probably derived by erosion of the Grand Coulee. There are also some granitic rocks thought to be from the granite outcrops at the head of the Grand Coulee near the present Grand Coulee Dam on the Columbia River, about 50 km to the north (Nummedal 1978).

"Mars Pathfinding in the Channeled Scabland"

The plan for combining Mars education and science goals in the Channeled Scabland was initiated by Jim Rice and Ken Edgett in 1994, a year before the workshop and field trip. Our very own Vic Baker led the field trip portion of the meeting, while Mars Pathfinder Project Scientist Matt

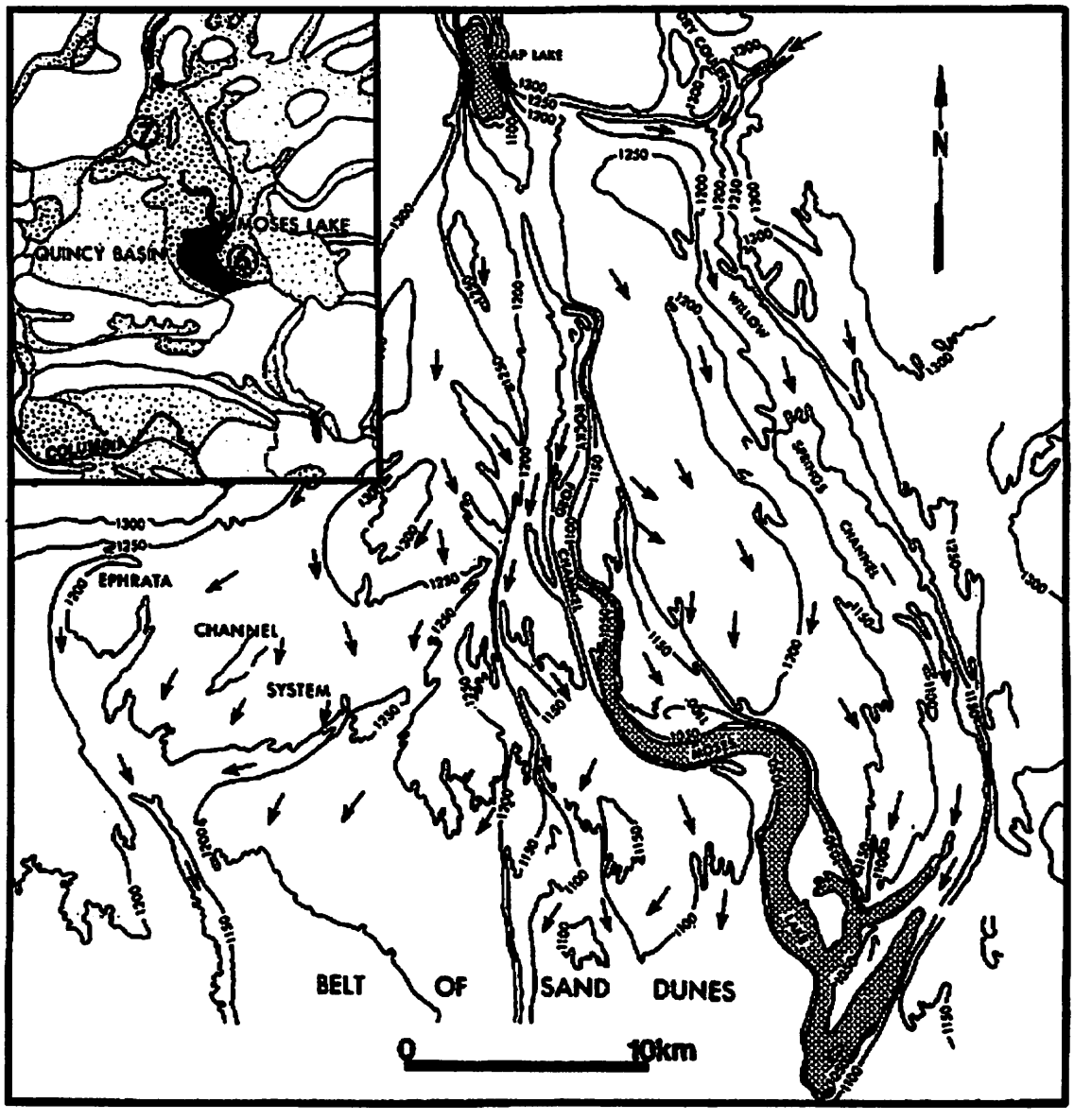

Figure 27.1: *Topographic map of the Ephrata Fan complex in the upper Quincy Basin. Arrows indicate inferred surface flow directions.*

Golombek led the workshop. A public open house, "Mars Night," held at a middle school in Spokane, was attended by 700 people including many K-12 students.

The field trips began with a flight over the terrain, which proved crucial for helping the scientists and engineers visualize the flood landforms in their full three-dimensional context and scale. The first ground-based excursion was designed to simulate a trip down Ares Vallis and out into the flood deposits where the landing site would be (Fig 2). It went down the Lower Grand Coulee from Dry Falls and out onto the Ephrata Fan. When the engineers responsible for the airbag landing system first saw the fan, they were quite alarmed - they were seeing the worst possible site, an area with giant boulders, the largest being "nearly the size of a small house" (Edgett 1978). Plans for the next day were revised so that they could return to the fan and see a different site that was thought

to be more typical of the terrain within the landing ellipse. It looked no rockier than the site where Viking 1 landed, and Pathfinder was designed to be able to land in places that are slightly more rocky than the Viking sites anyway (Edgett 1978). So the engineers were relieved!

The second trip onto the fan showed that most of it is not rocky at all, primarily just sand and gravel with no boulders. Mission Design engineer Rich Cook said, "There is a fairly high likelihood that we can handle [the Ares Vallis site on] Mars if the Channeled Scabland is a good analog." And, indeed, they were able to handle it remarkably well!

So, how well does the Ares Valles landing site compare with the Ephrata Gravel Fan?

REFERENCES

Edgett, K., 1995, Mars Pathfinding in the Channeled Scabland, TES News 4, No. 4.

Nummedal, D., 1978, Field Trip Stop Descriptions, in The Channeled Scabland, V. R. Baker and D. Nummedal (eds.), NASA, Washington, DC, pp. 131-168.

28 More Lœss

by JASON W. BARNES

Lœss (etymology: Scandanavian — Pronounced as $\frac{\text{luss+loose}}{2}$) is a weakly cemented deposit of wind-blown dust.

In arid areas of the world, prevailing winds entrain dust from dry lake beds, and to a lœsser degree dry riverbeds and banks, and blow it downwind. Glacial streams also provide a prodigious source of dust to be entrained. A map of dust source locations and wind directions is provided in Figure 28.1. This process is familiar to residents of Tucson, for whom the æolian transport of dust can coat exposed objects to about an optical depth in thickness in a few months of outdoor exposure (see my car). However, because there is a lot lœss dust accumulation than fluvial depsicion on average, there aren't any lœss deposits here in Southern Arizona.

The dust that makes up a lœss deposit has a median particle size between 1μm and 100μm, more or lœss. As the dust travels with the wind, larger particles fall out more quickly than smaller ones, leading to a negative gradient in median dust particle diameter as a function of distance from the source.

The dust particles that comprise a lœss deposit are composed of about 70% quartz and are usually high in carbonates. After deposition, rainfall dissolves some of the carbonate minerals and redeposits them, cementing the formerly loose dust together.

There is more lœss around than you might think: lœss covers 10%-20% of the Earth's land surface area (see Figure 28.2). The total mass of dust transported by æolian processes is quite large — comparable to the mass of silt transported by the Earth's river systems (see Figure 28.3). Though the mass of æolian dust transported is lœss than the mass of fluvially transported silt today, this has not been the case during dryer global climate regimes in the past. The prevalence of this deposit in currently wet regions or regions that are not currently in the path of windblown dust allows the determination of paleoclimate and paleowind circulation patterns.

Lœss deposits around the globe are quite young, varying in age from 11,000 years to 2.4 million years. Lœss deposits are vulnerable to water erosion, erasing them from the geologic record on Myr timescales (though some fossil lœss beds have been found).

At one time, lœss covered the entire area around southeastern Washington state. The silty dust that comprises lœss, mixed with volcanic ash from Cascades volcanoes, provides reasonably nutrient-rich soil for growing crops. The giant floods eroded away the lœss from many areas, leaving lœss islands that avoided erosion. The morphology of some of these islands resembles river islands, with teardrop shapes with the rounded edge into the direction of the water flow. There are flows around Martian craters that have similar morphologies.

On Earth, lœss formation seems to be sped up considerably by fluvial erosion and glacial erosion. On Mars, without such water to break up rocks into relevant particle sizes and without rainfall to coagulate the lœss sediments, dust may be transformed into lœss at a much lœsser rate.

nces: Livingstone & Warren, Aeolean Geomorphology. 1996, Addison-Wesley; Catt, J.A., Quaternary Geology for Scientists and Engineers. 1988, Ellis Horwood.

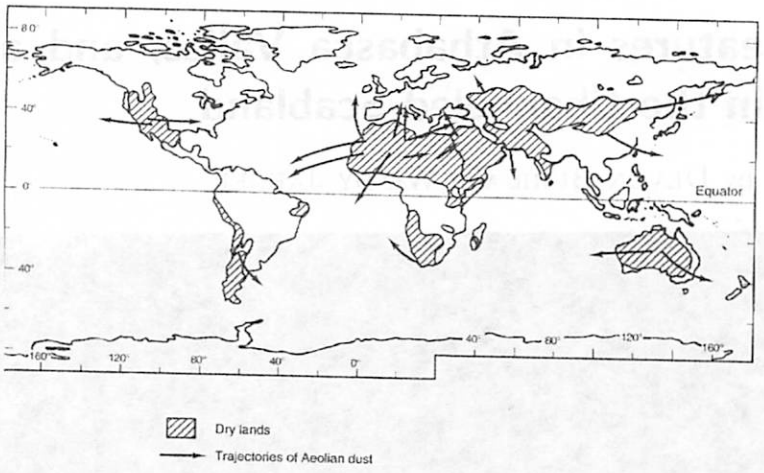

Figure 28.1: *Dust source regions and vectors on Earth.*

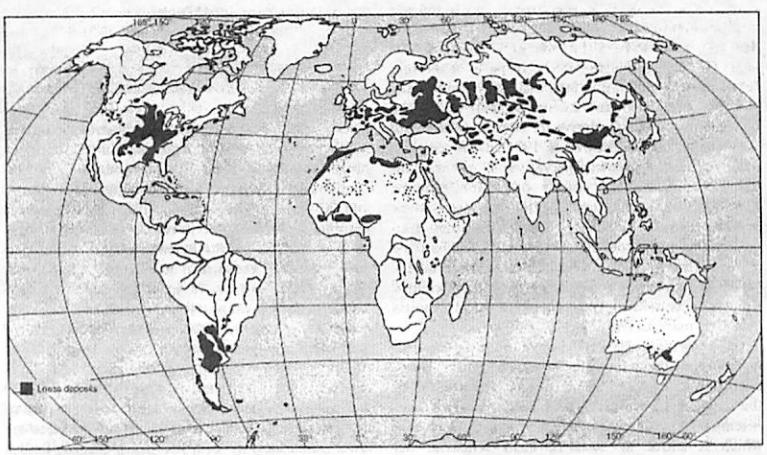

Figure 28.2: *Present-day distribution of læss.*

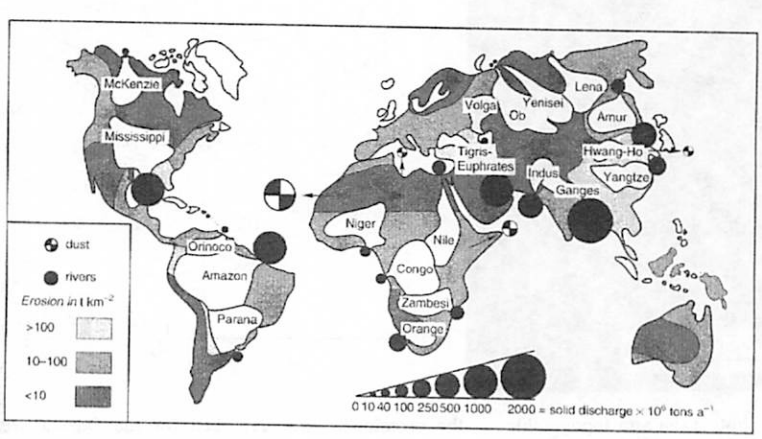

Figure 28.3: *Dust erosion rate compared to fluvial erosion.*

29 Circular/ring Features in Athabasca Valles, and a Possible Terrestrial Analog in the Channeled Scabland

by DEVON BURR AND WINDY JAEGER

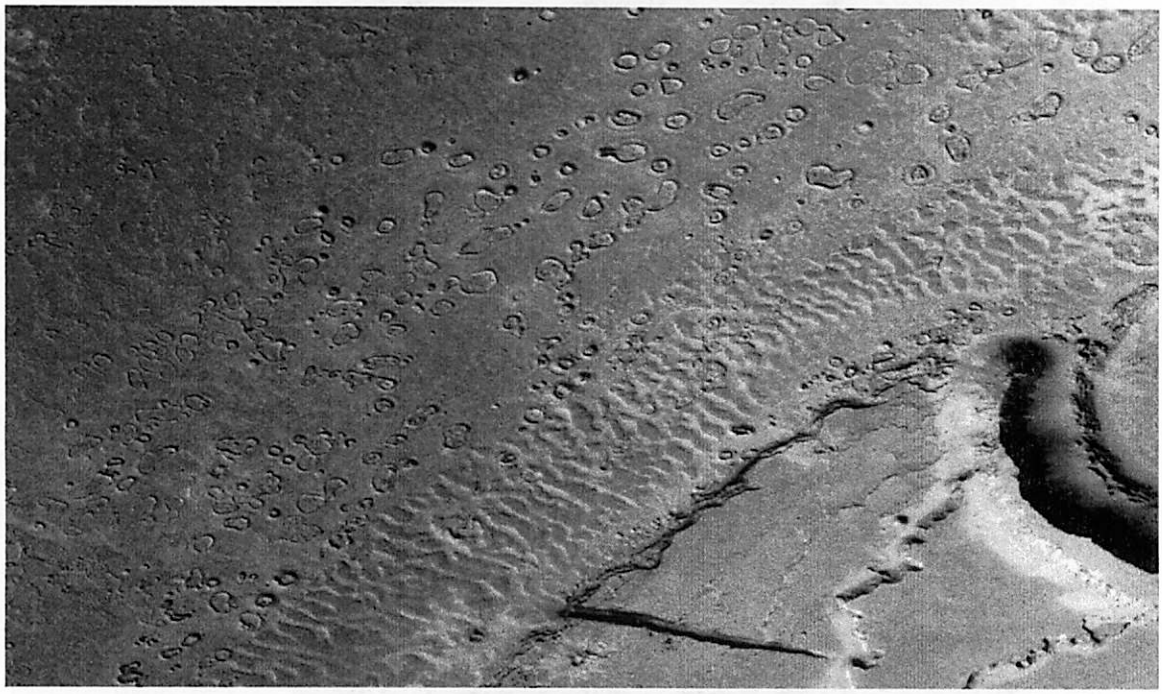

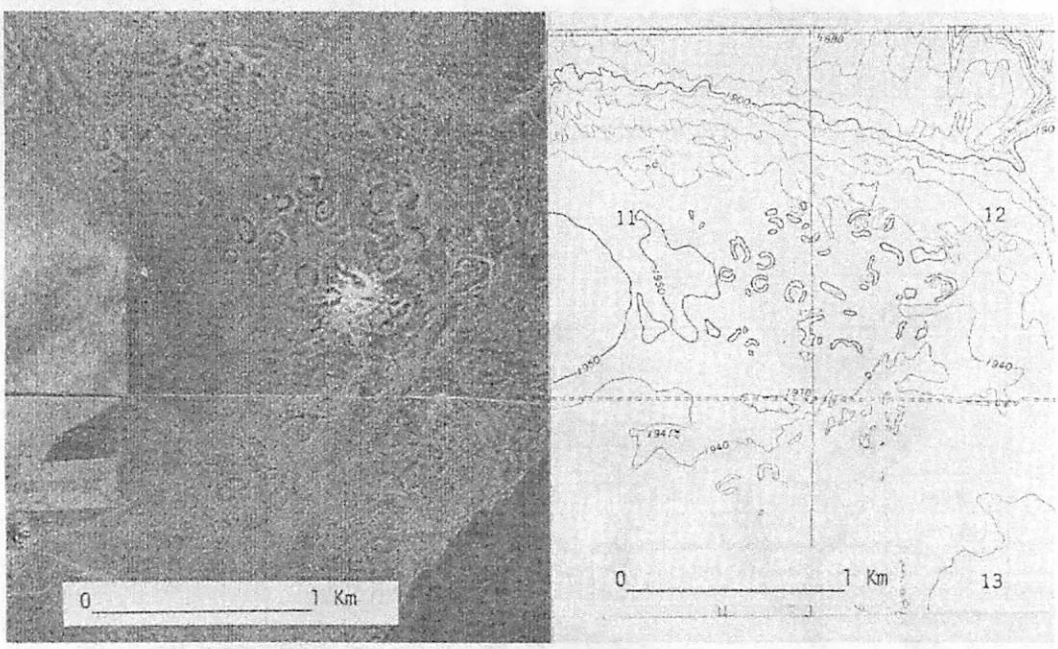

Figure 4.17. Vertical aerial photograph and topographic map (10 feet contour interval) of the ring structures shown in Fig. 4.16. These rings occur at 40 km east of the prominent rings described for the Odessa area by McKee and Stradling (1970) and by Hodges (1976).

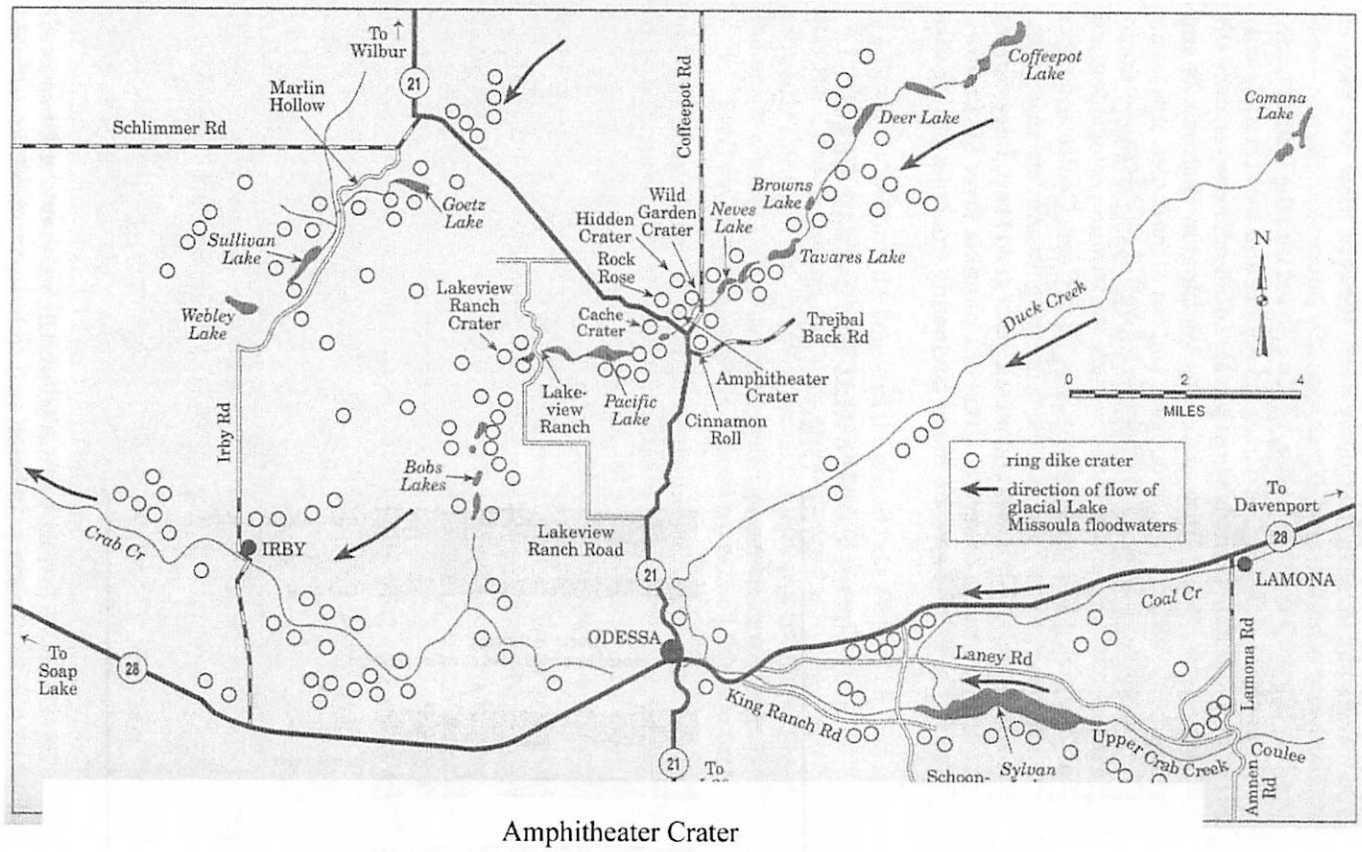

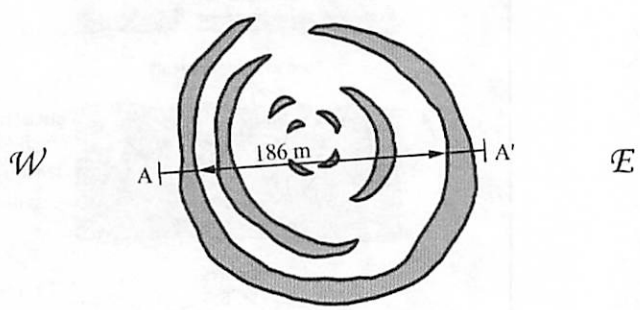

Plan View

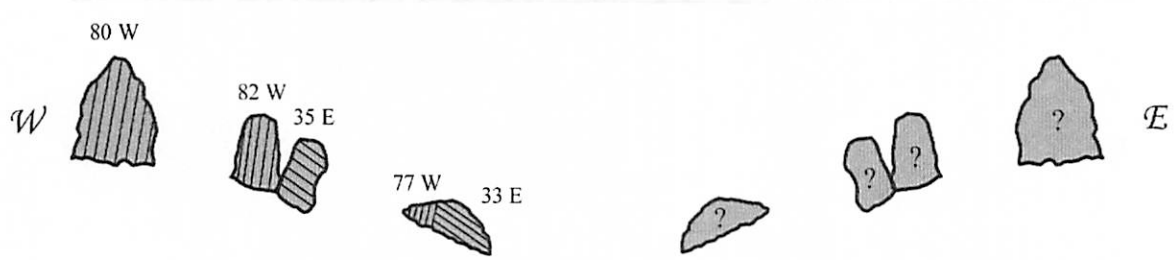

Schematic Cross Section with Measured Dips

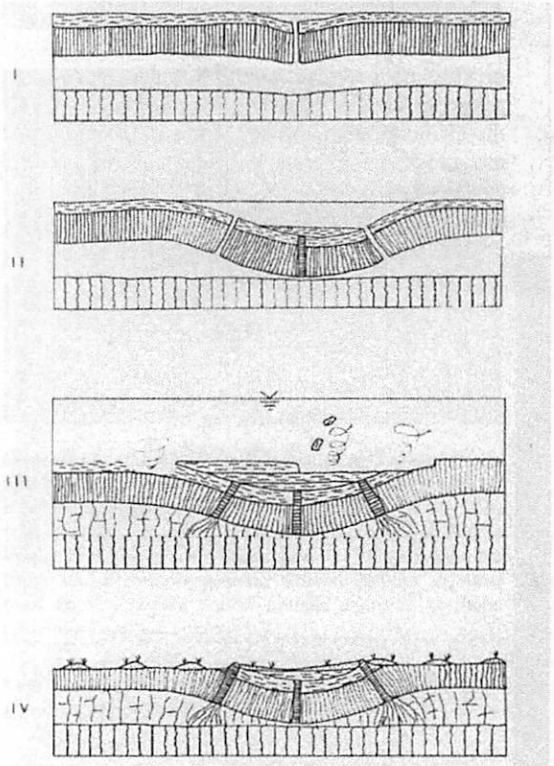

Fig. 4.18 from Baker (1978) after McKee and Stradling (1970)

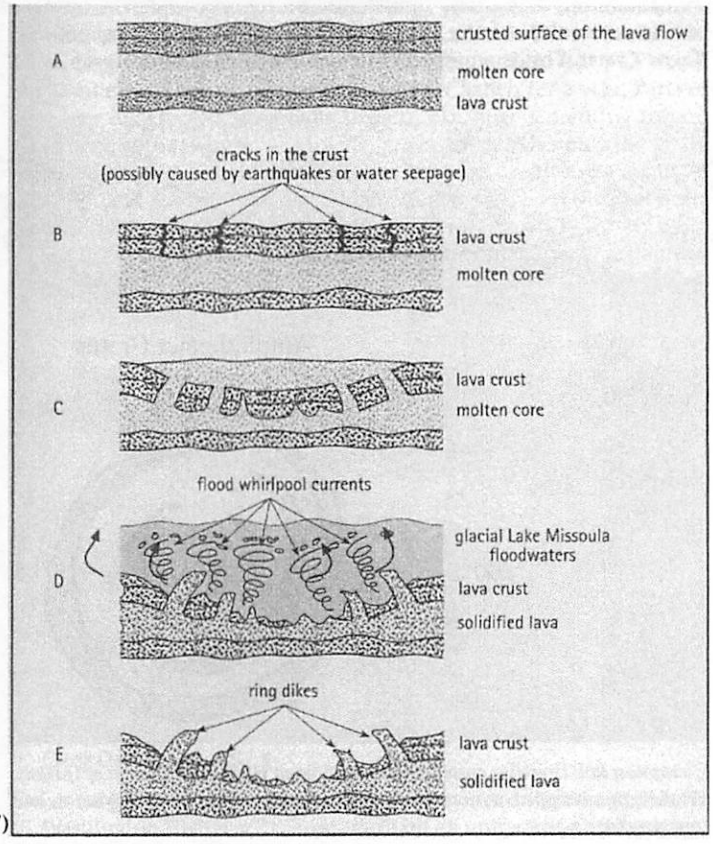

Fig. 2 from Mueller and Mueller (1997)

30 The Great Missoula Flood(s), or: One, two, many?

by YOUR FULSOME SPOUTER OF TALES, JAY MELOSH

The Controversy Did "the" great Missoula flood occur in one great spurt or in multiple mediocre pulses?

The Players J. Harlan Bretz, Advocate of a Single, Giant outbreak that inundated central Washington.
R. B. Waitt, Supporter of Multiple Bursts.
J. Shaw and company, 1999 Back to Bretz advocates.

The Evidence Repetitive sequences of "Rhythmites", sedimentary deposits recording time-varying sedimentary sequences, repeated 60 to 90 times in either (1) the bed of glacial Lake Missoula, or (2) in various locations in the Channeled Scablands.

Waitt says Rythmic sequences of sediments in the Ninemile Creek section comprising an arm of glacial Lake Missoula record 40 or more events in which the lake emptied and spilled over the scablands. Each unit is composed of a ca. 30 cm thick silt layer, overlain by a similar thickness of clay, which in turn is overlain by a large number of "varves": alternating silt and clay layers from 1 mm to 1 cm thick. Cracks within these layers show that each was exposed for a period of years following its emplacement, during successive high stands of Lake Missoula.

Shaw & Co say These rhythmic layers were all deposited under water by catastrophic water break-outs ("Jokulhlaups") that discharged from the northern ice sheet into the lake. They do not represent lowering of the lake, but simply strong influxes of sediment due to turbidity currents generated by these events.

Waitt says Rhythmic sequences also occur in the Scablands and adjacent areas. These sequences start with a basal layer of sand or sometimes angular basaltic cobbles and gravel that grades upward through silt and clay. Animal burrows and a volcanic ash bed occur in the tops of these deposits. *These deposits correlate in time with the layers in Lake Missoula. Each layer records a separate discharge/flood event, which therefore number* > 40.

Shaw & Co say These sequences record one, or only a few, massive outbursts. Each sequence records a mere resurge of a single event. The evidence for cracks and animal burrows is illusory: These apparent features are due to dewatering of sediment after the flood subsided. Large clastic dikes occasionally cut through the entire sequence. *The individual members of the rhythmites in the Scablands and in Lake Missoula are not correlated in time, since they record different events.*

Rejoinder by G. Komatsu (former LPL student of Vic Baker) New modeling of the flood shows that the total volume of the water in glacial Lake Missoula is insufficient to explain the observed flood high-stands. A second, much larger, source of water is needed, that Shaw & Co already argued must come from beneath the British Columbia lobe of the Cordilleran ice sheet. *Most of the water that formed the Scabland flood(s) did not come from Lake Missoula, further weakening the case for a putative correlation of rhythmite deposits.*

References

Atwater, B. F., et al (2000) Comment, *Geology* 574-575.

Komatsu, G., et al (2000) Comment, *Geology* 573-574.

O'Connor, J. E. and Baker, V. R., (1992) Magnitudes and implications of peak discharges from glacial Lake Missoula, *Geol. Soc. Amer. Bull.* **104**,267-279.

Shaw, J. et a1 (1999) The Channeled Scabland: Back to Bretz?, *Geology* **27**,605-608.

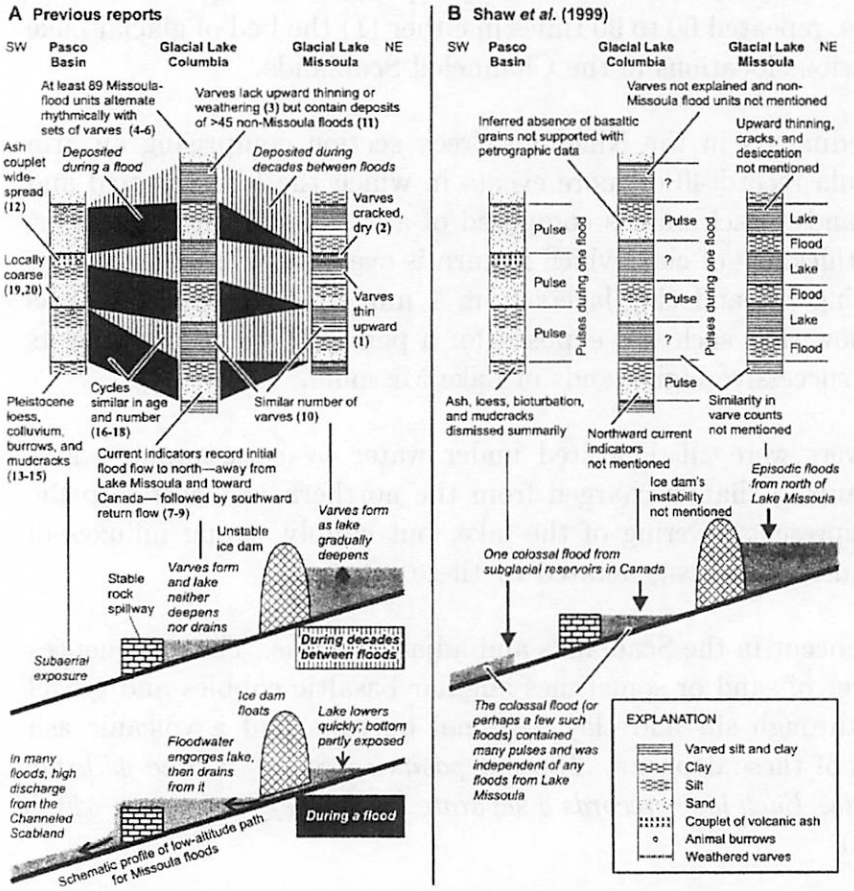

Figure 1. Two views of rhythmic deposits and their implications for last-glacial floods in the northwestern United States. Numerals in parentheses in A are keyed to an index map (Fig. 2, see footnote 1) and to details in Table 1 (see footnote 1).

from Atwater, et al (2000)

31 Mystery Mounds of the Puget Lowlands

by anti-mound mogul JAY MELOSH

What: Small black dirt mounds that dot the prairies in central and western Washington state (among other places).

Variously called "Mima Mounds" (after the type locality on Mima Prairie, WA), also "prairie mounds", "pimple mounds", "mounds", "those d*** piles of dirt!"

Where: Found in dense clusters in parts of Washington State, Wyoming, Minnesota, Iowa, the Mississippi lowlands (TX, LA), Cape Province, South Africa, Kenya, Argentina, etc.

Size: 0 to 3 m high, 2.5 to 15 m diameter, spaced at 1 to a few diameters crest to crest (see contour map and photo of occurrence below). Very circular to irregular in plan view. A few are surrounded by concentric ridges (multiring mima mounds)

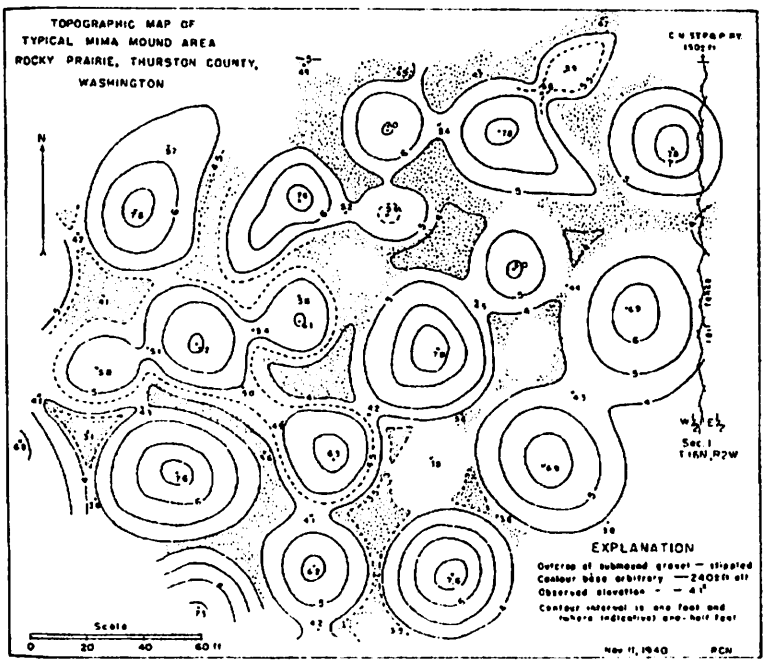

Figure 31.1: *An incompletely mounded average area inhabited by gophers. It is suggested that any subsequent growth, if present, might in the future be measured by resurvey, Newcomb (1962).*

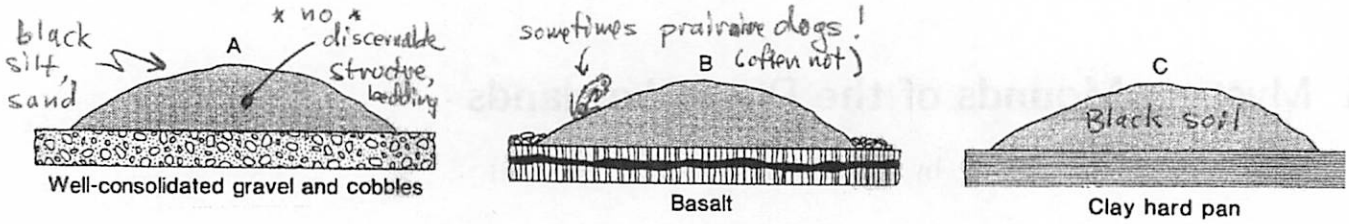

Figure 31.2: *Cross-section views of Mima mounts formed on various surfaces, Berg (1990).*

Composition: Unbedded, appaently structureless black sandy silt (loam) and fine sand. Sometimes contaIn cm-size gravel. Usually overlie a hard, bedded stratum of coarse gravel (containing cobbles to 20 cm), basalt or clay hardpan (see Figure 31.3). Intermound areas often cobbly, sometimes cut by branched troughs.

Age: In Washington, the mounds **post**date the Lake Missoula floods (15.3 –12.7 kyr) and predate the Mt. Mazama eruption (7 kyr).

Hypotheses for Origin :

Pocket Gophers (Dalquest and Schefer 1942)
Vegetation anchor (Washburn 1988)
Periglacial processes (humps between ice wedges Pewe, 1948, Taber 1943)
Glacial outwash/ice interactions (Bretz 1913)
Seismic shaking (Berg, 1990)

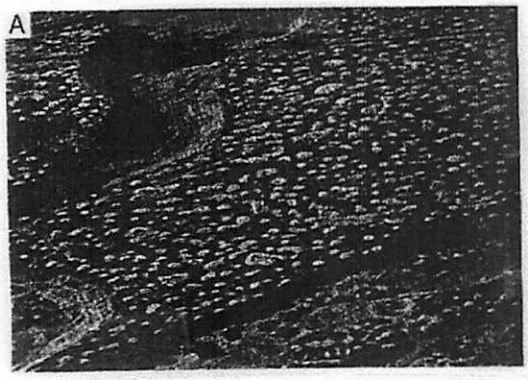

Figure 31.3: *Mima mounds near Rock Lake, Washington. A: Mima mounds formed on planar surfaces of the Columbia River basalts, from Berg (1990).*

References

Berg, A. W. (1990) Formation of Mima mounds: A seismic hypothesis, *Geology* **18**, 281-284.
Bretz, J. H. (1913) Glaciation of the Puget Sound Region, *Washington Geol. Survey Bull.* **8**, 244 pp.
Dalquest, W. W. and Scheffer, V. B. (1942) The origin of the Mima mounds of western Washington, *Jour. Geology*, **50**, 68-84.
Newcomb, R. C. (1962) Origin of the Mima mounds, Thurston County region, Washington, *Jour. Geology* **60**, 461-472.
Pewe, T. L. (1948) Origin of the Mima mounds, *Sci. Monthly*, **66**,293-296.
Taber, S. (1943) Perennially frozen ground in Alaska: Its origin and history, *Geol. Soc. America Bull.* **54**,1433-1548.
Washburn, A. L. (1988) Mima mounds, an evaluation of proposed origins with special reference to the Puget Lowland, *Washington Division of Geology and Earth Resources Report of Investigations*, **29**, 53pp.

32 Formation of Streamlined Forms

by DEVON BURR

Diluvial streamlined forms:

in plan view, teardrop or airfoil shape, with rounded end oriented up slope and pointed end pointing down slope;

in 3rd dim., positive relief with higher up slope end and lower down slope end;

N.B. Non-diluvial streamlined forms do exist, e.g. Drumlins (...or do they? Shaw)

Research highlights:

"discovery" as diluvial features (Bretz 1923, 1928 and other pubs)

dimensional analysis (Baker 1978, pp. 88-92)

K values: $K = l^2$??/ 4A quantifies elongation (value is 1 for a circle)

published values in Ch. Scabland are -2.3-4.9

related to Reynolds number? (Fig 5.14, K vs. Re, r = 0.778)

experimental work (Komar 1984)

flume experiments with med-grained sand and clay, Fr = 0.33-0.47, $Re = 10^4$

result: L/W = 3-4

i.e., minimum drag shape as hypothesized by Baker 1979)

balance between form resistance (decreases with decreasing width) and skin resistance (decreases with decreasing surface area)

Fr (total) = Fr (skin) + Fr (form)

Modes of formation:

erosional ("residual" Baker 1978 p. 88) –show:

flow obstacles that localized the resistant landform

upstream crescent-like scour marks

downstream tapering streamlines on the adjacent channel floor

oblique channels cutting through small divides at the crest of the form

formed in loess!! while elsewhere basalt is eroded — shows effectiveness of streamlining in reducing flow resistance

depositional –shows

grain size

foreset bedding

not pure deposition, but where inflow exceeds outflow

gradually built up beginning in the Early Pleistocene (Bjornstad et al. 2001)

Martian forms — located in:

circum-Chryse channels ie. Giant catastrophic outflow channels that feed into Chryse basin (Baker and Milton 1974)

Cerberus channels –smaller outflow channels around the Cerberus Plains (Burr et al. 2002), hypothesized that

main channel "streamlind mesas" are depositional

side channel forms are erosional

who cares??

— floodwater ht indicators

— sediment may be from Cerberus Fossae (origination pt of floodwater)

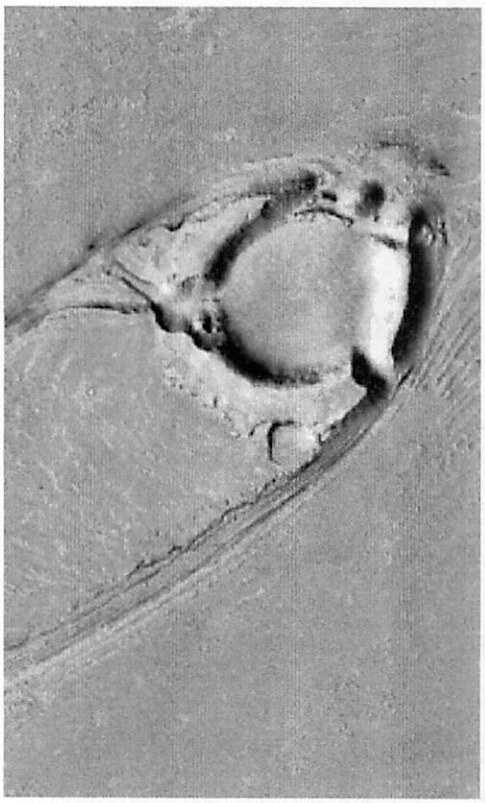

Depositional?

Erosional?

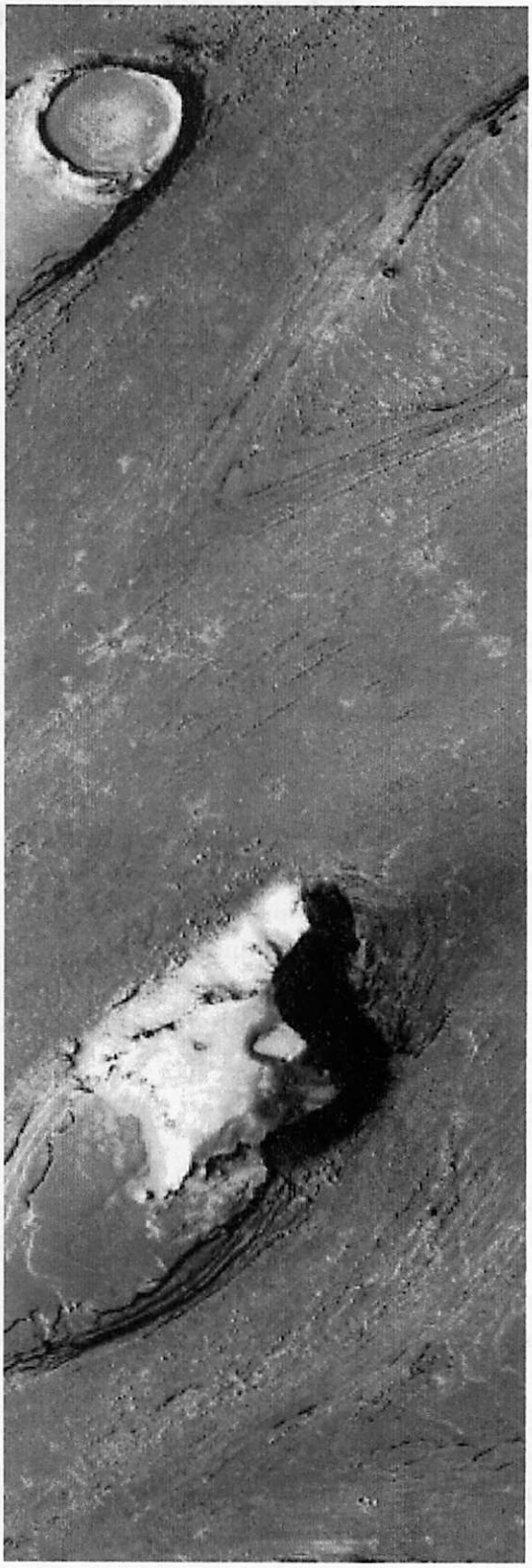

33 Remote Sensing to Interpret Volcanic and Fluvial Processes on Mars

by ALFRED MCEWEN

Interpretation of geologic processes on Earth is accomplished via field work, interpretation of air photos and other remote sensing, analysis of rocks in the lab, and modeling. On Mars we have had extremely limited opportunities for robotic field work and lab analysis is only possible for the Martian meteorites of unknown provenance. We can model all we want but the results shouldn't be entirely believed without good observational constraints. The great majority of our information about Mars comes from remote sensing.

When in the field I like to visualize how particular geologic deposits would appear in the remote sensing datasets available for Mars or expected in the near future. The orbital experiments on Mars that I like to think about are:

Experiment	Ground Sampling Scale	Spectral Capability	Expected Coverage	Other Capabilities
MOC	1.5 to 12 m	1 bandpass in visible	~2%	wide-angle camera
THEMIS	100 m	9 unique bandpasses from 6.8 to 15 microns)	100%	mapping of thermal inertia (*I*); visible imaging at 18 m
HiRISE	0.3 to 1.2 m	3 colors (green, red, near-IR)	~1%	stereo coverage and DEMs
CRISM	20 to 100 m	hundreds of wavelengths, 0.4-4.05 microns	a few % with full capability, global at 100 m and 50 bands	Will often cover same targets as HiRISE

MOC is Mars Orbital Camera on Mars Global Surveyor (in Mars orbit since 1997).
THEMIS is Thermal Emission Imaging System on Mars Odyssey (in orbit since 2001).
HiRISE is High Resolution Imaging Science Experiment on Mars Reconnaissance Orbiter (MRO; Mars orbit expected in 2006).
CRISM is Compact Reconnaissance Imaging Spectrometer for Mars, also on MRO.

What would these experiments detect from Martian deposits similar to those in MSH, the CRB, and the Channeled Scablands? Before attempting to answer that question, here is some background.

Some folks think HiRISE will be able to detect soccer balls on Mars, but that isn't the case. The

relations between optical resolution, ground sampling dimension (e.g., m/pixel) and the detection and characterization of features was studied in 1989 for the Mars Rover Sample Return Mission (remember that?). They concluded the following for images with a high signal-to-noise ratio (SNR > 150):

Feature	Optical Resolution Elements needed	Pixels Needed Across Feature
Detection of high-contrast linear feature (like a fissure)	1	2
Detection of most equant features (like boulders)	1.25	2.5
Minimal understanding of an equant feature (like whether a boulder is rounded or angular)	4 – 5	8 - 10

MOC has a ground sampling dimension of 1.5 m/pixel (but poor SNR) so high-contrast boulders larger than $\sim$ 4 m can be detected. Most MOC images are binned (averaged) over at least 2x2 pixel blocks to increase SNR, so only boulders larger than 7 to 8 m are detectable. That's half the size of the giant boulder in Vic's slide (and Fig. 4.15 of The Channelled Scabland), but such boulders are extremely rare in fluvial deposits. "Boulders" detected by MOC are mostly chunks of bedrock that broke off from cliffs and slid downhill a bit, or were exhumed in place. Such blocks can't move far without breaking up into smaller boulders, below MOC resolution. HiRISE will be able to detect boulders $\sim$ 1 m diameter or larger (limited by optical resolution rather than number of pixels) and will be able to show if boulders larger than 3 to 4 meters diameter are rounded, angular, tabular, etc. The resolution of compositional data like CRISM or THEMIS may be closer to the pixel scale. Thermal images can detect hot spots much smaller than the pixel scale.

For mineralogic studies, thermal emission is best for coarse crystalline materials while NIR reflectance spectroscopy is better for fine-grained materials (which cover most of Mars).

Thermal Inertia, I is given by $(K\rho C)^{1/2}$ where K is thermal conductivity, ρ is density, and C is heat capacity. I on Mars is dominated by K, which varies by several orders of magnitude as a function of grain size, porosity, and degree of bonding (cementation). Dust or reticulite have very low I, exposed rocks have high I, and medium I could be sand, cemented fines (duricrust), or a mixture of materials. Mixtures can be deconvolved to some degree because a mixture of pre-dawn temperatures (when I dominates the temperatures) will produce a non-blackbody thermal spectrum. THEMIS can map out regions with high rock abundances or bedrock exposures, which is very useful to a geologist.

Here are a few examples of how deposits or outcrops we will see on the field trip might appear in these remote sensing datasets if the same deposits were on Mars (and free of vegetation):

Mudflow deposits in N. Fork Toutle R. Debris flows transport unsorted materials including large boulders, some angular, whereas water is much more efficient at sorting, rounding, and producing bedfonns. The MSH rockslide-avalanche transitioned into a debris flow in the N. Fork of Toutle R., which then transitioned into a hyperconcentrated flood as the water:sediment ratio

increased downstream. MOC might see large boulders in the upstream reaches. HiRISE would see large boulders with a variety of shapes upstream, transitioning into smaller, better sorted, and more rounded boulder downstream. THEMIS will see moderately-high I (if not covered by eolian materials), and perhaps a gradient of I, decreasing downstream. CRISM and HiRISE color will show a variety of lithologies upstream, which appear more unifonn downstream. HiRISE stereo can be used to measure superelevation of the debris flow around channel bends, which enables determination of the flow velocity at that location and, along with measurements of flow depth provides a constraint on dynamic models that could help constrain the rheology (yield strength and/or viscosity in a Bingham model).

CRB outcrops in a steep canyon wall: MOC will see a stepped topography with 10-50 m thick layers, like the upper exposures in Valles Marineris (McEwen et al., 1999, Nature), and large (> 5 m) "boulders" (chunks of lava) that slid downhill a bit. (Such blocks would break up before tumbling 5-10 km to the floor of Valles Marineris so MOC can't resolve then, although Malin and Edgett (2001, massive isssue ofJGR-Planets) think the lack of resolved boulders indicates that the layers are sediment rather than lava). THEMIS will image high I layers, perhaps enabling the tracing and correlation of sets of thick flows, and detect emissivity variations consistent with basalt. HiRISE will see more detail in the stepped topography than MOC, better distinguishing the flow units, but can't resolve the cm-scale and smaller vesicles that Laszlo would love to study. However, HiRISE will detect the many basalt boulders ($\sim$ 1 m diameter) near the base of the cliff. CRISM will map out primary and secondary basaltic mineralogies, revealing areas where the basalt has been oxidized (near-vent regions?). HiRISE color will also show oxidized materials at sub-meter scales, perhaps detecting thin tephra or soil layers between flows.

Touchet beds of the Walla Walla valley: The Touchet beds are slack-water deposits associated with the Missoula floods. We should see these along the Columbia R. gorge. They consist of as many as 50 rhythmic layers up to $\sim$ 2 m thick consisting of mostly fine-grained fresh rock material. Although mostly fine-grained, there is gravel ranging up to the size of "large boulders" (Carson et al., The Channeled Scabland, p. 173). MOC will see relatively bright deposits and detect layers where exposures make them detectable. THEMIS and CRISM will see basaltic compositions and fail to detect carbonates, although a few diatoms are present. CRISM may detect clays and ferric minerals indicative of an aqueous environment. HiRISE will detect finer layers and may see a few boulders, and HiRISE stereo may prove useful for hydraulic models. Debates about the origin of these deposits will persist, since that is the case for the actual Touchet beds, which have been studied in much greater detail than would be possible on Mars.

In summary, these are examples of what I'll be thinking about at each stop; feel free to ask me to think out loud.